



Terms and Conditions of Use of Digitised Theses from Trinity College Library Dublin

Copyright statement

All material supplied by Trinity College Library is protected by copyright (under the Copyright and Related Rights Act, 2000 as amended) and other relevant Intellectual Property Rights. By accessing and using a Digitised Thesis from Trinity College Library you acknowledge that all Intellectual Property Rights in any Works supplied are the sole and exclusive property of the copyright and/or other IPR holder. Specific copyright holders may not be explicitly identified. Use of materials from other sources within a thesis should not be construed as a claim over them.

A non-exclusive, non-transferable licence is hereby granted to those using or reproducing, in whole or in part, the material for valid purposes, providing the copyright owners are acknowledged using the normal conventions. Where specific permission to use material is required, this is identified and such permission must be sought from the copyright holder or agency cited.

Liability statement

By using a Digitised Thesis, I accept that Trinity College Dublin bears no legal responsibility for the accuracy, legality or comprehensiveness of materials contained within the thesis, and that Trinity College Dublin accepts no liability for indirect, consequential, or incidental, damages or losses arising from use of the thesis for whatever reason. Information located in a thesis may be subject to specific use constraints, details of which may not be explicitly described. It is the responsibility of potential and actual users to be aware of such constraints and to abide by them. By making use of material from a digitised thesis, you accept these copyright and disclaimer provisions. Where it is brought to the attention of Trinity College Library that there may be a breach of copyright or other restraint, it is the policy to withdraw or take down access to a thesis while the issue is being resolved.

Access Agreement

By using a Digitised Thesis from Trinity College Library you are bound by the following Terms & Conditions. Please read them carefully.

I have read and I understand the following statement: All material supplied via a Digitised Thesis from Trinity College Library is protected by copyright and other intellectual property rights, and duplication or sale of all or part of any of a thesis is not permitted, except that material may be duplicated by you for your research use or for educational purposes in electronic or print form providing the copyright owners are acknowledged using the normal conventions. You must obtain permission for any other use. Electronic or print copies may not be offered, whether for sale or otherwise to anyone. This copy has been supplied on the understanding that it is copyright material and that no quotation from the thesis may be published without proper acknowledgement.

Characterisation and modelling of electro-pneumatic production systems

Paul Harris

University of Dublin,
Trinity College,
Department of Mechanical and Manufacturing Engineering

A thesis submitted in partial fulfilment for the degree of Doctor of Philosophy

May 2011

Dr. Garret O'Donnell

Project Supervisor



Thesis 9666

Declaration

Research has been carried out in the Mechanical and Manufacturing Engineering Department of Trinity College Dublin between October 2007 and April 2011. This thesis describes original work, which has not been submitted to any other University. The candidate agrees that the Library may lend or copy this thesis on request.

A handwritten signature in blue ink that reads "Paul Harris". The signature is written in a cursive style and is positioned above a dotted horizontal line.

Paul G. Harris

Summary

Compressed air is a widely employed energy source in modern manufacturing, accounting for a large percentage of plant electrical energy usage. However, the energy efficiency of such systems can be particularly low. Accurate models are essential in optimising the energy efficiency of pneumatic systems through model based design and control techniques. This study therefore aims to explore the dynamics, and in particular consumption characteristics, of pneumatic production processes with a focus on the development of scientific process models for industrial electro-pneumatic systems.

With a view to assessing compressed air usage and efficiency in automated production, an industrial case study was conducted on two assembly modules. An analysis of air flow to the module, under a variety of production rates and machine conditions, allowed for a characterisation of consumption and losses. The investigations showed that non-functional usage can account for approximately 34% of total machine air consumption. This figure represents a significant requirement on generation capacity. Such air losses can be reduced substantially with effective maintenance programs and control of open blow type devices. Both solutions are high return on investment projects and as such should be a priority target for industrial users. Additionally it has been highlighted that mathematical models are necessary to further quantify inefficiency in pneumatic systems due to design and exergy type losses such as pressure drop, friction and back-pressure.

A theoretical model was developed to predict the dynamics of an individual pneumatic drive system. The mathematical model considers non-linear flow through extended pneumatic circuits, direction dependent friction, dead volume in cylinder chambers, fittings and tubing, leakage between actuator chambers, time delays due to valve switching and long lengths of tubing, polytropic temperature model with optimisation of index and heat transfer. The simulation results were compared with the experimental results under different loading conditions using flow, pressure, position and acceleration sensors. The validation results indicate the model is accurate in tracking flow, pressure, pneumatic force and position trajectories. The mean absolute error in position prediction was less than 1 mm, and for pneumatic force was estimated to be 9.6N. These results are

good considering the maximum stroke length and theoretical force of the cylinder are 50mm and 245N respectively.

A scalable consumption model was developed for pneumatic production systems. The model was developed with a view to implementation in an industrial environment and can account for most types of active and all passive consumers. The Simulink model was interfaced with a programmable logic controller using an OPC server to allow for dynamic monitoring of control actions and air usage. The modelled and measured consumption of both active and passive consumers were compared, separately and as a system. The average error in consumption for three drives was estimated to be 13%. The error in passive consumer models depends on pressure, due to the assumption of sonic flow. The accuracy in modelling a combination of air knives and leakage was 5% at an upstream pressure greater than 3.5 bar. For pressures below 2.5 bar, the error increases from 15%. The accuracy of the simulation model in tracking the consumption of a prototype automation system under two different sequences was estimated to be between 7% and 13%. The results of the consumption model validation indicate that the proposed approach can be used with an acceptable level of accuracy for engineering applications.

It has been shown that the dynamics of an open-loop pneumatic drive system, common in industry, can be modelled with good accuracy, though the required identification effort is significant. The simplified consumption models reduce both modelling and identification effort and complexity. It has been demonstrated on a prototype machine that the predictive consumption approach can be used with reasonable accuracy. It is envisaged that the developed models will form part of a platform for improved measurement and control of industrial gas usage in manufacturing.

Acknowledgements

Thanks to;

- Dr. Garret O'Donnell, project supervisor, whose support is gratefully acknowledged.
- Mr. Tom Whelan, industrial supervisor, whose assistance throughout the project is appreciated. Thanks also to Garry Rooney and Ray O'Carroll for their support in Hewlett Packard.
- Dr. Petr Eret for his technical advice, in particular during the final stages of the project.
- Dr. Craig Meskell and Mr. Kevin Kelly for their input and advice at various stages of the project
- My fellow postgrads and friends John Gilchrist, Peter Ashmore, Kev Kerrigan, Emma Brazel, Paul Ervine, Peadar Golden and the rest of the 'manufacturing systems' team.
- On a more personal note, thanks to my girlfriend Molly for her patience and encouragement. In particular her assistance with the editing aspects of the thesis is much appreciated.
- Finally, and most importantly, many thanks to my parents, Anne and Gerry, for all their support over the years.
- The project has been funded by the Irish Research Council for Science, Engineering and Technology and Hewlett Packard Manufacturing under the Enterprise Partnership scheme.

Dedication

It is difficult to say what is impossible,
for the dream of yesterday is the hope of today
and the reality of tomorrow.

- Robert Goddard

This work is dedicated to my parents Gerry & Anne Harris,
and my grandfather Alec Harris.

Table of Contents

DECLARATION	II
SUMMARY	III
ACKNOWLEDGEMENTS	V
DEDICATION	VI
NOMENCLATURE	X
1. INTRODUCTION	1
1.1 Sustainable production and energy efficiency	1
1.2 Pneumatics in automated manufacturing	2
1.3 Challenges in pneumatics	3
1.4 Research focus	5
1.5 Scope & aim of research	6
2. LITERATURE REVIEW	8
2.1 Manufacturing Systems and Pneumatic Technology	8
2.1.1 Production paradigms	8
2.1.2 Manufacturing automation	10
2.1.3 Manufacturing energy usage and efficiency	16
2.1.4 Pneumatic and compressed air systems	18
2.1.4.1 Historical perspective	19
2.1.4.2 Compressed air system hardware	19
2.1.4.3 Pneumatic system hardware	20
2.2 Modelling and Analysis of pneumatic systems	25
2.2.1 Overview	25
2.2.2 Force dynamics models	27
2.2.3 Thermodynamic actuator models	32
2.2.4 Fluid Mechanic fundamentals, flow models and identification	38
2.2.5 Compressed air system models	66
2.3 Energy efficiency optimisation of pneumatic systems	71
2.3.1 Compressed air- energy consumption relationship	71
2.3.2 Energy saving in pneumatic systems	76
2.3.3 Energy saving in servo pneumatic systems	90

2.3.4 Compressed Air System Optimisation	94
2.3.5 Energy efficiency case studies in production	100
2.4 Summary	103
3. INDUSTRIAL INVESTIGATIONS: COMPRESSED AIR USAGE IN AUTOMATED PRODUCTION	105
3.1 Overview	105
3.1.1. Automated Assembly Production Module	105
3.1.2 Compressed air system	107
3.2 Investigations	108
3.2.1 Measurement equipment and setup	108
3.2.2 Investigation procedure	109
3.2.3 Accuracy of measurement system	112
3.3 Results and Analysis	114
3.3.1 Statistical analysis	114
3.3.2 Compressed air losses on AQT module	119
3.4 Summary	123
4. MODELLING & IDENTIFICATION OF INDUSTRIAL PNEUMATIC DRIVE SYSTEM	124
4.1 Model Development	124
4.1.1 System Dynamics	124
4.1.2 Software implementation	129
4.2 Parameter identification	131
4.2.1 Equipment and experimental setup	131
4.2.2 Flow identification	133
4.2.3 Leakage identification	139
4.2.4 Dead volume identification	140
4.2.5 Heat transfer identification	140
4.2.6 Polytropic index estimation	142
4.2.7 Friction identification	143
4.3 Model validation	148
4.4 Summary	156
5. PREDICTIVE CONSUMPTION MODELS FOR ELECTRO-PNEUMATIC PRODUCTION SYSTEMS	157

5.1 Model development	157
5.1.1 Consumption dynamics of production systems	158
5.1.2 Software implementation	162
5.2 Experimental setup	165
5.2.1 Consumption measurement	169
5.2.2 Flow model validation	170
5.3 Parameter identification	173
5.3.1 Circuit identification	173
5.3.2 Leakage characteristics	175
5.3.3 Consumption model estimation	177
5.4 Results and model validation	179
5.4.1 Active consumers	180
5.4.2 Passive consumers	184
5.4.3 Full system	186
5.5 Summary	190
6. CONCLUSIONS AND RECOMMENDATIONS FOR FUTURE WORK	191
6.1 Conclusions	191
6.1.1 Industrial investigations	192
6.1.2 Pneumatic drive dynamics model	192
6.1.3 Pneumatic system consumption model	193
6.1.4 Concluding remarks	195
6.2 Recommendations for Future work	196
6.2.1 Drive model and identification method development	197
6.2.2 Consumption model development	198
REFERENCES	201
Appendix A OPC data exchange protocol	213
Appendix B Matlab and Simulink programs	215
B1 Pneumatic drive Simulink models	215
B2 Identification scripts	217
B3 Pneumatic system Simulink models	220
Appendix C Prototype system details	222

Nomenclature

a	Cracking pressure ratio
A	Cross-sectional area, m^2
<u>A</u>	System activation matrix
Ae	Effective Area, m^2
Aq	Area of heat exchange surface, m^2
b	Critical pressure ratio
c	Speed of sound, m/s
C	Sonic conductance, $m^3/s.Pa$
C _d	Discharge coefficient
C _p	Specific heat capacity at constant pressure, J/kg.K
C _v	Specific heat capacity at constant volume, J/kg.K
d	Diameter (internal), m
E	Energy, kWh
f	Actuation frequency, cycles/min
F	Force, N
g	Gravitational acceleration, m/s^2
H	Total enthalpy, J
H _{sp}	Specific enthalpy, J/kg
h	Annual operating hours, h
I	Current, A
k	Heat conductance, W/K
L	Length, m
m	Gas mass, kg
ṁ	Mass flow rate, kg/s
M	Payload mass, kg
ms	Subsonic index
n	Polytropic index
P	Pressure, absolute pressure Pa or bar, gauge pressure bar(g)
Pr	Pressure ratio
P _w	Power, W
Q	Heat, J

q	Consumption, m ³
q _h	Enthalpy flow rate, W
q _v	Volumetric flow rate, m ³ /s or L/min
R	Gas constant, J/kg.K
Re	Reynolds number
S	stroke, m
s	Coefficient of compressibility
t	Time, s
T	Temperature, °C or K
u	Input signal, V
U	Internal energy, J
V	Volume, m ³
W	Total work, J
y	Position, m
<u>Z</u>	System transition matrix

Greek letters

β	Viscous friction coefficient
γ	Ratio of specific heat capacities
Δ	Increment
η	Efficiency
μ	Dynamic viscosity, kg/m.s
ν	Kinematic viscosity, m ² /s
ρ	Density, kg/m ³
φ	Flow function
λ	Heat transfer coefficient, W/m ² K

Subscripts

Amb	Ambient conditions
c	Choked
d	Downstream
df	Dynamic friction
f	Coulomb friction
u	Upstream

r	Rod
rf	Resistance force
t	Tubing
tr	Transmission
e	Equilibrium conditions
ex	Expansion
sw	Switching
sf	Static friction
1	Chamber 1, blind eye of cylinder
2	Chamber 2, rod end of cylinder
0	Reference conditions

Abbreviations

AQT:	Automated Quality Test
CA:	Compressed Air
CF:	Conversion Factor
DCS:	Distributed Control Systems
FRL:	Filter Regulator Lubricator
HMI:	Human Machine Interface
LCC:	Life Cycle Costs
MAE:	Mean absolute error
ME:	Mean error
MXR:	Maximum residual value
NEST:	Natural Environmental Societal Technological
OEM:	Original Equipment Manufacturer
OPC:	Object Linking and Embedding (OLE) for Process Control
PID:	Proportional-Integral-Derivative
PLC:	Programmable Logic Controller
RMSE:	Root mean square error
SCADA:	Supervisory Control and Data Acquisition
SEC:	Specific Energy Consumption, kW/lps
TCO:	Total Cost of Ownership
TU:	Transfer Unit

1. Introduction

1.1 Sustainable production and energy efficiency

The manufacturing industry is responsible for the generation of wealth, employment, quality of life and the promotion and sustaining of services, education, research and development [1]. The process, however, entails considerable environmental impact through pollution and particularly natural resource depletion: material and energy consumption [2]. Environmental benign or sustainable manufacturing incorporates the general concept that any business plan must address its relationship to the environment and suggests that business opportunity and social responsibility are ultimately intertwined [3,4]. Sustainability is emerging as a significant competitive dimension between large international companies for reasons such as risk mitigation, market advantage through 'green' product differentiation, regulatory flexibility and corporate image [4].

Energy is a key enabler in facilitating manufacturing operations and is provided for all aspects of a firm's value chain. Nevertheless, it is capital, labour and raw materials that are traditionally viewed as the prominent production factors in manufacturing organisations. There is an emerging paradigm that defines manufacturing, in a post-modern sense, as a process whereby "information is transformed into products by the controlled flow of energy" [5]. In this context, information and energy efficiency are the key critical success factors for future manufacturing operations. Energy efficiency is the ratio of energy consumed as useful work or output to the overall energy consumed [6], and is a key element in the development of sustainable production systems. In the national context, energy efficiency in manufacturing is a key factor in both retaining competitiveness in Irish industry and meeting strategic Irish government objectives [7,8]. However, it is important to acknowledge that energy efficiency is just one component of the sustainable production paradigm. In particular in the manufacturing context, there is a need for the integration of all sustainable production methods and tools including end of pipe approaches and prevention methods [9]. A longer term vision for sustainable production may encompass concepts such as industrial ecosystems [9] and closed loop manufacturing systems [10].

1.2 Pneumatics in automated manufacturing

In terms of automation and material handling, fluid power devices are used to move, position and clamp components, assemblies or other mechanisms on production machines [11]. Pneumatic systems refer to systems where the transmission of power is achieved through the use of a compressed gas. Since compressed air is the most commonly used gas, it has become synonymous with the term pneumatics [12,13]. In modern manufacturing pneumatic devices are widely used in conjunction with digital controllers, electrically operated valves and sensors, to automate production processes, but also significantly, for process control operations such as cleaning, cooling and drying. Additionally the availability of force and motion controllable servo-pneumatic systems, with performance similar to that associated with electric servo-systems, has extended the functionality and capability of pneumatic systems further [14]. Recent research has investigated the potential for pneumatics in advanced robotics with particular focus on robot teleoperation and haptic interface based applications, such as Exoskeletons and serpentine mobile robots [15-17]. The general application range for pneumatic actuators in terms of force and motion requirements is shown in figure 1.1 and indicates a wide range of applicability.

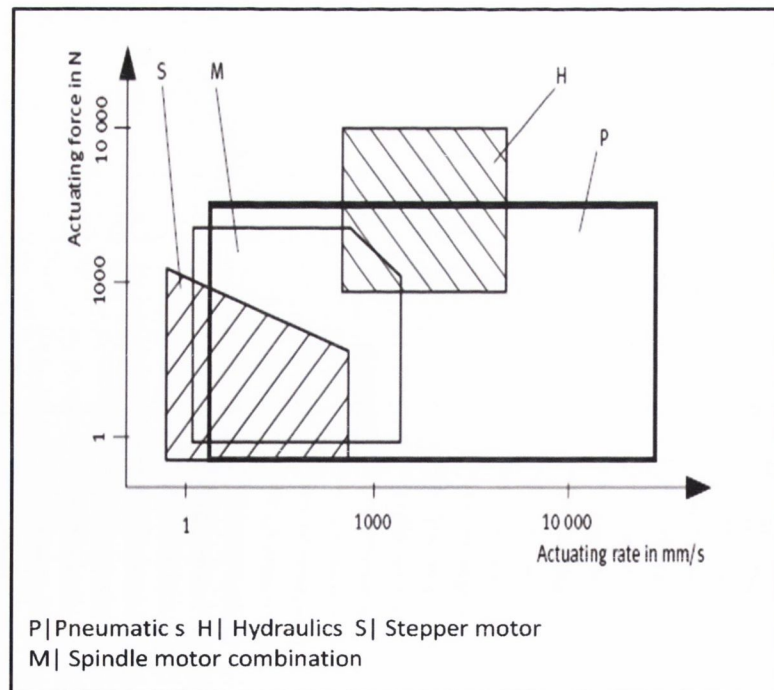


Figure 1.1: Application range for pneumatic drives [18]

The choice of actuation type for any machine (electrical, pneumatic or hydraulic) is driven by a combination of factors including speed, stroke length, load rating, duty cycle, accuracy, operating life, the requirement for multi-positional movement and cost [11]. There are a large number of advantages that ensure the use of pneumatics in most industrial facilities. These include low acquisition cost, long life time and rapid point to point positioning, which enables production machines to achieve high cycle rates. Pneumatic actuators have excellent power to weight ratios and since they do not overheat or generate sparks are very suitable for hazardous environments. Compressed air is safe, clean, poses no health hazard, and is a well established medium for converting pressure to force and translational displacement [13]. Pneumatic energy is easily stored and there is no requirement for the return lines associated with hydraulic systems. Unlike electromagnetic actuators, the pneumatic type can be directly coupled to a payload without the need for transmission, and is naturally compliant due to the compressibility of air. This compliance is beneficial when personnel must be inside the work envelope of the machine [19] or for mobile robots, where propulsion depends on optimal traction between propulsion elements and arbitrarily shaped environments [17]. Additionally the compliance is adjustable via pressure regulation. Finally pneumatic actuators can stall in extended positions indefinitely with no adverse effects and no additional energy consumption [14,20].

1.3 Challenges in pneumatics

One drawback of pneumatics is its low conversion efficiency, especially in comparison to equivalent electric drives. Conversion efficiency in this case refers to the ability to convert energy from a power source into mechanical work. Compressed air energy is expensive because compressing the air requires large amounts of electrical energy [21]. From an industrial perspective, compressed air is considered the fourth utility after electricity, gas and water. However, it can in fact be more expensive than any other industrial utility [22]. The overall energy efficiency of compressed air systems has been estimated to be between 5% and 15% (figure 1.2) [23,24]. However, since large energy savings are now achievable through heat recovery it is difficult to make general statements

about the true energy efficiency of such systems [13]. A common breakdown of energy usage and losses across the three main compressed air subsystems, generation, distribution and end-use, is shown in figure 1.2.

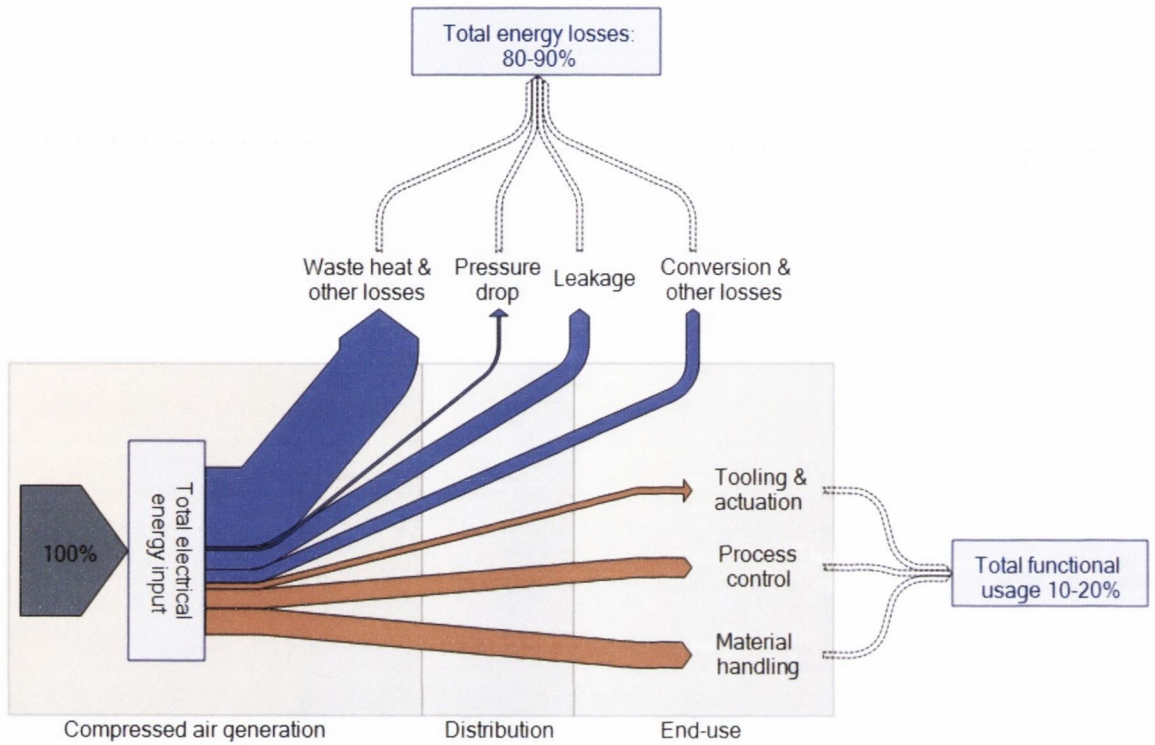


Figure 1.2: Sankey diagram of typical manufacturing CA system energy usage and losses, adapted from Eret et al [25].

The poor energy efficiency of pneumatic systems is important from a policy perspective since the production of compressed air accounts for 10% of the EU’s industrial electricity usage, equivalent to around 80 TWh annually [26]. This figure can be significantly higher for many manufacturing facilities where compressed air can account for, in some cases, 60% to 70% of total plant electrical energy consumption [27]. In general, energy costs can account for up to 75% of total ownership costs for pneumatic equipment [28,29]. With the adoption of life cycle cost metrics by OEMs, and the introduction of competitively priced electrically driven linear drive, energy efficiency is now also a strategic imperative for pneumatic suppliers to maintain competitiveness [11,20].

1.4 Research focus

Research in pneumatics employs a macroscopic view for the design and control of circuits and systems. Unlike in traditional fluid mechanics, phenomenon such as boundary layers, shock waves and velocity profiles are only considered qualitatively [30]. Most analysis of pneumatic devices utilises a lumped parameter approach so that one-dimensional flow and total differential equation formulae can be used for modelling and simulation purposes [13,30]. The air consumers of a pneumatic system are classified into two categories: active and passive [31]. Passive consumers refer to pneumatic devices such as blowers, air knives, nozzles and open pipes that consume air on a continuous basis. Active consumers include linear and rotary cylinders that draw pressurised air on a periodical basis and typically for a short duration.

The traditional focus for energy saving tends to be on generation of compressed air, since the direct consumer of electricity is the compressor and support equipment. In general in many production facilities compressed air is considered solely the responsibility of the technical building services department [26]. The energy efficiency of end consumers, the pneumatic systems embedded in production machines, has not been examined as extensively as other elements of compressed air systems. A reduction in end use, however, has the potential for a cascading energy saving effect, since losses are also reduced in generation and distribution.

The optimisation of energy usage must typically be balanced with sometimes competing objectives such as cycle time and capital costs. Therefore any air consumption minimisation strategy must consider the overall objective of the individual pneumatic drive or system, e.g. to move a specific mass along a specific stroke within a specified time [32,33]. Since constraints such as stroke time and final holding force must be considered, a full understanding of the system dynamics is necessary [33]. It is envisaged that scientific process models of pneumatic systems will form the basis for future energy optimisation through model based design and control. The modelling approach taken in this thesis considers both individual pneumatic components and systems of devices. In particular, passive consumers are considered in addition to active, since in many cases air knives and

nozzles on a machine can account for the majority of air energy usage, as shown in figure 1.2.

1.5 Scope & aim of research

The goal of the present research is to explore the dynamics, and in particular the consumption characteristics of pneumatic production systems. The objectives of the project may be stated as:

- To characterise compressed air usage and efficiency of an industrial production system and to investigate the state of art in energy optimisation methods and technology.
- To develop, and experimentally verify, dynamic models for both individual pneumatic drives and systems containing a multitude of pneumatic devices.
- To identify the flow characteristics of typical pneumatic circuits and assess viability of current identification techniques for industrial systems.

The investigation of machine level compressed air consumption focused on two operational production modules, and involved quantifying non-productive usage and identifying the underlying causes for such usage.

Two types of models were developed, the first a dynamics model of pneumatic drive, the second a consumption model for pneumatic system. All models were developed in the Matlab-Simulink software environment. Both are hybrid due to the discrete and continuous elements of any electro-pneumatic system. The first model takes a traditional approach to modelling the dynamics of an individual pneumatic drive system, consisting of cylinder-valve combinations, from first principles. The second consumption model employs simplified consumption equations and is interfaced with a programmable logic controller (PLC) to provide a dynamic consumption model suitable for industrial type pneumatic systems. The practicality of these models for use on full size production machines is discussed.

In order to validate the developed models an experimental rig was constructed and tested. The rig was designed to represent a typical electro-pneumatic system on an automated production machine, and consisted of a range of pneumatic consumers

including linear cylinders and air knives. Current parameter identification methods were assessed in terms of their practicality for use in industrial environments. The current identification techniques, described in ISO6358 standard for individual pneumatic components, were assessed with a view to their use on extended pneumatic circuits, with multiple devices in various configurations.

2. Literature Review

2.1 Manufacturing Systems and Pneumatic Technology

2.1.1 Production paradigms

The evolution of manufacturing paradigms has been driven by market conditions and society needs (i.e. NEST context changes) and realised through the development of enabling technology and processes [1,34]. At present the dominant production paradigm is one of mass customisation and personalisation, and is driven by consumer requirements for lower prices, customisation and innovation [34]. The paradigm is enabled by integration of state of art information technology and re-configurable manufacturing system (RMS) processes. RMS processes are developed such that production capacity is adaptable in order to respond rapidly to market demand.

It is widely theorised that environmental, economic and societal concerns will lead to the development of a sustainable production paradigm [1,3,4,35-37]. Sustainable production means that products are designed, produced, distributed, used and disposed with minimal environmental and occupational health damage, and with minimal use of resources; materials and energy [35]. The term is often used interchangeably with Environmentally Benign Manufacturing [4] and Environmentally Conscious Manufacturing [3]. The concept of Low Carbon Manufacturing is more specific and focuses on the carbon dioxide emissions resulting from energy usage [37]. The use of a Carbon Emissions Signature (CES) is a specific example of a structured LCM methodology that can account for CO₂ emissions in any system that uses an electric power grid [38].

A future vision for manufacturing, presented by Westkamper consists of processes characterised by distributed simultaneous development, virtual engineering, networked production and intelligent production systems [39]. This process will be enabled by three specific elements: 1/ Technical Intelligence 2/ Digital and virtual engineering tools 3/ Communication technology [39].

Technical intelligence refers to the ability of technological products to adapt themselves autonomously and in a situation dependant manner to ambient environmental

conditions. This is possible through mechatronic product developments. That is, products containing mechanical, electronic and software-based components as well as sensors and actuators that provides a machine with limited ability to adapt automatically to environmental conditions [39]. Specifically, this means that machines will be able effectively compensate for all system-based influences autonomously and adapt automatically to take account of prevailing conditions [39]. This concept is illustrated in figure 2.1.

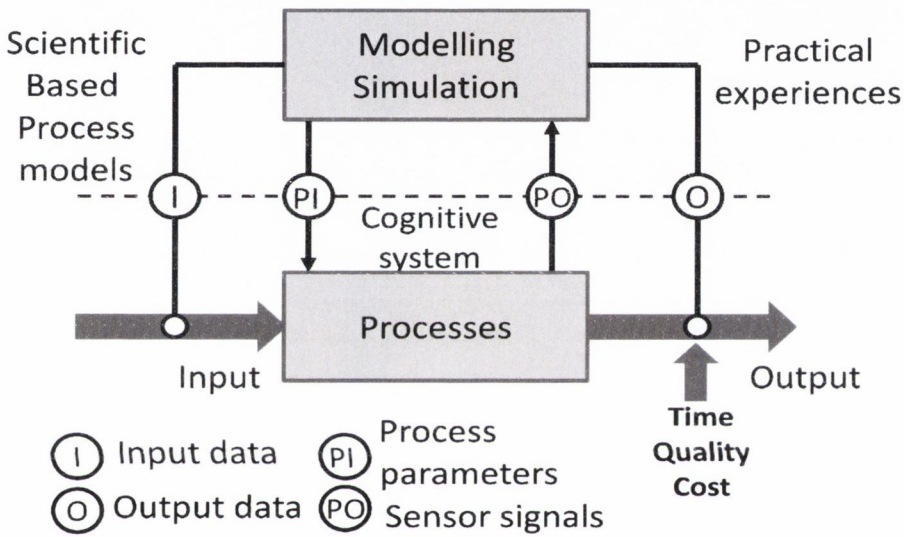


Figure 2.1: Technical intelligence [40]

Autodidactic software will play a key role in allowing machines to learn their own response characteristics and using this information to plan future process steps (e.g. correlations between parameter settings and quality). Sensors and integrated measuring technology will also play an important role in providing real-time process control capability. Due to the large number of features to be recorded simultaneously, solutions will most likely be based on multiple sensors [39]. Virtual engineering involves the design, development, modelling and analysis of prototypes on a computer, eliminating the need for physical prototypes [39]. This process will be enabled by the use of information technology methods such as process modelling and simulation to depict the physical properties of machines and processes and analyse the effects of varying parameters [39]. Finally the use of communication technology will be essential in the integration of

applications including the deployment of remote monitoring and control capability for machines in multiple locations.

Productivity, customisation and agility improvements are the key drivers in the transformation of production processes and paradigms [34]. In industrial engineering productivity is generally defined as the relation of output to input in the manufacturing transformation process [41]. In contrast, efficiency is strongly connected to the utilisation of resources and mainly affects the inputs of the productivity ratio [41] i.e. efficiency is only one aspect of productivity.

<i>Production drivers</i>	<i>Enabler</i>
Productivity	Fixed automation Programmable automation
Customisation	Flexible automation Lean production Computer Integrated Manufacturing
Agility	Virtual enterprise Holonc manufacturing Reconfigurable manufacturing Service manufacturing

Table 2.1: Production paradigm drivers and corresponding enabler technology, adapted from Jovane et al [34]

2.1.2 Manufacturing automation

It is clear from table 2.1 that automation is one of the key technological enablers in the development of production technology. Automation refers to the machine driven execution or implementation of a process. Fixed automation is defined as a system in which the sequence of processing or assembly operations is fixed by the equipment configuration. Examples include machine transfer lines and automated assembly systems that are used in high volume production. Programmable automation involves equipping production systems with the capability to change the sequence of operations to

accommodate different product configurations. The operation sequence is controlled by a program (coded instructions or algorithm) that can be changed for each new product. Typically, the scale of production volume with programmable systems is comparatively less than the equivalent for fixed automation. Flexible automation is an extension of programmable automation. Flexible automated systems possess the capability to produce a variety of parts with virtually no time lost for product changeovers. This is possible as the differences in the parts processed by the system are not significant [42]. Each type of automated system with its corresponding output volume and product variety is illustrated in figure 2.2.

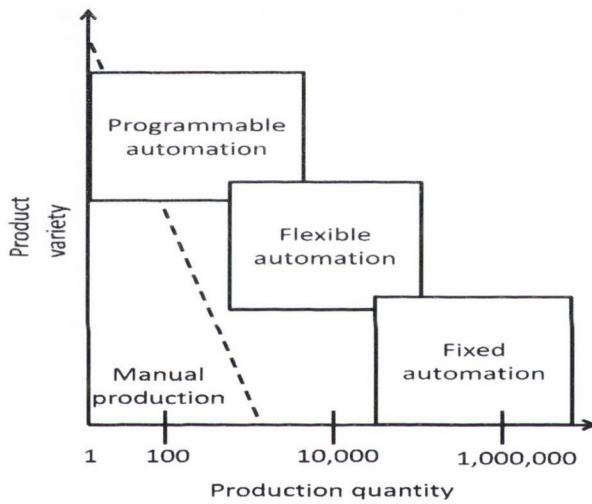


Figure 2.2: Types of automation relative to production quantity and product variety [42]

Reconfigurable Manufacturing Systems are a relatively new class of system that are designed to combine the high throughput of dedicated manufacturing lines with the flexibility of flexible manufacturing systems, but also able to react to changes quickly and efficiently [43]. This concept is enabled through the development of reconfigurable machine tools whereby new machine components, such as spindle or axis, can be added to the machine depending on new product requirements [44]. Computer Integrated Manufacturing (CIM) is a broad paradigm involving the extensive use of computer systems within manufacturing firms [45]. Automation solutions that can integrate all factory

levels, from machine controls to shop-floor supervision and production planning, will be essential in the future development of automated manufacturing systems [46].

Pneumatic applications

Pneumatics plays a major role in mechanisation and automation of production, and material handling [18]. For example, many of the material handling functions shown in figure 2.3 are performed by pneumatic or electro-pneumatic systems. Pneumatics has universal applications in automation; handling of work pieces, packaging and assembly but also for process control, conveying, metal forming and stamping operations [47]. Some specific applications for pneumatics in the production context are shown in table 2.2. The development of servo-pneumatic drives has expanded the application potential of pneumatics further to flexible and reconfigurable type automated machines.

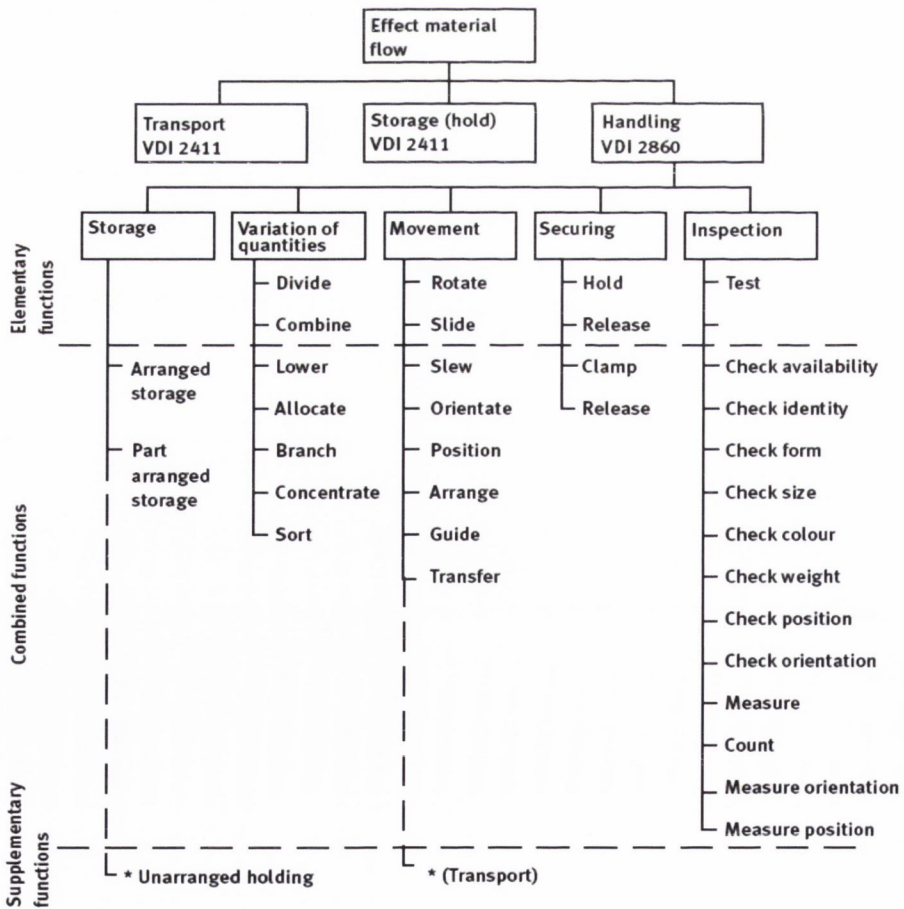


Figure 2.3: Structure and subdivision of the material handling function [48]

<i>Application</i>	<i>Enabling pneumatic devices</i>
Machine tooling	Linear cylinders
Instrument control	Semi-rotary actuators
Process air (cooling, drying et cetera)	Air motors
Cleaning & purging	Grippers
Paint spraying	Positioning valves
Air gauging	Screwdrivers
	Nutrunners
	Grinders
	Air bearings
	Vacuum generators (venturi)
	Air nozzles/knives/ guns
	Open pipes
	AODD pumps

Table 2.2: Application examples for pneumatics in production

Most modern automation systems are electro-pneumatic such that the power section is pneumatic but the signal control section consists of electrical components. The directional control valves form the interface between the signal control and power sections and control the motion of the actuator. Signal control is implemented with Programmable Logic Controllers (PLC) in most industrial facilities, and the position of the piston is reported by proximity switches on the actuator [12]. The control function of most pneumatic systems is open loop so that the control valve is simplified to binary mode (on-off) operation and mechanical stops provide the required positive positioning action. The simplest form of positioning control uses a mid-position cylinder switch [12]. When the PLC receives the input, it signals the control valve to block the air flow to the cylinder. This system combined with a brake can be used to stop a horizontally mounted piston at medium speed to within $\pm 1\text{-}2\text{mm}$ [12]. However if any changes occur in the load, friction, pressure or leakage, then repeatability will be lost.

Closed loop servo-pneumatic systems continuously monitor feedback from sensors to control the position or force output of an actuator. Their development has been driven to an extent by their potential for certain robotic applications. For example, applications such as teleoperation master arms with gravitational compensation, require long duration static high force output [15]. Pneumatic actuation is considered a better alternative for such applications, since direct drive electrical actuators necessitate special cooling systems to dissipate the excessive heat [15]. The main elements of both electro-pneumatic and servo-pneumatic systems are illustrated in figure 2.4.

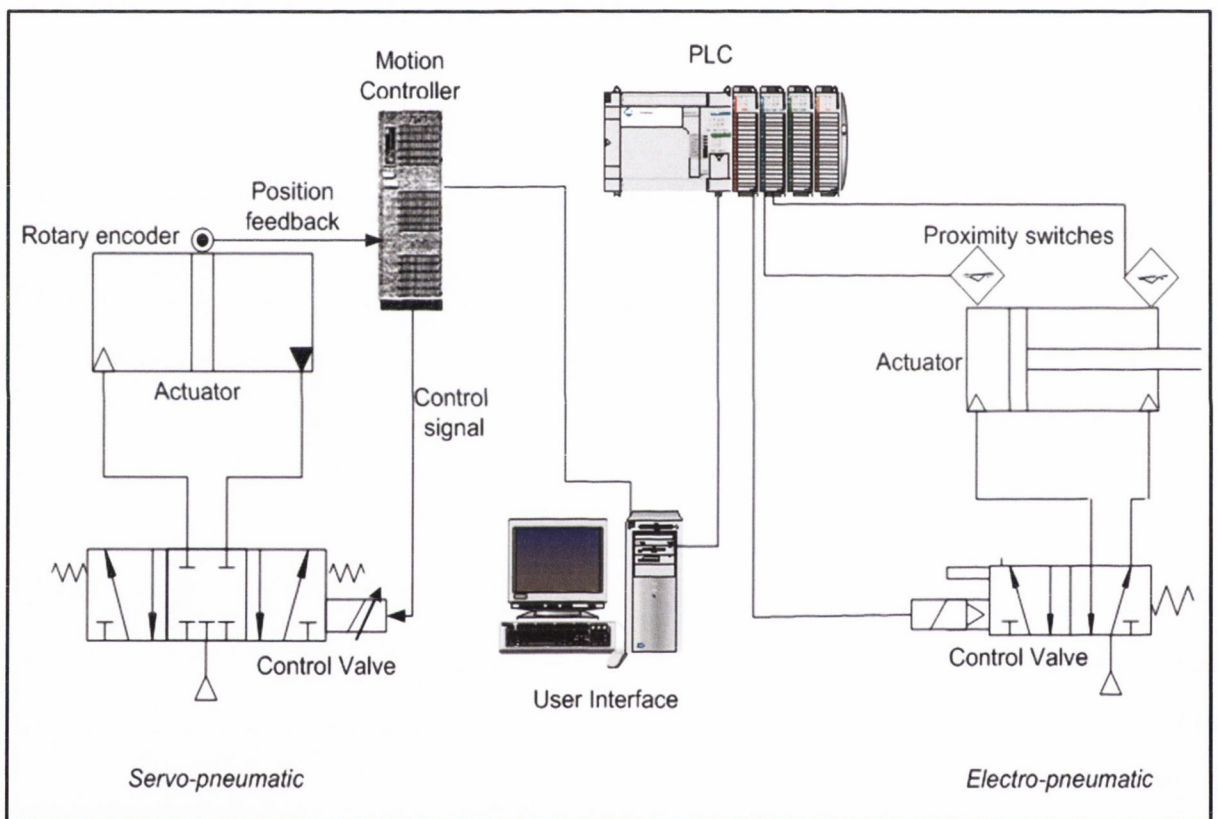


Figure 2.4: Components of a electro-pneumatic and servo-pneumatic actuator systems adapted from [14]

Servo-pneumatic actuator technology is particularly suited for linear motion as no transmission mechanism is normally needed, and in the manufacturing context have found applications in automated assembly systems where their high speed and precision can be utilised effectively [14]. Other production applications include force-controlled pressing of

work pieces and automated handling tasks [49]. The typical static position accuracy of purchasable servo-pneumatic drives is about 0.2mm [49].

Interoperability of manufacturing systems

In order to realise a totally integrated and automated factory there needs to be communication between all levels of plant information systems, from top level Enterprise Resource Planning (ERP) systems to lower automation levels [50]. While there has been extensive work on the development of individually optimised manufacturing systems, for example machine tool design, process planning optimisation, intelligent control, there is a need for increased interoperability and communication between the different system types [51].

In general connectivity, the ability of multiple disparate devices to communicate, is a key driver of industrial automation allowing further integration of process, factory and business management levels (figure 2.5). The use of standardised interfaces for machine enhances integration and interoperability, thereby improving coordination and optimisation capabilities. The OPC data exchange protocol is discussed in appendix A.

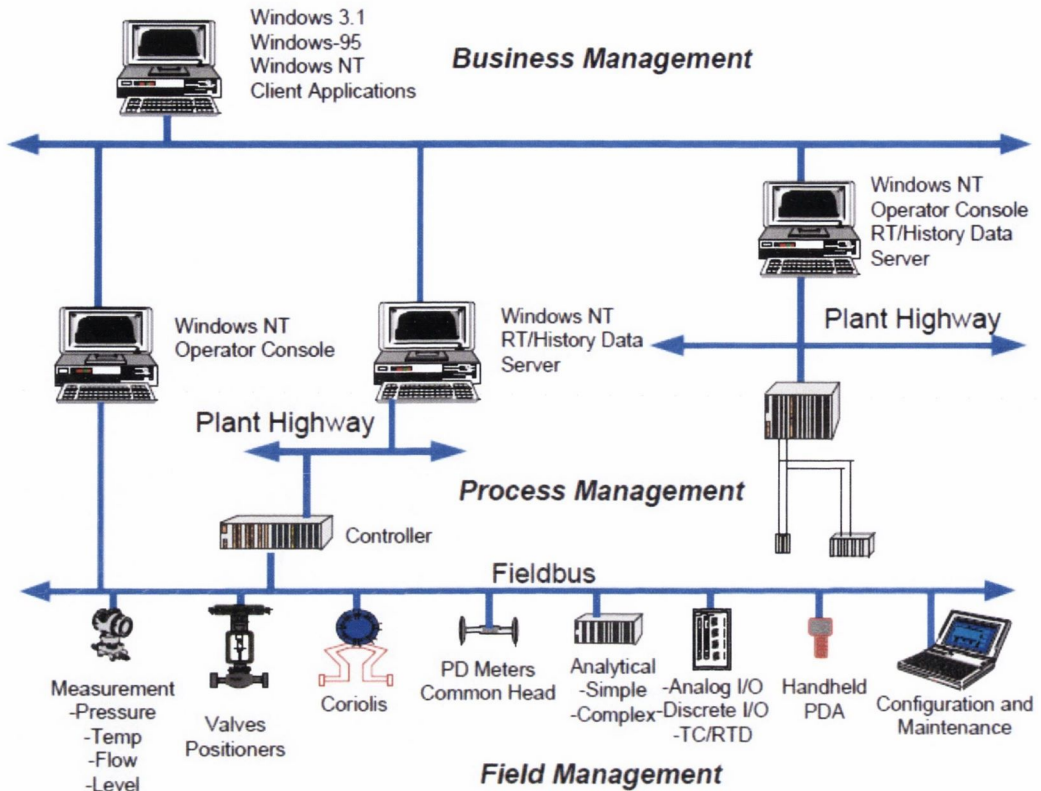


Figure 2.5: Process control information architecture [52]

2.1.3 Manufacturing energy usage and efficiency

Energy is a key enabler in the manufacturing process. As modern manufacturing processes are usually highly automated, this entails that in addition to the energy requirements for the primary function of the process, machining, forming, assembly, there is also significant energy requirements for support operations such as work handling, lubrication, material removal and tool condition sensor systems [53]. In fact, as the primary process energy consumption is dependant or proportional to the quantity of material being processed, some equipment's specific electrical energy requirements can be dominated by support features [53]. Evidence from Toyota Motor Corporation demonstrates that up to 85.2% of the energy consumed by a machining process can be used in non-machining operations which are not directly related to the production of parts (figure 2.6). The machining centre in question was part of an automated mass production line, inclusive of support equipment such as lubrication and chip recovery [4]. Further work by Dahmus and Gutowski characterising the breakdown of energy usage in

machining [54,55] indicates that even for smaller, less automated, low throughput type systems (including manual machines) between 30% to 50% of energy is consumed by auxiliary equipment. Actual machining energy consumption is variable and dependant on working conditions while the energy usage of support equipment is typically constant. These results imply that while the specific energy consumption per product can be significantly lower for highly automated, mass production systems due to economies of scale, a major percentage of the energy consumed is required by non value add processes.

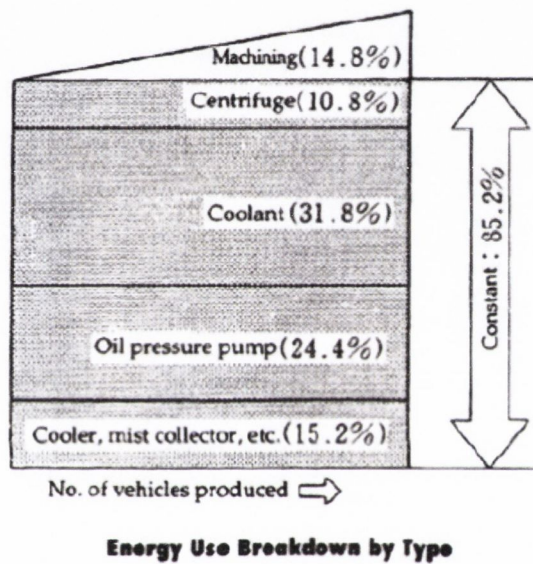


Figure 2.6: Energy used as a function of production rate for an automobile production machining line [4]

This entails that machine state operating characteristics (shutdown and start up capabilities) should be targeted to ensure stable and efficient state changeovers during non-operational periods i.e. idling and other machine downtime. A substantial energy consumption is involved in the starting up and maintaining many equipment sets in a 'ready' position [53]. Therefore two strategies are suggested for minimising energy usage in manufacturing processes; 1/ the redesign of support equipment and 2/ an increase in the processing rate of a machine's primary function [53]. However, it is also noted that the integration of support equipment is usually done precisely to increase throughput rates. Therefore any decisions made with the objective of reducing energy usage must be based

on careful analysis of the total specific energy cost per unit of product, inclusive of primary and support function energy requirements. The consumption of compressed air and associated energy costs has not been considered.

2.1.4 Pneumatic and compressed air systems

Compressed air is an essential energy source and is considered the fourth industrial utility, after electricity, natural gas, and water, in facilitating production activities [22]. Failure of the compressed air system in some industries can shut down the entire manufacturing process [28]. Typical pressure ranges for pneumatic systems are given in figure 2.7. For process control, drives and mobile applications (truck/train brakes) with operating pressures up to 20 bar, the ideal gas law is valid. In the pressure range of 0.1 MPa to 10MPa and temperature range of 200K to 800K, the error between calculated density and relevant tabulated (measured) data is less than 5% [13]. However, for aerospace applications where very high pressure exhaust gas is utilised for hot gas servomotors, alternative laws are required [13,56].

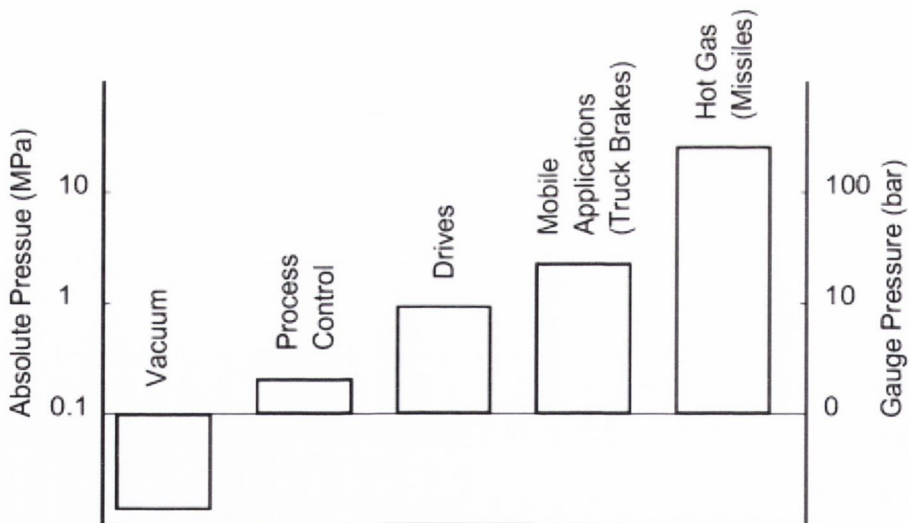


Figure 2.7: Pressure ranges of pneumatic systems [13]

2.1.4.1 Historical perspective

The term pneumatics comes from the Greek 'to breath'. The concept of using a compressed gas to transmit power is very old. Heron of Alexandria is reported to have developed automatic temple doors with the use of hot air [13]. During the industrial revolution, circa 1888, a large scale compressor plant was installed in Paris to supply the city with compressed air, which was used to power clocks, elevators and other industrial equipment [57]. However, the modern industrial application for pneumatics began around the 1950's with the demand for automation of production processes and the availability of suitable elastomeric materials for valve and piston seals [13]. Shearer [58] is widely credited with the original development of an analytical model for pneumatic processes, that forms the basis for modern servo-pneumatic research and technology [13,56].

2.1.4.2 Compressed air system hardware

An extensive infrastructure is required to supply the pneumatic systems with an energy source. Compressed air systems consist of a supply side, transmission and demand side. The supply side refers to the generation, treatment and storage of compressed air, and consists of the compressor, air receiver, dryer, filters and drains [59-68]. Typically, in industrial facilities the compressed air production and treatment occurs at a centralised plant. The transmission usually consists of a ring main with multiple dropdown points serving various production areas. The demand side refers to the production equipment that consume pressurised air in operation (i.e. actuators in machines), and also includes air preparation and control. The layout for a compressed air system, excluding the demand side, is illustrated in figure 2.8.

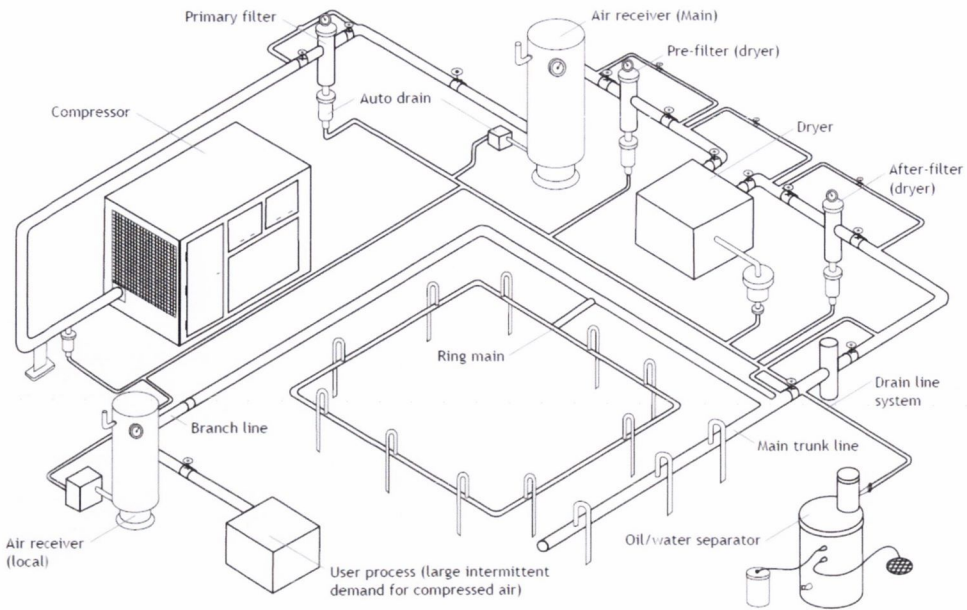


Figure 2.8: Compressed air system layout [24]

2.1.4.3 Pneumatic system hardware

Modern electro-pneumatic systems consist of actuators and valves which provide power and control capability to machines. Valves fulfil a number of functions such as signalling, to trigger another event, power/direction control and flow and pressure control [12]. Pneumatic valves can be divided into three main categories: directional control, flow control and pressure control and further divided into valves that control airflow for power or control functions.

Fluid control valves and air preparation

Fixed restrictions which have a constant area are usually called orifices and variable restrictions are called valves. A capillary is a long thin tube and it is distinguished from orifices by the fact that the main resistance to flow is wall friction rather than gas momentum [30]. Note the rounding of the entrance turns the orifice into a nozzle [30].

Regulating valves are employed in compressed air systems in order to ensure that the pressure in the system is not exceeded. This is important from both a safety and functionality point of view. Most pneumatic components have a maximum operating pressure, which if exceeded can cause damage, in the form of stressed parts. Secondly it

allows parts of the system to operate at a lower pressure than the main supply. As air is generated at higher pressures (usually 7 to 8 bar in a typical plant), regulators can be used to step down the pressure locally to provide the requirements of lower pressure applications. Unregulated or improper pressure settings can increase compressed air demand, resulting in higher energy consumption [67].

There are various types of regulating valves, the most common types being pressure reducing valves, pressure relief valves and safety valves. Pressure relief valves limit maximum system pressure by exhausting fluid when the system exceeds a preset value. Similarly safety valves protect the system from over pressurisation, in this case in the event of a component malfunction. The valve opens, to exhaust fluid, when the system pressure exceeds design pressure by a selected amount [69].

Pressure reducing valves, also known as pressure regulators, reduces a high variable primary pressure to a lower secondary pressure; it measures and corrects deviations in pressure [69]. The regulator works by maintaining a pressure balance across a piston or diaphragm (figure 2.9) [12]. A bleed valve is usually included, so that if secondary pressure exceeds the setting of the valve, excess pressure can be vented. Pressure droop refers to the drop in output pressure with increased flow through a regulator [13,67]. In addition to pressure droop, there can be considerable hysteresis i.e. a different pressure for the same flow rate depending on whether the flow rate has been increasing or decreasing [13].

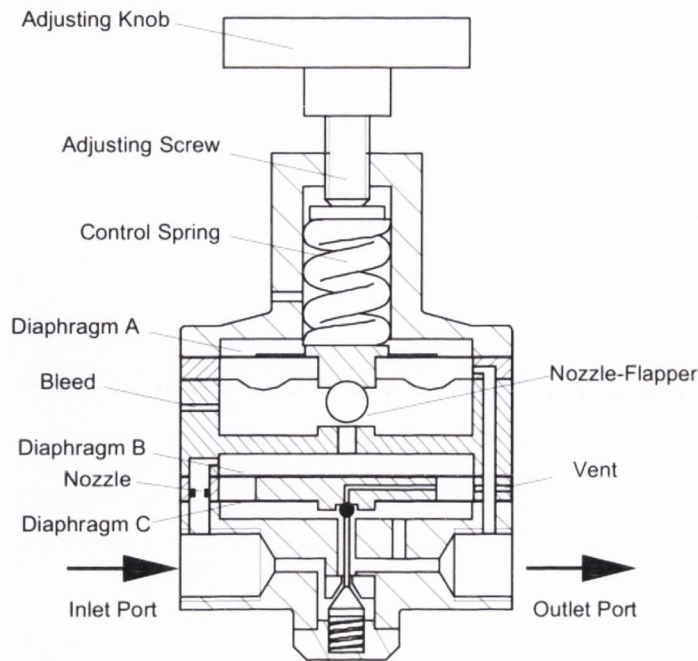


Figure 2.9: Cross-sectional view of precision pressure reducing valve [13]

Filters and regulators are widely available from manufacturers as compact modular or combination units [68]. The filter is installed upstream of the regulator to protect it from any dirt or water in the compressed air [67]. Lubrication of compressed air is required before some power applications, such as cylinders, air motors and other high speed applications, in order to reduce friction and allow pneumatic components to operate effectively [68]. Typically high grade oil is used for this purpose [12]. The oil is delivered, in the form of atomised droplets, into a high speed air flow that is created by passing the air across a nozzle. The air is accelerated through the nozzle and its pressure reduced, thus drawing up the oil (venturi effect). Typically filters, pressure regulators and lubricators are combined into a single bank, called a FRL (Filter, regulator, lubricator) bank, to prepare the compressed air before its final application. The lubricator is located downstream of the filter and regulator [68]. However, the trend in modern pneumatic systems is to use unlubricated air and components, cylinders and valves, that are lubricated for life [68].

Directional control valves are used to control the direction of flow between components in a pneumatic circuit. They are distinguished by the number of ports, number of switching positions, internal design and type of operation [13]. Some typical

valves and their symbols are shown in figure 2.10. For cylinder drives 5/2 valves are often used. Due to their internal resistance, the control valves throttle airflow [13].

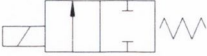




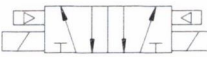

Symbol	Name/Description
	2/2-way valve NC, direct electrically operated
	3/2 Valve NC, electrically operated with pilot valve
	3/2 Valve NO, electrically operated
	4/2 Valve, mechanically operated
	5/2 Valve, electrically operated, monstable
	5/2 Valve, electrically operated, bistable
	5/3 Valve, pneumatically operated

Figure 2.10: Typical configurations of directional control valves [13]

Flow control is achieved by a sliding spool that opens or blocks passages between ports. Other designs use poppets or diaphragms, in particular for 2/2 and 3/2 valves. Failure of the valve is now defined as unacceptable leakage, as opposed to the previous definition as failure to function [13]. Lapped spool valves consist of steel spools in steel housings, and require no seals. This type of design offers low friction and thus longer comparative service life of more than 200 million switching cycles [13]. However, a drawback of the lapped spool type valve is that it is not completely leak free. The alternative valves with elastomeric seals have a life of approximately 50 million switching cycles but are completely leak free and have lower internal resistance [13].

Typically, directional control valves work in binary mode where the flow path is either completely open or closed. However, using a pulse-modulated voltage, direct acting valves can be used as nozzles with variable conductance [13]. The effective conductance of the valve is then given by the relative duty, the ratio between the time the voltage is on to off [13]. The solenoid is the device that converts an electric current (signal output from

controller) to a force which opens or closes a flow path in a valve [13]. Proportional solenoids are used in proportional directional control valves to generate a force that is ideally proportional to the electric DC current and independent of the stroke of the armature [13]. Proportional pressure control valves are also available and can be used for force and torque control applications [14].

Non-return or check valves allow almost unrestricted flow of air on one direction while blocking it in the opposite direction. Throttling valves are used to control flow rate and consist of an adjustable needle with tapered nose, that is used to throttle air flow by reducing the cross-sectional area of the flow path [13]. A one way flow control valve contains a throttle valve and non-return valve so that free flow is allowed in one direction and controlled flow in the other. These valves are often used for the speed control of pneumatic cylinders. Note for both flow directions there is an influence of the setting of the needle [13].

Actuators

Actuators convert pneumatic energy to mechanical work [13]. They provide the motive force in pneumatic systems by moving, clamping or vibrating some sort of output device. Pneumatic cylinders are the most commonly found actuator [69], however there is wide range of different types including grippers, rotary actuators and vane actuators. A single acting cylinder (figure 2.8) uses compressed air in one direction of operation and an internally mounted mechanical spring in the other. Most single acting cylinders are in the small bore and light duty model ranges [13]. Typical examples are stopper cylinders used to stop a pallet on a conveyor. A double acting cylinder (figure 2.11) uses compressed air to extend and retract, making them suitable for work in both directions [12]. The force exerted by the cylinder is determined by the effective surface area and the pressure acting on the piston. The thrust for the return stroke is reduced due to cross sectional area of the piston rod which means the effective surface area is smaller. Frictional losses must also be accounted for [12]. The minimum velocity where the piston moves without sticking and slipping will depend on the load [13]. Double acting single rod cylinders, with bore range of 8 to 25mm, are standardised in ISO6432 [70].

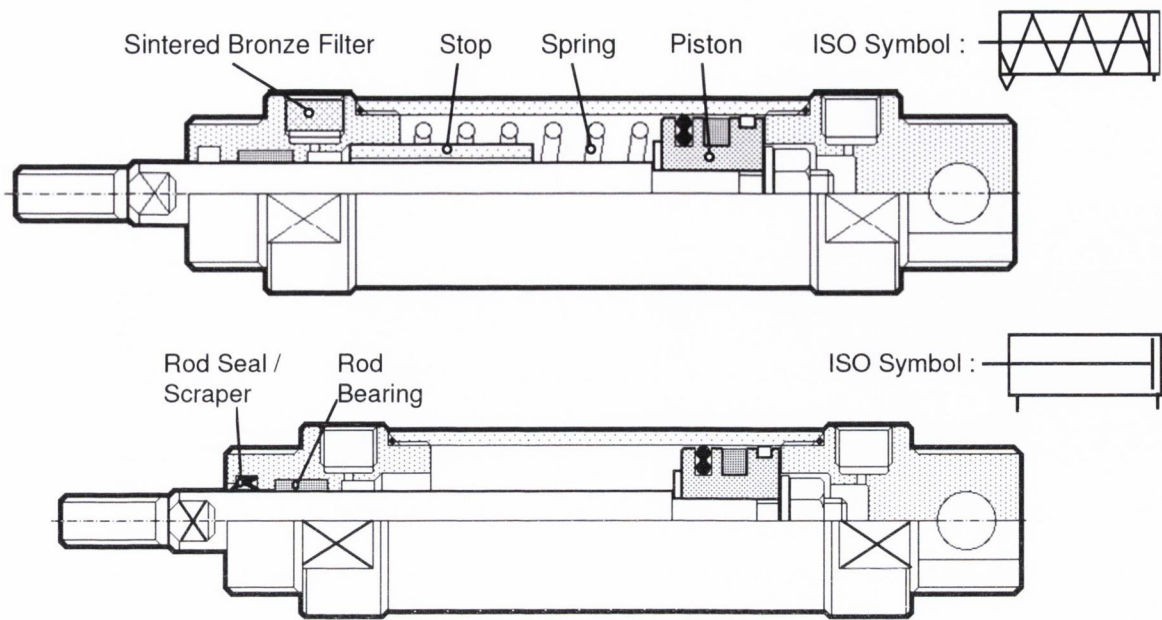


Figure 2.11: Single and double acting cylinders with ISO symbols [71]

Pneumatic cylinders are well suited to rapidly accelerate a mass to a high speed, however at the end of the cylinder stroke, the mass must be decelerated gently to avoid damage and noise [13]. This is achieved through fixed cushioning with shock absorbing pads or for larger cylinders industrial shock absorbers are often used. Adjustable cushioning is suited for some applications [13].

2.2 Modelling and Analysis of pneumatic systems

2.2.1 Overview

Accurate models are of crucial importance in the design of pneumatic drive systems, and also for control and maintenance purposes. In industrial design practise, steady state assumptions are often used for component sizing problems e.g. drive needs to perform automation task with desired speed, force and accuracy [49]. However, this procedure fails if there is significant non-linearity in the system. Therefore there is a move towards more systematic design/sizing processes that are based on dynamic models of the pneumatic

drive system [49]. With regard to control, there are two main tasks to solve when dealing with pneumatic servo systems: modelling of the system and synthesis of a suitable control law [72]. In developing a controller however, there exists an additional trade-off between accuracy of the model and its suitability/complexity for online implementation [73]. Finally such models are now also being used in the condition monitoring of pneumatic production systems found in industry [74].

The development of a mathematical model for a pneumatic drive system (figure 2.12) involves three major considerations [56]:

1. The determination of mass flow rate through a pneumatic circuit consisting of directional control valve, fittings and tubing.
2. The determination of pressure, volume and temperature of the air in the actuator chambers.
3. The determination of the dynamics of the load.

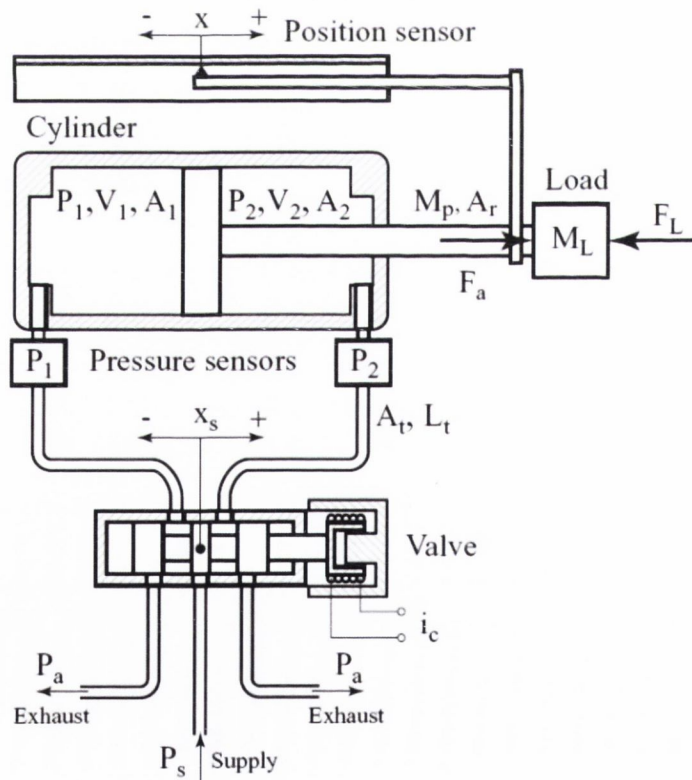


Figure 2.12: Schematic representation of pneumatic actuator system [15]

The combination of the three individual models describes the dynamics of pneumatic subsystems completely. The following sections describe the derivation of the three mathematical models respectively.

2.2.2 Force dynamics models

The load and the friction force can have considerable effect on the dynamic behaviour of a pneumatic actuator, and the accuracy of a system model depends heavily on a good description of those forces [13]. The piston-payload dynamics are modelled using Newton's second law (eq. 2.1). The right hand side of the equation represents the active (applied) force, produced by different pressures acting on opposite sides of the piston [15]. The moving mass includes both the payload mass and the mass of the piston and rod assembly. The external load force F_L is zero for horizontal orientation but for any other orientation the external force must be accounted for (e.g. for vertical orientation, $F_L = mg$). Additionally for asymmetric cylinders, the load dynamics model can be improved further by considering the difference in active area of the piston due to the rod [15].

$$(M_L + M_p)\ddot{y} + F_L + F_f = P_1A_1 - P_2A_2 - P_aA_r \quad (2.1)$$

Friction is perhaps the most important nonlinearity that is found in any mechanical system with moving parts [75]. It occurs in pneumatic cylinders because a sliding piston seal has to push outwards against the sliding surface with enough force to prevent compressed air from escaping from the cylinder [13]. The total (internal) friction force is considered the sum of the friction forces at the seals of the piston and rod cover [76].

Friction forces in pneumatic cylinders depend on cylinder characteristics such as piston diameter and type of seals, and operating conditions such as the relative pressures acting on the seals, temperature and velocity [13,76]. Belforte et al have been shown experimentally that friction force varies according to piston position and among cylinders of the same specification [76]. This is attributed to tribological factors including the tolerance between cylinder barrel and seals, roughness of cylinder barrel and amount of

lubricant. Additionally the piston rod seal act differently according to direction of motion of the piston [76]. Friction is also a function of time, as it can change over the actuator's life time [77]. Therefore if a good model of the friction is important, the actual values have to be experimentally identified at appropriate operation conditions.

An early friction model suitable for digital simulation is given by equation 2.2 and can be used for pneumatic drives if the influence of the chamber pressure is small (e.g. because the friction forces are dominated by the load) [13]. This model is sometimes termed a static stribek curve model [49]. In equation 2.2, δ is an arbitrary exponent.

$$F_f = F_{df} + (F_{sf} - F_{df})e^{\left(-\frac{\dot{y}}{sv}\right)^\delta} + \beta\dot{y} \quad (2.2)$$

The static friction force is the break-away friction force that has to be overcome to begin a relative motion of the piston [13]. Since seals inherently need to exert an outward radial force, the static friction will also depend on the dwell time of the piston i.e. time between movement of the piston [13]. Dynamic friction force occurs when the piston is moving arbitrarily [13]. Simplified rule of thumb equations 2.3 and 2.4 for estimating static and dynamic friction are given by Fleischer [32] (d is bore in mm).

$$F_{\text{static}} = 0.67 \frac{\text{N}}{\text{mm}} \cdot d \quad (2.3)$$

$$F_{\text{dynamic}} = 0.4 \frac{\text{N}}{\text{mm}} \cdot d \quad (2.4)$$

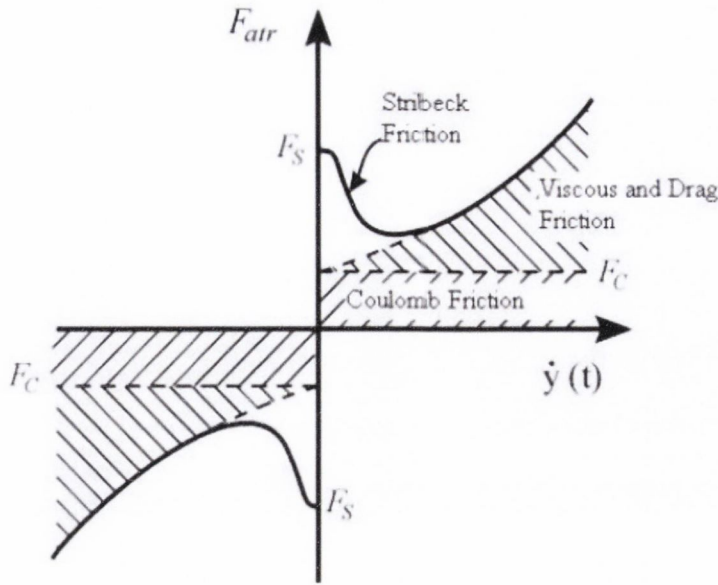


Figure 2.13: Friction force characteristics combined in steady state [78]

Another widely used friction model in the pneumatic literature considers the dynamic friction a combination of coulomb and viscous friction (equation 2.5) [15,79,80]. However, if dealing with low velocity cylinder motion, the Stribeck effect should be included in the friction model (figure 2.13) [81]. Friction in servo-actuators has also been represented by the LuGre model (eq 2.6), though Valdeiro et al have noted it can be difficult to identify the coefficients σ_0 and σ_1 of the model [78].

$$F_f = \beta \dot{y} + F_C \quad (2.5)$$

$$\text{Where } F_C = \begin{cases} F_{sf} & \text{if } \dot{y} = 0 \\ F_{df} \text{ sign}(\dot{y}) & \text{if } \dot{y} \neq 0 \end{cases}$$

$$F_f = \sigma_0 z + \sigma_1 \frac{dz}{dt} + \beta \dot{y} \quad (2.6)$$

A list of proposed mathematical (friction) models and the coefficient of determination of the equations for measured data is presented in figure 2.14. With the exception of model A, they include the pressure difference between cylinder chambers [13]. The coefficient of determination is a measure of the closeness of agreement between measured data points and the corresponding predicted values of a model [82].

Model number	Dynamic friction model	Coefficient of determination
A	$F_f = F_o + c \cdot v$	0.90
B	$F_f = F_o \cdot e^{-\xi v} + c \cdot v + \beta \cdot \Delta p$	0.91
C	$F_f = F_o + c \cdot v + \beta \cdot \Delta p$	0.93
D	$F_f = F_o + (1 + c \cdot v^n) \cdot (\beta \cdot \Delta p + \beta_1 \cdot p_1)$	0.94
E	$F_f = F_o + c \cdot v^n + \beta \cdot \Delta p^m$	0.91
F	$F_f = F_o \cdot e^{-\xi v} + c \cdot v^n + \beta \cdot \Delta p^m$	0.95
G	$F_f = F_o \cdot e^{-\xi v} + c \cdot v + \beta \cdot \Delta p + \beta_2 \cdot p_2$	0.93

Figure 2.14: Empirical friction models [13]

Nouri et al investigated friction forces in a servo-pneumatic actuator system [75]. Experimental results of friction as a function of velocity at different nominal chamber pressures, corresponding to supply pressures of 2 to 7 bar(g), are shown in figure 2.15. The hysteretic behaviour of friction is clearly present and means that the friction force is higher for increasing speed and lower for decreasing speed [75]. This is termed frictional lag. The Stribeck behaviour is well illustrated by the increasing velocity part of the loop and is best modelled by equation 2.2. For decreasing velocity, however, the behaviour seems to resemble best that of Coulomb plus viscous friction (eq 2.5) [75]. In order to model this gross sliding behaviour, a friction model can be fitted for each branch of the hysteresis loop [83]. In this case, a static Stribeck curve can be used for the increasing velocity part of the loop and Coulomb plus viscous friction model for decreasing speed. Hildebrandt et al have noted that the dry friction can be high for pneumatic actuators in comparison to their full theoretical force output [49].

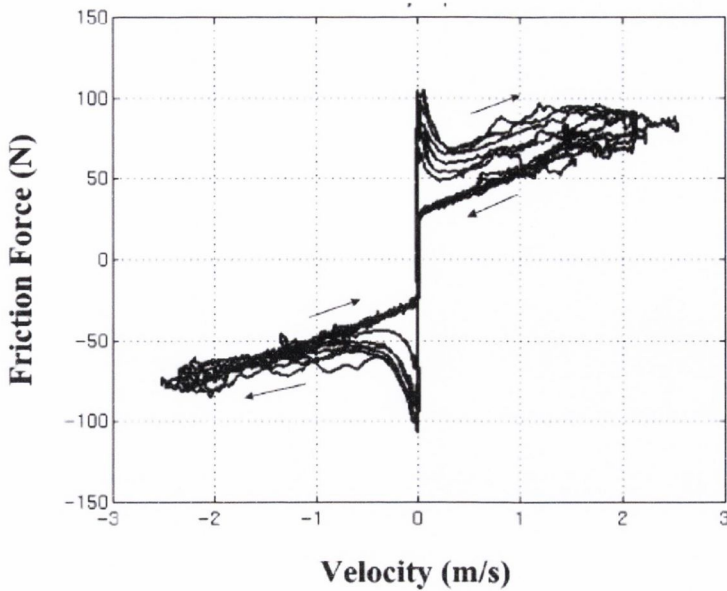


Figure 2.15: Measured velocity dependent friction force in the positive and negative directions, and for different supply pressures [75]

The most comprehensive friction models account for both the gross sliding and pre-sliding or micro slip regimes. In the pre-sliding regime, adhesive forces are dominant such that friction force appears to be a function of displacement rather than velocity [84]. This is because asperity junctions deform elasto-plastically leading to non-linear spring like behaviour [83]. In contrast to classical models where friction force experiences a step jump at the origin, the saturation of pre-sliding force (increase in displacement) leads to gross sliding, in which all asperite junctions have broken apart [83,84]. The Leuven model, developed by Swevers et al, improves the LuGre model further by accounting for nonlocal memory and accommodating arbitrary force-displacement transition curves in pre-sliding friction [84]. Hysteresis behaviour with nonlocal memory is defined as an input-output relationship for which the output at any time instant depends not only on the output at some time instant in the past and the input since then, but also on past extremism values of the input and output as well [84]. Such dynamical models are recommended if highly accurate control via servo-pneumatic mechanisms is necessary [75] but requires additional programming, to implement memory stacks, and identification procedures and equipment, to determine friction forces during micro-sliding (0 to max 0.1/0.2mm).

2.2.3 Thermodynamic actuator models

The mass conservation law and energy conservation law enable the complete description of the dynamic behaviour of the gas in the chamber [85]. The first law of thermodynamics, conservation of energy, can be applied to the control volume to determine pressure and temperature (eq 2.7) [58,86]. The full derivation of the thermodynamic model is presented by Beater [13]. The pressure and temperature dynamics of a single variable volume chamber are described by equations 2.8 and 2.9.

$$\frac{dU}{dt} = dW + dQ + (dm_{out}h_{out} - dm_{in}h_{in}) \quad (2.7)$$

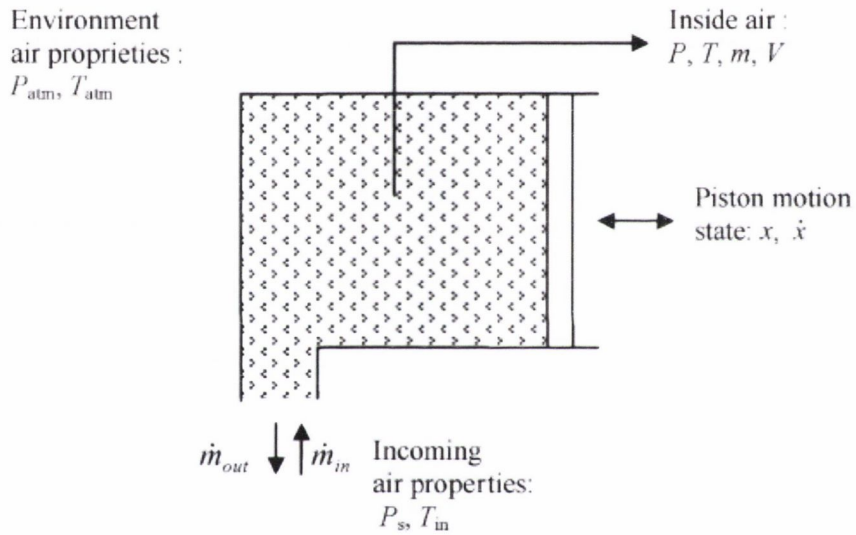


Figure 2.16: Pneumatic cylinder chamber [72]

$$\frac{dP}{dt} = -\gamma \frac{P}{V} \frac{dV}{dt} + \gamma \frac{R}{V} \dot{m}_{in} T_{in} - \gamma \frac{R}{V} \dot{m}_{out} T + \frac{\gamma-1}{V} \frac{dQ}{dt} \quad (2.8)$$

$$\frac{dT}{dt} = \frac{T}{V} \frac{dV}{dt} (1 - \gamma) - \dot{m}_{out} \frac{RT^2}{VP} (\gamma - 1) + \dot{m}_{in} \frac{RT}{VP} (\gamma T_{in} - T) + \frac{(\gamma-1)T}{PV} \frac{dQ}{dt} \quad (2.9)$$

Classical hypotheses used in modelling the heat exchange in pneumatic actuators, rely on the assumption that the heat conductivity of air is much less than the conductivity of the actuator wall material [72,85]. This means the cylinders internal wall temperature is essentially equal to its average temperature [72]. Secondly it is assumed that the thermal

capacitance of the wall material is sufficiently large compared to capacitance of the air, so that average wall temperature is equal to ambient temperature e.g. $T_w = T_{amb}$ [72,85]. Neglecting radiation heat transfer, the heat exchange can be described by a convection heat transfer model (eq 2.10) expressed by Newton's Law of cooling [13,72,85].

$$\frac{dQ}{dt} = \lambda A_q(y)(T_w - T) \quad (2.10)$$

However, since the heat transfer coefficient is difficult to determine and it is known to vary with pressure, temperature and actuator velocity, the most typical solution is to simplify the model by neglecting heat exchange dynamics, and to instead consider a polytropic process with a tuneable index (eq 2.11), ranging from isothermal process ($n=1$) to adiabatic reversible process ($n=1.4$) [30,58,72,79,80]. Equation 2.11 is produced by directly differentiating the ideal gas law ($PV = mRT$).

$$T = T_0 \left(\frac{P}{P_0} \right)^{\frac{n-1}{n}}$$

$$\frac{dP}{dt} = -n \frac{P}{V} \frac{dV}{dt} + n \frac{R}{V} T (\dot{m}_{in} - \dot{m}_{out}) \quad (2.11)$$

In some cases the model is further simplified by neglecting temperature changes with respect to ambient temperature. Note that even though the model (eq 2.12) was deduced assuming a polytropic law, the temperature is fixed at ambient temperature while the polytropic index of pressure dynamics is tuneable [80].

$$T = T_0$$

$$\frac{dP}{dt} = -n \frac{P}{V} \frac{dV}{dt} + n \frac{R}{V} T (\dot{m}_{in} - \dot{m}_{out}) \quad (2.12)$$

However experimental measurements by Otis et al of the temperature inside a pneumatic cylinder during the charging and discharging processes, indicate that the temperature change can be significant (figure 2.17) [87]. Otis et al found the charging process was better approximated using an adiabatic index while discharging was closer to isothermal, though neither predicted the temperature exactly [87]. According to Carneiro

et De Almeida the temperature change is comparatively not as pronounced in servo-pneumatic systems [80].

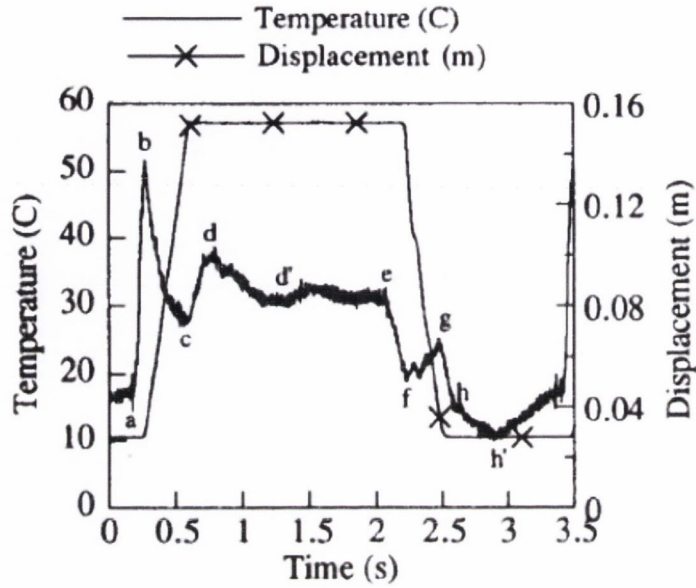


Figure 2.17: Cap-end temperature history during charging and discharging [87]

Based on this experimental evidence, an alternative thermodynamic model (eq 2.13), with different polytropic indexes was developed by Richer et Hurmuzlu [15]. This model uses an adiabatic evolution for the charging process, isothermal for discharging and intermediate ($n=1.2$) polytropic index for movement of the piston [15,80].

$$T = T_0$$

$$\frac{dP}{dt} = -1.2 \frac{P}{V} \frac{dV}{dt} + 1.4 \frac{R}{V} T \dot{m}_{in} - \frac{R}{V} T \dot{m}_{out} \quad (2.13)$$

Despite being used successfully in the past [15] more recent research by Carneiro et De Almeida has shown that this model is not suitable for a wider variety of industrial cylinders [80]. As De Las Heras points out assuming a wrong value for the polytropic index represents an exponential error estimating gas pressure history [88].

Equation 2.14 was developed by Carneiro et De Almeida based on a simplified heat transfer model and provided the best results in terms of balancing performance and

complexity [80]. The simplified heat transfer model 2.17 was achieved by neglecting temperature and pressure changes with regard to their equilibrium values (eq 2.16) and considering an average heat transfer area (eq 2.15) [80].

$$T = T_e \left(\frac{P}{P_e} \right)^{\frac{n-1}{n}}$$

$$\frac{dP}{dt} = -\gamma \frac{P}{V} \frac{dV}{dt} + \gamma \frac{R}{V} T (\dot{m}_{in} - \dot{m}_{out}) + \frac{\gamma-1}{V} k_e (T - T_{amb}) \quad (2.14)$$

$$A_q(av) = A_q(y_e) = \frac{\pi}{2} d^2 + \left| \pi d \left(y_e + \frac{1}{2} \right) \right| \dots y_e = 0 \quad (2.15)$$

$$k_e = \lambda_e A_q(av) \quad (2.16)$$

$$\frac{dQ}{dt} = k_e (T_{amb} - T) \quad (2.17)$$

Equilibrium conditions are defined for servo-valves, when the spool is at central position, temperature in cylinder is steady state and therefore same as ambient temperature, and the leakage mass flows are equal (figure 2.18).

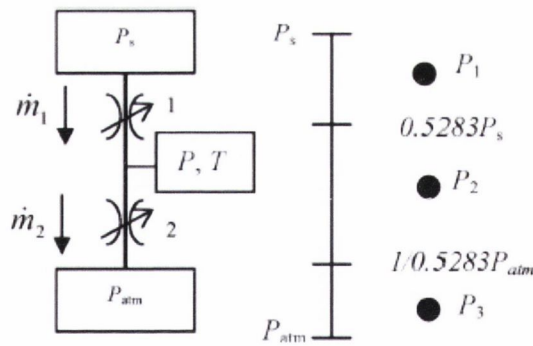


Figure 2.18: Half-bridge model of servo-valve [72]

According to Carneiro and De Almeida model 2.14 only contained 10% of errors of standard polytropic models (eqs 2.12 and 2.13) in comparison to the datum model. Additionally results showed that taking into account temperature change significantly reduced pressure prediction error [80]. In order to determine the heat transfer conductance, required by the equations above, a heat transfer evaluation method was

presented by Carneiro et De Almeida based on thermal time constant [72]. The thermal time constant is the time it takes for the gas pressure (or temperature) to reach 63.2 percent of the difference caused by a step input [13]. In fact the thermal time constant is not really constant as the convection heat transfer coefficient and the effective wall (heat transfer) area both change with time [88]. However, it has been shown that a constant does fit experimental data quite well [88]. Additionally a comparison of the thermal time constant with the cycle time helps to understand the effects of heat transfer for a particular process e.g. if the thermal time constant is an order of magnitude smaller than the cycle time, an isothermal process can be assumed [13].

The thermal time constant is determined by fitting a first order equation to the pressure response in a closed chamber of the cylinder to a change in volume (eq 2.18). The cylinder piston-rod was moved to its extended position and the exhaust port (chamber 1) plugged (figure 2.19). The piston-rod was pushed by an external force to about its half-length position, where it remained until pressure reached a stationary value. Applying the ideal gas law, the temperature evolution inside the chamber can also be estimated based on the pressure measurements.

$$P(t) = P_f + \nabla P e^{-\frac{t}{\tau}} \quad (2.18)$$

The average thermal conductance and average heat transfer coefficient can then be determined using the thermal time constant and equations 2.19-2.21. Eichelberg's simplified model (neglecting piston velocity) is then used to relate the reference coefficient of heat transfer to equilibrium or operating pressure and temperature conditions (eq 2.21).

$$\hat{k}_{av} = \frac{\hat{m}c_v}{\tau} \quad (2.19)$$

$$\hat{\lambda}_{av} = \frac{\hat{k}_{av}}{\hat{A}_q} \quad (2.20)$$

$$\hat{\lambda}_e = \hat{\lambda}_{av} \cdot \left(\frac{P_e T_e}{P_{av} T_{av}} \right)^{0.5} \quad (2.21)$$

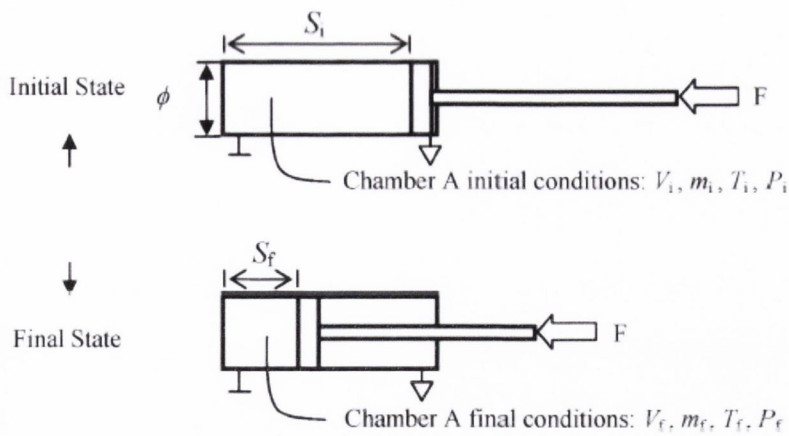


Figure 2.19: Evaluation of heat transfer coefficient [72]

The dynamic response of the thermodynamic model can be improved further by accounting for dead/inactive volume in the pneumatic cylinder, fittings and tubing (eq 2.22). Richer et Hurmuzlu measured the inactive volume by positioning the piston at each end of the stroke and filling the port cavities with a liquid such as lubrication oil [15]. The volume of the used liquid can then be measured with a graduated cylinder. Alternatively Carneiro et De Almeida estimate the dead volume using a closed volume experiment (figure 2.19). Since the chamber a inlet is closed, $m_i = m_f = m$, and the experiment started and finished with steady situation in chamber a, $T_i = T_f = T_{amb}$. Equation 2.24 is applied to solve for the mass in the cylinder chamber and applying the ideal gas law the dead volume can then be estimated [72].

$$V = V_d + A \cdot y \tag{2.22}$$

$$\hat{m} = \frac{V_i - V_f}{RT_{amb}} \cdot \frac{P_i P_f}{P_f - P_i} \tag{2.23}$$

Cushioning sections of pneumatic cylinders must also be accounted for in the thermodynamic model, where applicable, since as Najafi et al point out these sections affect the positioning accuracy of the piston [89]. The leakage between chambers can be neglected for regular pneumatic cylinders with rubber type seals, but can be significant for low friction cylinders that have graphite or Teflon seals [15]. To test for leakage in the cylinder, pressure can be applied to one port while venting the other and vice versa [90].

The time delay for the input pressure wave to propagate the entire length of tubing is estimated by Lt/c [15].

2.2.4 Fluid mechanic fundamentals, flow models and identification

Theoretically, the *motion* of a given fluid particle in chemical and physical equilibrium can be completely defined if the pressure, temperature and velocity as a function of space and time are known [13]. To determine the *state* of a fluid particle, density and viscosity are required. Therefore, seven variables are required to describe fluid dynamics: three velocity components (of three co-ordinates), pressure, temperature, density and viscosity [13]. In order to solve for the seven variables, seven equations are required which are given by the following relationships [13]:

- Newton's laws of motion, conservation of momentum, must hold for every fluid particle at every instant (Navier Stokes equations)
- The law of conservation of mass must apply (continuity equation)
- The conservation of energy or first and second laws of thermodynamics must hold
- The equation of state must apply i.e. ideal gas equation
- The empirical viscosity equation as a function of pressure and temperature must hold

However, in order to simplify this system of equations, a number of assumptions and restrictions are made [13]:

- The gas obeys the equation of state for an ideal gas, specific heat capacities are constant and inertial effect are negligible
- The viscosity is constant
- The flow is one-dimensional

The one dimensional gas flow dynamics can then be described by flow velocity, pressure, temperature and density [13]. During steady flow the mass flow rate at any cross section of a duct will be the same [13], this relationship is described by the continuity equation 2.24.

$$\dot{m} = A_1 \cdot v_1 \cdot \rho_1 = A_2 \cdot v_2 \cdot \rho_2 = A \cdot v \cdot \rho \quad (2.24)$$

In pneumatic systems there are many restrictions that have to be modelled [13]. The flow rate characteristic of pneumatic components is an important index in their design and selection, and in evaluating and comparing performance [91]. In this section the traditional flow equation for a restriction is derived from first principles. Consider a large reservoir discharging air through a nozzle to the atmosphere (figure 2.20). Due to the size of the reservoir, upstream pressure, temperature and temperature remain constant. The atmosphere pressure is lower than the upstream tank pressure.

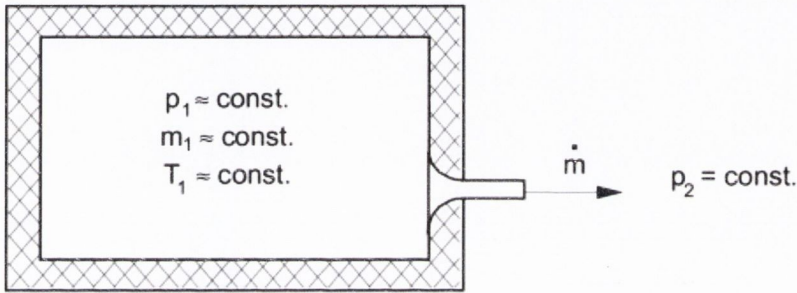


Figure 2.20: Discharge from a reservoir to atmosphere [13]

The velocity of the air can be found from the general energy equation assuming no heat exchange (adiabatic, $Q=0$), and no work done, $W=0$. Additionally potential energy changes can be ignored (i.e. $z_u = z_d$) and the velocity of the air in the reservoir is zero [13].

$$-\int V dp = \frac{m \cdot v_d^2}{2} - \frac{m \cdot v_u^2}{2} + m \cdot g \cdot (z_d - z_u) + W \quad (2.25)$$

$$v_d = \sqrt{2 \cdot R \cdot T_u \cdot \left[\frac{\gamma}{\gamma-1} \right] \cdot \left[1 - \left(\frac{P_d}{P_u} \right)^{\frac{\gamma-1}{\gamma}} \right]} \quad (2.26)$$

The isentropic process relating P_1 and P_2 determines the relationships between density and pressure [30]. Substituting the ideal gas law, into equation 2.27, results in the relation between static density to pressure ratio and total pressure (eq 2.28).

$$\frac{\rho_d}{\rho_u} = \left(\frac{P_d}{P_u} \right)^{\frac{1}{\gamma}} \quad (2.27)$$

$$\rho_d = \frac{P_u}{RT_u} \left(\frac{P_d}{P_u} \right)^{\frac{1}{\gamma}} \quad (2.28)$$

Substituting 2.27 and 2.28 into the continuity equation 2.24 and combining terms allows for the subsonic mass flow rate to be calculated with equation 2.29.

$$\dot{m} = \frac{C_d \cdot A \cdot P_u}{\sqrt{T_u}} \left\{ \frac{2\gamma}{R} \frac{\gamma}{\gamma-1} \left[\left(\frac{P_d}{P_u} \right)^{\frac{2}{\gamma}} - \left(\frac{P_d}{P_u} \right)^{\frac{\gamma+1}{\gamma}} \right] \right\}^{0.5} \quad \dots \text{if } Pr \geq b \quad (2.29)$$

$$A_e = C_d \cdot A \quad (2.30)$$

The discharge coefficient C_d is introduced as a correction factor, mainly to take into account jet contraction [13]. Due to abrupt area changes at the entrance section to the orifice, flow separates from the orifice wall forming, in a sense, its own nozzle [30]. This is illustrated in figure 2.21. The minimum-area cross section is called the vena contracta and is considered the effective area of the orifice (eq 2.30). The effective area is essentially empirical, even for simple restrictions where the geometrical area is known, since the discharge coefficient still must be found experimentally [92]. Figure 2.22 illustrates that C_d depends heavily on the geometry of the orifice [13,32,92]. The discharge coefficient also accounts for reduction in mass flow due to friction, heat losses and velocity profile effects [13].

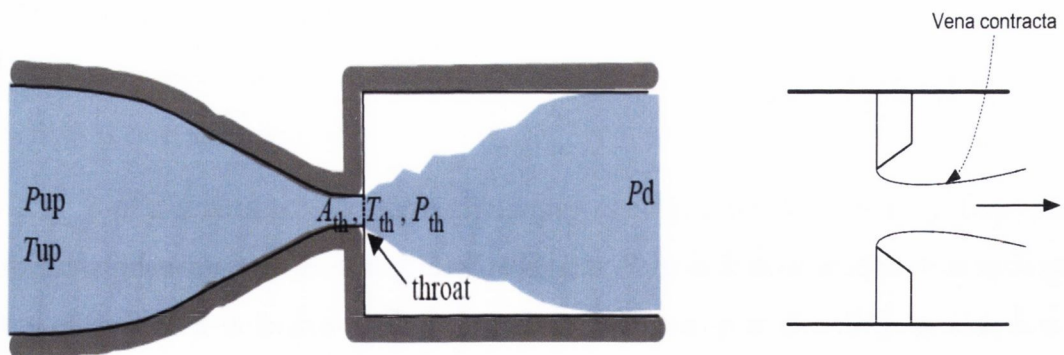


Figure 2.21: Converging nozzle and flow pattern at orifice inlet [30]

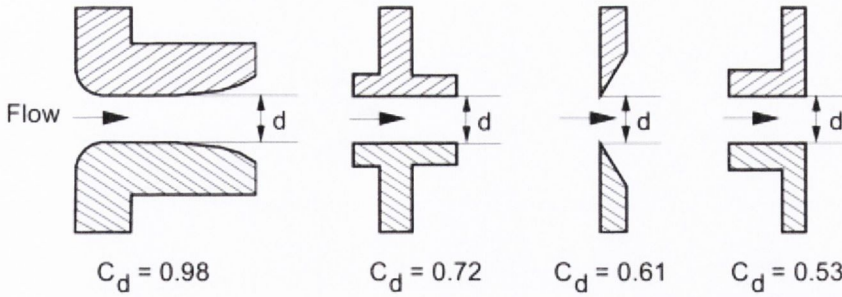


Figure 2.22: Various orifices and respective discharge coefficients [32]

To obtain the pressure ratio corresponding to the maximum mass flow, equation 2.29 is differentiated and the derivative set to equal zero [30]. This is called the critical pressure ratio b and at this point the velocity at the throat just attains the speed of sound [92]. The theoretical critical pressure ratio for air ($\gamma = 1.4$) is 0.528.

$$\left(\frac{P_d}{P_u}\right)_{cr} = b = \left(\frac{2}{\gamma+1}\right)^{\frac{\gamma}{\gamma-1}} \quad (2.31)$$

Substituting the equation for critical pressure ratio 2.31 into equation 2.29 allows calculation of the choked mass flow rate (eq 2.32). Choked flow occurs when the ratio of downstream pressure and upstream pressure (pressure ratio) is less than the critical pressure ratio of the component [13]. A further reduction in downstream pressure will not increase the mass flow.

$$\dot{m}_c = \frac{C_d \cdot A \cdot P_u}{\sqrt{T_u}} \left\{ \frac{\gamma}{R} \left(\frac{2}{\gamma+1}\right)^{\frac{\gamma+1}{\gamma-1}} \right\}^{0.5} \quad \dots \text{if } Pr < b \quad (2.32)$$

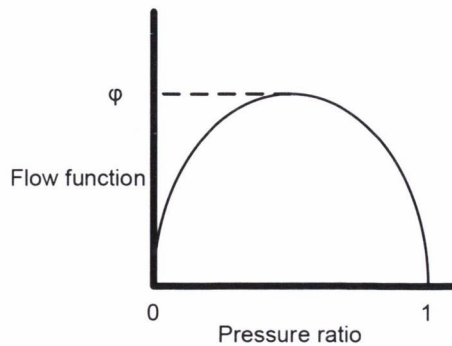


Figure 2.23: Flow function for air [30]

Finally, divide equation 2.29 by 2.32 and let:

$$K = \left\{ \frac{\gamma g}{R} \left(\frac{2}{\gamma+1} \right)^{\frac{\gamma+1}{\gamma-1}} \right\}^{0.5} \quad (2.33)$$

$$\frac{\dot{m}}{\dot{m}_c} = \left\{ \frac{2}{\gamma-1} \left[\left(\frac{P_d}{P_u} \right)^{\frac{2}{\gamma}} - \left(\frac{P_d}{P_u} \right)^{\frac{\gamma+1}{\gamma}} \right] \left(\frac{\gamma+1}{2} \right)^{\frac{\gamma+1}{\gamma-1}} \right\}^{0.5} = f \left(\frac{P_d}{P_u} \right) = \varphi \quad (2.34)$$

Applying equations 2.30, 2.33 and 2.34 simplifies equations 2.29 and 2.32 to a single expression 2.35 which applies to all pressure ratios [92]. Unlike incompressible fluid flow, where flow is a function of pressure drop, compressible fluid flow through a restriction is a function of pressure ratio across the restriction [93].

$$\dot{m} = \dot{m}_c \cdot \varphi = \frac{K \cdot A_e \cdot P_u}{\sqrt{T}} \cdot \varphi \quad (2.35)$$

Limitations of orifice flow equation

When the assumptions are met, the theoretical orifice flow equation can describe the mass flow rate through a simple restriction with an error of less than 1%, accurate enough for measurement purposes [13]. However, for predictions to be accurate there must be no significant friction loss, meaning the use of traditional orifice flow models is essentially limited to simple converging nozzles of short length [92]. Additionally, for compressible flow the discharge coefficient varies with pressure ratio, sometimes considerably, meaning equation 2.35 does not have universal application [13,92].

However, the main issue with the single orifice model is its inability to account for a reduction critical pressure ratio for typical pneumatic devices such as control valves [94]. Fluid power components and circuits are better represented by a cascade of orifices (figure 2.24), nozzles or both [94]. While equation 2.35 can be applied to the individual restrictions within a valve it cannot predict the combined effect of the multiple restrictions of the valve or other pneumatic component.

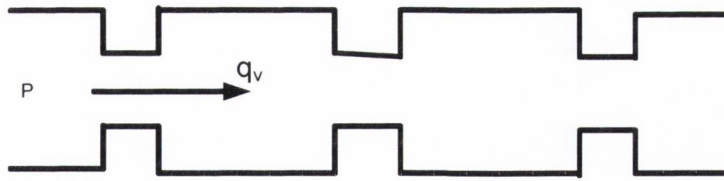


Figure 2.24: Multi-nozzle representation of a spool valve [92]

The depression of the critical pressure ratio is caused by choking of one of the restrictions within a valve [92]. The valve exhibits a critical point which occurs at the theoretical pressure ratio of 0.528 at the choked restriction, but this causes a pressure drop across the other restrictions. Consequently the overall pressure ratio for the component is less than 0.528 [92]. For directional control valves, the typical critical pressure ratio is between 0.2 to 0.5 [13].

Experimental investigations by Shannak of straight bore and sharp-edged test orifices have also demonstrated that the critical pressure ratio for air flow through single orifices can also be considerably lower than that for an ideal nozzle [95]. In the case of a single orifice the depression of the critical pressure ratio is due to the following: With a decreasing pressure ratio, a minimum local velocity develops in the vena contracta as the flow velocity reaches its maximum there [95]. As the pressure downstream of the orifice decreases, the density of air decreases and the air volume expands. This results in the cross-sectional flow area (vena contracta) becoming larger and moving toward the orifice [95]. Even though the local velocity of the air flow is constant at sonic velocity, as the vena contracta increases, the mass flow will reach its maximum. With further decrease in pressure ratio below the critical point, the vena contracta remains invariable and mass flow through orifice becomes choked [95].

ISO model development

In order to allow for reduction in critical pressure ratio, an approximation was developed by Sanville based on two parameters: the effective area and critical pressure ratio which are the intrinsic characteristics of any pneumatic device [92-94]. The parameters

must be determined empirically. Although, flow equations are expressed naturally in terms of mass flow rate, there is a widely shown preference for using volumetric flow rate [94].

$$q_v = \frac{\dot{m}}{\rho_0}$$

The density ρ of air is defined under standard reference conditions. Additionally because the gas is always air, the constants in equation 2.35 can be lumped to produce equation 2.37. Sonic conductance is lumped parameter (eq 2.36), that represents the ratio between the mass flow rate through the component and the product of upstream pressure and mass density at standard conditions when flow is choked [13]. If the actual temperature is significantly different to reference temperature, a temperature correction factor is included.

$$C = \frac{K}{\rho_0 \cdot \sqrt{T_0}} \cdot Ae \tag{2.36}$$

$$q_v = C \cdot P_u \cdot \sqrt{\frac{T_0}{T}} \cdot \varphi \tag{2.37}$$

Sanville [92,94] discovered that flow function (eq 2.38) of most pneumatic directional control valves could be approximated using quarter curve of an ellipse (figure 2.25). This approach allows for a reduced critical pressure ratio, b .

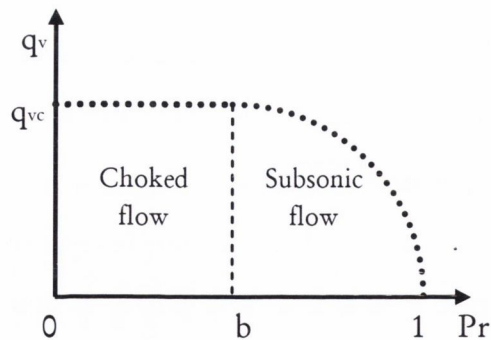


Figure 2.25: General presentation of flow rate against pressure ratio with fixed upstream pressure [96]

$$\varphi = \begin{cases} \left[1 - \left(\frac{\text{Pr}-b}{1-b} \right)^2 \right]^{0.5} & \dots \text{if } \text{Pr} > b \\ 1 & \dots \text{if } \text{Pr} \leq b \end{cases} \quad (2.38)$$

The equations 2.37 and 2.28 form the basis for the ISO 6358 standard [96]. The values of the critical pressure ratio and sonic conductance depend on the particular design of a component [13]. It is important to note that the performance of any pneumatic component is modified by the addition of fittings and to a lesser extent tubing [94]. If the purpose of a test is to examine the flow characteristics of a single component (i.e. valve), then it is recommended that fittings and tubing are oversized such that they have negligible effect on the component performance [94,96]. However, since an assembly of components behaves as a single component to the extent that an effective area and critical pressure ratio can be identified, a pneumatic circuit can be tested as one unit [94]. Although in this case, the elliptical flow function may not be followed as closely and calculated values of b may vary with pressure ratio [94].

The standard also provides an alternative set of characteristics, effective area A_e and coefficient of compressibility s . The coefficient of compressibility (eq 2.39) takes into account gas compressibility when flow is subsonic [96]. This is set of characteristics of recommended when the flow characteristics of several components connected in series is to be estimated [96].

$$s = \frac{1}{1-b} \quad (2.39)$$

$$A_e = C \cdot \rho_0 \cdot \sqrt{s \cdot R \cdot T_0} \quad (2.40)$$

The International Standard 6358 specifies a method for testing the flow characteristics of pneumatic fluid power components which use compressible fluids [96]. It specifies requirements for the test installation, procedure and presentation of results [96]. The test circuits are illustrated in figure 2.26 with key to circuit components in table 2.3 [97].

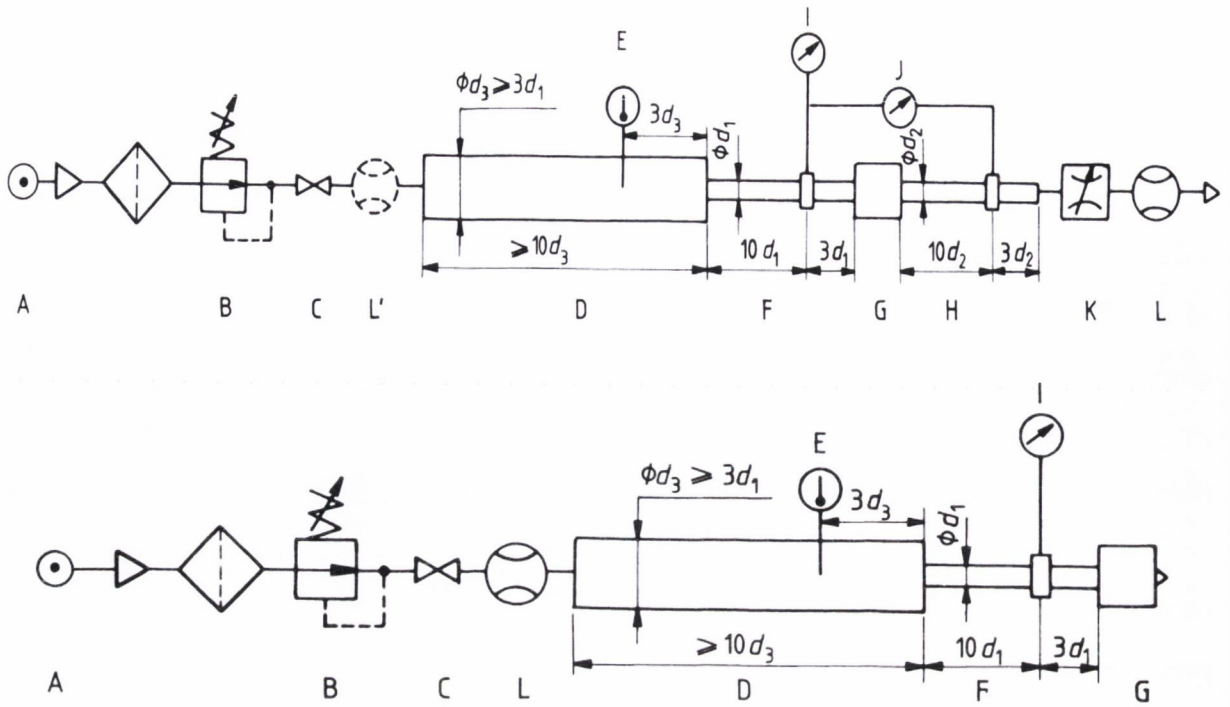


Figure 2.26: ISO6358 test circuit for components with inlet and outlet ports (top) and exhausting directly to atmosphere (bottom)

Reference letter	Description
A	Compressed gas source and filter
B	Adjustable pressure regulator
C	Shut-off valve
D	Temperature measuring tube
E	Temperature measuring instrument
F	Upstream pressure measuring tube
G	Component under test
H	Downstream pressure measuring tube
I	Upstream pressure gauge or transducer
J	Differential pressure gauge or transducer
K	Flow-control valve
L/L'	Flow rate measuring device

Table 2.3: Key to ISO test circuit components

Test procedures

ISO test method 1 determines the flow rate characteristics, C , b , for pneumatic components with inlet and outlet ports i.e. valves. First, the upstream pressure is set at a certain value and the flow control valve fully opened so that the maximum flow can be measured [98]. By adjusting (partly closing) the flow control valve, the flow rate is successively reduced to 80%, 60%, 40% and 20% of the maximum flow rate [96]. At each step, the flow rate, temperature and pressure differential are measured. The resulting curve resembles figure 2.25. The sonic conductance C and critical pressure ratio b are then determined from the following equations [96,98]:

$$C = \frac{q_{vc}}{P_{uc}} \sqrt{\frac{T_c}{T_0}} \quad (2.41)$$

$$b = 1 - \frac{\frac{P_u - P_d}{P_u}}{1 - \sqrt{1 - \left(\frac{q_v}{q_{vc}}\right)^2}} \quad (2.42)$$

The critical pressure ratio is the mean of b for each value of q_v [96]. If the lowest pressure ratio achieved in the experiment is higher than the estimated critical pressure ratio, the test must be repeated with higher upstream pressure or lower downstream pressure such that choked flow is achieved [96].

ISO test method 2, for components exhausting to atmosphere specifies that the upstream pressure is increased successively from atmospheric pressure to 1.1, 1.5, 3 and 5 bar (absolute)[96,98]. The sonic conductance is calculated by eq 2.41 using the mean of values in straight line region (figure 2.27). The test point which is on a straight line through the origin of coordinates is considered the choke point, and the critical pressure ratio can be obtained from the pressure of this point [98].

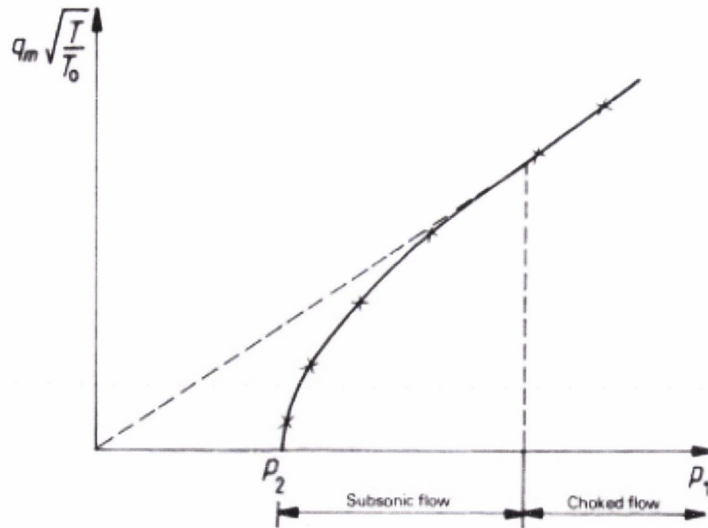


Figure 2.27: Example flow-rate versus pressure characteristic [96]

The permissible systematic errors of measurement instruments, determined during calibration, for the standard are documented in table 2.4.

Parameter of measuring instrument	Class A	Class B
Flow rate, %	± 2	± 4
Pressure, %	± 1	± 2
Temperature, K	± 1	± 2

Table 2.4: Permissible errors of measurement instruments in ISO6358 [96]

Critique of ISO6358 and proposed improvements

There has been criticism about the way the coefficients b and C are determined according to the ISO6358 standard [13]. It stipulates that only four points on the ellipse have to be measured and used for computation of the critical pressure ratio b . This small number of measurements can lead to a poor fit of the model [13]. Additionally for the ISO test method 2, the inlet pressure at the choke point and thus the critical pressure ratio

cannot be determined exactly [98]. In order to improve the accuracy of both ISO test methods, Kuroshita has recommended that the flow rate characteristics are obtained with smaller pressure intervals [98]. Additionally for second test method, it has been proposed by Kuroshita that the pressure ratio versus flow rate ratio characteristics are determined using the pressure versus flow rate characteristics (fig 2.27), so that the critical pressure ratio can be calculated using equation 2.42 specified in the ISO test method 1 [98]. The choked flow rate is the theoretical choked flow-rate calculated by equation 2.37 using each measured upstream pressure and temperature values. A comparison of the improved test method 2 with test method 1 for a number of valves and restrictions clarified the accuracy and consistency of this improved method [98].

The ISO6358 standard has also been criticised by Hubert and Sesmat for incoherence with regard to the nature of measurements made for characterisation of a pneumatic component [99,100]. The parameters b and C are based on upstream and downstream static pressure measurements done on measuring tubes that match the port size of the component under test [100]. This means that the fluid velocity, and consequently the Mach number, at the upstream and downstream pressure sensor locations may not be negligible and the flow characteristics will depend on the diameter of the connecting tubes [99]. Additionally according to the test circuit used, the nature of the *downstream* pressure is not the same nature: static pressure for in-line test circuit, ISO method 1, and stagnation pressure for exhaust to atmosphere circuit, ISO method 2 [100]. The measured temperature in the ISO test circuits corresponds to a stagnation pressure which means the nature of the *upstream* temperature and pressure measurement is also not consistent [100]. In figure 2.28, $P1$ and $T1$ correspond to upstream pressure and temperature respectively, $P2$ the downstream pressure.

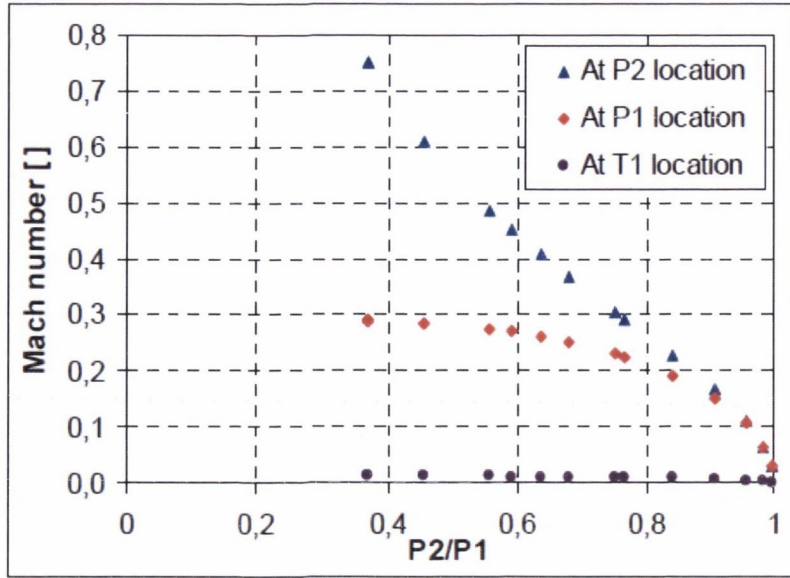


Figure 2.28: Mach numbers at locations in ISO test circuit [100]

Based on the fluid mechanic theory and experimental investigations, Sesmat et al concluded the use of stagnation pressure instead of static pressures is preferable [100]. By definition, the stagnation pressure is the pressure the flow would reach if brought isentropically to rest [101]. The total pressure is the sum of the static and dynamic pressures [100] and it can be calculated from the static pressure P , with knowledge of the local geometrical section A (eq 2.43). Typically the flow is assumed adiabatic so that upstream temperature is used as stagnation temperature T_t [99]. This method allows the stagnation pressures to be derived from the static pressure measurements made on the ISO6358 standard test benches.

$$P_t = P \left[\frac{1}{2} + \sqrt{\frac{\gamma-1}{2\gamma} RT_t \left(\frac{\dot{m}}{PA} \right)^2 + \frac{1}{4}} \right]^{\frac{\gamma}{\gamma-1}} \quad (2.43)$$

However in some cases, in particular for the in-line ISO test method 1, it will not be possible using this method to obtain the sonic part of the conductance curve leading to a poor estimate of the critical pressure ratio [100]. The underlying assumptions are not always true [100]. Therefore it is recommended to use an expanded section to directly measure the stagnation pressures [99,100].

Extended ISO representation

A limitation to the ISO standard models is that they are limited in scope to certain pneumatic components such as directional control valves and nozzles, that exhibit an elliptical flow-rate characteristic [91,102]. However, not all flow characteristic curves are elliptical. This includes common pneumatic circuit components such as check valves, silencers and components in series [102]. An extended version of the ISO6358 model (eqs 2.44 and 2.45) has been proposed by Kagawa et al, based on the introduction of two additional flow characteristic parameters (figure 2.29), in order to improve the accuracy of the model for all pneumatic components [102]. The cracking pressure ratio a accounts for the fact that in one way flow control valves the flow-rate can be zero for a pressure ratio of less than one [102]. A one flow control consists of both a speed control valve and a check valve, and the reduction in a is due to the cracking characteristic of the check valve [103]. The subsonic index ms allows for increased flexibility in the flow function as illustrated in figure 2.30.

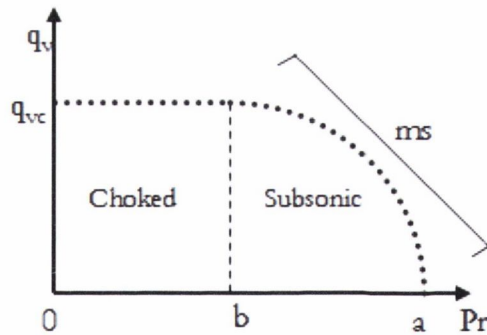


Figure 2.29: Extended representation of ISO6358 model

$$q_v = q_{vc} \left[1 - \left(\frac{Pr-b}{a-b} \right)^2 \right]^{ms} \quad (2.44)$$

$$\dot{m} = \begin{cases} \rho_0 \cdot C \cdot P_u \cdot K_t \cdot \left[1 - \left(\frac{Pr-b}{a-b} \right)^2 \right]^{ms} & \dots \text{ if } Pr > b \\ \rho_0 \cdot C \cdot P_u \cdot K_t & \dots \text{ if } Pr \leq b \end{cases} \quad (2.45)$$

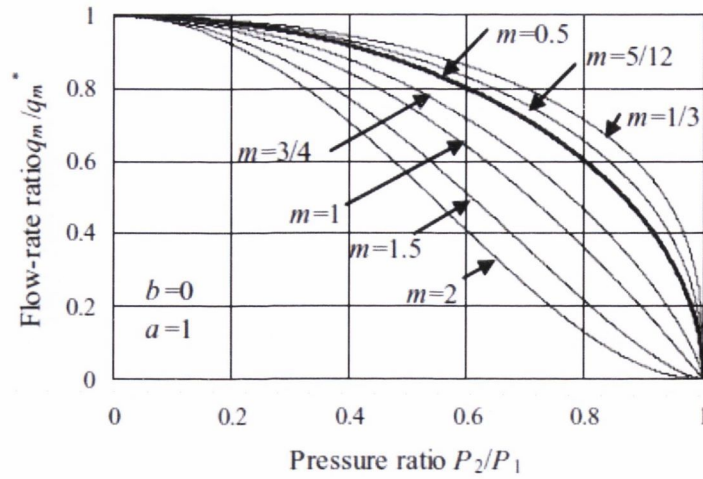


Figure 2.30: Influence of index m on flow-rate characteristics [91]

Jungong et al use a minimal least squares method in Matlab in order to fit the extended equation to experimental data with best fit. Figure 2.31 shows the experimental data of a one way flow control valve in the free flow direction (i.e. through check valve) and its characteristics determination by several methods. It is clear the original ISO6358 equation cannot fit the measured results and that introduction of the additional parameters, to account for cracking pressure and flexible flow function, improves the approximation considerably [103].

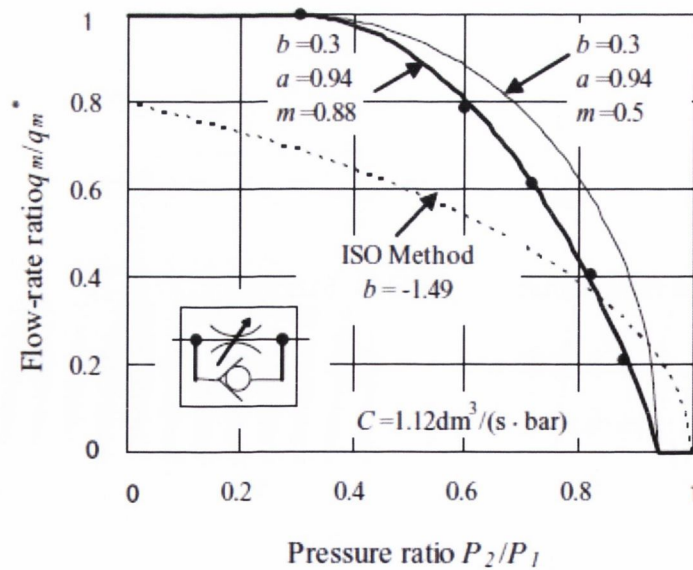


Figure 2.31: Flow-rate characteristics of one way flow valve [91]

Figure 2.32 illustrates the distribution of b and m for a range of pneumatic components and is based on tests of over 179 components made by 7 manufacturers [103]. It can be seen from the figure that while the critical pressure ratio b can vary from 0.05 to 0.53 for solenoid valves, the subsonic index m_s is consistent around 0.5. This highlights the fact that the original ISO6358 equation can correctly represent the flow characteristics of directional control valves and also the consistency of the new extended representation [103]. In contrast to solenoid valves, it can be seen from that the characteristics b and m_s can vary significantly for components such as silencers and speed control valves. Theoretically, it is impossible for a fixed orifice to have a subsonic index greater than one [103]. However, some silencers have a special flexible area flow passage that allows flow area to expand with higher air pressure [103]. This can result in a subsonic index m_s that exceeds one. With increased length, resin tube exhibits a decreased critical pressure ratio and increased subsonic index. Note for silencers, directional control valves and blow nozzles the cracking pressure a will be one.

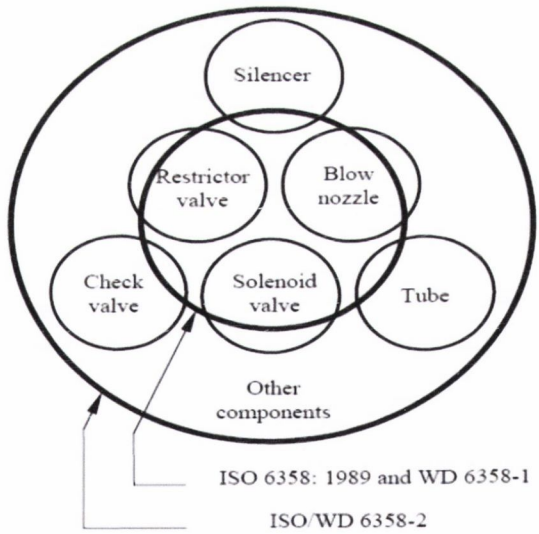
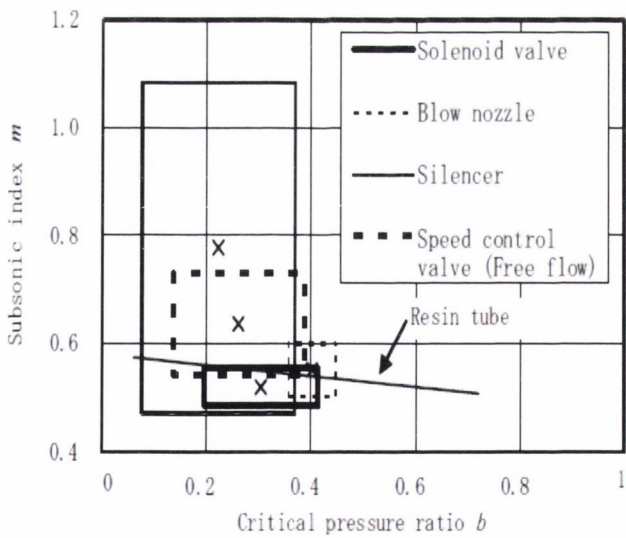


Figure 2.32: (a) Distribution of b and m for various components [102] (b) Applicable range of ISO and improvement methods [104]

Another objection to the ISO6358 methods is the large amount of compressed air required, in particular to test high capacity valves, the long test times and high noise levels generated [13,105]. There have been a number of alternative test methods proposed to overcome these problems. These include simple discharge tests from a general air tank, Isothermal discharge tests and Vacuum charge test methods [91].

Isothermal discharge method (IDM)

This alternative method, originally developed by Kawashima et al, tests a component by discharging air to atmosphere from an isothermal tank, which is pre-charged with compressed air at a specified pressure [91]. The isothermal chamber can almost realise isothermal conditions due to the large heat transfer area and heat transfer coefficient [106]. This is achieved by stuffing the tank with steel wool [106]. The principle of the method involves directly differentiating the ideal gas equation. Since the volume of the tank is fixed, and the state of the air while discharging remains isothermal equation 2.46 is reduced to equation 2.47.

$$V \cdot \frac{dP}{dt} = \dot{m} \cdot R \cdot T + m \cdot R \cdot \frac{dT}{dt} \quad (2.46)$$

$$\dot{m}_{out} = \frac{V}{RT_{amb}} \cdot \frac{dP}{dt} \quad (2.47)$$

Using this procedure allows the instantaneous flow rate and thus flow characteristics to be obtained by only measuring the pressure in the chamber [107]. According to Kawashima et al the instantaneous flow rate can be measured within a 1% error [106-108]. This method is also applicable for measuring the dynamic performance of air flow meters [106]. The proposed test bench for the isothermal discharge method is illustrated in figure 2.33.

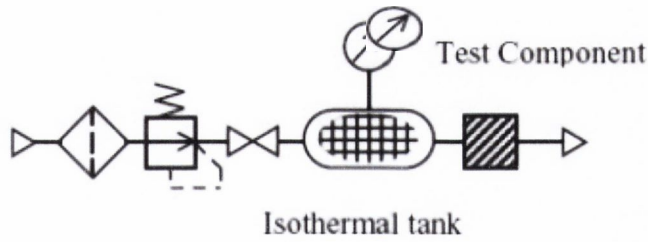


Figure 2.33: Experimental setup for the isothermal discharge test [91]

The IDM method determines the sonic conductance and the critical pressure ratio by fitting the experimental pressure response with the theoretical pressure response [108]. The Gauss-Newton method, a non-linear least squares method is used to fit the pressure response (figure 2.34) [108]. The isothermal discharge procedure resulted in a maximum sonic conductance uncertainty of 1.2% [108]. An isothermal chamber based method has also been proposed by Ji-Seong et al [109] to measure very small leakage flow rates in pneumatic drives.

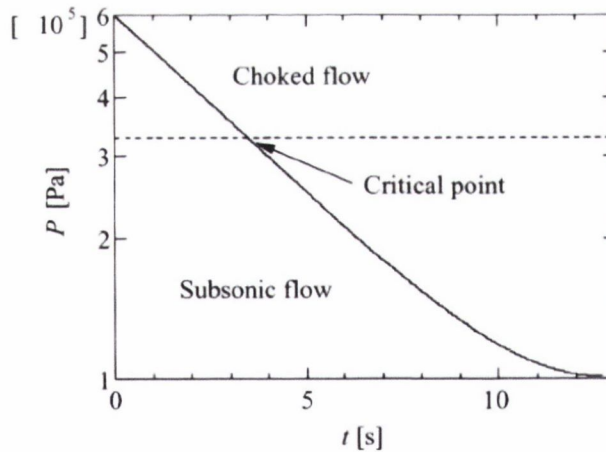


Figure 2.34: Pressure response during discharge from isothermal tank [108]

Simple discharge & hybrid method

Since it is expensive and practically difficult to construct a isothermal chamber or tank there is considerable interest in using the discharge of air from standard tanks to characterise pneumatic components [85,98,110-112]. The simple discharge method allows

the estimation of sonic conductance of a test component based on the principle that the amount of air discharged from the tank can be calculated from pressure changes in the tank and the discharge time [91].

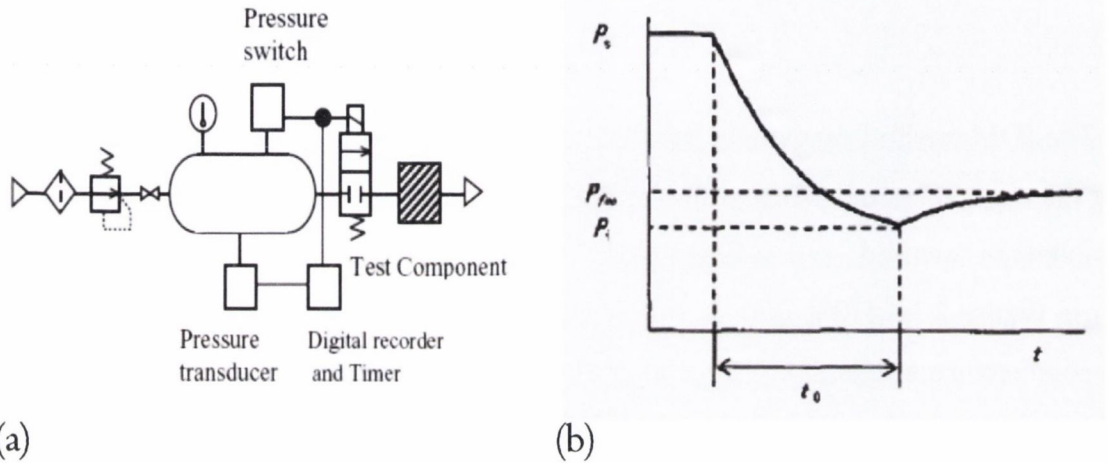


Figure 2.35: (a) Simple discharge test circuit [91] and (b) pressure change in tank [98]

Figure 2.35 shows the test circuit for the discharge method. Valves and tubing are oversized as in the ISO6358 standard. The experimental procedure is described by Kuroshita et al as follows [98]:

1. Open shut-off valve and set pressure in tank to 7 bar absolute (P_s). Allow temperature and pressure to reach steady state conditions.
2. Close the shut-off valve and measure initial charge pressure and temperature in the tank.
3. Open the solenoid valve to allow air to discharge through the component to the atmosphere until the pressure in the tank drops to 3.5 bar. Stop the discharge using a pressure switch and measure the discharge time (t_0).
4. Let the air in the tank reach steady state conditions and measure residual pressure (P_f).

The pressure change is shown in figure 2.35 and the sonic conductance can be calculated using equation 2.48 [98].

$$C = \frac{2}{\gamma-1} \cdot \frac{V}{P_0 t_0} \cdot \sqrt{\frac{T_0}{T_s}} \cdot \left\{ \left(\frac{P_s}{P_f} \right)^{\frac{\gamma-1}{2}} - 1 \right\} \quad (2.48)$$

For a component under test with a critical pressure ratio less than 0.29 (1/3.5), the flow includes a subsonic component and thus an error is produced in the calculation of sonic conductance [98]. However the error in sonic conductance is estimated by the authors to be less than 4% [98].

Since the simple discharge method only provides a means for determining sonic conductance, a hybrid test method was proposed by Kuroshita et al to obtain the other flow parameters [98]. This method obtains the sonic conductance by the simple discharge method and the critical pressure, subsonic index and cracking pressure ratio from the improved ISO method 2, exhaust to atmosphere, test [91]. This allows the flow rate at high pressures to be calculated using the sonic conductance obtained via the discharge method meaning a large pneumatic pressure source (tank or compressor) is not required [98].

The vacuum charge method tests a component by charging atmospheric air to a tank which has already been evacuated [91]. The method is reviewed fully by Zhang and Kuroshita [91,105]. The applicability of the different alternative test methods for different sized components, flow parameters and connection types is illustrated figure 2.36.

Test types	Test components								
	Parameter				Size			Connection	
	C	b	m	a	1/8	1	2	In-line	Exhaust
Part1: In-line test									
Part1: Exhaust-to-atmosphere test									
Part2: Isothermal discharge test									
Part3: Vacuum charge test									
Part4: Simple discharge test									
Part4: Hybrid test									

Figure 2.36: Applicable ranges of ISO6358 and alternative test methods [91]

Temperature measurement

A limitation to the discharge methods in general is that is necessary to know both the instantaneous pressure and temperature [111]. While the instantaneous pressure of the gas in a tank can be measured readily, it is difficult to measure the instantaneous temperature due the time response of thermocouples [110]. In addition the temperature field in the tank is not uniform [111]. In the isothermal discharge method, the discharge from a tank is approximated as an isothermal process while the proposed vacuum charge and simple discharge methods assume polytropic charge or discharge processes [98,105,108,111]. All of the above methods correspond to an inverse approach to identifying the flow characteristics of a pneumatic component [110]. The sonic conductance and critical pressure ratio are obtained from the pressure response using an approximation of tank state equation [110].

Although these inverse methodologies allow flow rate characteristic testing time and air consumption to be reduced, the accuracy of the results are strongly related to the parameters of the experimental rig i.e. different shaped vessels can lead to difference in heat transfer [110,111]. De Giorgi et al and Yang et al have shown that the polytropic index also varies continuously during the charging or discharging of compressed air [110,111]. Figure 2.37 illustrates that a polytropic law cannot properly describe the heat transfer during a fixed volume discharging process.

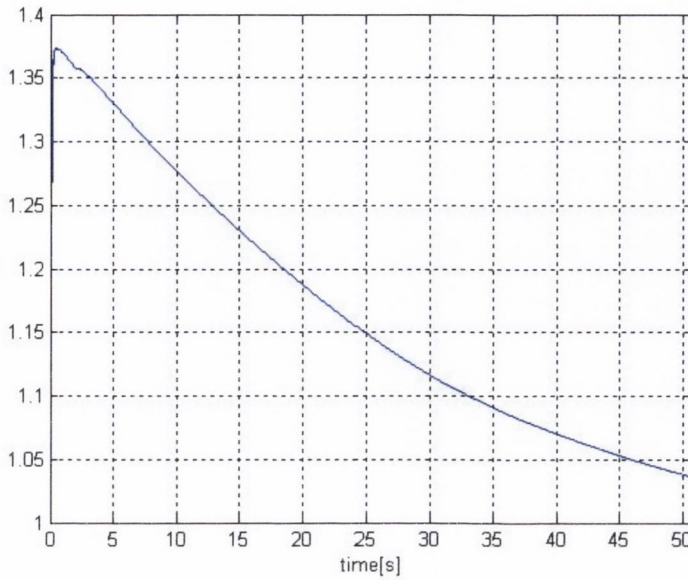


Figure 2.37: Polytropic index during discharging process [110]

One solution is to measure the average temperature during discharge indirectly using the ‘stop method’ proposed by Kawashima et al [106,110]. The procedure consists of several discharges always starting from the same initial conditions, which have the initial conditions of the complete discharge test [110]. When the pressure reaches a certain specified value or time, the discharge is interrupted by closing the solenoid valve, and the pressure $P(t)$ is measured [106,110]. When the pressure becomes stable (P_f), the temperature in the chamber recovers to room temperature [106]. As the mass of the gas in the tank is constant, the temperature at time the discharge was stopped (t) can then be accurately calculated using [107,108]:

$$T(t) = \frac{P(t)}{P_f} \cdot T_{\text{amb}}$$

By changing the time to stop the discharge, the average temperature at any time can be measured [108]. The uncertainty of this method is reported to be within 3% [106]. Figure 2.38 gives an example of measured temperature using the stop method and the polynomial approximation introduced to solve the inverse problem [110].

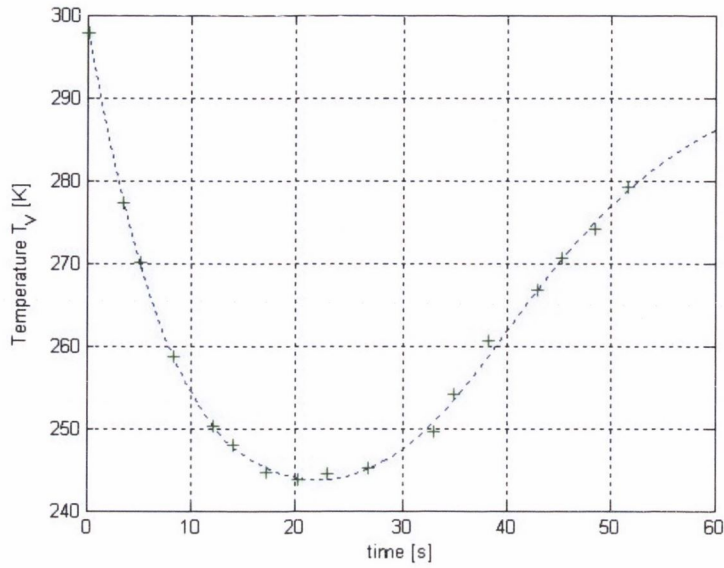


Figure 2.38: Temperature measurements during discharge [110]

As an alternative, Qian et Xiang have suggested using the stop method to obtain the instantaneous polytropic index using equation 2.49 [110,112]. P_i and T_i are the pressure and temperature before discharge respectively. It is important to note that the instantaneous polytropic index will vary for the same circuit if started from different initial pressures [85].

$$n(t) = \frac{1}{1 - \frac{\ln\left(\frac{T}{T_i}\right)}{\ln\left(\frac{P}{P_i}\right)}} \quad (2.49)$$

According to the inverse method proposed by De Giorgi et al, if the temperature and pressure are known, the heat transfer and mass flow rate can be calculated using inverse models (eqs 2.50 and 2.51) [110]. As pressure and temperature are obtained from measurements, a noise reduction procedure is typically required [110]. This is accomplished through median filtering and under sampling of pressure measurements prior to differentiation [85].

$$\frac{dQ}{dt} = \frac{\gamma VP}{(\gamma-1)T} \cdot \frac{dT}{dt} - V \cdot \frac{dP}{dt} \quad (2.50)$$

$$\dot{m}_{\text{out}} = -\frac{V}{RT} \cdot \frac{dP}{dt} + \frac{VP}{RT^2} \cdot \frac{dT}{dt} \quad (2.51)$$

According to De Giorgi et al, this approach allows the identification of the flow characteristics of a component using only pressure measurements during discharge from any type of tank, providing the heat transfer phenomenon is well known [110].

However the 'Stop method' is a time costly since each measured temperature point requires stabilisation of pressure and temperature in the tank [110]. An alternative solution that avoids the measure of temperature relies on either knowledge of the heat exchanged for a given tank or the use of an accurate thermal exchange model [110]. A number of macroscopic models based on dimensional analysis theory have been developed that allow identification of the main heat transfer mechanisms according to flow conditions, pressure levels and tank shape [85,111,112].

Convection can be split into two categories according to the phenomenon influencing mass transfer [85]:

1. Natural convection occurs when the mass transfer is due to a temperature gradient
2. Force convection occurs when mass transfer is imposed by a difference in pressure

For convection three dimensionless groups are required, Nusselt, Prandtl and Grashof and are related by 2.52 [85].

$$Nu = \zeta \cdot Gr^{\delta_1} \cdot Pr^{\delta_2} \quad (2.52)$$

The Nusselt number corresponds to the ratio between heat power exchanged by convection and conduction (eq 2.53). The Grashof number is the ratio between product of Archimedes and inertial force, and viscous forces (eq 2.54). The Prandtl number characterises the velocity distribution versus temperature distribution (eq 2.55). The Rayleigh number is used for natural convection modelling in order to determine the transition between laminar and turbulent convection (eq 2.56).

$$Nu = \frac{\lambda D}{k} \quad (2.53)$$

$$Gr = g \cdot \frac{(T_w - T) \cdot D^3 \cdot \rho^2}{\mu^2 \cdot R^2 \cdot T^3} \quad (2.54)$$

$$Pr = \frac{c_p \mu}{k} \quad (2.55)$$

$$Ra = Gr \cdot Pr \quad (2.56)$$

Therefore:

$$\frac{dP}{dt} = -\frac{\gamma RT}{V} \cdot \dot{m}_{out} + \frac{\gamma-1}{V} \cdot \frac{k}{D} \cdot \zeta \cdot Gr^{\delta 1} \cdot Pr^{\delta 2} \cdot Aq \cdot (T - Tw) \quad (2.57)$$

$$\frac{dT}{dt} = \frac{(\gamma-1)T}{PV} \cdot [-RT\dot{m}_{out} + \frac{k}{D} \cdot \zeta \cdot Gr^{\delta 1} \cdot Pr^{\delta 2} \cdot Aq \cdot (T - Tw)] \quad (2.58)$$

A similar physical based approach is taken by Yang [111]. A drawback of these approaches is that they rely on natural convection heat transfer models [111]. However, if the conductance of a discharge circuit is large or volume of tank small the discharge time will be short and forced convection heat transfer more prevalent [112]. In this case an increased error will be observed in the test method.

Qian et Xiang have improved the simple discharge method further by considering a hybrid forced and natural heat transfer model [112]. This type of discharge method looks promising for future industrial applications but requires further model validation to verify shape factors in order to extend the approach to tanks of all shapes [85].

Drive circuit flow models

In modelling a pneumatic drive system, a pressure regulator, working within its capacity, is considered a low-impedance source of compressed air and is therefore the start of the total inlet flow path [93]. The highly non-linear characteristics of pneumatic systems due in part due to the compressibility of air, has in the past made pneumatic systems difficult to model. However, the traditional flow models, used widely in the literature [15,16,80,113-115], rely on standard orifice theory and are not suitable for components with complex flow paths or multiple devices in series [92]. The discrepancy between theoretical orifice and measured flow function for an actuator circuit is illustrated in figure 2.39. In particular, the flow function during discharge is considerably different to predicted.

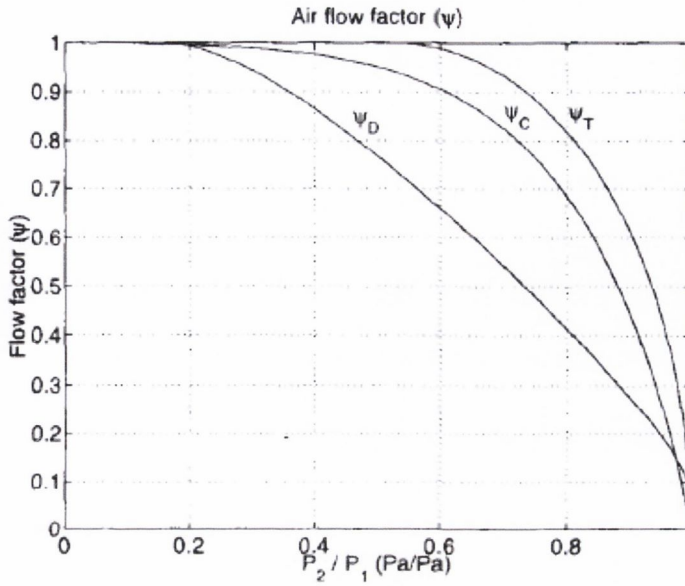


Figure 2.39: Comparison between theoretical and measured air flow factors for charging and discharging [75]

For this reason some data based flow models have also been investigated by Nouri et al [75] and Bobrow et McDonnell [116]. However, since these approaches depend heavily on curve fitting using experimental values they are limited in application to even slightly different systems [15]. Recent research by Thomas et al has modelled the flow function with an ISA model [19] while Najafi et al and Hildebrandt et al [49] model the flow with the ISO6358 equation [89].

In modelling a circuit, the control valve itself is usually only a minor part of the total flow impedance in a pneumatic circuit and the pipe work, fittings and other components must be accounted for [93]. Richer et Hurmuzlu have shown that flow attenuation due to long signal lines can be significant. To account for this behaviour the authors added an attenuation component (eq. 2.59) to the flow model [15]. The tube resistance R_t depends on whether the flow through the tubing is laminar or turbulent.

$$\Phi = e^{-\frac{R_t R T}{2P}(L_t / c)} \quad (2.59)$$

Hildebrandt et al have suggested that the pneumatic network for a servo-system is best represented using a Wheatstone bridge model (figure 2.40) since the leakage across the spool can be considerable for proportional valves. The mass flow model can then be expressed in the manner of equation 2.60, though the flow functions are not necessarily symmetric [49]. This is not an issue for standard binary mode switching valves with elastomeric seals, typical in industry, since leakage is negligible [13]. However for the low friction type directional control valves with lapped spool design, leakage in the valve is relevant and should be included in the flow model.

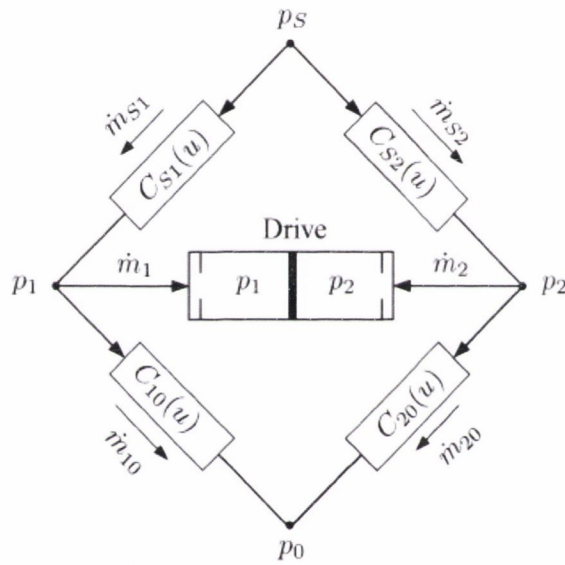


Figure 2.40: Pneumatic Wheatstone bridge for servo system, each C depends on u [49]

$$\dot{m}_1 = \dot{m}_{s1} - \dot{m}_{10} = C_{s1}(u)P_u\rho_0\varphi - C_{10}(u)P_1\rho_0\varphi \quad (2.60)$$

Finally, the switching time of solenoid valves can be significant and should also be included in the flow model (figure 2.41).

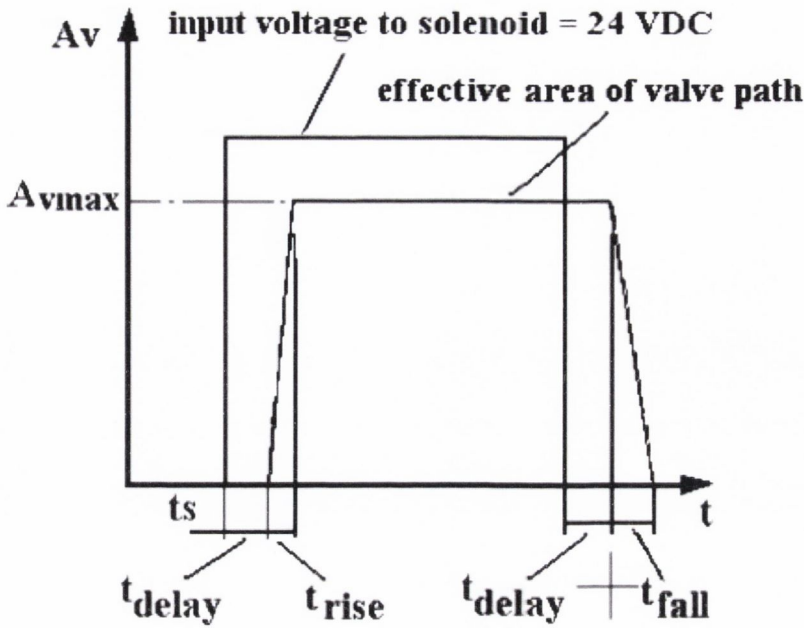


Figure 2.41: Change of cross-sectional area of the valve orifice [89]

Circuit analysis

If the flow characteristics of the individual components are known (from measurement or catalogue), the flow characteristics of a pneumatic system consisting of devices connected in series can be calculated using two methods presented by Eckersten. The first additivity method is a simple approach that allows the calculation of the flow characteristics of a system with an error of less than 10% [117]. Considering a system of n components connected in series, the total conductance of the system can be calculated using equation 2.61 and the critical pressure ratio using equation 2.62.

$$\frac{1}{C_s^3} = \sum_{i=1}^n \frac{1}{C_i^3} \quad (2.61)$$

$$1 - b_s = C_s^2 \sum_{i=1}^n \left[\frac{1 - b_i}{C_i^2} \right] \quad (2.62)$$

The second method of consecutive additions considers the order of components and provides the characteristics of a system more accurately, with an error below 5% [117]. The calculation is performed in $n-1$ steps and the first two components are considered in the first step. If α is less than 1, the flow first becomes choked in component 1. Choked

flow in component 2 occurs after further increase in pressure drop [117]. If α is greater than 1 then the flow only becomes choked in component 2 and if α is equal to 1 choked flow occurs in both components at the same time [117]. The conductance of the compounded component is calculated using equations 2.64 and 2.65.

$$\alpha = \frac{C_1}{C_2 \cdot b_1} \quad (2.63)$$

If $\alpha \leq 1$

$$C_{1,2} = C_1 \quad (2.64)$$

If $\alpha \geq 1$

$$C_{1,2} = C_2 \cdot \alpha \cdot \frac{\left[\alpha \cdot b_1 + (1 - b_1) \cdot \left\{ \alpha^2 + \left[\frac{1 - b_1}{b_1} \right]^2 - 1 \right\}^{0.5} \right]}{\left[\alpha^2 + \left[\frac{1 - b_1}{b_1} \right]^2 \right]} \quad (2.65)$$

For all α

$$b_{1,2} = 1 - C_{1,2}^2 \cdot \left[\frac{1 - b_1}{C_1^2} + \frac{1 - b_2}{C_2^2} \right] \quad (2.66)$$

The second step in the procedure is to add the third component of the system to the first two and continue until all components of the system have been included [117]. Using either of the above approaches, the flow through passive components can then be calculated using the standard Sanville/ISO6358 equation [96,117]. No derivations are provided for either method. Tables with typical values of b and C for standard fittings (seat valves, elbows, hose couplings, reducers) are given by Eckersten [117].

2.2.5 Compressed air system models

A mathematical model of an overall compressed air system requires models of the subsystems; Production, transmission and storage, and consumption [31,118]. Such an approach is useful in the optimal dimensioning of distribution pipes for example, in order to reduce energy consumption, and also general network analysis [119]. A lumped circuit parameter model is an analytical approach that has been explored by Hyvarinen et al [119,120]. The general structure of a pneumatic network is illustrated in figure 2.42 and

consists of pressurised air centres, which are producers and consumers of compressed air, and a distribution loop where the air centres are attached through nodes [119].

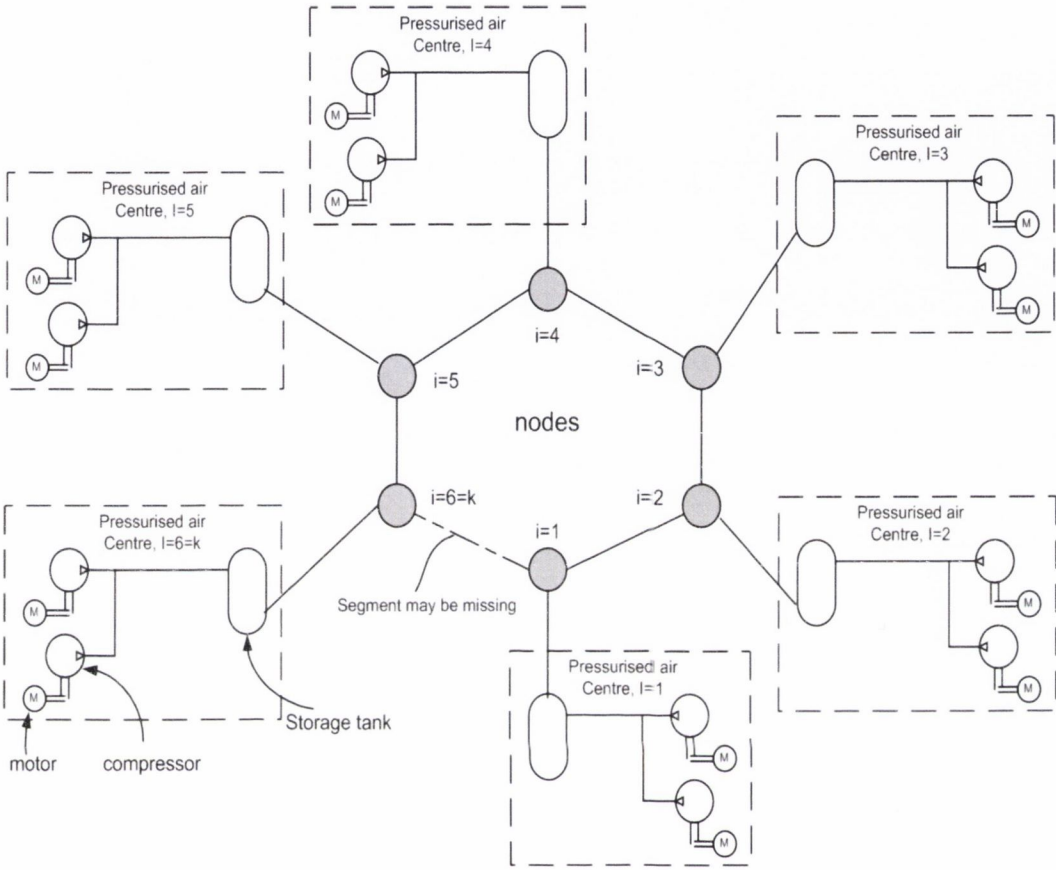


Figure 2.42: Pneumatic loop network [119]

Each air centre consists of zero to several compressor units, a storage tank, network and consumer valves, and a number of consumers (figure 2.43). If the number of compressors is zero, the centre is a pure consumer and storage may or may not be included in the centre [119]. The network valve separates the air centre from the distribution network and the consumer valve's function is to provide adequate air supply to high priority consumers by blocking the air supply to low priority consumers in the case of pressure shortage [119].

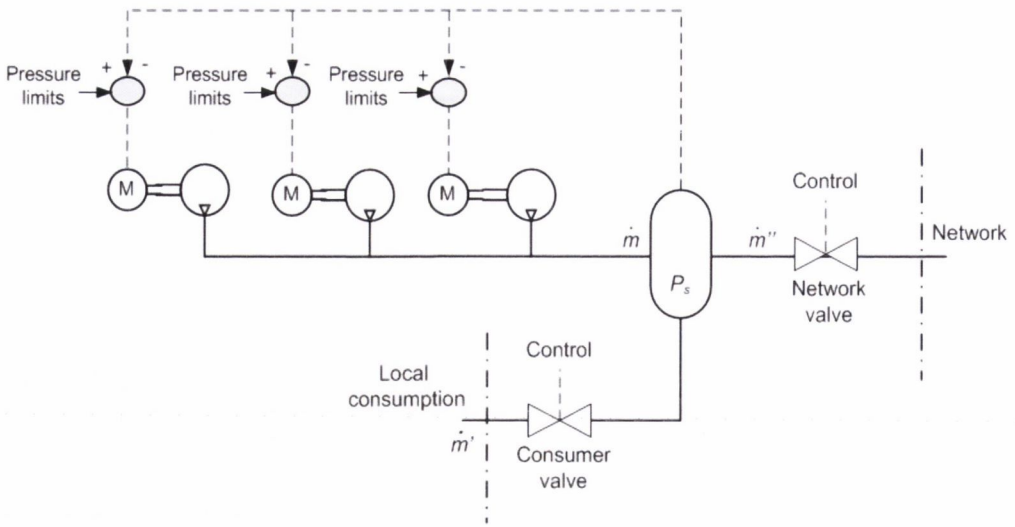


Figure 2.43: Structure of pressurised air centre [119]

An air centre with several compressors is modelled as a lumped air generator with stepwise constant air production capacity (eq 2.67). Air centres are indexed by $i=1,\dots,k$, compressors in the centre by $j=1,\dots,a_i$ and nodes $l = 1,\dots,k$. (In this case $u(t)$ is the unit step function, t_j is activation and deactivation time).

$$\dot{m}_i = \sum_{j=1}^{a_i} \dot{m}_{ij} [u(t - t_{jon}) - u(t - t_{joff})] \quad (2.67)$$

Assuming an isothermal thermodynamic process, the storage of compressed air is modelled using equation 2.68 where the storage volume V is taken as the sum of the capacity of the storage tank and half the capacity of the pipe which connects the centre to the network [119]. (\dot{m}_i is the production mass flow of centre, \dot{m}_i' is the consumption mass flow of centre, \dot{m}_i'' is the mass flow of the centre to the network).

$$\frac{d[p_i(t)]}{dt} = \frac{(\dot{m}_i - \dot{m}_i' - \dot{m}_i'')RT}{V_i} \quad (2.68)$$

The model of the node, which connects the air centre to the network, is the same as equation 2.68 except only the mass flow from the centre to the network is considered [119]. The capacity of the node is equal to half the sum of volumes of the connecting pipes to neighbouring nodes and to the air centre involved e.g. capacity of the node is lumped

network parameter. In this approach the connecting pipes in the model have the ability to conduct the compressed air, but they do not have the capacity to store it [119]. The next step pressure for the discrete model can then be calculated as a function of present pressure, air production and consumption [119]. See [119] and [120] for further details.

From the viewpoint of energy saving, to know the energy consumption of a system is very important and for pneumatic systems the energy consumption is dominated by air consumption [121]. The consumption of pneumatic drives can be difficult to measure due to dynamic and unsteady flow behaviour [121].

A general model for total factory consumption was presented by Parkkinen [31] based on application of the superposition principle to pneumatic systems. This means that the overall consumption is the sum of the individual consumptions. Passive consumption, such as leakage, is modelled by the Sanville equation assuming choked flow. Active consumers, such as cylinders and semi-rotary actuators, are modelled using simplified consumption equation 2.69.

$$q_v = \left[s \cdot \left(\frac{\pi d^2}{4} \right) \right] \cdot \frac{P}{P_0} \cdot f \tag{2.69}$$

The general consumption model considers a number of devices scattered across a factory, whose characteristics are known [31]. The consumption matrix is thus given by:

$$q(t) = \begin{bmatrix} q_1(t) \\ \vdots \\ q_n(t) \end{bmatrix} \tag{2.70}$$

The activation and deactivation of individual devices during a subinterval are also known and given by the activation matrix A. There are N columns in A each representing one subinterval of the time interval I. Each row represents the activation of an individual device [31].

$$A = \begin{bmatrix} a_{11} & \dots & a_{1N} \\ \vdots & \dots & \vdots \\ a_{n1} & \dots & a_{nN} \end{bmatrix} \tag{2.71}$$

$$a_{ij} = \begin{cases} 1 & \text{if device activated during time interval} \\ 0 & \text{otherwise} \end{cases}$$

By multiplying the activation matrix by the consumption matrix, the instantaneous total consumption during the sub-periods can be obtained [31]. Execution of the matrix multiplication yields eq 2.72.

$$q_{\text{total}}(t) = A^T q(t) = \begin{bmatrix} a_{11} & \dots & a_{1N} \\ \vdots & \dots & \vdots \\ a_{n1} & \dots & a_{nN} \end{bmatrix}^T q(t)$$

$$q_{\text{total}}(t) = [\sum_{i=1}^n a_{i1} q_i \quad \sum_{i=1}^n a_{i2} q_i \quad \dots \quad \sum_{i=1}^n a_{iN} q_i]^T \quad (2.72)$$

The transitions from one value of the function to another takes place at the moment when individual loads are activated and deactivated (figure 2.44). The consumption function is defined for every subinterval, if the moments of switching of loads is known [31].

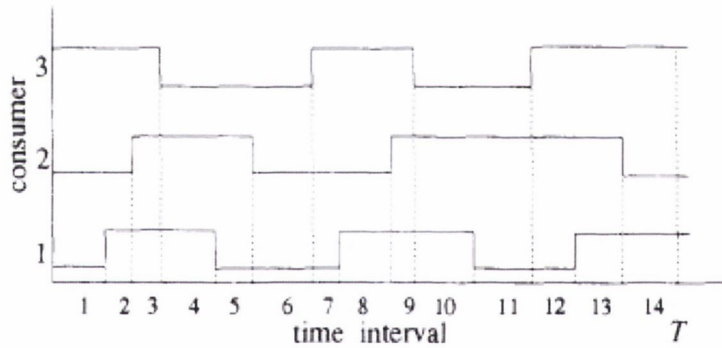


Figure 2.44: Example consumption profile for system [31]

Since the consumption of pressurised air was assumed a random function of time, the developed deterministic approach was considered by Parkkinen et al as a first step towards a fully stochastic model [31]. The approach is useful for quantifying the consumption behaviour of pneumatic systems.

2.3 Energy efficiency optimisation of pneumatic systems

A major criticism of pneumatic systems is its low energy efficiency [122]. Additionally in the industrial context compressed air usage is one of the most costly and least understood processes in a manufacturing facility [22,27].

2.3.1 Compressed air- energy consumption relationship

In a pneumatic system the electrical energy consumed in producing a volume of compressed air, occurs at the supply side by the compressor and dryer [123]. The part load efficiency of a compressor is an important aspect in calculating overall energy costs, as depending on the flow-rate required, the power consumed by the compressor motor will vary [124] e.g. when unloaded the motor can still consume considerable amounts of power. Therefore the specific energy cost (SEC) of compressed air needs to be calculated based on a period of compressor runtime data that is representative of typical working conditions. An average value for power consumed per volume of compressed air produced can then be determined using equation 2.73 [22,125]. The variables such as percentage of time the compressor is running fully loaded $L\%$ and unloaded $u\%$, and electrical power consumption P_w during load and unload are determined from compressor runtime data.

$$\text{Energy} \left(\frac{\text{kWh}}{1000\text{m}^3} \right) = \frac{(P_{w\text{load}} \times h \times L\%) + (P_{w\text{unload}} \times h \times u\%)}{\eta \times q} \times 1000 \quad (2.73)$$

Determining overall costs involves a consideration of electrical energy costs, capital costs, equipment footprint and related space costs, and other maintenance costs [124]. The capital costs include installation, inflation, depreciation, cost of water and water disposal costs. Due to the large amount of data required to estimate each individual plants specific compressed air energy consumption, there are a number of widely accepted SEC figures that are illustrated in table 2.6. The most commonly cited of these is the US Department of Energy, Office of Energy Efficiency and Renewable Energy [125].

	DOE EERE P = 7 bar(g)	Carbon Trust P = 7 bar(g)
kW/ lps	0.347	0.3

Table 2.6: Comparison of specific compressed air energy consumptions

If the rate of air consumption by a pneumatic actuator is known, the actuators equivalent electrical energy usage can be calculated based on the compressor’s efficiency or approximated using a standard specific compressed air energy consumption figure (eq. 2.74)

$$\text{Energy} \left(\frac{kWh}{\text{year}} \right) = \frac{q_v \times SEC \times h}{\eta} \quad (2.74)$$

Exergy and life cycle costs

While pressure is an essential factor in calculating overall energy costs, many studies tend to only consider flow rate as representative of air consumption and thus energy usage. Unlike hydraulics, this is not an appropriate method for pneumatics due to the compressibility of air i.e. a compressor will consume more power, outputting same volume flow rate of compressed air at higher pressure. Therefore flow rate is not proportional to energy costs for compressed air [126].

A more fundamental approach to analysing the efficiency of pneumatic systems is to examine the work producing potential or exergy of compressed air [126]. The exergy represents the amount of useful energy, which can theoretically be converted to mechanical work [25]. This concept is illustrated in figure 2.45. Air power has been defined by Cai et al as the “flux of the available energy that can be theoretically extracted from air to do mechanical work” and is represented mathematically in equation 2.75 [126], where P_w represents air power.

$$P_w = P q_v \ln \frac{P}{P_0} \quad (2.75)$$

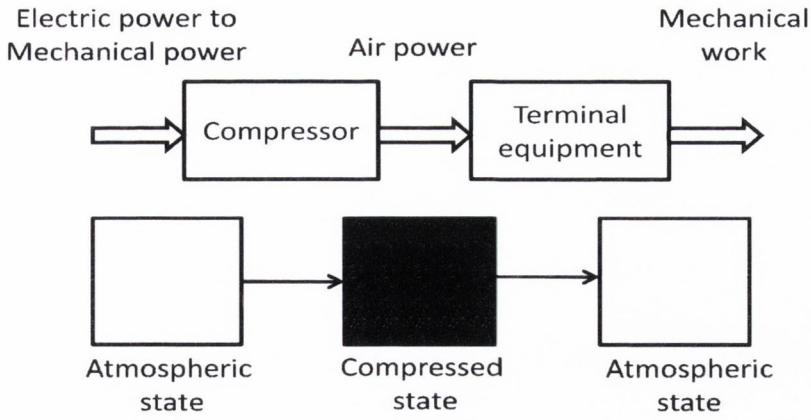


Figure 2.45: Energy flow and air state change [126]

Air power (eq. 2.76) consists of two parts: 1/ Transmission power (eq. 2.77) and 2/ Expansion power (eq. 2.78). Transmission power represents the pushing power from the upstream to downstream of flowing air. Expansion power is the work ability of air expansion. Increasing the delivery pressure, while keeping volume flow rate constant, thus has the effect of increasing air power. Temperature is also an important factor. However as compressed air usually flows in pipes at atmospheric temperature, this variable can be eliminated [126].

$$P_w = P_{wtr} + P_{wex} \quad (2.76)$$

$$P_{wtr} = P_0 \cdot q_v \cdot \left(1 - \frac{P_0}{P}\right) \quad (2.77)$$

$$P_{wex} = P_0 \cdot q_v \cdot \left(\ln \frac{P}{P_0} + \frac{P_0}{P} - 1\right) \quad (2.78)$$

Not all energy is consumed in producing compressed air and to dry the air requires additional energy input. Similarly, transmission efficiency can be low due to pressure losses at filters, valves, piping distribution and air leaks throughout the system. The air power concept is based on ideal conditions and can be improved by incorporating an approximate transmission efficiency figure into the calculations [126]. Eret et al and Zhang et al have improved the exergy analysis further by incorporating the efficiency of the drier [25] and aftercooler [123].

Zhang et al have applied the air power concept to assess the overall energy efficiency of lubricant-injected rotary screw compressors [123]. The efficiency of compressor and aftercooler can be calculated using equation 2.79 where E_o is the air power of the output air flow after the compressor's aftercooler, $E_{compressor}$ and E_{cooler} are the electricity supplied to the compressor and aftercooler respectively [123].

$$\eta_{total} = \frac{E_o}{E_{compressor} + E_{cooler}} \times 100\% \quad (2.79)$$

Pneumatic actuation systems are typically considered less energy efficient than their equivalent electric counterparts. However, this is not always the case, as actual conversion efficiency is a function of actuation conditions [127]. A comparative study of both systems by Cai et al, utilising the air power method, indicated that the energy consumption of an actuation system was dependant on its duty cycle, that is the ratio of moving time to the total time for one actuation cycle [127]. At a duty ratio of 1 (e.g. the actuator does not stop), the electric actuators were more efficient. However, for functions that require infrequent actuation, or maintaining loads over a periods of time, less energy is consumed comparatively by the pneumatic cylinders [128].

While in practise many actuators will often have a higher duty cycle, for clamping and gripping operations pneumatics is particularly efficient, since an air buffer provides continuous force without the need for continuous feeding of energy [20,25]. Therefore it is not always clear, in particular for a workshop consisting of thousands of actuators, with large ranges of duty cycle ratios across applications, which technology is optimal from an energy efficiency perspective [127].

Additionally many comparisons of pneumatic and electric systems are based on different technologies such as open loop versus closed loop control systems with considerably different capital costs [33]. In order to assess the full costs when comparing pneumatic and electro-driven systems, life cycle costing approaches particularly from a product user perspective, are useful [128]. Life cycle costing allows for the identification of main cost drivers by considering all economically relevant monetary flows over the whole life cycle [129]. Alternative life cycle cost concepts are available and differ with respect to their scope e.g. life cycle phase, manufacturer or operator costs [129]. A total cost of

ownership approach specifically considers all operator related costs. Such an approach, LCC based on users, has been developed by Zhang et al for pneumatic and electric actuators, and is composed of three parts; acquisition cost, energy consumption and maintenance cost [128].

The acquisition cost of pneumatic actuators must include the cost of compressor, receivers, dryer, pipe, valves and other components that are required to operate the actuator while the acquisition cost of the electric system consists of the electric actuator itself and its controller [128]. Depreciation costs over appropriate periods must also be included. The results for the total acquisition costs of equivalent pneumatic and electric actuators and their support equipment are shown in figure 2.46.

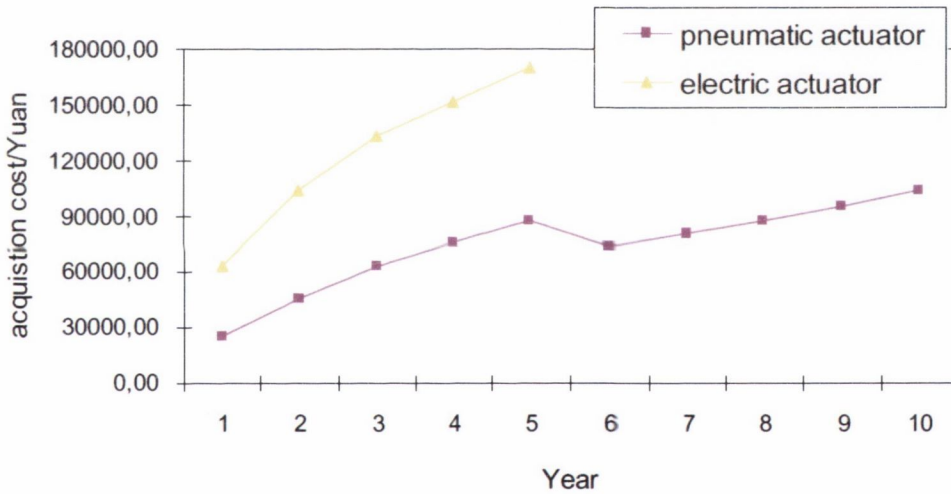


Figure 2.46: Comparison of two actuators total acquisition cost [128]

In terms of energy consumption for electric systems, power is consumed by the actuator and the controller while for pneumatic systems it is based on volume of air consumed and compressor efficiency [128]. Maintenance charges for both systems are assumed the same [128]. As with the exergy based approach, analysis from a LCC-operator perspective indicates the dependence of energy consumption on actuation frequency (figure 2.47). A more comprehensive approach involving dynamic life cycle costing based on lifetime prediction has been proposed by Hermann et al [129].

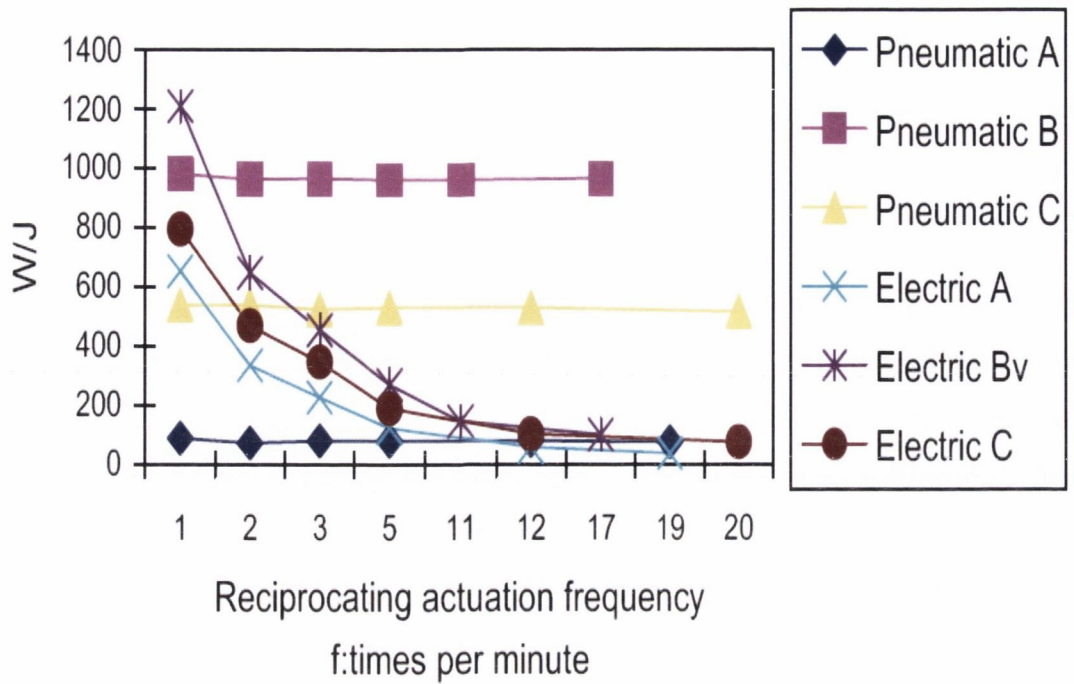


Figure 2.47: Energy consumption for electric and pneumatic actuators [128]

2.3.2 Energy saving in pneumatic systems

Pneumatic drives

The reference literature describes two variants for improving the energy efficiency of pneumatic drives: energy recuperation and the reduction of energy consumption where the latter can be broken into the use of different pressures and the utilisation of expansion energy [122,130]. The design of pneumatic circuits is critical in determining the system's overall compressed air consumption. The best component for any circuit will depend on accompanying objective such as minimisation of energy consumption or capital costs, or maximisation of productivity [131]. A trade off analysis is required for such competing objectives. The use of total cost of ownership models allows for efficient prioritisation of objectives for the designer [132,133].

Actuators form a critical element in any pneumatic circuit but consume significant amounts of compressed air and are often improperly sized [131]. In many cases this is due to the lack of reliable formulas for actuator selection, leading engineers to integrate

excessive safety factors in the selection calculations [22]. Cylinders are also over dimensioned due to the fact that rather than exactly meet force requirements, the next largest cylinder in the range of sizes defined in DIN ISO 6431/2 is selected [130]. This combined with a common supply pressure for all cylinders ensures that excessive energy is consumed [130].

Simulation based design allows for optimal component selection in pneumatic systems [134], and is available from OEM's such as Festo and SMC. The energy consumption can also be reduced by adapting the pressure to each cylinder or group of cylinders. For specific applications that require higher pressure than necessary elsewhere in a plant, pressure boosters are useful and avoid over pressurisation of the entire compressed air system (figure 2.48) [135]. An exergy based approach to pressure booster design has also been proposed by Yan et Cai [136].

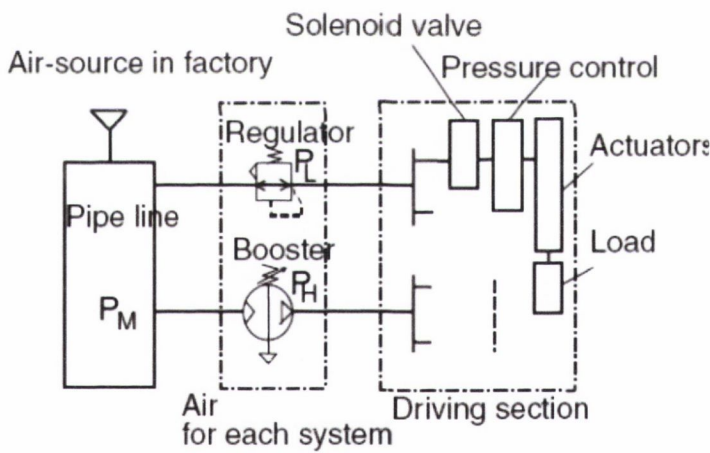


Figure 2.48: Local pressure boosters for high pressure consumers [135]

The design concept of dual pressure pressurisation has been developed extensively by Fleischer and has proven effective in reducing energy usage [32]. Actuator motion involves either extension or retraction of a load, however the loads on both strokes are rarely equal [131]. Building on this fact, dual pressure pressurisation involves the use of two different pressures to move each load [131]. Furthermore a reduction in pressure in one end of the actuator usually permits a pressure decrease in the other end, since there is a

smaller exhaust-pressure load to overcome [32]. Single and dual pressure circuit designs are illustrated in figure 2.49.

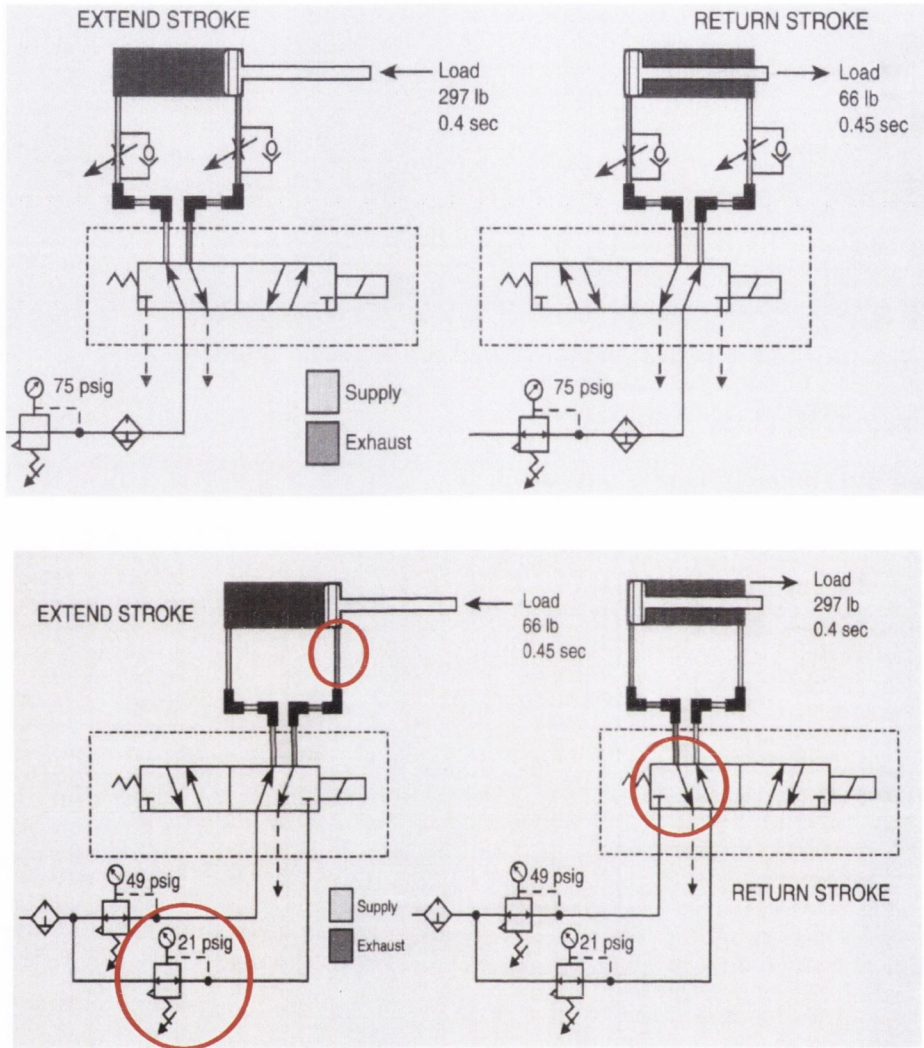


Figure 2.49: Single (top) and dual-pressure (bottom) design with highlighted circuit alterations, from Fleischer [131]

In the single pressure design example, the system uses 75 psig to move variable loads in both directions, and flow controls throttle exhaust airflow without altering regulated pressure levels to achieve required performance times [32]. In the dual pressure system, adjustable regulators are used to move loads at required speed and two pressures were utilised for extend and retract strokes respectively. In this case (figure 2.49), lower dual pressures moved the same loads as single pressure system in the same time whilst

simultaneously consuming less air. Fleischer reported that for one industry case study, energy cost were reduced by 51.6% [32]. In many cases, it was noted that productivity was also improved through shorter cycle times. Average energy savings of 25% using dual pressures are reported by Beater [13].

An alternative pneumatic circuit design for dual pressure circuit is shown in figure 2.50. This design is useful for manifold mounted valves, since a lower pressure retract may not be desirable in all situations. This circuit is effectively a combination of meter in, for the retract stroke, and meter out control, for the extend stroke [13].

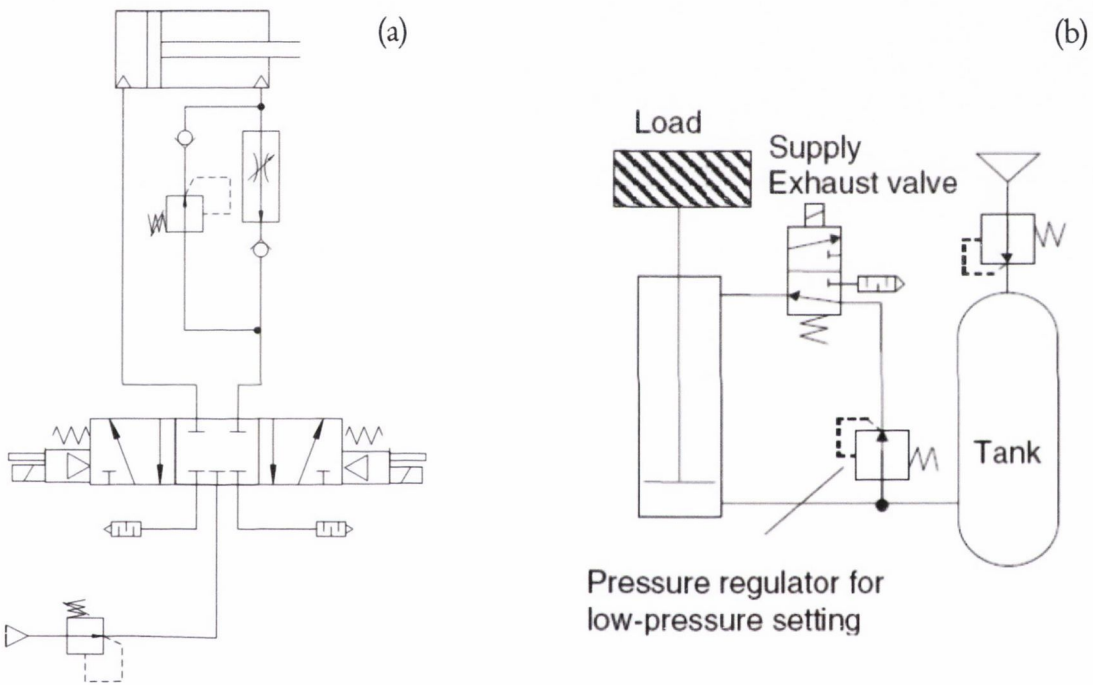


Figure 2.50: (a) Alternative dual pressure pneumatic circuit design [13] and (b) energy saving lifter [135]

A similar method has been proposed by Senoo et al [135] for application to lifting drives (figure 2.50). The compressed air in the under chamber will be balanced with the heavy load and is not exhausted but flows to and from the tank. By reducing the pressure to the upper chamber (return stroke), air consumption was reduced by 75% because exhaust occurs only once a cycle [135].

Cylinders are usually driven during their entire stroke, and at the end of the stroke the entire cylinder is filled with air at high pressure. When the cylinder motion is reversed, the compressed air is vented with a destruction of the potential to do work by the expansion of the air [137]. However, if the air supply valve is closed after the piston has advanced some fraction of the stroke; the air will expand during the remainder of the stroke. The drawback of this approach is that the cylinder force begins to drop as the gas expands, and this decrease may not be compatible with the force required to accomplish the task [137]. To overcome this problem, the use of a linkage mechanism to match the cylinder force to the load was proposed and investigated by Otis et al [137].

In figure 2.51 the cylinder is trunion mounted at fixed pivot B and connected to a single link at pinned joint C with the other end of the link connected to fixed pivot A. When air is supplied to the cylinder, the rod extends but the cylinder is constrained to rotate about pivot B, shifting the load from the cylinder to the link [137]. When the air supply is cut-off, the piston will continue to extend while expanding the air in the cylinder [137].

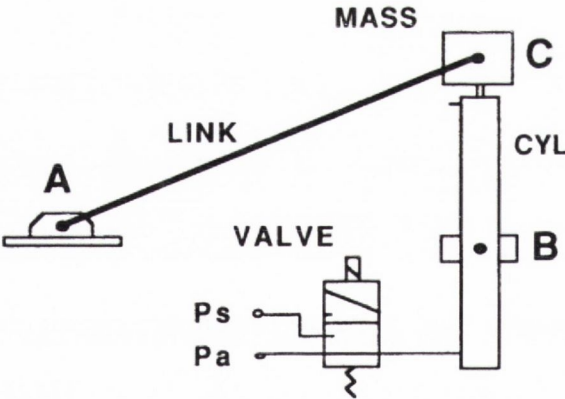


Figure 2.51: Pneumatic lifter with inverted slider-crank mechanism [137]

Otis et al estimated that consumption savings of up to 50% were theoretically possible using this approach but no experimental results were provided and the effect on savings of pressure drops and friction in real pneumatic systems remains to be quantified [137].

If the input air to a cylinder is throttled (i.e. meter in), the air consumption can also be reduced through the use of expansion energy [130]. The pressure in the driving chamber will build up a slower rate while the second chamber is evacuated completely. If the pressure supply is cut-off once the cylinder reaches its final position, the pressure in the first chamber will be well below the supply pressure in final state [130]. However a drawback of throttling the input air is stick-slip behaviour at the start of motion and the stroke time dependence on load [130].

Another circuit modification introduced by Li et al uses an accumulator and pressure boost valve in the exhaust line of a cylinder (figure 2.52). Using this approach exhaust air can be recycled for another actuator circuit. Alternatively the recovered air could also be redirected back for use in the same circuit [138].

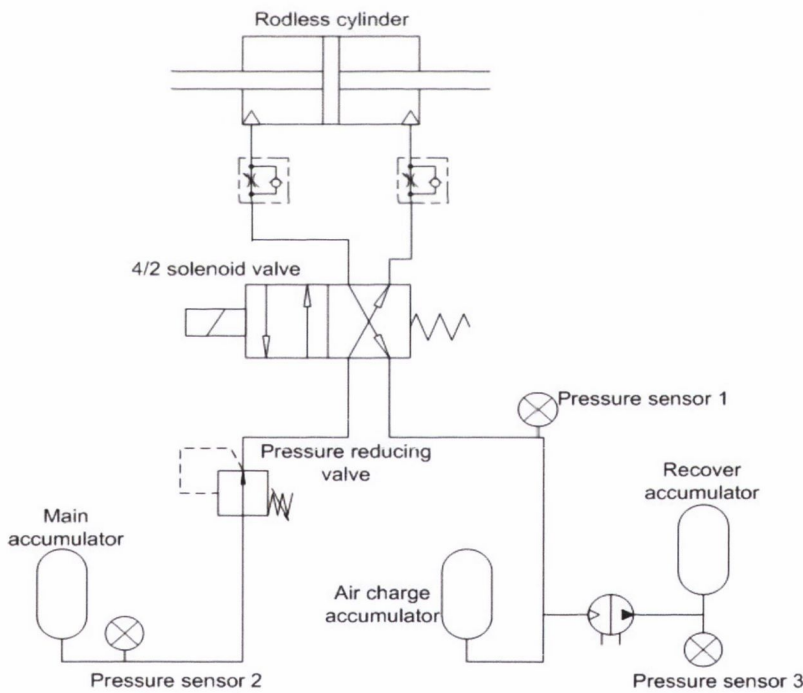


Figure 2.52: Recovery of exhaust air to accumulator and boost valve [138]

Savings of 20% were estimated using this approach though the savings are limited by the capability of the boost valve [138]. Instead of using a boost valve, Li et al and Mutoh et al suggest using the recovered exhaust air directly for lower pressure applications such as unloaded return strokes or air blowing [138,139]. The concern with taking this approach

is that the backpressure in exhaust line might decrease the performance of the actuator. Experimental investigations by Mutoh et al [139] on a meter out pneumatic actuator system indicate that the response of the cylinder is almost unaffected by higher exhaust line pressure once there is choked flow on the exhaust side (figure 2.53). In the case of figure 2.53 choked flow occurs for exhaust line pressures between 0.1 to 0.3 MPa.

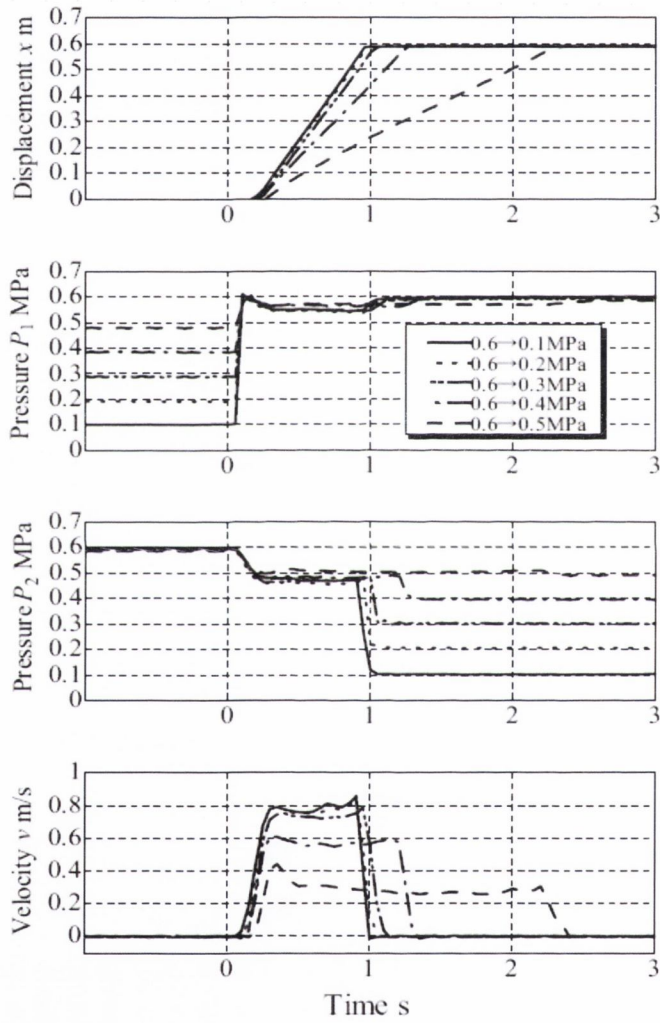


Figure 2.53: Cylinder performance with range of backpressures [139]

Additionally the start-up delay is decreased due to higher initial pressure on the primary side. However, this approach is load dependant since the movement of the load depends on the pressure differential and means that, even with a short delay, a larger load will lead to reduced velocity and increased position time with higher exhaust line pressures

[139]. Typically in the industrial context, meter out stroke time control is employed and the retract stroke is unloaded, so this approach could still be useful.

Air Blowers

Compressed air is widely used in industry for cleaning, cooling, drying parts and removing material: metal chips and other scrap. This is typically achieved through open blow operations using air nozzles, knives or simple orifices/open pipes. Since in many cases over 50% of the total air consumption in a plant can be due to blow operations it is an important area for energy savings [135].

In many situations simple open pipe blow-offs are employed to fulfil these functions. In contrast, engineered air nozzles and jets use the Coanda effect to amplify air flow by capturing free surrounding ambient air. In the case of the nozzle in figure 2.54, compressed air ejects out a thin ring on the outer perimeter and travels along the outer wall of the nozzle. The high velocity air entrains surrounding air into the stream and a centre hole concentrates the air stream into a high volume, high velocity, blast of air [140]. The impinging pressure, often the variable of interest for an air blow nozzle, is determined by the nozzle diameter, nozzle inlet pressure and distance from nozzle to work [135].

The dimensions of the nozzle are important in determining the efficiency of the blow process. For example, it has been shown that by decreasing the length to diameter ratio, the supply pressure can be reduced without affecting the net blowing force [141]. The nozzle internal geometry has been investigated using a computational fluid dynamics approach by Lovrec et al [23]. The design object was to achieve minimal air flow to the nozzle with maximal output by optimising the suction effect. It has been shown that using energy saving nozzles can reduce compressed air consumption by up to 40% [23]. Additionally nozzles can be cycled on and off eliminating idle or non-functional usage [140].

Optimisation programs, based on the simulated pressure distribution of a jet for a single orifice, are available to designers. Based on desired flow force/impinging pressure, the simulation tools optimally determine nozzle size, supply pressure and blowing distance

[141]. Air consumption reductions of up to 70% have been reported for air blow systems using such tools [135]. Lovrec et al [23] also used a CFD-based approach to design a more complicated cooling block for a blow moulding process with similar good results.

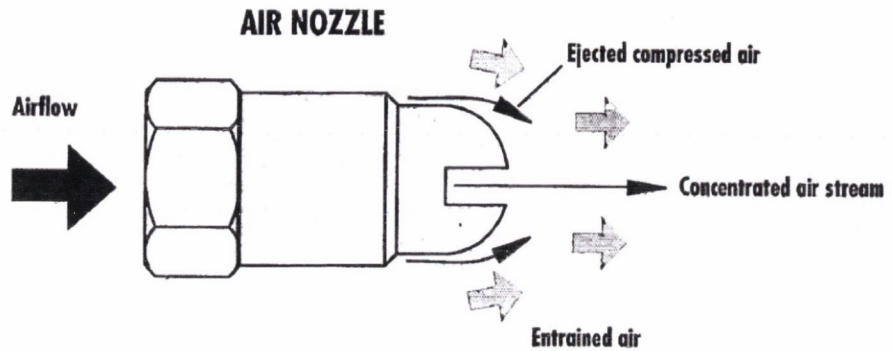


Figure 2.54: Coanda effect on air nozzle [140]

Generally, air flows to blowing systems through pressure regulators in most industrial facilities. Using the air power concept, Cai et Xu have shown that up to 39% to 47% of the energy potential of compressed air is lost in this process [141]. In order to avoid energy losses at the regulator, Cai et Xu have proposed a pulsed air blowing system as shown in figure 2.60. In the proposed system, the supply pressure to the nozzle rises, from the typical regulated pressure of 3 bar to the air system pressure of 6-8 bar, but the output flow is pulsed. This is achieved by outputting a pulsed signal from the PLC to drive the solenoid valve [141]. To reduce the overall pneumatic power consumed, the duty ratio must be small. An investigation of the pulse frequency and duty ratio indicated that with optimal parameter selection, energy savings of 70% were achievable in comparison to standard blow system.

Since the complexity associated with a PLC based pulsed blow system may not be robust enough for an industrial environment, Cai et Xu also proposed a self-oscillated system as shown in figure 2.55. In this system an air operated valve starts in the right position and air flow through two branches, to the nozzle and to the pilot port (G) of the valve through a throttle (1). The air in the right operating chamber of the valve flows through another throttle (3) to the atmosphere. When the pressure differential across the

valves V1 and V2 supply the chambers with pressure, valves V3 and V4 exhaust air from the chambers and valve V5 is a by-pass valve that permits cross-flow [33].

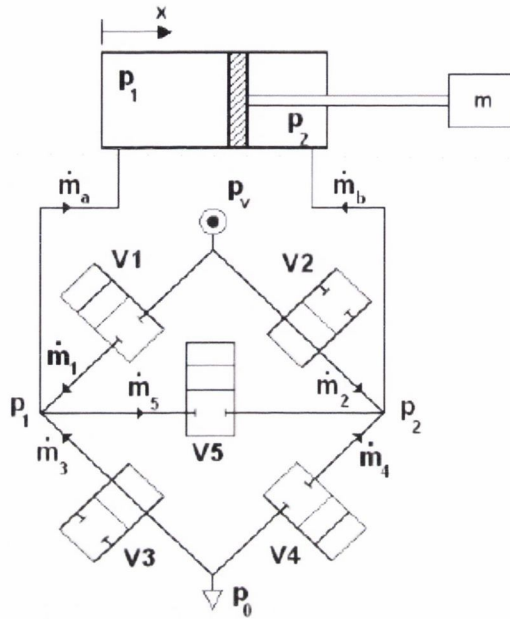


Figure 2.56: Five valve bridge connection for energy optimal open loop control [33]

The optimisation problem considered the movement of a specific mass along a stroke within a specific time, with the objective of minimising air consumption [33]. The optimisation strategy involved using a genetic algorithm and strategy of evolution [33]. If only the minimisation of air consumption is considered, it was shown that up to 61% of air could be saved [33]. However, this was caused by the low pressures in final positions which implies the system would be sensitive to external forces. This approach is not comparable to standard pneumatic control which achieves the maximum possible final force [33]. Additionally, a large reduction could be achieved without the use of a bypass valve [33].

In order to investigate the savings due to the bypass valve, Doll et al considered another scenario in which the cycle time, pressurisation in final position, mass and cylinder were all the same [33]. Results indicated that significant air savings of up to 30% could be made with the use of an optimised control sequence and a bypass valve active

before and during movement of the piston [33]. A drawback of the bridge connection in combination with the optimised open loop control approach, however, is that it is difficult to find a general rule for parameterised control [33]. However, it does demonstrate the potential for significant improvements in drive energy efficiency.

Condition monitoring and diagnostics

Condition monitoring for pneumatic systems is an important means of reducing costs, machine downtime and improving life expectancy of machinery [74]. According to Kambli [142] many users tend to run pneumatic systems until they fail, typically because it is difficult to isolate the process or component contributing to higher consumption.

In particular from an energy efficiency perspective, leakage is an expensive waste of compressed air. For example, a single ¼” leak can incur an annual cost of \$12,000, based on an energy cost of \$0.07/kWh [143]. In many plants demand due to leakage, can account for 20% to 30% of total compressed air production capacity [125]. Common problem areas for leakage include couplings, hoses and tubes, fittings, pressure regulators and valves (i.e. mainly at point of use) [125,143]. The standard approach to leak detection and repair involves regular audits, several times a year, with the use of ultrasonic detection equipment or manual inspection [143-145]. However, it is now recommended that system air consumption be monitored on an on-going basis in order to pinpoint leaks and losses [142].

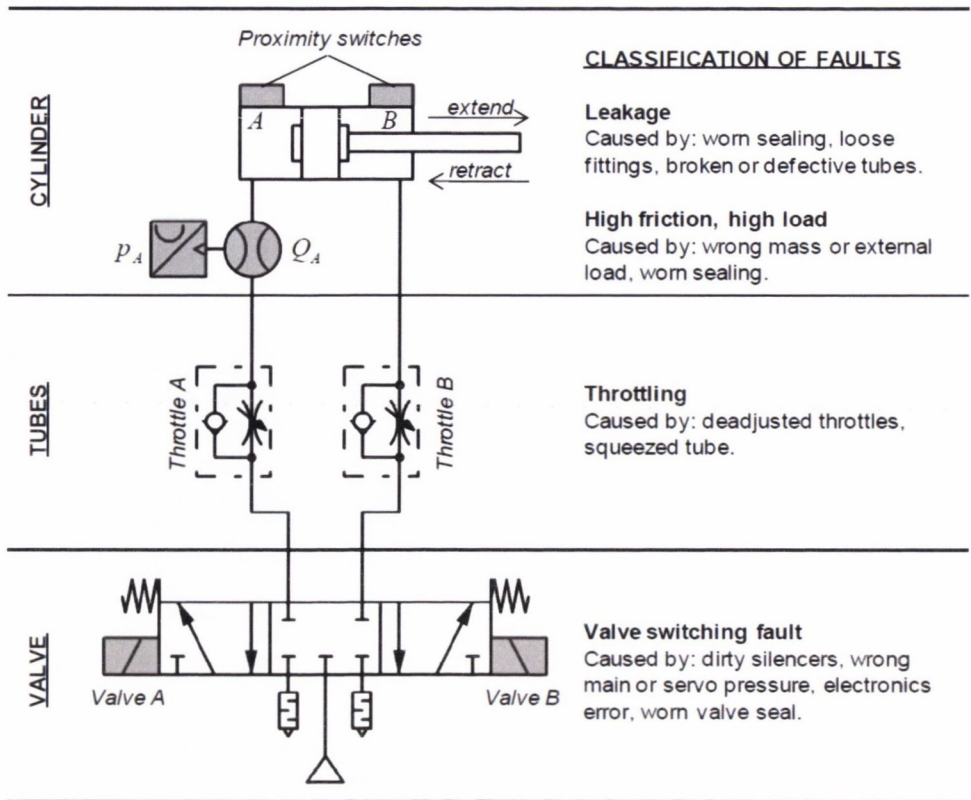


Figure 2.57: Pneumatic subsystem with possible faults [74]

Faults manifest through symptoms such as increased or decreased pressure or position speed (figure 2.57) [74]. Positioning times and average speed can be assessed with the use of end-position switches, stroke counters and valve control signal [20,74]. However, a detailed diagnosis is only possible by using additional pressure and flow sensors though only if they are required [74]. A list of diagnostic approaches with different diagnosis depth is presented in figure 2.58.

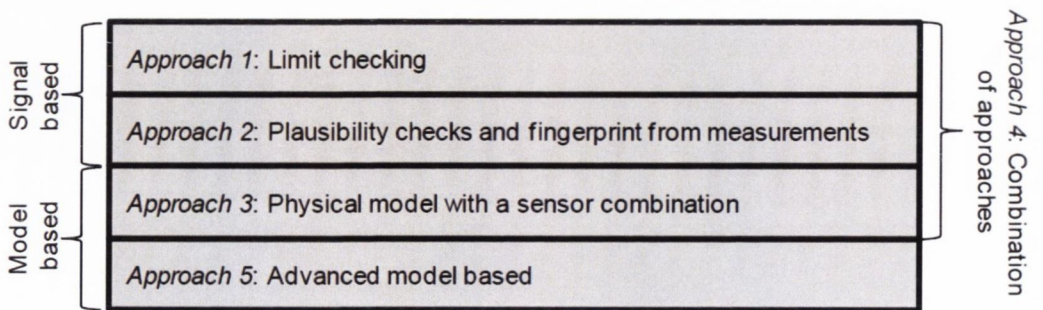


Figure 2.58: Diagnostic approaches [74]

Limit checking, the simplest approach, consists of producing symptoms with available signals (valve, proximity, pressure, flow etc) [74]. Examples include supervision of pressure or characteristic values (i.e. average speed of piston) within specific limits. The disadvantage of this approach is that the observation of symptoms alone is not enough for fault isolation[74].

Plausibility checks is a type of limit checking technique except with wider tolerances i.e. measurements are evaluated with regard to credible values [74]. An example is the detection of increased friction by increased or decreased pressure during the extend and retract strokes. This approach is also useful for detecting valve switching faults, leakage and higher loads [74]. The disadvantage of plausibility checks is that there is not a 100% guarantee that the faults are detected since many faults can have similar symptoms on the measured pressure [74]. However, plausibility checks can be combined with fingerprint tables for confirming diagnosis and as a first step in identifying faults before quantifying their value [74]. Fault detection will still depend on the available sensors.

Using a model based approach the position of the cylinder can be calculated, based on measured mass flow and standard polytropic chamber models, and used as a parameter for further diagnostics, for example to detect leakage (figure 2.59). Throttling of the flow by squeezed tube can also be determined by detecting changes in circuit conductance [74]. This is achieved by monitoring the pressure (upstream and downstream) and flow.

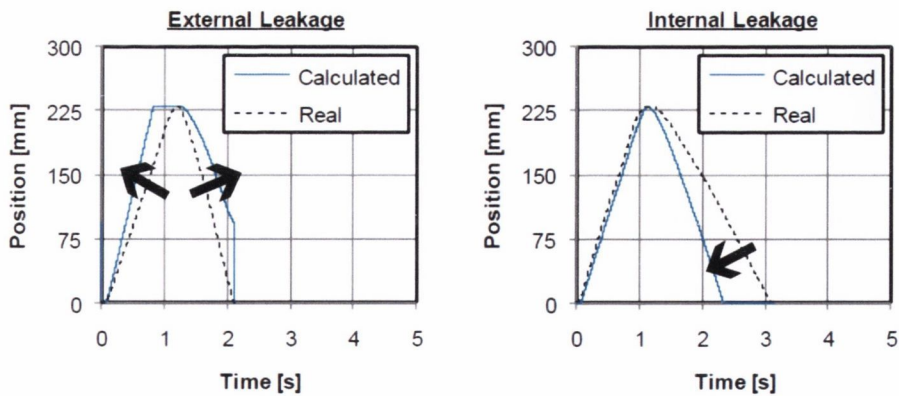


Figure 2.59: Behaviour of calculated position when leakages occur [74]

If the all the diagnostic approaches are combined and work in sequence, then it is possible to detect all the faults shown in figure 2.57 [74]. The procedure then consists of isolating any faults through elimination. Commercial condition monitoring solutions are available from Festo AG. Their condition monitoring system monitors flow and pressure, and air consumption by using regular flow and pressure sensors, a diagnostic controller and a graphical display [142].

2.3.3 Energy saving in servo pneumatic systems

In order to improve the energy efficiency of a servo-drive system, Yang et al installed a bypass valve in the pneumatic circuit to allow for recycling of some exhaust air [122]. The typical speed response for a traditional type controlled servo-pneumatic drive is shown in figure 2.60.

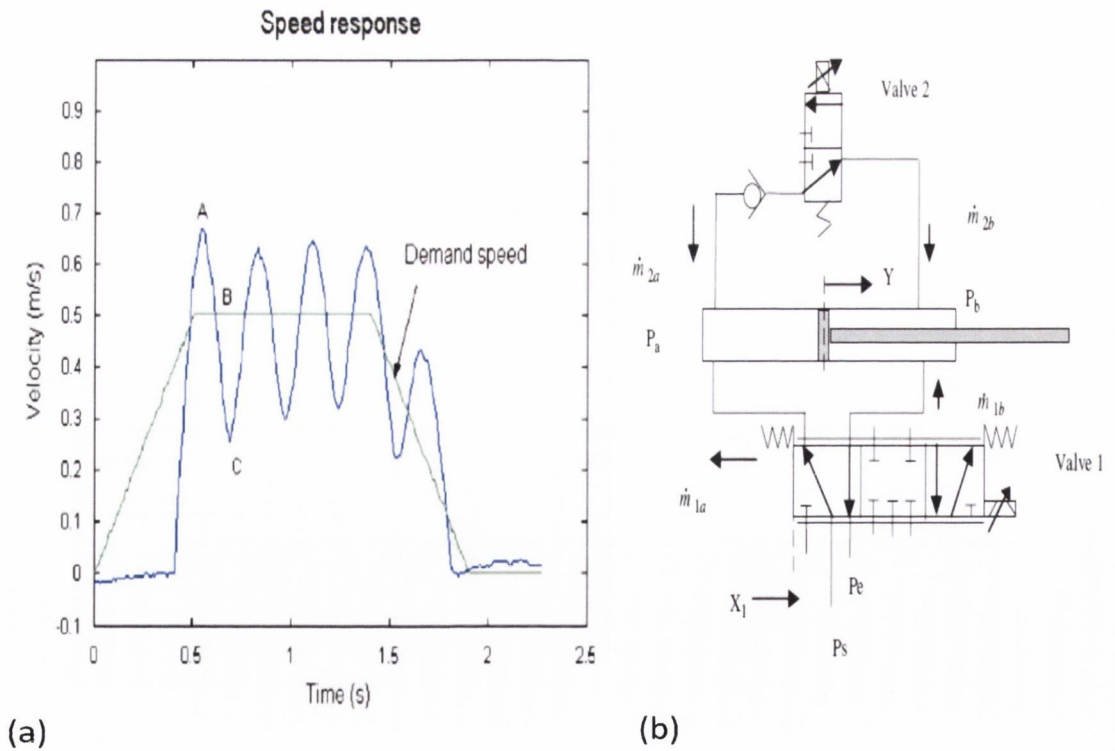


Figure 2.60: (a) Typical speed response of traditional control and (b) by-pass valve control of an asymmetric cylinder [122]

From the maximum speed point A, the controller will reduce the speed which means the pressure in the drive chamber (A) will be reduced and the exhaust pressure in chamber B will increase, until the minimum point C is reached [122]. If the bypass valve is open (figure 2.60) from point A to point C the exhaust pressure can be greater than the charge pressure and some of the exhaust air will be recycled into the drive chamber [122]. In order to guarantee the system working in case that pressure in chamber a is greater than chamber b, a check valve is fixed in the bypass path to allow flow in only one direction. This avoids the need for open and close control of the bypass valve according to piston position and chamber pressures which is complicated to control [122].

Results indicate that 12-28% air consumption savings can be made using the bypass valve method, depending on supply pressure and stroke length. Based on the additional costs (extra valves) for building the system, the payback for the method was approximately 2.6 years [122]. Additionally system performance can be improved since pressure in both chambers can balance quicker leading to reduced overshoot [122].

A similar cross-flow valve configuration for recycling pressurised air (figure 2.61) was developed by Xiangrong et Michael [146]. However, a nonlinear control approach was utilised that constrains the valves only by tracking and energy saving objectives [146].

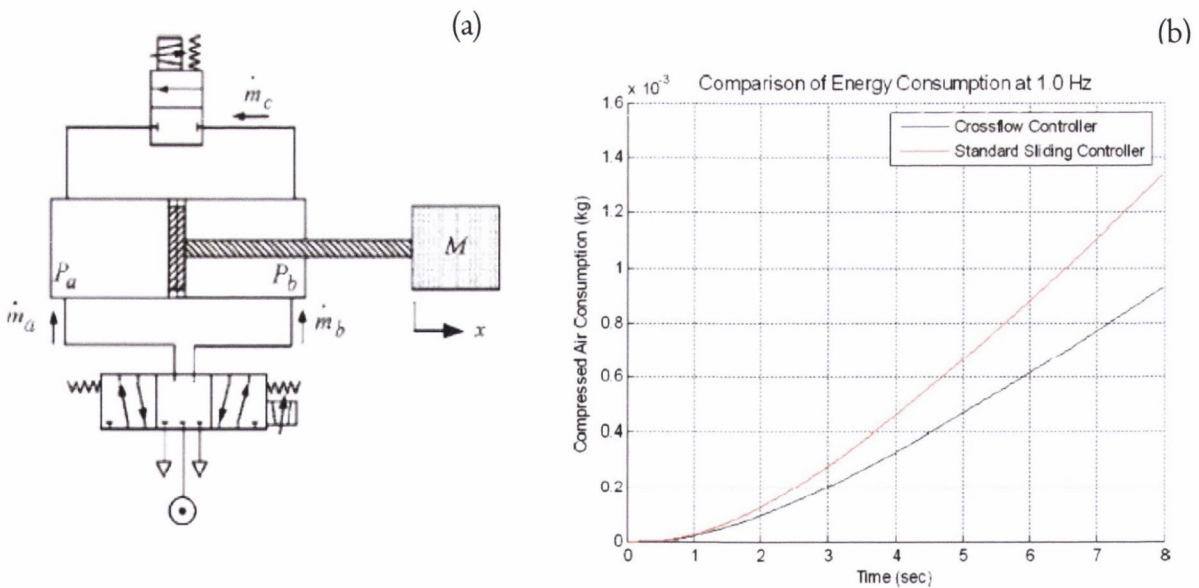


Figure 2.61: (a) Pneumatic servo with inter-chamber flow path and (b) air consumption in comparison to standard controller [146]

The proposed controller was developed by calculating the control effort (i.e. differential mass flow rate) required for tracking, and second by calculating the extent to which the cross flow can contribute to that differential mass flow rate [146]. Results demonstrated that energy consumption could be reduced by 25-52% depending on tracking frequency [146]. Additionally it is noted that symmetric (e.g. rodless or double rod) cylinders would provide greater opportunity for cross flow energy savings [146].

The energy efficiency of pneumatic systems and their control method's is of particular interest in the field of mobile robotics where local power source (air supply) is limited [147,148]. In traditional servo pneumatic systems the area that connects one cylinder chamber to supply pressure is constrained to be the same area that connects the other area to exhaust [149]. An energy saving method is presented by Al-Dakkan et al [147,150,149] that involves decoupling a standard 4 way valve into two 3 way servo valves (figure 2.62). This decoupled configuration enables independent control of charging and discharging valve areas and thus cylinder chamber pressures [149]. The resulting two control degrees of freedom can be used to satisfy a performance constraint and an energy saving constraint, which in this case minimises cylinder pressures i.e. the modified servo is a two input single output system [149]. The proposed control approach is based on a standard sliding mode control approach, in which the single control degree of freedom is utilised to satisfy a sliding condition, which in turn provides stable tracking with a desired dynamic error [147]. The proposed energy saving approach modifies the standard sliding mode controller to provide only the actuator output impedance necessary to achieve desired tracking performance [147].

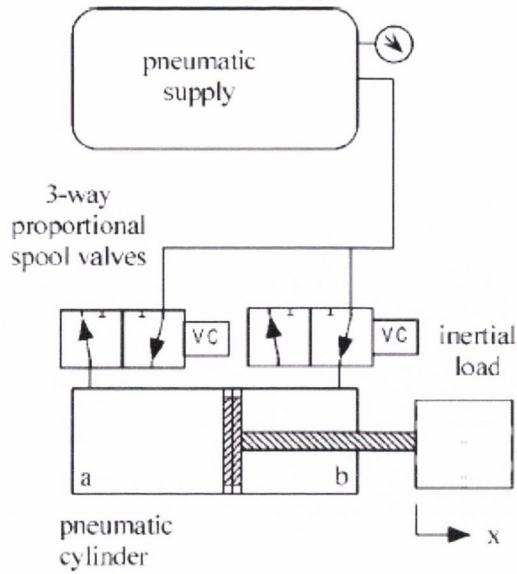


Figure 2.62: Modification of standard pneumatic servo actuator for accommodating dynamic constraint based control [149]

This control approach is essentially variable impedance controller which maintains an output impedance required to track a desired trajectory, and this minimises the required air mass flow rate [149]. Experimental results indicated that energy savings of up to 45% were possible with essentially no sacrifice in tracking performance. The energy savings were dependant on the tracking frequency with less savings possible at higher frequencies [149]. This is due to great actuator demands and output impedance must be higher to provide the desired degree of tracking performance [149].

A similar methodology for energy saving using a decoupled valve configuration with separate adaptive robust controllers for motion and pressure trajectories has been proposed by Xiaocong et al [151]. Other research by Ke et al has shown that optimal control velocity profile is obtained by using a shape close to a sine function [152].

Two pulse width modulation (PWM) type control methods were investigated by Granosik et al in order to assess their air consumption efficiency. The first system consisted of two on-off (2/2) valves, and is the least expensive solution for implementing proportional control of a pneumatic cylinder since it requires only the two valves and position feedback [148]. The second system consists of four 3/2 control valves and is called proportional position and stiffness controller (figure 2.63).

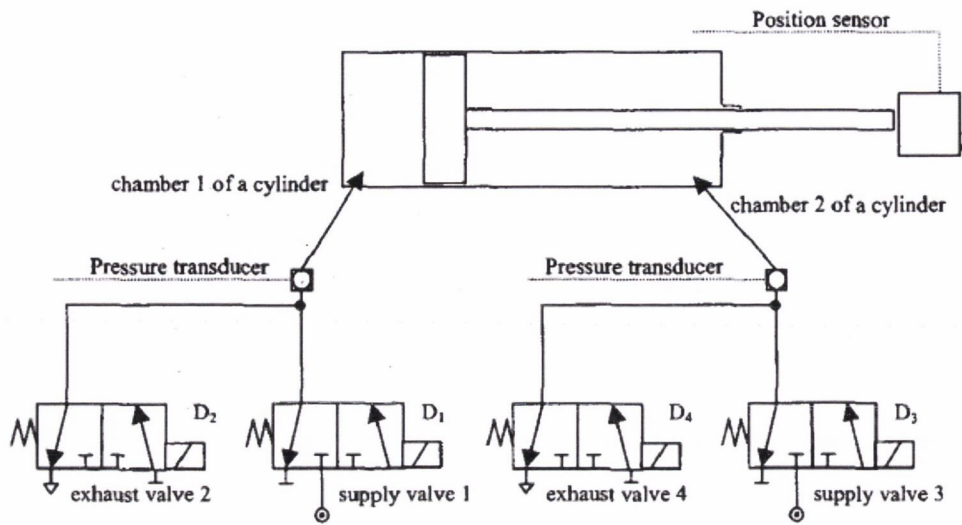


Figure 2.63: Pneumatic circuit for PPS controller [148]

The conventional control method results in continuous airflow even during steady states, causing excessive air consumption [148]. In comparison using four valves per cylinder and a PID controller that shut off air flow when position error reached a reasonable minimum, allowed the air consumption to be reduced from 3.37L to 0.4 L [148]. The PPS method reduced the consumption even further to 0.11 L [148].

2.3.4 Compressed Air System Optimisation

Best practise technical measures for energy efficient compressed air systems are widely reviewed in trade journals [28,29,47,61,123,153-156]. The focus for this discussion is on research based energy saving methods.

Two level system design

The power needed to drive a compressor is primarily dependant on the pressure ratio, but the energy available at point of use is dependent on the pressure difference between inlet and exhaust [69]. Therefore for energy savings there should be an objective to generate a high pressure differential with a low pressure ratio [157]. In two level systems

there is a high pressure delivery line and a lower pressure return line to form a closed circuit (table 2.7) [157].

	P_u	P_d	ΔP	CR
Conventional	6	1	5	6
Two-level	11	6	5	1.83

Table 2.7: Typical values for standard and two-level CA systems [157]

Energy savings of up to 50% have been estimated by implementing such closed loop compressed air systems [157]. However, there are a number of disadvantages that restrict two level system's industrial implementation. The distribution network design and installation complexity is increased as a double main is required to take exhaust air back to the compressor inlet and also provide lower pressure to blow devices. Tools that operate with back pressure at the exhaust port are not available and modifications would be necessary [69].

Optimal compressor control

The interaction of generation, transmission and consumption subsystems of a compressed air network strongly affects overall system energy requirements [118]. While the isothermal coefficient of efficiency is provided by compressor vendors, it is difficult due to the complexity of the overall pneumatic line to quantify the energy efficiency of the system [118]. Based on the overall models of compressed air systems developed in [31,119,120] a compressed air energy efficiency index has been proposed [118]. Minimisation of the index (CA-index) allows the optimal operation policy for compressor systems to be formulated [118]. The efficiency of the CA system (eq. 2.80) is determined from the relation of theoretical minimum power (i.e. isothermally) to the average power during duty cycle [118]. The real power is determined by computational means or measurements.

$$CA_{\text{index}} = \frac{\eta_{\text{isot}} P_{\text{isot}}}{P_{\text{real}}} \quad (2.80)$$

The energy efficiency of the compressor system depends on adjustable parameters; minimum compression pressure and pressure difference (between control points) [118]. The theoretical solution to the CA-index optimisation problem is to keep maximum pressure difference and minimum compression pressure as low as possible. However the maximum permitted switching frequency of electric motors forms a hard, system specific, constraint on the lower limit of the maximum pressure difference [118]. There is a trade-off between using idle run, where a small pressure difference between cut-off is possible, or switching the motor off completely and using a larger pressure difference [118]. If the maximum switching frequency and the parameters of the system are known, the minimum average power during duty cycle for switching or idle running can be compared. This approach (CA index) allows for the optimal two-point control strategy for a multi-compressor system to be determined, based on the energy efficiency during a given interval [118]. However, this approach does not account for changes in production conditions.

Localised Air Generation

Another aspect of compressed air usage that is widely believed to be inefficient, from an energy efficiency perspective, is the generation and distribution of air from a centralised plant [22]. A number of factors hinder the system efficiency including infrastructure complexity, energy storage and excess supply [22]. Plant air systems can be extremely complicated, especially in large scale plants. Extensive distribution pipe work can lead to high maintenance and operational costs through low efficiency [22]. Constant pressure is difficult to maintain due to inevitable leakage and limited storage capacity but is essential for the practical operation of production equipment [22]. This means that excess compressed air is generated in order to meet the maximum demand at any time. In addition, to increased energy consumption, this can lead to reduced equipment life through increased wear.

A quantitative analysis of three compressed air supply patterns for an automotive manufacturing plant was presented by Yuan et al [22]. Environmental value system tools

were employed to analyse the economic and environmental impact of plant air, point of use and local generation type supply of compressed air. Plant air refers to the supply of compressed air from a centralised compressor plant and distribution through the factory via pipe work. Point of use involves each machine being exclusively supplied by an independent compressor. In local generation, a compressor supplies compressed air to a number of machines that are grouped together. Each supply pattern is illustrated in figure 2.64.

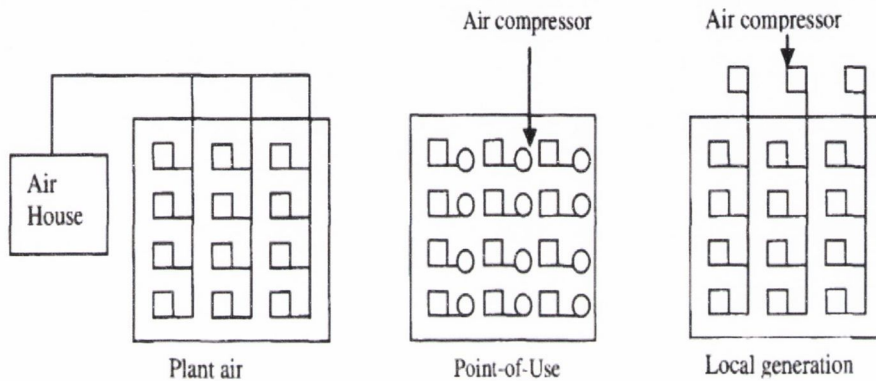


Figure 2.64: Air Configuration diagrams [22]

In considering the alternative options, a full cost of ownership study is necessary [22]. This includes setup costs, depreciable costs and annual costs for the operation of equipment and presents a complete picture of the costs involved with each option. The total cost of ownership (TCO) can be determined using equation 2.81, where M is the number of compressors needed to supply all machines, q is annual consumption of compressed air on all machines (m³/year) and N is the total number of machines.

$$TCO \text{ (cents/1000 ft}^3 \text{)} = \frac{(C1+C2+C3) \times M \times 100}{q \times N} \times 1000 \quad (2.81)$$

The depreciable cost (C1), setup cost (C2) and annual cost (C3) are calculated using equations 2.82 to 2.84. The variables for the environmental value system are shown in table 2.8.

Variable	Definition	Unit
D	Equipment cost	\$
Y	Equipment life	Years
I	Installation fee	\$
T	Transportation fee	\$
P	Number of people to be trained	-
F	Training fee for each person	\$
S	Footprint for the equipment	ft ²
R _s	Footprint cost rate	\$/ft ² /year
E	Electricity consumed	kWh/year
R _e	Electricity rate	\$/kWh
O	Cost of various consumable	\$
H	Downtime	Hours
R _m	Maintenance cost	\$/hour

Table 2.8: Environmental value system definitions and units [22]

$$C1 = \frac{D}{Y} \quad \$/\text{year} \quad (2.82)$$

$$C2 = I + T + \sum P \times F \quad \$ \text{ in first year} \quad (2.83)$$

$$C3 = S \times R_s + E \times R_e + \sum O + H \times R_h \quad \$/\text{year} \quad (2.84)$$

The analysis indicated that POU generation is the most expensive in terms of the costs associated with generating 1000 cubic feet of air [22]. The costs for local generation are comparable to the operational cost for the plant air supply pattern. However, if the setup costs, which consist of many onetime costs, are taken from the equation, operational costs for some configurations of local generation are slightly lower than plant air over a five year period [22]. From an energy conservation perspective, the study found local generation to be the best solution, as the energy required (kWh) to produce 1000 cubic feet

of air was significantly less for local generation than plant air or point of use. As such the quantitative analysis favours local generation from both a cost and energy efficiency consideration [22].

However, the issue of noise levels in a working environment was not addressed. The addition of a compressor into a working production environment may mean the cumulative effect would bring the noise above acceptable regulated levels. This problem could likely be solved through strategic placement and installation of an acoustic enclosure for the compressor [61]. The study was also specific to an automotive production facility. Therefore in the wider context, the cost of ownership and energy consumption will be dependent on individual plant configurations. The division of responsibilities between manufacturing and facilities in some organisations may also dictate the favouring of plant air configuration due to cost and ownership issues. This can be unfortunate from an energy efficiency perspective as ownership of energy usage is widely seen as a critical factor in reducing consumption levels [26].

Organisational & statistical approaches

There are a number of organisational barriers that need to be addressed in order to improve compressed air system energy efficiency. These include a lack of compressed air cost accounting, lack of awareness to potential savings and complex management structure [26]. Due to the nature of compressed air energy costs, responsibility for cost reduction measures is often divided between managers for maintenance, production, facilities, finance and purchasing [26]. In particular the use of local (machine or process) level compressed air cost metrics could be useful in ensuring responsibility for the efficiency of pneumatic production equipment.

Value stream mapping is a another tool for uncovering hidden sources of waste, such as unnecessary energy usage [158]. Incorporating energy usage into value stream mapping allows energy reduction opportunities to be considered in conjunction with other process improvement opportunities Other methodologies have been developed for graphically and statistically analysing plant energy use in terms of the major end uses [159]. These

approaches use energy-use breakdowns and statistical analysis to find energy saving opportunities and later track energy savings.

2.3.5 Energy efficiency case studies in production

Jarvensivu et al [160] present an intelligent control system for the improved control of an existing industrial lime kiln process. The supervisory-level control system was designed to be modular and hierarchically structured system. The core system components consisted of neural network models used in conjunction with high level controllers, based on fuzzy logic principles. The control of the process was carried out by feed-forward controllers, stabilising controllers and constraints handling (figure 2.65).

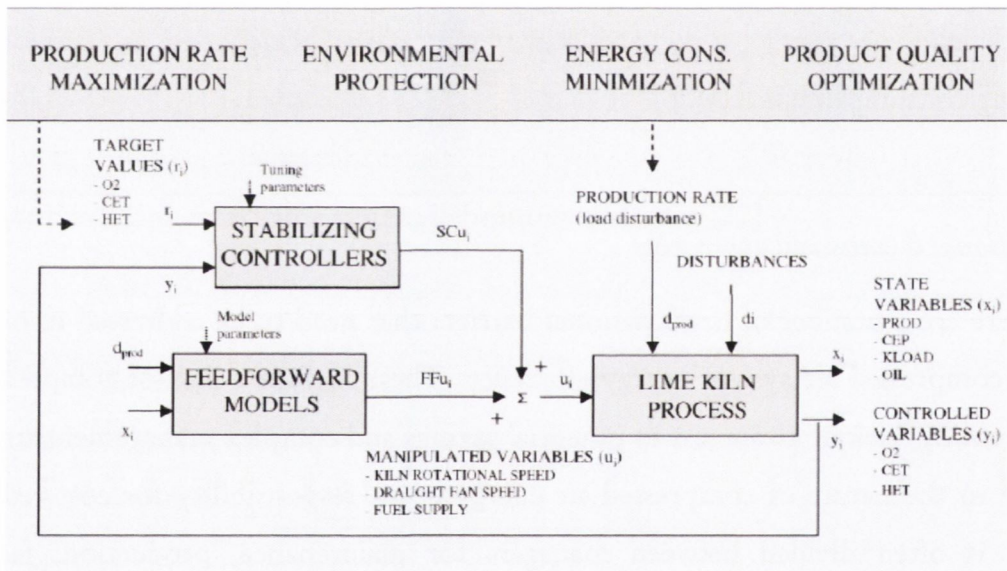


Figure 2.65: Schematic presentation of control structure for lime kiln process [160]

In order to optimise the process, it was operated closer to constraints (e.g. narrowed safety margin) with additional supervision to enable adjustment of controlled variables in order to fulfil objectives, in this case improved lime quality, energy efficiency and emissions. The target values were the adjustments necessary to maintain the process close to the optimal state and were based on operating conditions. The necessary adjustments (target values) applied by the control module were based on neural network models, developed on the basis of process data i.e. empirical models. The models took into account

moving averages, for a range of times, for a number of measurable (controlled) variables. Those measurable variables, in this case excess oxygen content of flue gas and temperature of flue gas in hot and cold end of kiln, were selected for having a known correlation with primary process outputs (quality, efficiency, emissions).

Results from the new system indicated that heat energy consumption was reduced by 7% in comparison to manual operation. This reduction was attributed to a decrease in the energy required to heat up cold burning air, reduction in hot and cold end temperatures which subsequently implied a reduction in heat loss by radiation [160]. The reduction in energy consumption was greatest at low production rates. This case study provides a good demonstration of how experimental knowledge of process behaviour combined with intelligent techniques, can be used to improve process efficiency considerably [160].

Operational methods to minimise the energy consumption of manufacturing equipment have been developed by Mouzon et al [161]. The methods include both dispatching rules and multi objective optimisation techniques. Following on previous research that observed the considerable energy consumption by support functions of manufacturing equipment [53-55], the focus for the study was shutting down underutilised (non-bottleneck) equipment sets when idling.

The logic for the first dispatching rule follows that a machine should be shutdown based on the following conditions and assumes jobs should be processed as soon as a machine becomes available i.e. no scheduled idle time is allowed: 1/ There is no part waiting in the queue 2/ There is enough time for a turn off-turn on operation before the next job arrives 3/ the total idle energy consumption is greater than the energy to shut down and restart the machine [161]. These rules were integrated into a controller that successfully reduced energy consumption in comparison to a no-controller case. Additionally a number of alternative algorithms were tested utilising various levels of information (release dates and arrival time distributions) with varied success. Typically lower energy consumption entailed greater total completion time.

Lean manufacturing principles dictate that a priority focus should be on reducing setups, turning on-off machines, and waste energy consumption. The use of batching was proposed to achieve this aim. By queuing a number of jobs before they can be processed, both objectives can be achieved. The machine processes jobs until the queue is empty and

if there is sufficient time until the arrival of the next batch will turn off to realise energy savings [161]. However, while this algorithm was successful in reducing total energy consumption, the total completion time was increased due the postponement of job processing. A variation of batch sizes caused the energy consumption to change predictably, with higher batch size leading to lower energy consumption, but the effect of batch size on total completion time was not as predictable [161].

To summarise, the success, in terms of energy saved by the dispatching rules, was dependant on inter-arrival time, processing time of jobs and break-even time of machine. This outcome is intuitive since the lower the warm up time, stop time, on/off energy consumption and machine utilisation rate, the larger the potential savings in energy consumption [161].

Due to the importance of information (arrival time etc), an artificial neural network based forecasting model was developed in order to predict arrival times. Neural networks make predictions based on preceding arrivals and are particularly suited to short term predictions [161]. This method is therefore more suitable than probability distribution modelling when the rate of arrival depends on the time (e.g. rate of arrival is higher in morning and afternoon and less around lunch break). The artificial neural network model was integrated with the dispatching rules so that the controller would make the decision to shut down the machine or leave it running idle based on the model forecast. This combination was successful in reducing energy consumption by more than 10% in comparison to the no controller approach and may be appropriate for 'unusual' scheduling situations [161].

Multi-objective programming was investigated due to the requirement in manufacturing to optimise more than one objective. In this case the criteria selected to optimise were energy consumption and total completion time. A mathematical model was developed so that users can weight the importance of several factors and prioritise their own minimisation objective, in this case completion time or energy consumption. The developed models provided non-dominated solutions and assisted the controller in choosing the best schedule [161]. However, this model did not factor in issues associated with re-establishing the equipment within a stable process window following an on-off cycle, and this factor is known to be critical from an operational perspective. Shutdown

and start up procedures have been known to cause significant disruption and production downtime in many industrial facilities. In any case the applicability of such operational methods to pneumatic production systems is limited, since they are based on the electrical consumption of machines during non-productive periods. In fact pneumatic systems are more efficient in this situation, as an optimised system (e.g. without leakage) will not consume energy during non-operational periods [20].

2.4 Summary

Automation is a key driver in the development of manufacturing systems. The importance of compressed air in facilitating automation has been discussed. However, it has noted that automation can lead to an increase in non-value add energy usage so improving energy efficiency is of critical importance. The interoperability enabled by standards such as OPC can potentially provide the mechanism for process and system monitoring and optimisation with respect to energy and resources [51].

Modelling approaches for simulating the dynamics of individual pneumatic drives and the consumption of larger systems have been reviewed. The state of art in energy efficiency for pneumatic and compressed air systems has been discussed. A number of production related case studies were highlighted that are of relevance in particular for the control of compressors.

Within the scope of exploring the dynamics and consumption characteristics of electro-pneumatic systems, a number of challenges have been identified.

1. To investigate air usage characteristics of manufacturing systems. Previous work has focused on electrical energy consumption of manufacturing equipment [53], however the breakdown of compressed air usage and losses in manufacturing has not been assessed.
2. To investigate the suitability of process models for industrial pneumatic systems with dynamic conditions. Within this focus, a number of issues must be addressed:
 - The appropriateness of linear statistical methods
 - The application of servo based models to open loop pneumatic drives

- The accuracy of simplified consumption models
3. To investigate the Kagawa flow model [103] for industrial pneumatic drive circuits consisting of multiple devices such as flow controls, silencers and long lengths of tubing. Additionally an assessment the applicability of flow identification techniques to an industrial environment is required.

3. Industrial Investigations: Compressed air usage in automated production

3.1 Overview

The objective of the industrial case study was to investigate compressed air consumption and losses on typical automated assembly type modules with a view to understanding the sources of inefficiency in pneumatic production machines. The investigations focused on one cell, an automated quality test (AQT) unit, of an overall flexible automation type production process. The manufacturing facility consisted of a number of different discrete manufacturing processes with mass production of individual parts/products at high volume with some level of product mix capability. Generation of compressed air was the largest electrical energy consumer on site, accounting for 23-24% of overall energy usage. Compressed air was used for a variety of applications on site, including actuation, process control and material handling purposes.

Two AQT modules were investigated. The compressed air consumption of the quality testing units was analysed primarily in terms of quantifying non-productive usage and identifying the underlying causes for such usage.

3.1.1. Automated Assembly Production Module

The function of the Automated Quality Test (AQT) unit on the production line is to monitor product quality. The module receives partially completed product assemblies from an upstream module, prepares the product for testing, tests the product, after which it is cleaned and dried, then returns the product to a downstream module, via a conveyor, for further processing. An overview of the machine's layout and pneumatic components is illustrated in figure 3.1. Compressed air is consumed primarily by pneumatic drives and open blow type devices on the assembly station.

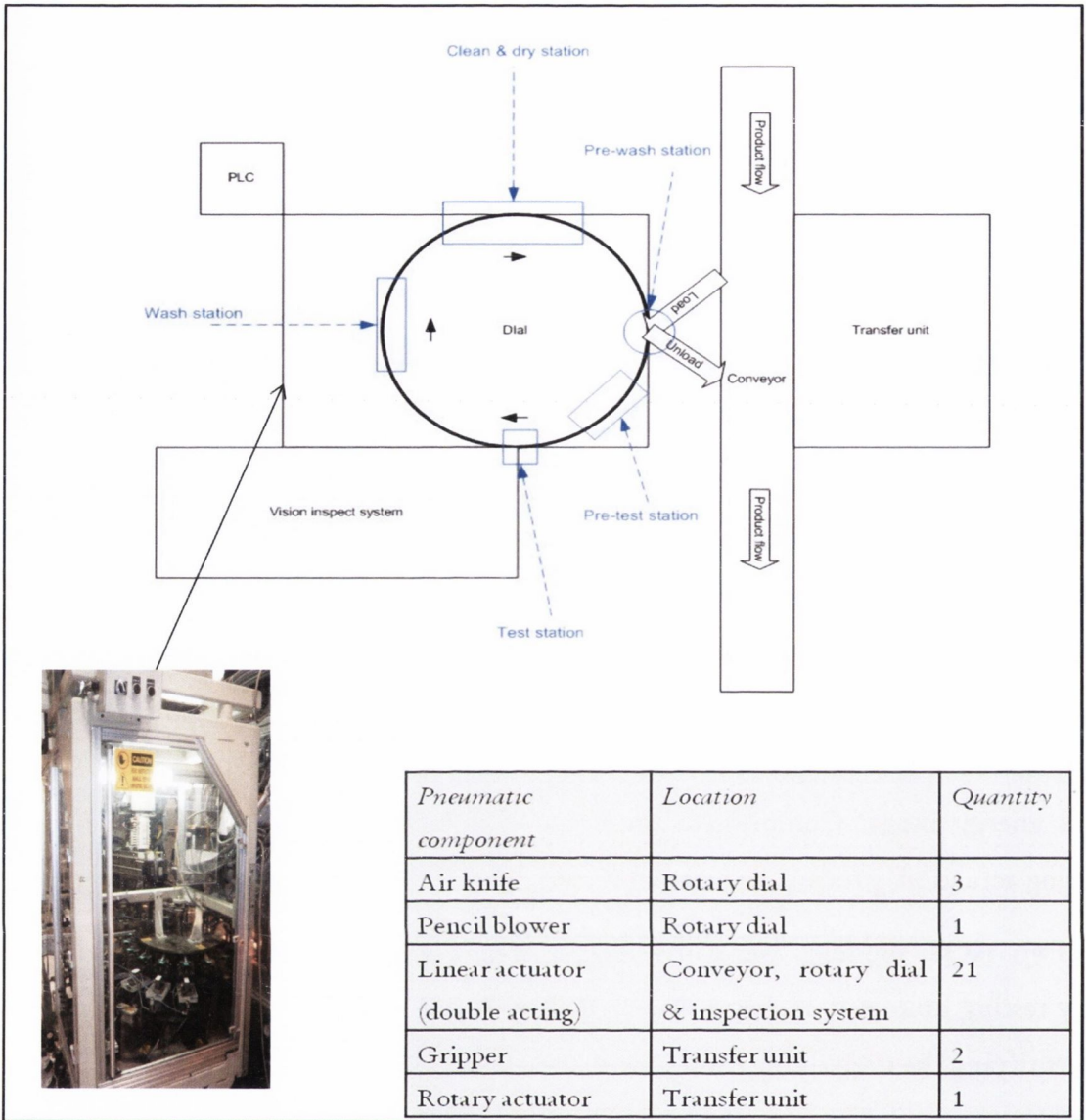


Figure 3.1: Automated quality testing unit system layout and pneumatic components

The transfer unit (TU) in figure 3.1 retrieves the product from a pallet on the conveyor and transfers to a fixture on the indexer dial. The pre-wash station scrubs nozzles on the product with a wetted roller pad, after which the product is indexed to the next station. Contact time during the pre-wash stage is approximately 0.25 to 0.5 seconds. The pre-test station is used to warm up the product head prior to testing by repeatedly firing the nozzles and a vacuum system is used to collect any waste material. The product is moved to the test station where its quality is evaluated by a vision inspect system. The following wash station's function is to clean residual material from the product head after testing. Three different wash pads, saturated with de-ionized water, are run across the head

of the product in three successive dial positions and a vacuum is then applied to drain used de-ionized water. Two air knives are used in the next clean and dry station to dry the head of the product. Finally after being rotated back to the starting point of the cycle, the product is retrieved by the TU from the indexer dial, rotated about its X-axis, and placed back in a pallet on the conveyor belt for further processing. The total processing time for each product is approximately 40 seconds. However, since the indexer dial contains 16 nests, the module is capable of outputting a product every 2.5 seconds approximately at maximum cycle rate.

3.1.2 Compressed air system

There were seven compressors in total supplying pressurised air for the entire production facility. Two of the compressors were used for higher pressure applications operating at 13 bar(g), with the remaining five supporting general pneumatic operations in production, including the AQT modules. All compressors were rotary screw type and details of the five low pressure units can be found in figure 3.2. Each compressor had a dedicated receiver for air storage. A schematic of the low pressure compressed air system is illustrated in figure 3.2. The AQT module was located in B2 of the facility. The air was dried and filtered to an appropriate ISO8573 quality class. Both refrigerant and desiccant type driers were employed for this purpose.

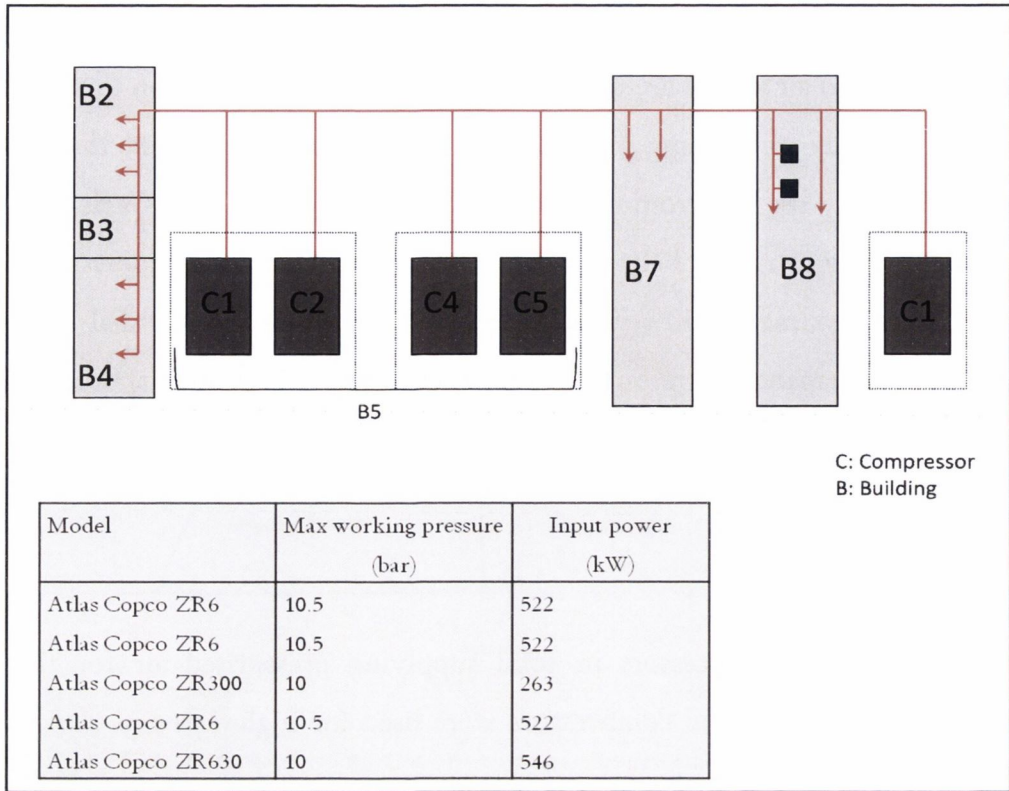


Figure 3.2: Schematic of compressed air system and compressor specifications

3.2 Investigations

3.2.1 Measurement equipment and setup

The main equipment used in the investigations were: the AQT production module, a flow meter, PC Oscilloscope and a laptop computer. The flow meter was used to measure the volumetric flow rate of compressed air consumed by the AQT unit. The flow meter employs thermal mass flow principles to measure the volumetric flow rate. This means that the measurements are pressure and temperature independent. All results are based on the ISO 2533 standard reference conditions (i.e. 15°C/ 1013hPA/ 0% RH). A dedicated dropdown pipe supplied air to the quality test module and was retro-fitted with additional valves and fittings to enable the air flow to be re-directed to the flow sensor before entering the air preparation (FRL) bank (figure 3.3). The PC oscilloscope, laptop and PicoLog software formed the data acquisition system, used to measure and log the output signals from the flow sensor.

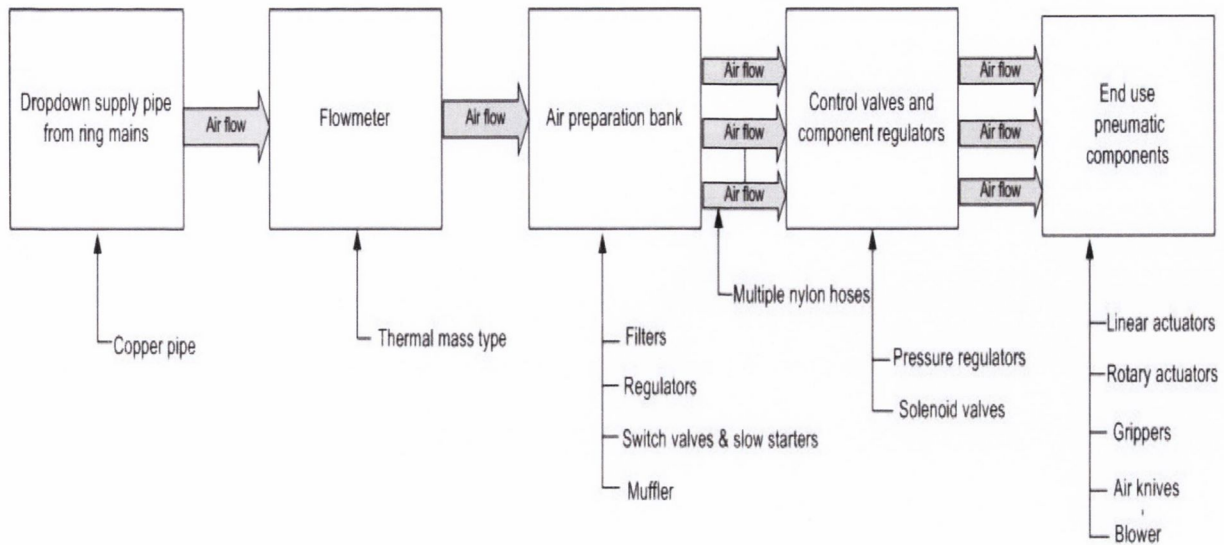


Figure 3.3: Local compressed air system layout with sensor augmentation

3.2.2 Investigation procedure

The methodology followed in the investigations was to monitor and record the volume flow of air consumed by the AQT unit with corresponding machine output. The PicoLog software allowed for the sensor signals to be recorded over typically sixty minute periods. The maximum possible sampling rate for the flow measurements over this period was 2 Hz. A sampling rate of 100Hz was also used, over shorter periods, to test the sensitivity of the DAQ system to faster changes in flow.

The corresponding machine output figures were visually inspected and noted every minute from the AQT module's HMI. Additionally, the causes for machine downtime during each test were documented. The information flow underpinning the investigation procedure and measurement equipment details are outlined in figure 3.4. The air consumed by the machine in operation was calculated as the mean of the 120 flow measurements (i.e. based on 2Hz sampling) taken over a one minute period. This allowed the average consumption to be correlated with production output.

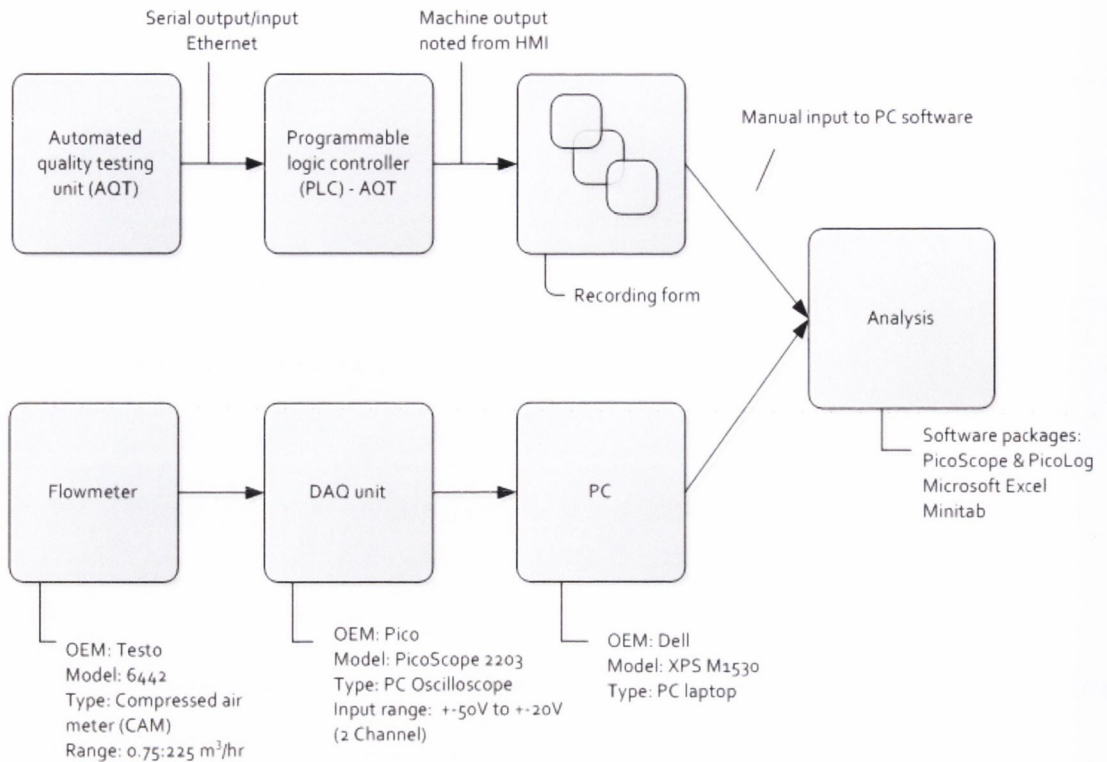


Figure 3.4: Measurement system setup & information flow

Two assembly stations were investigated as part of the industrial investigation. For the first assembly machine, the investigation procedure was carried out twenty times at random intervals over approximately a one month period. In total approximately 20 hours of data was collected. For the second assembly module, ten tests of sixty minute duration were conducted also over a one month period.

Machine model

The control setup for the AQT unit is typical of many automated production machines, with a combination of PLC controlled sequential operations and integrated analog control loops (i.e. PID modules) for motion control. When the AQT machine is processing product, it is considered by the PLC to be 'In Cycle', although under dry run conditions it can be operated with no product throughput. Any event that causes machine downtime is documented by the PLC and placed in one of seven categories for storage in a database. The main categories are; Machine Idle, Machine Blocked, Machine Stop, Operator Stop, Material Stop, Machine starved, System stop and Island stop.

Each category contains multiple event types, such as ‘process power not on’, ‘velvet wash not clear from dial’ or ‘ethernet timeout error’, with different air consumption characteristics. For example, the operator stop category includes the “process power not on” and “cycle stop by operator” events. ‘Process power not on’ exhibits a volumetric flow of approximately 50% of the maximum flow rate whereas ‘cycle stop by operator’ exhibits minimum air consumption levels (e.g. leakage rate).

In order to analyse the compressed air consumption and losses of the AQT unit, the machine was simplified to a single input single output (SISO) system and the number of finite machine states was reduced to three (figure 3.5). In this context, machine state indicates the operational status of the machine for any minute time period. In-cycle means the unit is processing product, usually at its maximum output rate. The not-in-cycle state includes all of the downtime categories such as idle and blocked, and entails that no product is outputted during that period. The combined-cycle state takes account of the fact that in any minute the machine may be both processing product and experiencing downtime for any range of reasons. Machine condition refers to the air consumption characteristics of the machine state. As each state consist of multiple events with different air flow characteristics, each state can have multiple machine conditions (e.g. MS=NiC with MC=cS & MS=NiC with MC=pA).

Finally production output specifies the number of products fully processed in any minute. Minimum output is zero and maximum is limited by safety factors at twenty four.

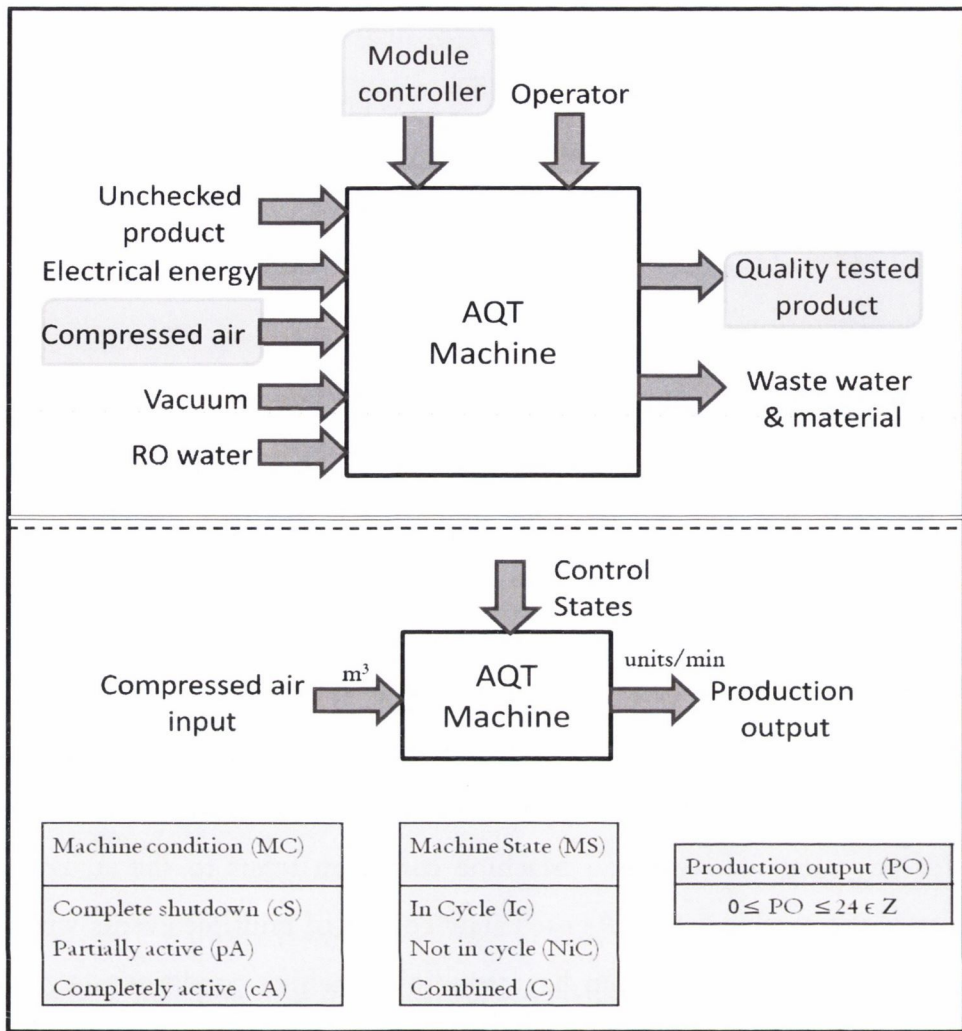


Figure 3.5: Black box model of AQT unit and simplified Finite State Machine

3.2.3 Accuracy of measurement system

The total accuracy of the measurement equipment is a function of the accuracy of both the flow meter and the PC oscilloscope. The technical data [162] for the Testo 6442 flowmeter indicates an accuracy of $\pm 3\%$ of reading and $\pm 0.3\%$ of final value. Likewise, the specifications for the PicoScope 2203 [163] provide an accuracy of 100 ppm (0.01%). The flow-rate measurement is therefore subject to an approximate total error of $\pm 3.02\%$. The main measurement error associated with production output is alignment of time and display but this is difficult to quantify.

In an industrial investigation, ideal experimental conditions are difficult to achieve, and it must be acknowledged that a larger degree of uncertainty is present. Additional potential sources of error in the investigation are listed below.

- The PLC approximated the production output by using a counter to monitor the number of times the rotary table indexes. The output figure is thus not based on the physical presence of products in the system.
- The PLC for the AQT module updated the 'output per minute' figure every full dial rotation (e.g. after 16 dial indexes). As the machine could process up to 24 products per minute, this meant that usually two output figures were displayed in any minute. Only one of these values was typically recorded.
- When the AQT was not-in-cycle, the PLC did not update the output figure. Therefore at times, the output figure was not accurately represented, when the machine experienced multiple states (e.g. in cycle and not) in any minute period.
- Multiple events were difficult to track.
- The accuracy of the measurement system was limited significantly by the response time of the flow sensor and maximum possible sampling rate of the data acquisition equipment for long durations.

The response time of the flow sensor was by default 0.6s. However, this could be adjusted to a minimum of 0.1s, by reducing the amount of damping via an embedded digital filter. This response time is typical for industrial thermal-mass based flow sensors. The maximum allowable sampling rate on the PicoLog software, for a sixty minute test period, was 2Hz. The trade-off between dynamic response of the measurement system and the quantity of data generated is an important issue for fast acting pneumatic systems since many linear cylinders, particularly for unloaded short strokes, can actuate in less than 0.5s. Other factors limiting the industrial adoption of flow sensors include high cost, installation complexity, limited range ability and diminished circuit performance.

3.3 Results and Analysis

The analysis focuses on two aspects: the applicability of linear regression techniques for modelling machine air consumption and an assessment of compressed air losses. The statistical analysis was carried out in Minitab. An example of one of the test results is illustrated in figure 3.6. The figure shows the measured air consumption with corresponding machine output over a typical one hour period. Each major event causing a change in consumption or output has also been highlighted.

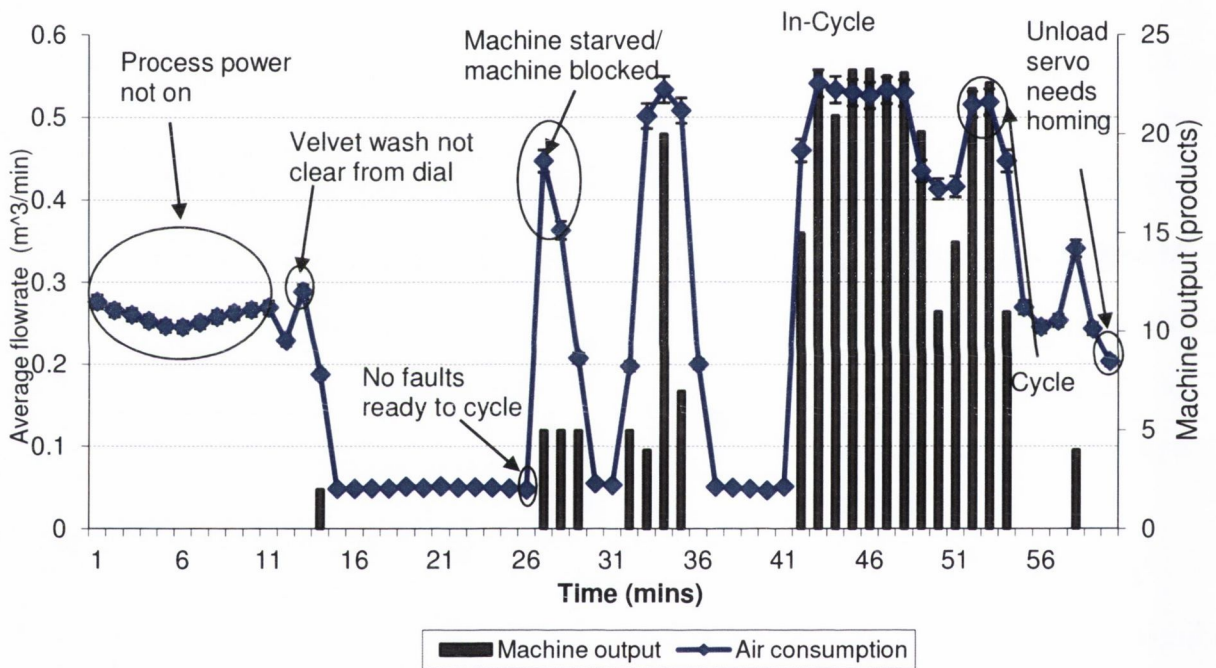


Figure 3.6: Example flow test, 60 minutes at sampling frequency 2Hz

3.3.1 Statistical analysis

The total compressed air consumption and product output for the entire test period is detailed in table 3.1. The specific air consumption metric refers to the amount of pressurised air consumed by the quality testing module in processing one product. This metric can be useful as a quality benchmark. An air consumption of 0.027 m^3 per product is equivalent to 27 Litres per product. Note this figure refers to the specific air

consumption of one stage of process and represents only a fraction of the total compressed air consumed in the production of the overall product.

Total compressed air consumption (m ³)	Total production output (products)	Specific CA usage metric (m ³ /product)
363.11	13,599	0.027

Table 3.1: Totals for test period, assembly station 1

In an industrial environment many data distributions do not follow the Normal distribution model that underlies many standard statistical tools [82]. Due to the constantly shifting nature of many industrial process conditions, long term process means for variables such as energy consumption can be difficult to predict with accuracy. It is therefore essential to test the ‘Normality’ assumption for each data set in order to validate the use of statistical tools such as process control charts, which could potentially be useful in monitoring air usage.

Figure 3.7 contains the histogram, box-plot and summary statistics for the volumetric flow-rate of compressed air at maximum output rate. The sample statistics in this case are based on 521 observations at maximum production rate. Note the flow rate units in figures 3.7 and 3.10 are m³/h.

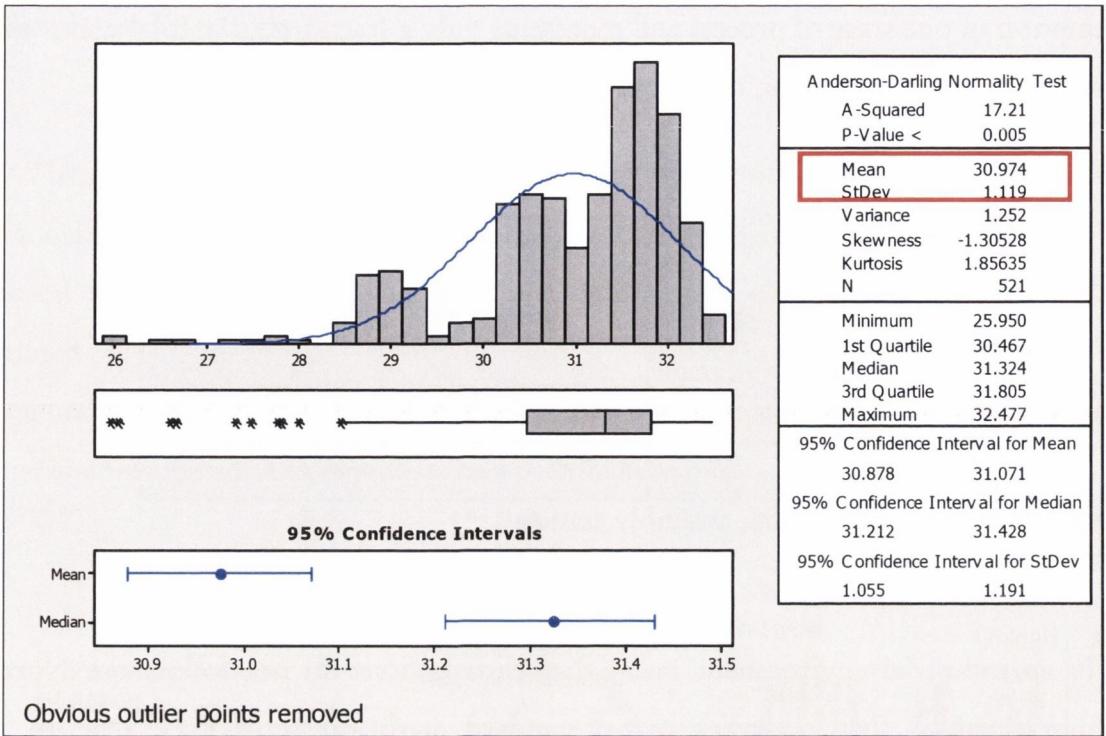


Figure 3.7 Summary statistics for air consumption at maximum machine output

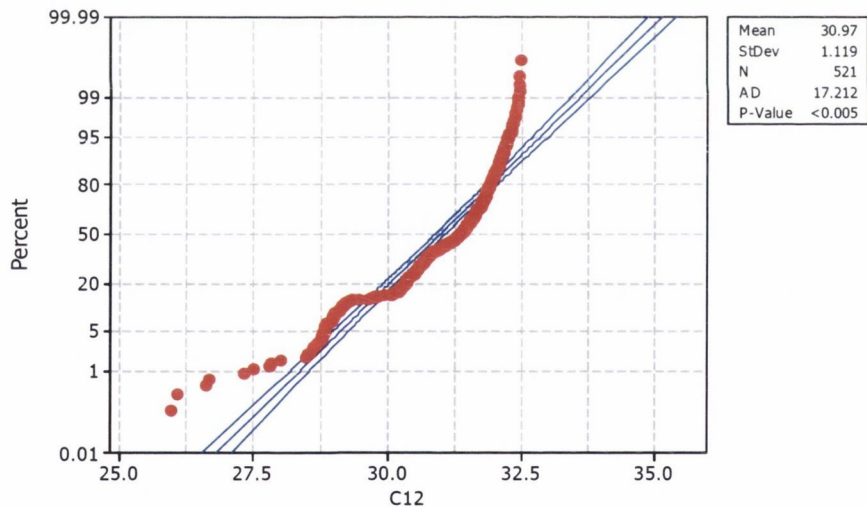


Figure 3.8: Probability plot of air consumption at maximum machine output

The normal probability plot (figure 3.8) indicates the data does not follow a normal distribution even after existing outlier points had been removed. As the p-value is less than 0.05, the null hypothesis that the data comes from a Normal distribution is rejected. Therefore it is not possible to use confidence intervals to predict future air consumption at maximum output.

Similarly, the histogram, box-plot and summary statistics, with obvious outlier points removed, for flow at no production output are illustrated in figure 3.9. Additionally the machine condition was that of complete shutdown, so that any air consumption is due to leakage. The statistics are based on 284 points (minutes) worth of data. The normal probability plot indicated a p-value of less than 0.05 which means the data is not normal. It is again not possible to estimate the long term process mean for leakage flow rate based on the sample data. This is typical for an industrial process with frequently changing conditions. Planned maintenance periods and wear of components means that the process mean for leakage rate is likely to change depending on the frequency and type of maintenance (e.g. preventive or corrective) and the age of equipment i.e. there is a time based element to the leakage rate. Some of the variability in the flowrate can also be attributed to an unstable pressure supply, since if the leak occurs upstream of the pressure regulator it will be subject to pressure fluctuations in the compressed air network.

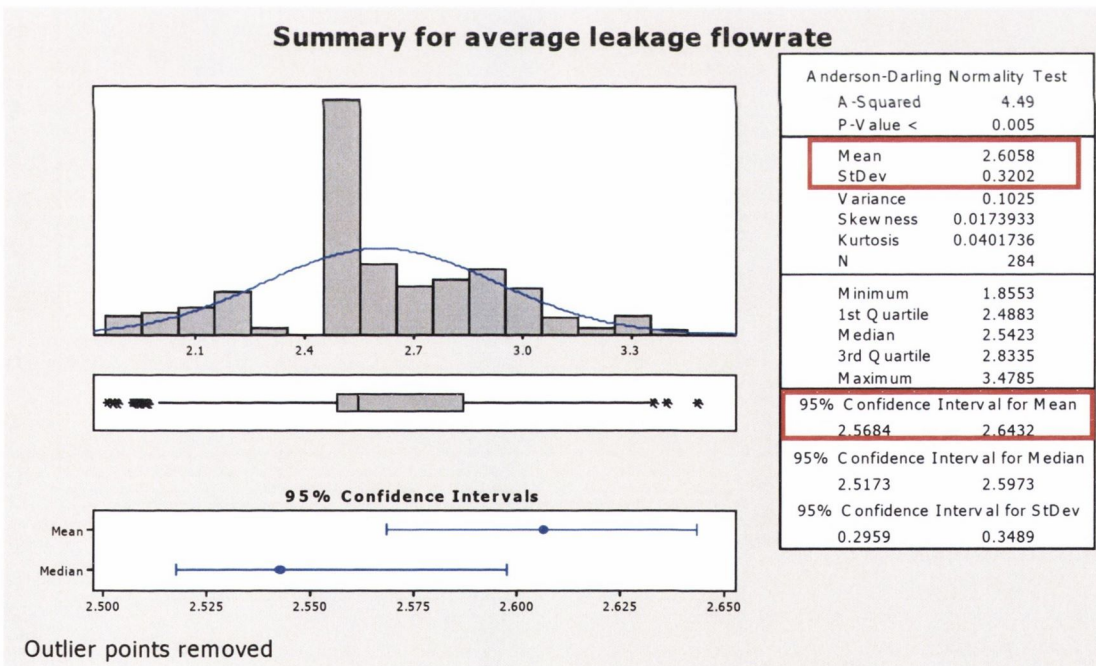


Figure 3.9: Summary statistics for air flow rate at PO=0, MS =NiC, MC=cS

The box-plot and regression analysis for compressed air consumption and machine output are shown in figure 3.10. It was assumed that production output would be the primary driver of compressed air consumption. However, it is clear from the box-plot that

air consumption varies widely with production output, in particular at no output. The regression analysis indicates that there is a relationship between compressed air consumption and production output, as is expected intuitively, but that output alone cannot be used as an accurate predictor of consumption. It is clear from the box-plot that the data is not normally distributed along the linear regression curve, a key assumption underlying the regression analysis. Therefore, it is clear that air consumption is a function of multiple variables, such as output and machine state, even at machine level.

The scatter plot for the power consumption of all operational compressors against total production output of the factory, over a four year period are shown in figures 3.11. The coefficient of determination calculated by the regression analysis was 50%, significantly less than the equivalent R^2 value at machine level. This indicates a very poor prediction level and thus demonstrates the difficulty in accurately predicting compressor energy consumption with only production output as a predictor variable.

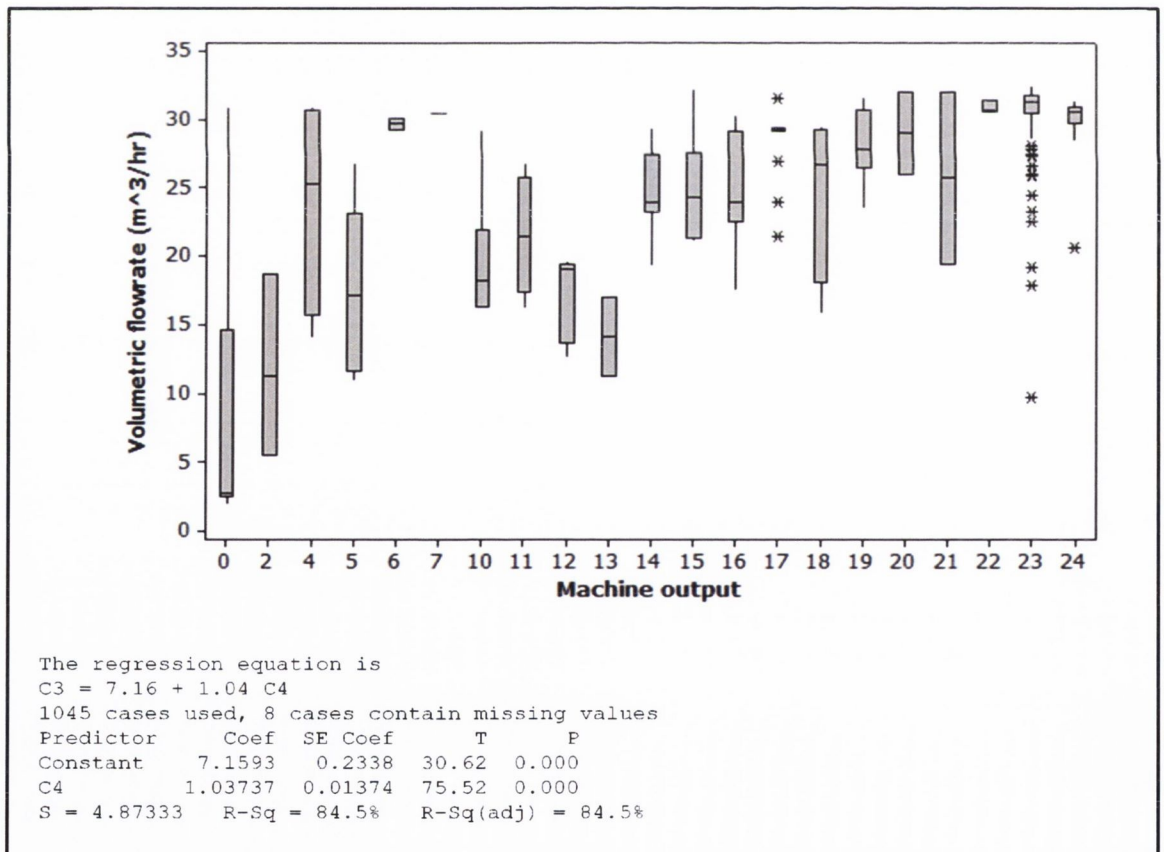


Figure 3.10: Box-plot of air consumption for a range of production rates and regression analysis (C3: Volumetric flow-rate, C4: production output)

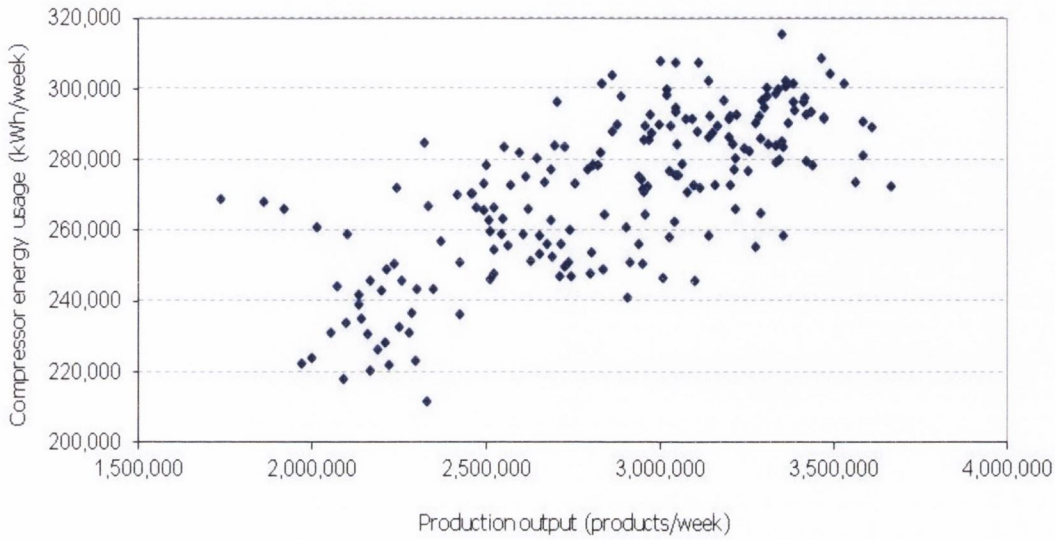


Figure 3.11: Scatter plot of total compressor system energy usage with production output at factory level

3.3.2 Compressed air losses on AQT module

Non-functional usage is defined as compressed air consumed during periods of non-value-add activity. Examples of non-functional usage in this particular case include the air consumption of active components when machine is not processing product and air exhausted to the atmosphere by leakage. The compressed air losses were divided into three primary categories, leakage, control and design, that describe the underlying drivers of non-functional air usage.

Leakage refers to compressed air that escapes to the atmosphere if the system is not perfectly sealed. Leakage typically occurs across worn seals in actuators and spool valves, and at threaded joint connections and push-in fittings [143]. The total leakage calculation is based on the sample mean flow rate of air at no output, machine state of not-in-cycle and machine condition of total shutdown.

The control losses category accounts for excess compressed air consumed, during non-productive periods, due to a lack of control capability or inadequate control settings. This category is based on the observation that the machine would still consume

compressed air even when it was not producing any output and not-in-cycle. This occurred during particular machine events such as 'system start-up' and 'process power not on'. Additionally this category includes compressed air consumed when there is no machine output but the machine is still in cycle (e.g. $MS=Ic$, $Mc=A$, $PO=0$). This happens when the machine is in dry cycle, usually for maintenance or product changeover purposes. The control losses category also includes compressed air consumed during idling before shutdown (e.g. $PO=0$, $MS=C$, $MC=pA$). Usually, this can happen if the upstream module is blocked or idle causing a delay. The machine is usually left active for 30s to 60s in order to re-engage rapidly. Finally, it was observed during the investigations that the air-knives on the clean and dry work station remain active during the transfer period when product is being moved between stations on indexing dial. During this time a quantity of compressed air is discharged to the atmosphere without providing either cleaning or drying function to the product. The transfer time between stations was timed with a stopwatch at approximately 0.4s. Estimated losses due to non-functional usage during transfer were also included in the control category.

Design losses refer to the higher than necessary air consumption, caused in the machine design stages, by utilisation of poor design methodologies with respect to energy efficiency. This includes design choices based on capital not life cycle costs, such as the use of open pipes for blowing purposes or bridge type circuits for pneumatic gauging [164,165]. Additionally this category could potentially include the use of excessive design safety factors and other issues such as component sizing and valve to actuator tubing lengths [164]. However, these losses are difficult to determine without the use of a comparable system model and therefore remain outside the scope of the study. Nevertheless, the category is included to highlight the fact that further energy losses occur in pneumatic systems in addition to those documented in this study.

Total losses

The breakdown of air consumption and losses of the first assembly module during the investigation period are illustrated in figure 3.12. Total non-functional usage, not including potential design losses, accounts for 27% of total compressed air consumption. It can be seen from the figure 3.12 that a major cause of non-functional usage is leakage,

consuming 13% of all air supplied during the investigation period. Total control losses account for 14% of compressed air consumed. The same methodology applied to the second assembly station investigated revealed similar results (figure 3.12). Total non-functional usage increased to 41% of overall machine consumption due nearly wholly to increased leakage rates. Total control losses were consistently in the 12-14% range.

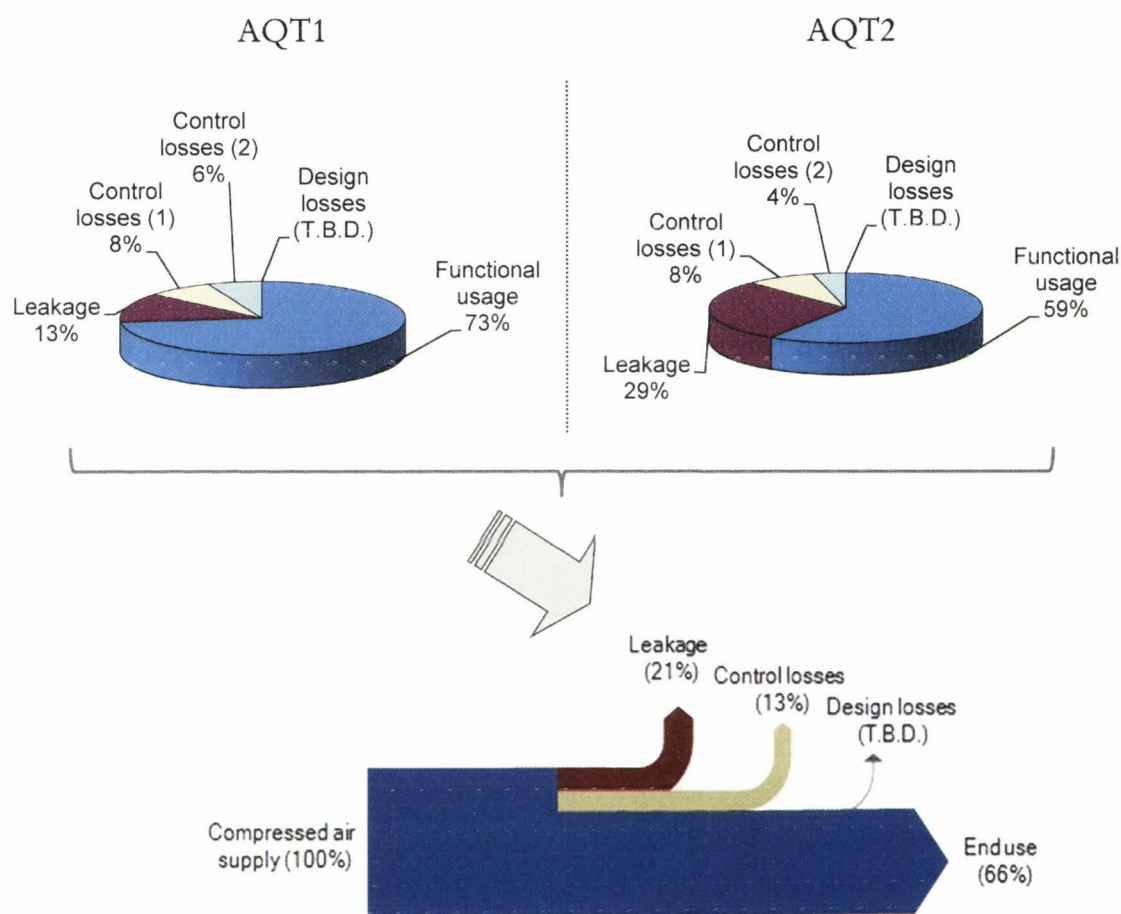


Figure 3.12: Breakdown of air consumption and losses on automated assembly units

The results from both assembly units demonstrate the need for regular and preventative maintenance. Notably, the leakage rate in the second case is particularly striking, accounting for nearly a third of all machine consumption. It is also clear there is scope for improved control of air consumption during non-productive periods. This can be achieved with additional control valves and control settings (programming). Design

losses are difficult to assess without a suitable model and this reason constitutes part of the rationale for the work carried out in chapters 4 and 5. Figure 3.12 highlights the potential for immediate energy savings in industrial facilities. The literature review has shown the potential for considerably more energy savings with better design, monitoring and control of pneumatic systems.

To assess further the control losses categories, the breakdown of consumption between active and passive consumers in the assembly module, was also investigated (figure 3.13). The passive consumers included the air knives, pencil blower and leakage. Active consumers included the linear and rotary actuators and grippers. Figure 3.13 demonstrates that passive consumers account for a large part of consumption during full production and also for a majority of losses during non-productive periods.

It is clear from the figure that tighter control of passive consumers during non-productive periods is necessary to improve energy efficiency. An additional control valve for the air knives was installed and programmed to shut off the air supply when the machine was not-in-cycle. This resulted in air savings of approximately 8%. Leakage can be reduced with regular maintenance. According to best practise, the percentage of compressed air lost to leakage should be less than 10% in a well maintained system [125].

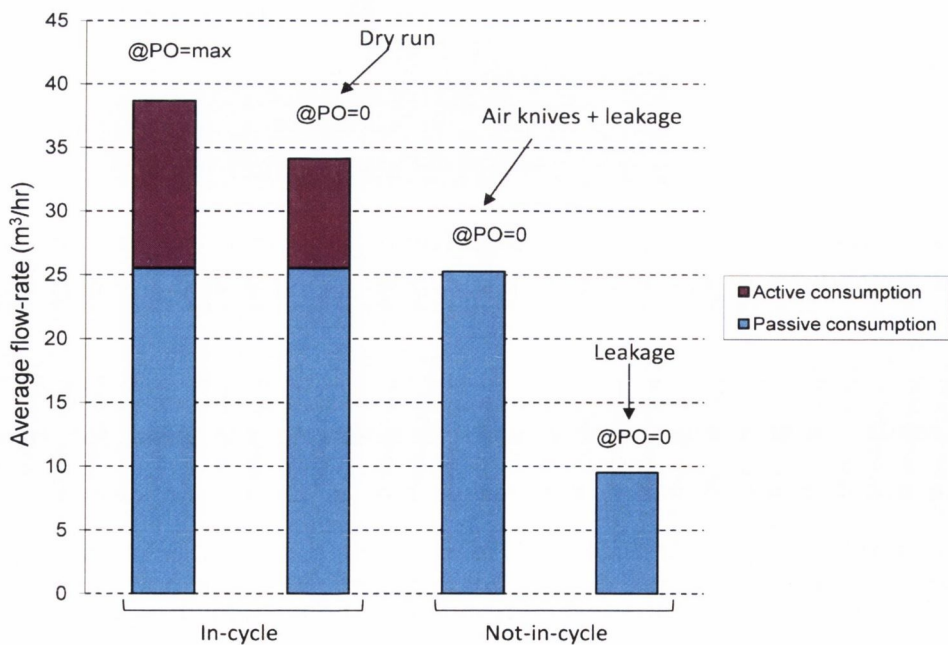


Figure 3.13: Breakdown of air flow for range of production conditions

3.4 Summary

1. Based on the investigations of the two assembly stations, losses were estimated to account for 34% of total machine air consumption. It is clear that a significant amount of such energy losses can be addressed with current technology, little investment and better maintenance. The losses estimate does not include further energy savings possible using more advanced methods in design. A system model would be useful in allowing such energy losses to be quantified.
2. The dynamic response and accuracy of the measurement chain is limited by the response time of air flow sensors. For fast acting pneumatic drives, the consumption may not be accurately captured using only a flow sensor.
3. Linear regression, a widely employed tool in industry, is of limited use in predicting machine air consumption with confidence. This is due to non-normal distribution of underlying data and dependence of air consumption on more than one predictor variable. Additionally the variability of leakage flowrate over time during machine shutdown periods has been highlighted.
4. Due to the demonstrated limitations of the standard statistical approach, a more transparent type of modelling approach is therefore taken in subsequent chapters. As a prerequisite to modelling large scale pneumatic production systems, a fundamental understanding of the most common pneumatic consumer devices is first required. The flow of compressible fluids (air) through orifices, nozzles and pipes is well documented in the literature. However, the consumption dynamics of pneumatic cylinders has received less attention. Since linear cylinders are one of the most common pneumatic devices found in industry and account for a significant portion of machine consumption, it is necessary to develop a detailed dynamic model of such air consumers. Moreover, since the measurement system resolution is limited by flow sensor response time, detailed dynamic models of pneumatic cylinders are also required to calculate the air consumption of fast acting drives with better accuracy.

4. Modelling & identification of industrial pneumatic drive system

4.1 Model Development

The model development consists of the theoretical development of non-linear mathematical model for the system dynamics, and its implementation in Matlab-Simulink software. An advantage of using Simulink is that post-process simulation analysis and experimental validation can be carried out in Matlab. The model is developed specifically for a double acting asymmetric linear cylinder, one of the most commonly found pneumatic actuators in industry. The motivation for the development of a comprehensive actuator model was two fold:

1. To utilise the short response time of pressure sensors to accurately model the flow/consumption of fast acting pneumatic drives
2. To understand the phenomena that contribute to the dynamic characteristics of the system, such as output force, cycle time and air consumption.

4.1.1 System Dynamics

The pneumatic drive system under consideration is shown schematically in figure 4.1 with a flow chart of the model development stages. The full system model for the drive includes a flow model, thermodynamic model and force dynamics model. When the valve in figure 4.1 switches position one of the cylinder chambers is connected to an energy supply while the other is vented to atmosphere. This allows mass flow to and from the system. The mass flow drives the pressure response, and the subsequent pressure differential across the chambers drives the force and position output of the cylinder. The flow model considers the aggregate flow characteristic of a pneumatic circuit. The thermodynamic model predicts the pressure, temperature and heat transfer in both of the drive cylinder's chambers. The force dynamics model considers inertial and frictional effects.

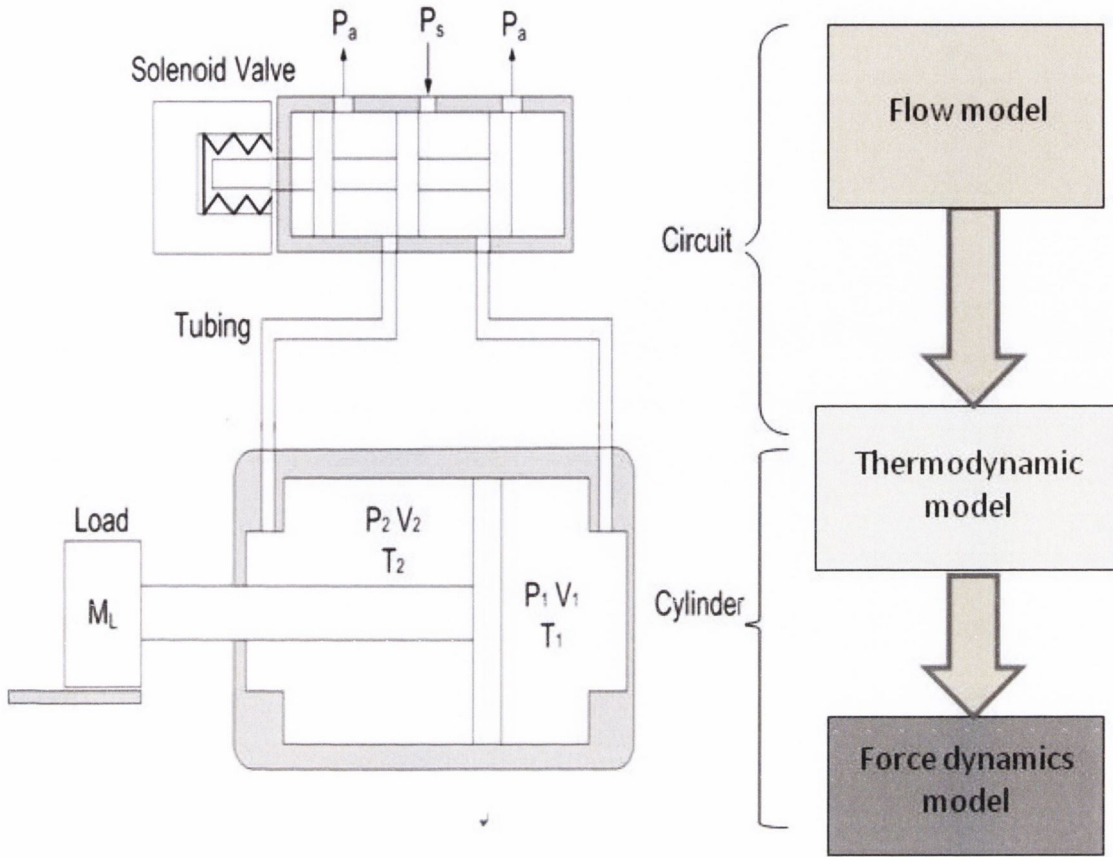


Fig. 4.1 Pneumatic drive system schematic with model development stages

Flow model

A typical pneumatic circuit in an industrial environment consists of a directional control valve, one way flow control valve, silencer, multiple fittings and in some cases long lengths of tubing. The extended ISO6358 equation (eq 4.1) introduced by Kagawa [103] for component characterisation is proposed for modelling industrial type pneumatic circuits. The flow characteristics depend on the particular design of components, and circuit configurations. The extended ISO/Sanville model allows for increased flexibility in accounting for the flow behaviour of circuits with common components [103].

$$\dot{m}_i = \rho_o \cdot C_i \cdot P_u \cdot \sqrt{\frac{T_o}{T_u}} \cdot \varphi_i \tag{4.1}$$

$$\text{Where } \varphi_i = \begin{cases} \left[1 - \left(\frac{\text{Pr} - b_i}{a_i - b_i} \right)^2 \right]^{ms} & \dots \text{ if } \text{Pr} > b \\ 1 & \dots \text{ if } \text{Pr} \leq b \end{cases}$$

$$i = 1 +, 1 -, 2 +, 2 -$$

The sonic conductance C and critical pressure ratio b of the circuit can be significantly less than that of the directional control valve due to additional impedance of flow control valves, pipe work and fittings. The cracking pressure ratio accounts for the fact that in one way flow control valves, the flow rate can be zero for a pressure ratio of less than one due to cracking characteristic of the check valve [103]. This occurs when the spring force in the non-return valve is significant [13]. If there is no check valve in the circuit, the cracking pressure ratio a can be eliminated e.g. $a = 1$. The subsonic index allows for increased flexibility in the flow function and is essential to accurately model components such as silencers and one way flow controls [102]. Potentially the Kagawa model is ideal for circuits consisting of several devices in series.

The time delay due to switching of directional control valve can be considerable for solenoid actuated control valves, and is modelled as a unit step delay (figure 4.2). In equation 4.2 \tilde{u} represents the input signal u delayed by the time it takes for the valve to switch; including both delay and rise time. The threshold voltage is 24V for typical solenoid actuated valves. The total delay time t_{sw} of solenoid control valves is typically available in OEM data sheets. However, it is best to identify the delay experimentally since pilot supply pressure effects switching time performance.

$$\dot{m}_i = \begin{cases} C_i \cdot P_u \cdot \sqrt{\frac{T_0}{T_i}} \cdot \varphi_i \cdot \rho_o & \dots \text{ if } \tilde{u} \geq u_{th} \\ 0 & \dots \text{ if } \tilde{u} < u_{th} \end{cases} \quad (4.2)$$

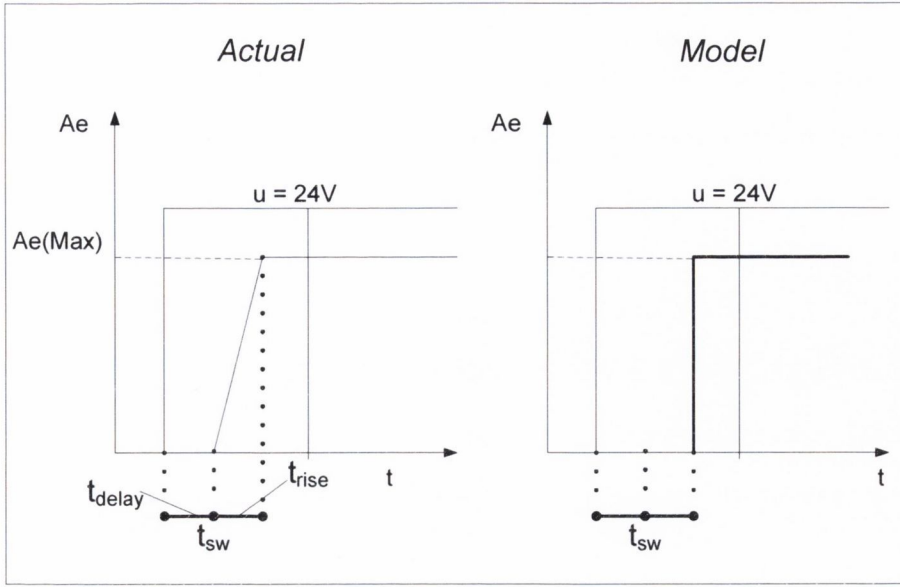


Figure 4.2: Valve switching delay and conceptual model delay

Thermodynamic model

Based on the recommendation of Carneiro et De Almeida [80], equation 4.4 is used as the thermodynamic model for the cylinder with temperature following a polytropic process (eq. 4.3). To account for asymmetric cylinder, equation 4.4 allows for a difference in a cylinder's active and dead volume for both chambers. The heat transfer model was simplified by considering an average heat transfer surface area, equation 4.4. Additionally, the changes in the heat transfer coefficient, with pressure and temperature, are neglected i.e. a static equilibrium value is used.

$$T = T_e \left(\frac{P}{P_e} \right)^{\frac{n-1}{n}} \quad (4.3)$$

$$\frac{dP}{dt} = -\gamma \frac{\bar{P}}{V} \frac{dV}{dt} + \gamma \frac{R}{V} T (\dot{m}_{in} - \dot{m}_{out}) + \frac{\gamma-1}{V} \lambda_e A_q(av) (T - T_{amb}) \quad (4.4)$$

Where $V_i = V_{di} + A_i \cdot y$

$$A_q(av) = \frac{\pi d^2}{2} + \pi d \left(\frac{S}{2} \right)$$

The pressure P is also delayed using a transport delay in Simulink to account for the time delay for the pressure wave to propagate the length of tubing. For servo-valves equilibrium conditions were defined as the point where the spool was at central, closed position, temperature in the cylinder was steady ambient temperature and leakage mass flows were equal [80]. This approach was adapted for dual position valves. A leakage term can be included, as in equation 4.5, or excluded as in equation 4.6 based on identification results.

$$\dot{m}_i = \dot{m}_{i \text{ in}} - \dot{m}_{i \text{ out}} \quad (4.5)$$

$$\dot{m}_i = \begin{cases} \dot{m}_{i \text{ in}} \dots & \text{if } u \geq u_{\text{th}} \\ \dot{m}_{i \text{ out}} \dots & \text{else} \end{cases} \quad (4.6)$$

Force dynamics

The piston-payload dynamics is modelled using Newton's second law (eq. 4.7). The right hand side of the equation represents the applied pneumatic force, F_p , produced by different pressures acting on opposite sides of the piston [15]. The moving mass includes both the payload mass and the mass of the piston and rod assembly. The external load force, F_L , is zero for horizontal orientation but for any other orientation the external force must be accounted for e.g. for vertical orientation, $F_L = mg$.

$$(M_L + M_p)\ddot{y} + F_L + F_f = P_1A_1 - P_2A_2 - P_aA_r \quad (4.7)$$

$$F_p = P_1A_1 - P_2A_2 - P_aA_r \quad (4.8)$$

The friction force is modelled using a combination of two approaches; the first simple model assumes friction is the traditional combination of Coulomb and viscous components (eq. 4.9), as used by Richer et Hurmuzlu [15] and Ning et Bone [79], while the second model uses static Stribeck curves (eq. 4.10) to model the friction force [49,75]. Using both models based on the data allows part of the hysteretic behaviour in velocity (frictional lag) to be captured for increasing/decreasing velocities, if necessary. In a study by Nouri et al [75] for increasing velocity, friction was best represented using a Stribeck

model and for decreasing velocity by Coulomb plus viscous model but this cannot be generalised. Equation 4.10 is only valid for frictional forces that are symmetric in both motion directions.

$$F_f = \beta \dot{y} + F_C \quad (4.9)$$

$$\text{Where } F_C = \begin{cases} F_{sf} & \text{if } \dot{y} = 0 \\ F_{df} \text{ sign}(\dot{y}) & \text{if } \dot{y} \neq 0 \end{cases}$$

$$F_f = \text{sgn}(\dot{y})F_{df} + \text{sgn}(\dot{y})(F_{sf} - F_{df})e^{\left(\frac{-|\dot{y}|}{sv}\right)^\delta} + \beta \dot{y} \quad (4.10)$$

4.1.2 Software implementation

The mathematical model of the actuator system was implemented in Matlab Simulink (figure 4.3) based on the equations described in section 4.1.1. The inputs to the model are the upstream pressure and the control signal to valve. Within the flow and pressure models there are further subsystems representing the individual chamber and circuit configurations. In figure 4.3, the pneumatic circuit model consists of four flow models and the cylinder-pressure models of two thermodynamic equations for both chambers.

A variable step ODE45 (Dormand Prince) solver with maximum step size of 0.001 was used for the simulations. The flow, pressure and force subsystems within the overall model were masked to allow for easy changes to parameters. Call-back functions were used to initialise variables on loading of the model and to automate some post-process data analysis. The top level subsystem depth is five. Examples of lower level models in Simulink can be found in appendix B.

In contrast to servo systems, point to point pneumatic drive systems are hybrid in the sense that the control element is discrete (on/off valves) but the output in terms of position or force of the actuator or air flow through the circuit is continuous and typically non-linear. In order to create a fully dynamic model this means that an additional number of loops, switches and logic are necessary, and this can increase computational time.

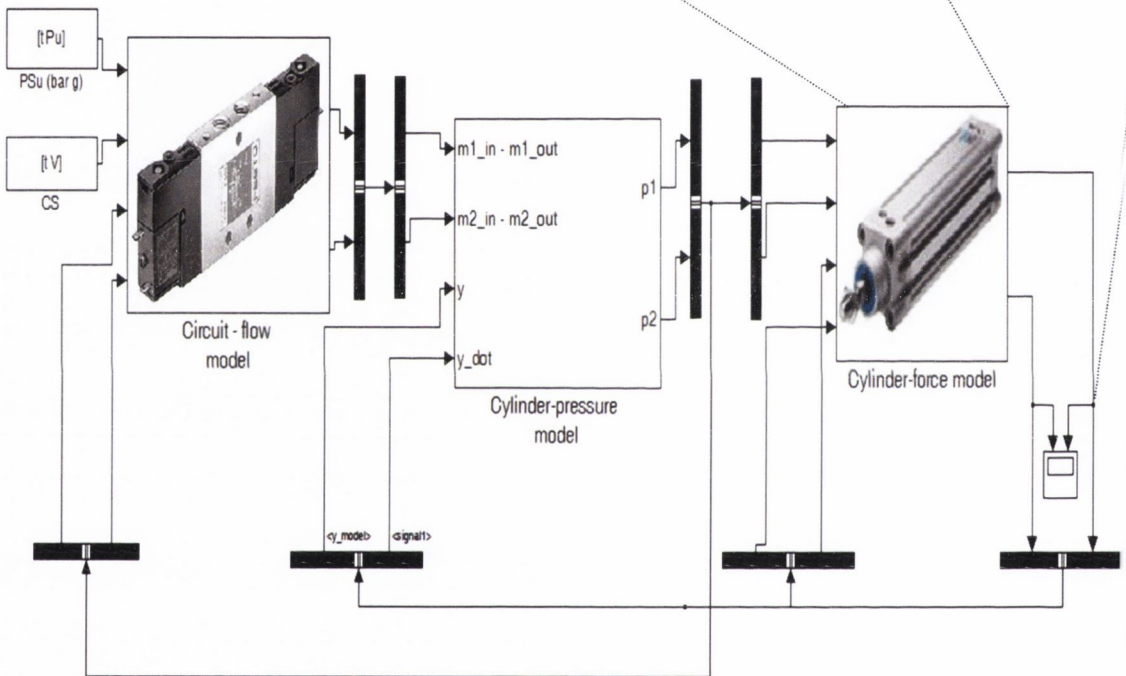
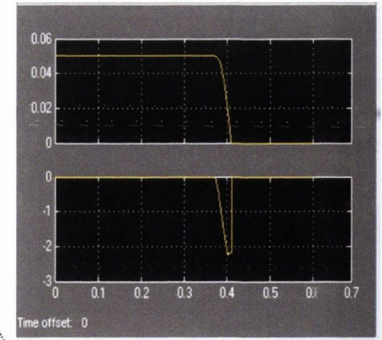
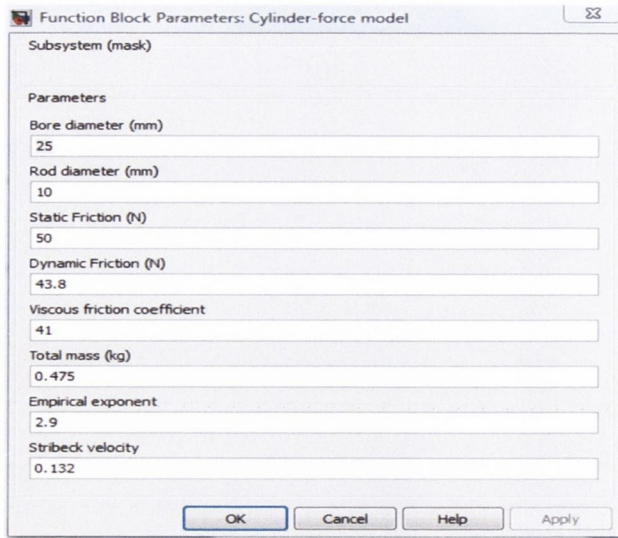


Figure 4.3: Top level drive system model in Matlab-Simulink

Boundary conditions

To account for the external force when the piston reaches the end caps of the cylinder, the velocity is reset when position reaches the defined saturation limits of: retracted, 0 mm, and extended 50 mm. The lower saturation limits for pressure and position are set to 101325 Pa and 0 mm respectively. Initial velocity is set to zero. The initial position can be set externally before each test so that the simulation can be started in

the extended or retracted position. Additionally the inertial force term Ma is equal to zero if the resultant pneumatic force F_p is less than static friction force and the piston is in its extended or retracted position. This is described mathematically in equation 4.11. The polytropic index n of the temperature model is set for each test and is limited to the range 1 for an isothermal process, to 1.4 for an adiabatic process.

$$Ma = \begin{cases} 0 \dots \text{if } y = 0 \text{ AND } F_p < F_{sf} \\ 0 \dots \text{if } y = 0.05 \text{ AND } F_p > -F_s \\ F_p - F_f \dots \text{else} \end{cases} \quad (4.11)$$

4.2 Parameter identification

4.2.1 Equipment and experimental setup

A schematic of the pneumatic drive with attached sensors is illustrated in figure 4.4. In addition to pressure, linear displacement and acceleration sensors, upstream flow, temperature and the command signal from the PLC to the directional control valve were also measured. Flow was measured to ISO2533 reference conditions by the Testo sensor and converted to the DIN1343 standard (figure 4.5). Details for the sensors used can be found in table 4.1. All sampling was conducted at 1000 Hz.

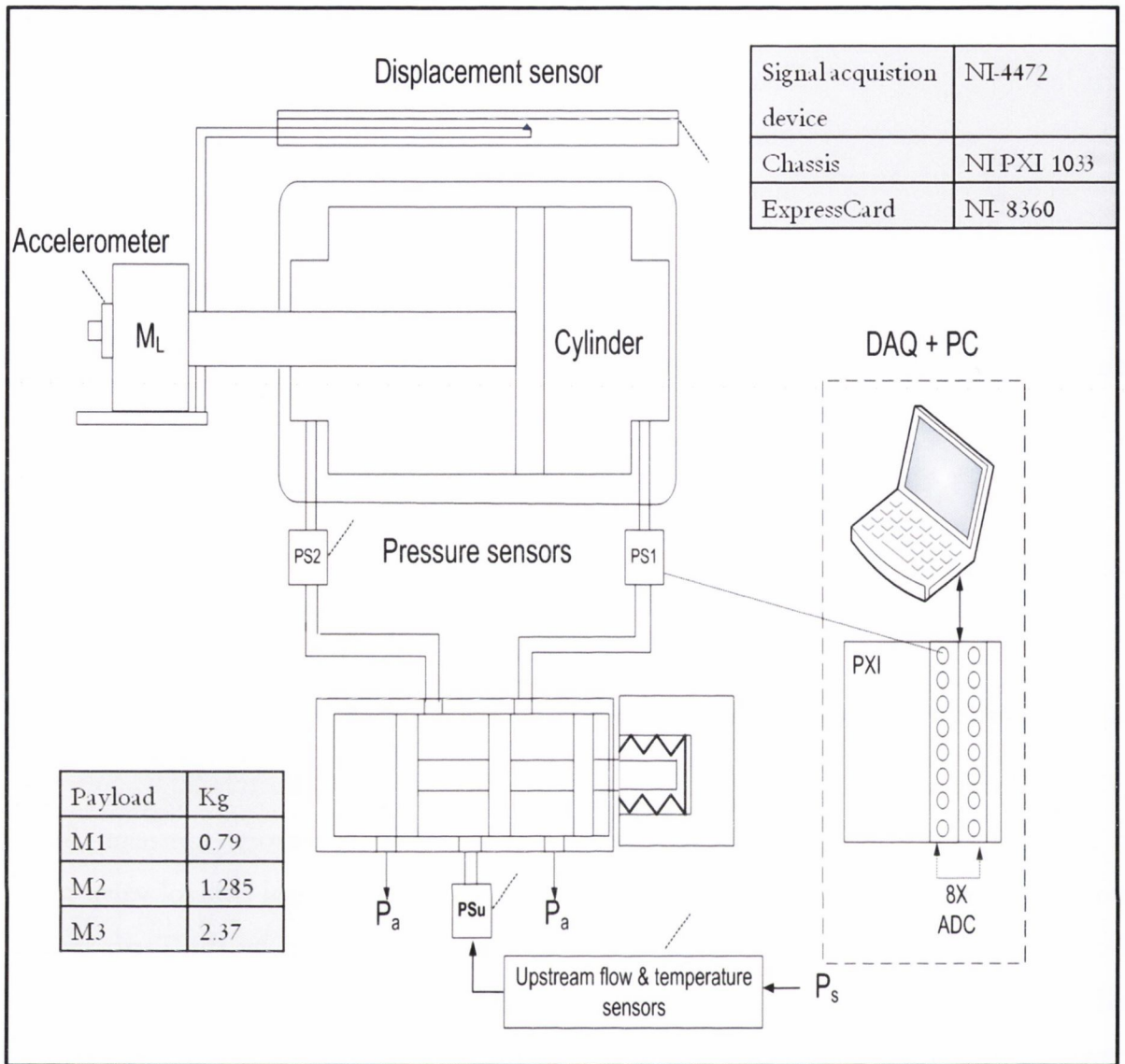


Figure 4.4: Experimental setup of drive with sensors, and details of experimental loads and DAQ system specifications

The NI signal acquisition device allowed for simultaneous sampling and analog to digital conversion, on 8 input channels with 24 bit resolution (figure 4.4). Additionally the input channels incorporated Integrated Electronic Piezoelectric (IEPE) signal conditioning for the accelerometer.

Sensor	Model	Range
Flow	Testo 6442	0-3.75 m ³ /min
Pressure	SMC PSE530	0-1 MPa
Temperature	Testo 6442	0-60 °C
Linear displacement	MTS EP2	0-200 mm
Acceleration	PCB 353B	± 500 g

Table 4.1: Measurement equipment

4.2.2 Flow identification

In industrial pneumatic actuator systems, the circuit flow paths are rarely symmetric. The flow characteristics of the charge flow paths can be significantly different for each chamber due to the presence of flow controls valves and the difference in tubing lengths. Additionally, the exhaust lines characteristics for both chambers will also be different as they typically contain components such as throttle or quick exhaust valves and silencers in the flow path. Individual fitting configurations also effects circuit performance. Since, the back-pressure is a critical aspect from a modelling accuracy perspective, it is crucial the exhaust line characteristics are known. Therefore the drive circuit is well represented using the Wheatstone bridge model in figure 4.5, to emphasise the need to identify the flow characteristics of four flow paths of the pneumatic drive. Such models are used in a different context in servo-pneumatics to describe the leakage across the spool in proportional valves [49] which is typically not an issue for standard binary mode control valves with elastomeric seals.

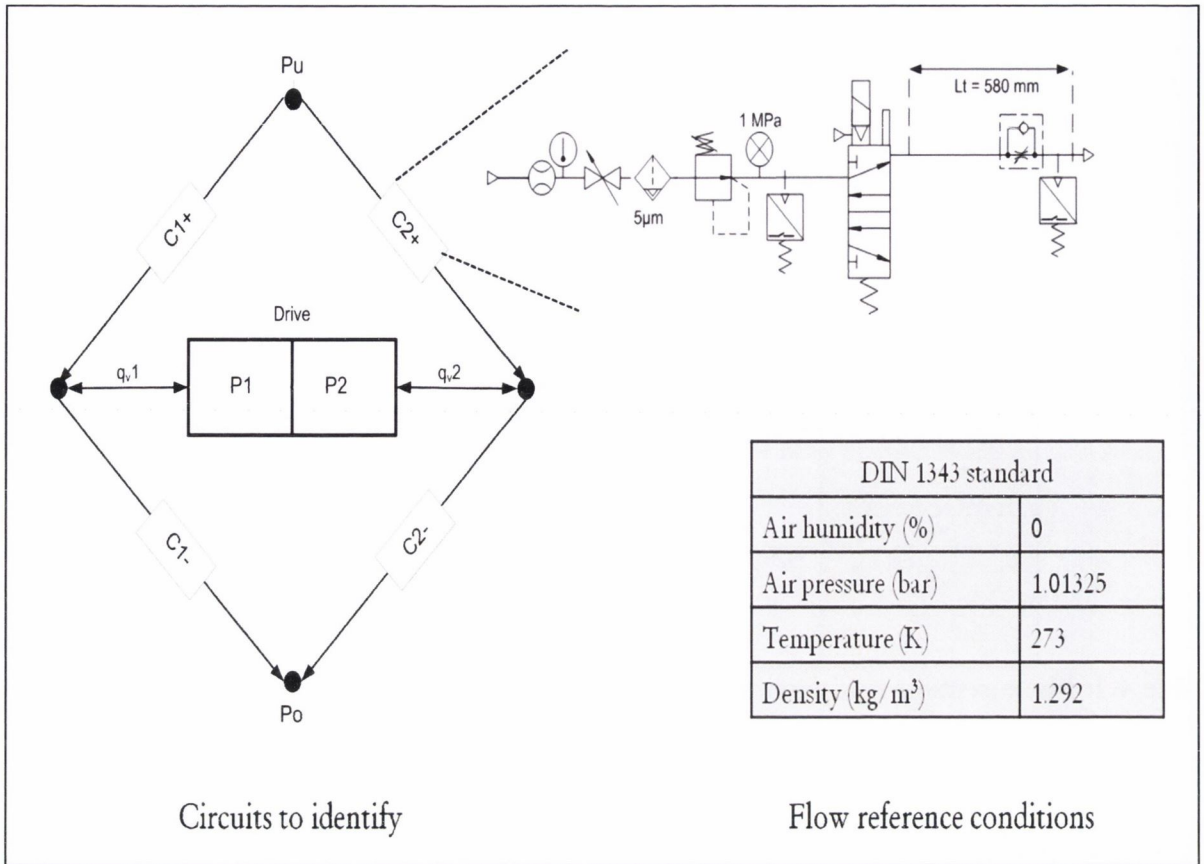


Figure 4.5: Pneumatic Wheatstone bridge model to indicate flow paths that require identification and volumetric flow reference conditions to DIN standard

Since an assembly of components behaves as a single component to the extent that an effective area and critical pressure ratio can be identified, a pneumatic circuit can be tested as one unit [94]. In this manner attenuation of flow due to tubing and fittings can be accounted for without the requirement for further terms in the model. A pressure regulator, working within its capacity, is a low-impedance source of compressed air and is therefore the start of the total inlet flow path.

The first test (steady flow) method, specified in ISO6358, for characterisation of devices in series involves reducing the flow rate successively with the use of a throttle valve, downstream of the device, while keeping the upstream pressure fixed. However this method is not suitable for industrial circuits, where the tubing and fittings are not oversized, since attaining a sufficient pressure differential across the device, in order to achieve choked flow, may not be feasible. Instead an improved test method [98] is used for

identifying the characteristics of the charge and exhaust flow paths, whereby the conductance is determined from the pressure versus flow and the remaining parameters are determined based on the flow ratio versus pressure ratio characteristics. In this method, the upstream pressure was gradually increased in increments and the pressure and flow through the circuit to the atmosphere was recorded, details of measurement equipment can be found in table 4.1. The sonic conductance C can then be solved using the gradient of the mean straight line region through the origin (figure 4.6a) and the flow ratio Qr from the conductance and equation 4.2. The critical pressure ratio b , subsonic index ms and cracking pressure ratio a are then determined by fitting the extended flow function, equation 4.1, to experimental data, figure 4.6b, using least squares method in Matlab (Trust-region algorithm).

Examples of selected identification results are given in figures 4.6 and 4.7 and demonstrate the affect of a silencer on the circuits flow function. Based on the accuracy of the flow, pressure and temperature sensors, shown in table 4.2, the conductance is subject to an estimated measurement accuracy of 6.32%.

Parameter of measurement system	Sensor/system accuracy
Flow rate, %	± 6 (3:4:4)
Pressure, %	± 2
Temperature, K	± 2
Conductance, %	± 6.32

Table 4.2: Accuracy of sensors and measurement system for flow identification

Experimental ambient conditions

The upstream temperature sensor indicated an ambient temperature of approximately 25 °C. Compressed air is produced by a compressor unit on the roof of the building and dried with a refrigerant drier, which means that the minimum dewpoint is limited to 0°C. The air was filtered locally to 5µm, which is equivalent to an ISO particle purity class of 3. In terms of oil content, the Dominik Hunter filters used in the

compressor house have a range of 0.01-0.6 mg/m³ oil content, equivalent to ISO classes 1 to 3. Based on the above deductions the air supplied to the experimental equipment is estimated to range between the ISO8573 quality classes: 3:4: 1 to 4:4:3.

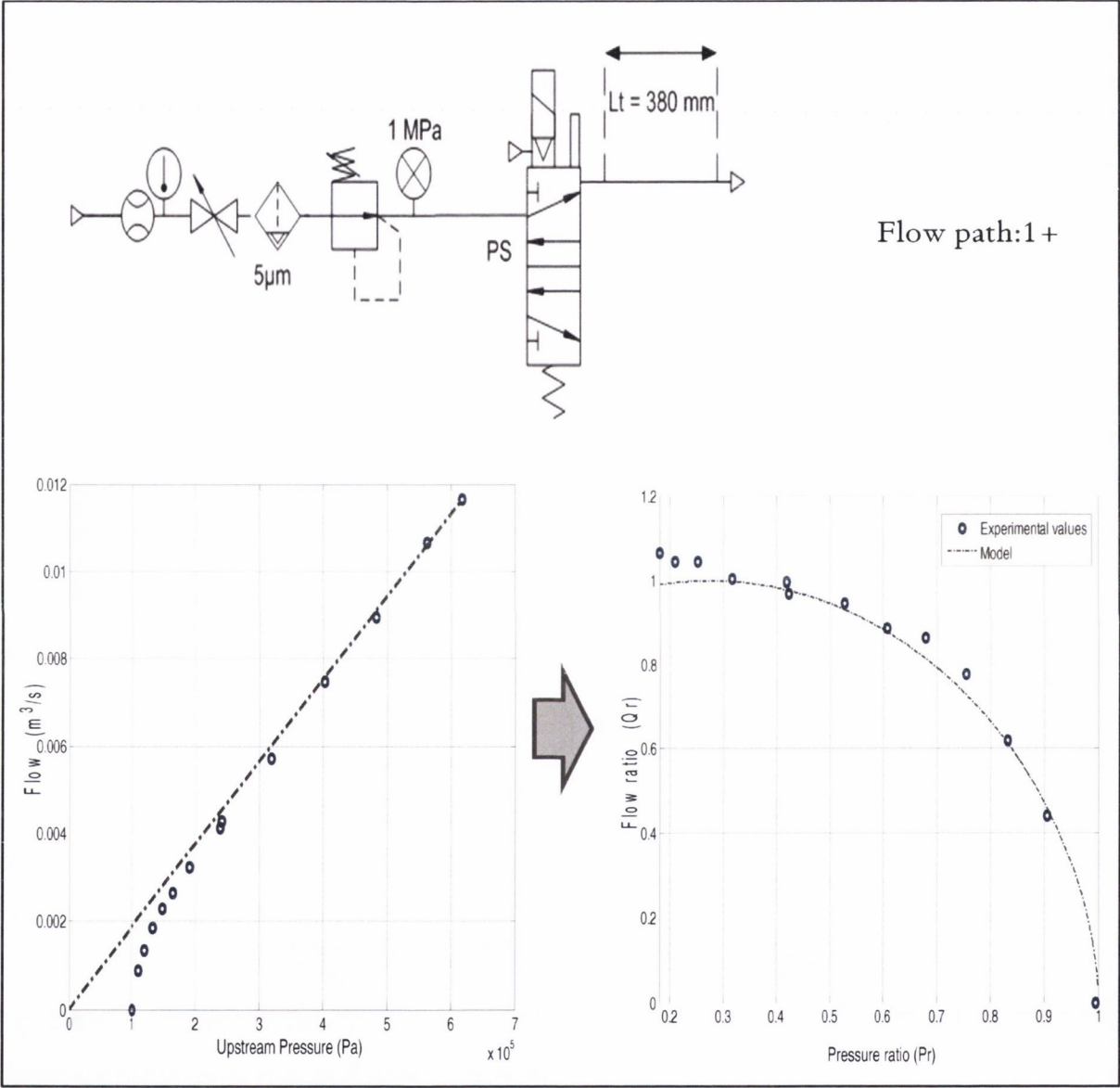


Figure 4.6: Flow characteristics of circuit flow path 1+ (a) Flow as function of upstream pressure (b) Flow ratio as function of pressure ratio

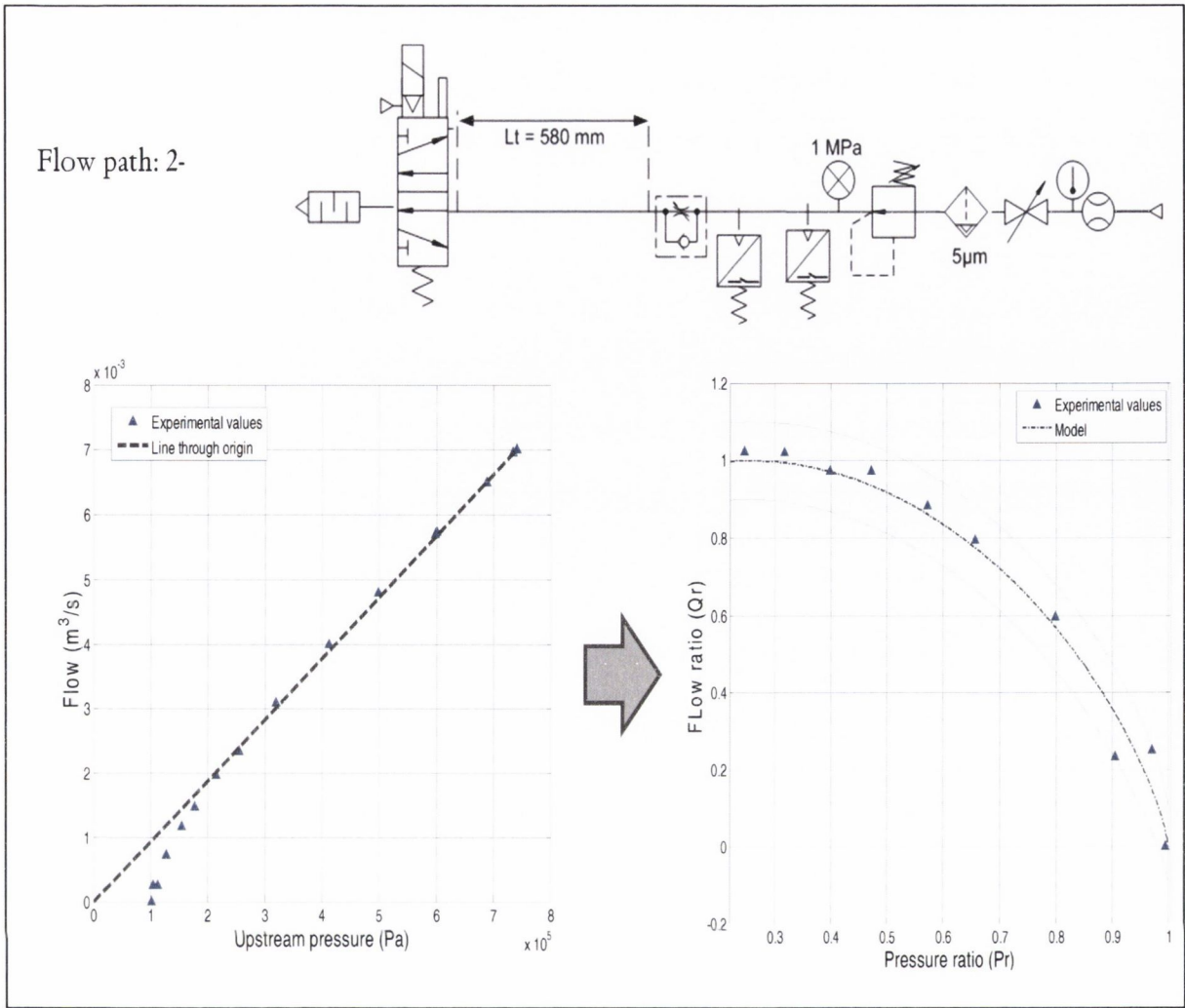


Figure 4.7: Flow characteristics of flow path 2-

The characteristic identification procedure was automated using Matlab and the algorithm's script can be found in appendix B. The mean results for the four flow paths are shown in table 4.3. Each parameter is an average of 5 test runs.

The conductance of the second chamber's flow path is considerably less (50% difference) than the first chamber's due to the presence of a one way flow control in the second chamber circuit. While the original ISO ellipse function is suitable for flow paths 1+, 1- and 2+ since m varies about 0.5, it is clear that the extended version is necessary for the exhaust path of chamber 2. A negative critical pressure ratio means that the flow never saturates(chokes)[75]. However, it is important to note that the critical pressure ratio for chamber 1 exhaust circuit is not based on physical behaviour but model best fit. This is

caused by a change in conductance of a circuit due to the silencer. When the pressure reaches a certain level the effective flow area can expand for some silencers [103], though since the conductance of the second chamber is less, this only occurs for the exhaust path from chamber 1 of the pneumatic drive. The existing ISO6358/Sanville equation is suitable for fixed area orifices only. Nouri et al [75] have also noted a discrepancy in flow function for charge and discharge circuits. The standard deviations indicate a reasonable level of precision in the identification results.

	1+		1-		2+		2-	
	Mean	Std dev.	Mean	Std dev.	Mean	Std dev.	Mean	Std dev.
C	1.79E-08	2.76E-10	2.31E-08	5.01E-10	8.69E-09	1.64E-10	9.45E-09	3.95E-11
b	0.2293	0.0348	0.01	0.0223	0.2925	0.0200	0.24	0.0076
m	0.4973	0.0422	0.52	0.0289	0.5163	0.0556	0.69	0.1203
a	1.0000	0	1.0000	0	1.0000	0	1.0000	0

Table 4.3: Summary flow characteristics for circuit flow paths with highlighted cases (+ inflow, - outflow paths)

To validate the flow model further, the model was used with equation 2.4 to predict the pressure response in a constant volume tank. The piston-rod was moved to its extended position and its entry port vented to atmosphere. The valve was then switched so that air flows to the cylinder chamber (1) and the pressure was recorded. The measured and predicted pressure trajectory is shown in figure 4.8. The maximum residual during transient pressure state was 12% of measured value and absolute steady state error was 0.3%.

The switching time for the directional control valve is different for on/off movements and is available in the data sheets of most OEM's. However, for accuracy purposes it is best to measure experimentally since in practise a drop in supply pressure can increase the switching time. This was done by measuring the time lag for pressure response in fixed volume chamber to a step input (figure 4.8) and subtracting the time it

takes for the pressure wave to propagate the tube/hose. The time delay for pressure wave to propagate the length of tubing is estimated by Lt/c . Mean results for delay times are also shown in figure 4.8 and are based on five test runs.

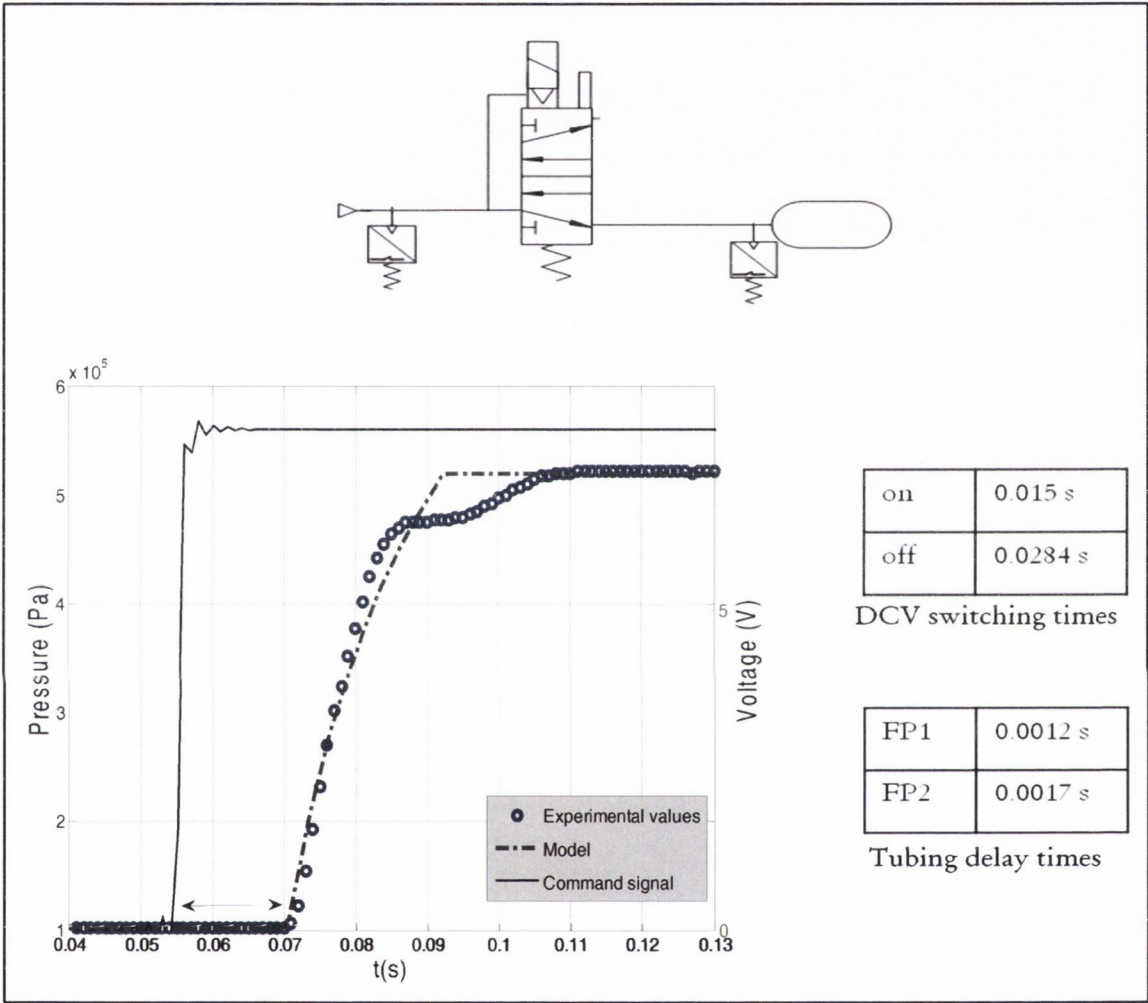


Figure 4.8: Measured and predicted pressure trajectory during constant volume charging with switching and estimated tubing delay times

4.2.3 Leakage identification

To test for leakage in the cylinder, pressure was supplied at 150 kPa and 630kPa at the rear port while venting the opposite port to atmosphere. The same procedure was applied to the front port, and in both cases the drive was cycled several times before testing. No leakage was detected above 0.1 L/min using a Festo SFE3 flow sensor.

Similarly to test for leakage in the valve, the open working port was closed with a plug and pressure was applied at the supply port. The procedure was repeated for the alternative valve state (e.g. on/off). Again no leakage could be detected above 0.1 L/min. Since the leakage is negligible equation 4.5 can be simplified to 4.6 for modelling purposes.

4.2.4 Dead volume identification

The dead volume at stroke ends was originally measured using a cutting fluid liquid and graduated cylinder. However, since the dead volume includes any additional fittings at the chamber port, it was instead estimated by equation 4.12 using the closed chamber method described by Carneiro et De Almeida [72]. The tubing lengths can easily be measured.

$$\hat{m} = \frac{V_{cyl_i} - V_{cyl_f}}{RT_o} \cdot \frac{P_i P_f}{P_f - P_i} \quad (4.12)$$

4.2.5 Heat transfer identification

The thermal time constant is determined by fitting a first order equation to the pressure response in a closed chamber of the cylinder to a change in volume. The cylinder piston-rod was moved to its extended position and the exhaust port (chamber 1) plugged. The piston-rod was pushed by an external force to about its half-length position, where it remained until pressure reached a stationary value. The pressure in the closed chamber was recorded.

Applying the ideal gas law, the temperature evolution inside the chamber can also be estimated. The thermal time constant is estimated using the first order equation 1 in figure 4.9. The average thermal conductance and average heat transfer coefficient was determined using the thermal time constant and equations 2-3 in figure 4.9. The mean results and standard deviation for five test runs can be seen in figure 4.9 and indicate a good level of precision.

Eichelberg's [72] simplified model (neglecting piston velocity) is then used to relate the reference coefficient of heat transfer to equilibrium or operating pressure and

temperature conditions (eq 4.13). While the Eichelberg model has been shown to be insufficiently accurate in identification of flow characteristics using fixed volume discharge methods, due to the fact that heat transfer coefficient changes with pressure and temperature [110], it does offer modest improvement for dynamic simulations [80] where temperature measurement is practically infeasible.

$$\hat{\lambda}_e = \hat{\lambda}_{av} \cdot \left(\frac{P_e T_e}{P_{av} T_{av}} \right)^{0.5} \tag{4.13}$$

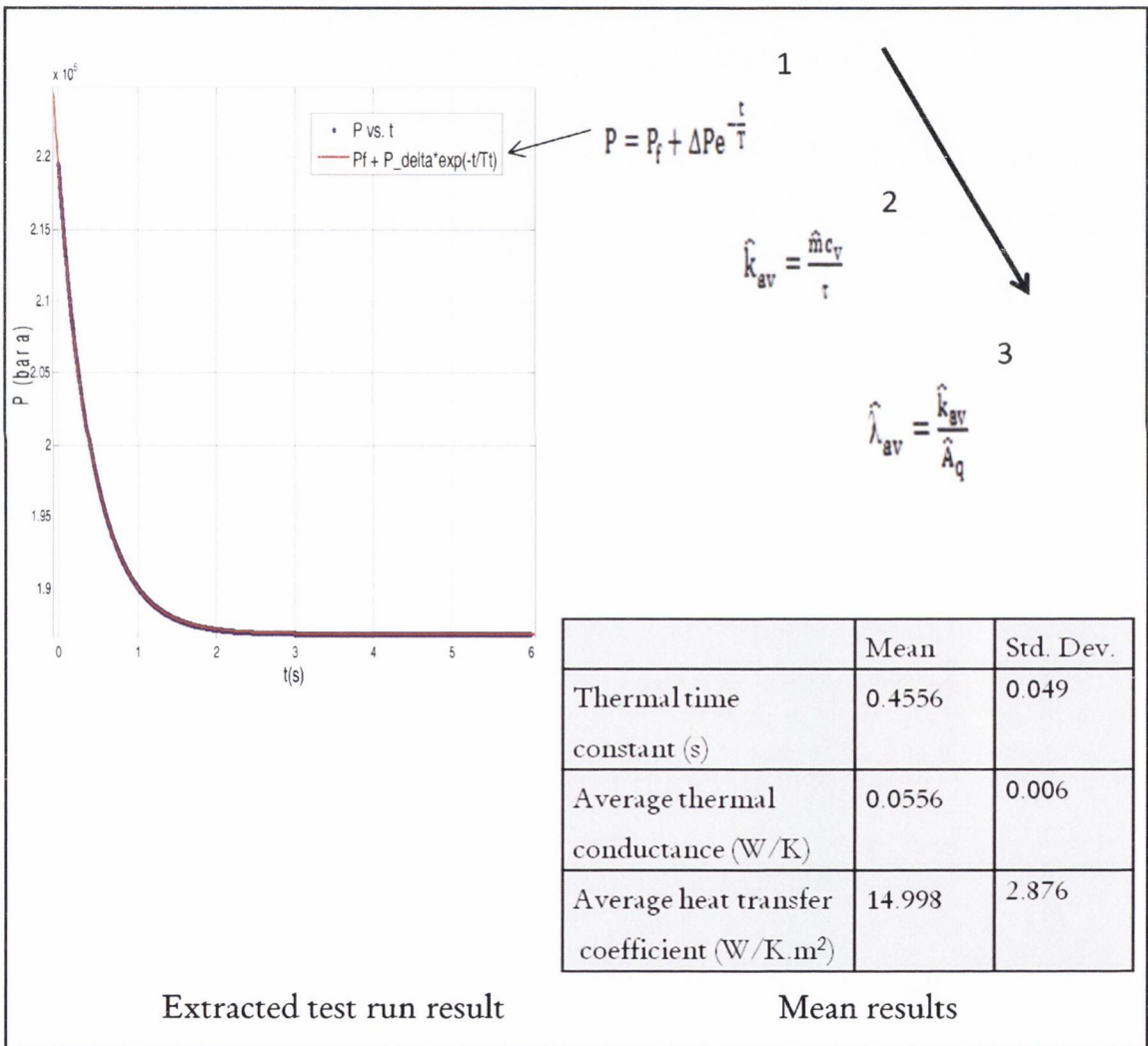


Figure 4.9: Pressure response (after motion ends) with fitted first order equation and heat transfer characteristics

4.2.6 Polytropic index estimation

Simulink design optimisation was used to estimate the polytropic index for each simulation. The thermodynamic model for chamber one of the pneumatic actuator in Simulink is shown in figure 4.10. The estimation tool minimises the cost function, in this case difference between simulated and empirical pressure signals, using a nonlinear least squares method. Figure 4.11 shows the trajectory of the estimated polytropic index and cost function for the procedure. The example given in figure 4.11 shows the optimisation results for the fixed volume charging illustrated in figure 4.8.

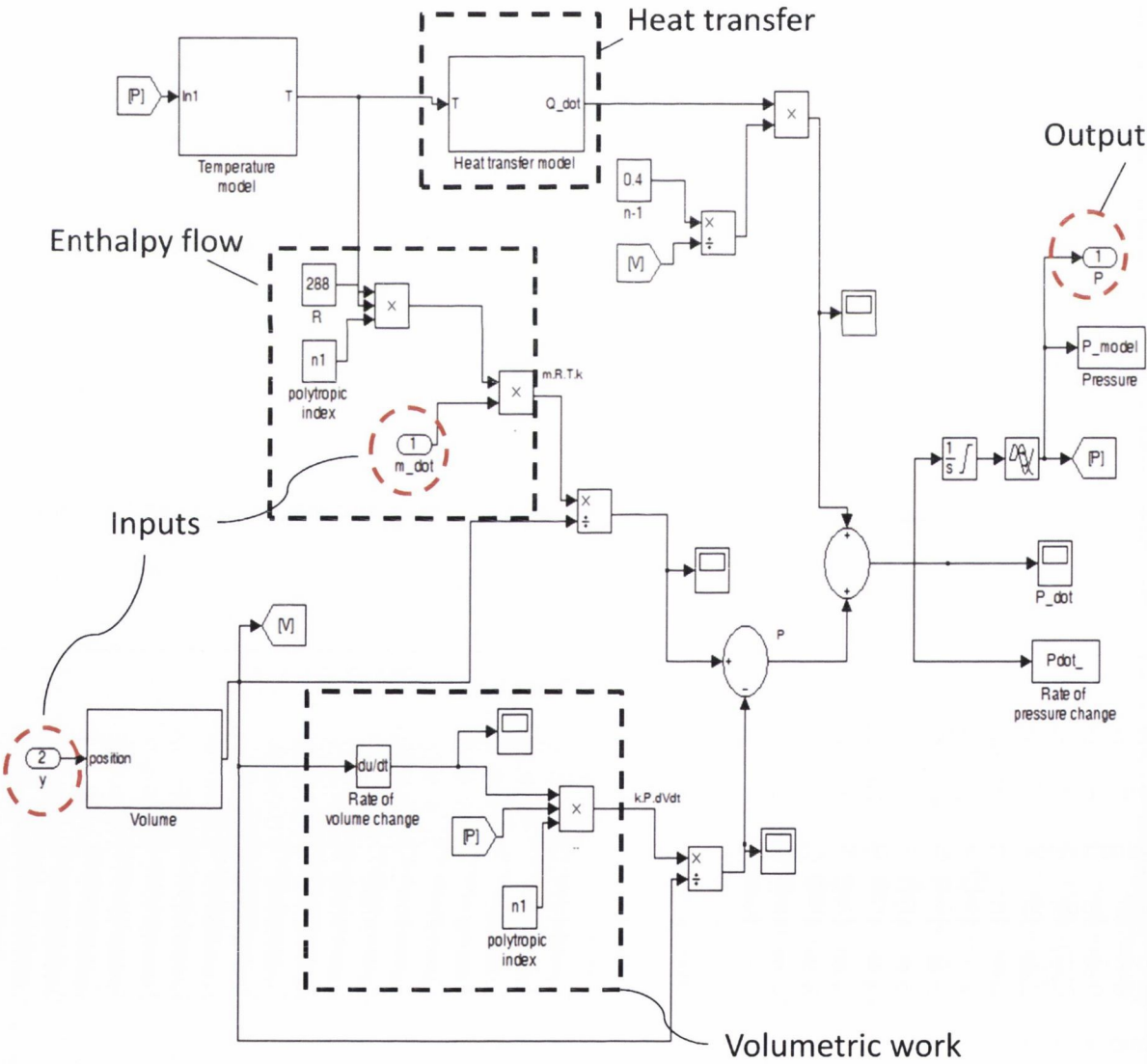


Figure 4.10: Chamber 1 thermodynamic model for polytropic index estimation

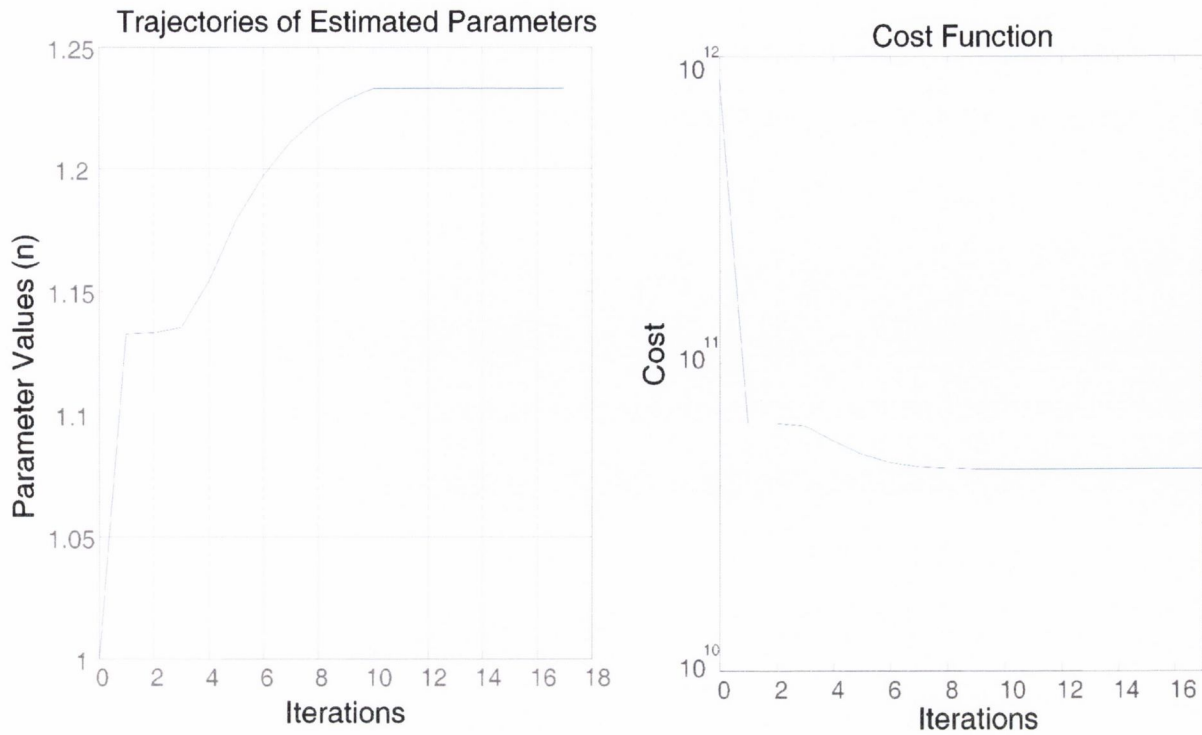


Figure 4.11: Trajectory of estimated polytropic index parameter and cost function

4.2.7 Friction identification

To identify the friction forces, the cylinder piston was cycled using the PLC and the acceleration, displacement, command signal, chamber and upstream pressures were measured using the setup shown in figure 4.4. For all tests the regulated pressure was held constant at approximately 5 bar. The friction force is estimated by subtracting the inertial force from the resultant pneumatic force (eq 4.14). The parameters static friction, Coulomb friction, viscous coefficient, Stribeck velocity and arbitrary exponent are then solved by non-linear least squares method in Matlab, using a Trust-region algorithm. The friction model identification procedure was automated in Matlab. An extracted test result from the procedure is shown in figure 4.12.

$$F_f = F_p - Ma \tag{4.14}$$

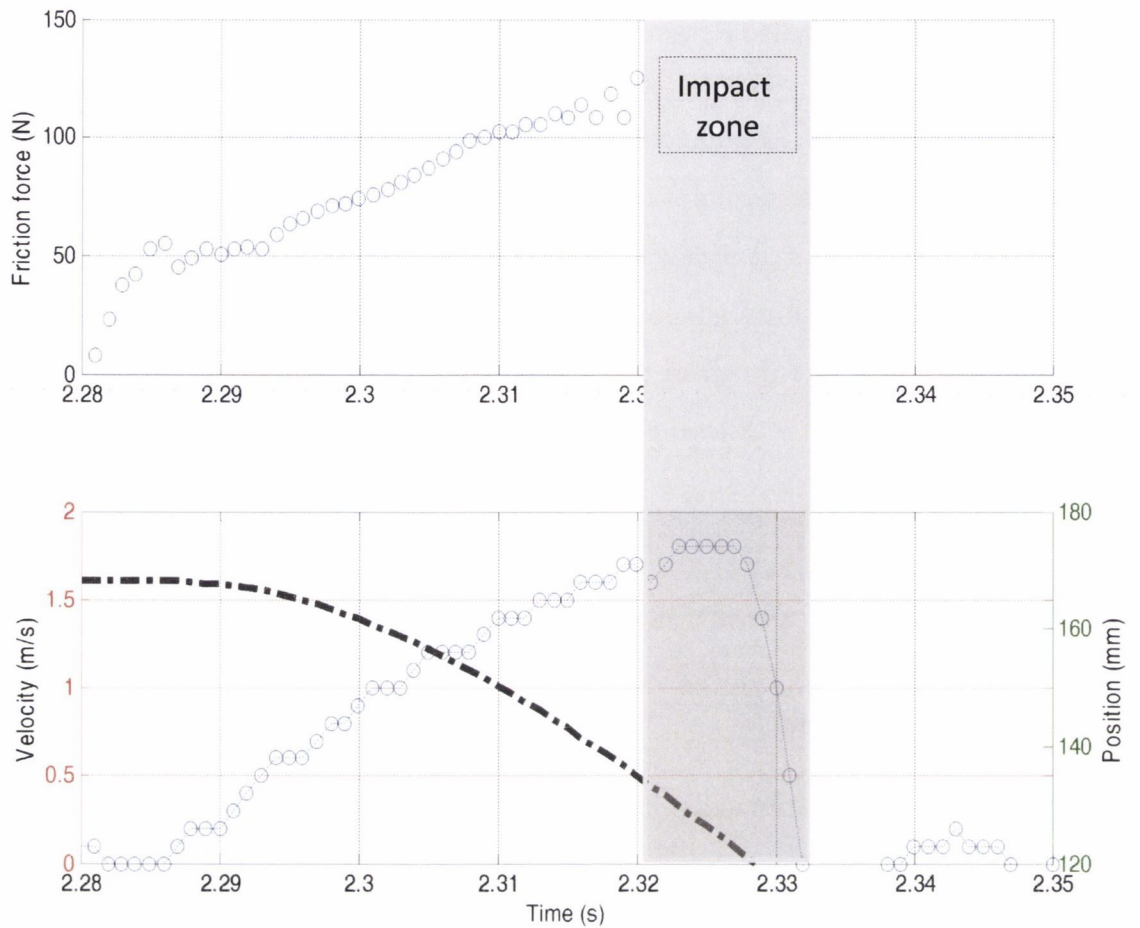


Figure 4.12: Friction, velocity and position with time over cycle

Based on the sensor specifications shown in table 4.4, the accuracy for the resultant pneumatic force is estimated to be 2.8%, and for friction force is approximately 5.7%.

<i>Parameter of measurement system</i>	<i>Accuracy of sensor/system</i>
Pressure	$\pm 2 \%$
Acceleration	$\pm 5 \%$
Mass	$\pm 0.1\%$
Pneumatic force	$\pm 2.83\%$
Friction force	$\pm 5.75 \%$

Table 4.4: Accuracy of sensors and measurement system for friction identification

The choice of friction model is data dependant, in some cases the simple combination of coulomb and viscous components may suffice but in this case the Stribeck model best fit the data. This is shown clearly in figure 4.14. Hysteretic frictional lag behaviour can be captured by fitting separate models to both increasing and decreasing velocity frictional forces [22,27]. However in this case, since the piston is relatively short stroke, the piston tends to accelerate to impact or accelerate initially to a constant velocity, and an additional decreasing velocity friction model is not necessary.

The friction parameters were identified at required operating conditions (pressure, payload and cycle time identified to simulation), since pressure effects the contact force between the piston and rod seals and the chamber walls [27] and the dwell time effects breakaway friction [13]. If the nominal chamber pressure or cycle time for the cylinder is changed the friction model must therefore be re-identified. Additionally care must be taken with open loop controlled pneumatic positioning systems not to include the impact acceleration due to an external force, the piston reaching the end cap of cylinder, which can distort the friction calculations. The results were found quite repeatable for both extend and retract strokes. Figure 4.13 demonstrates the scatter of friction force with velocity for the extend stroke and is based on 5 test runs. There is some variation in the frictional forces due to inexact upstream pressure settings on an analog regulator.

In reality pre-sliding or micro-slip occurs where the friction is better represented as a function of displacement and the saturation of pre-sliding force is the breakaway friction which leads to gross sliding [27]. However, in practice pre-sliding models can be difficult to identify without high resolution equipment and a special experimental setup.

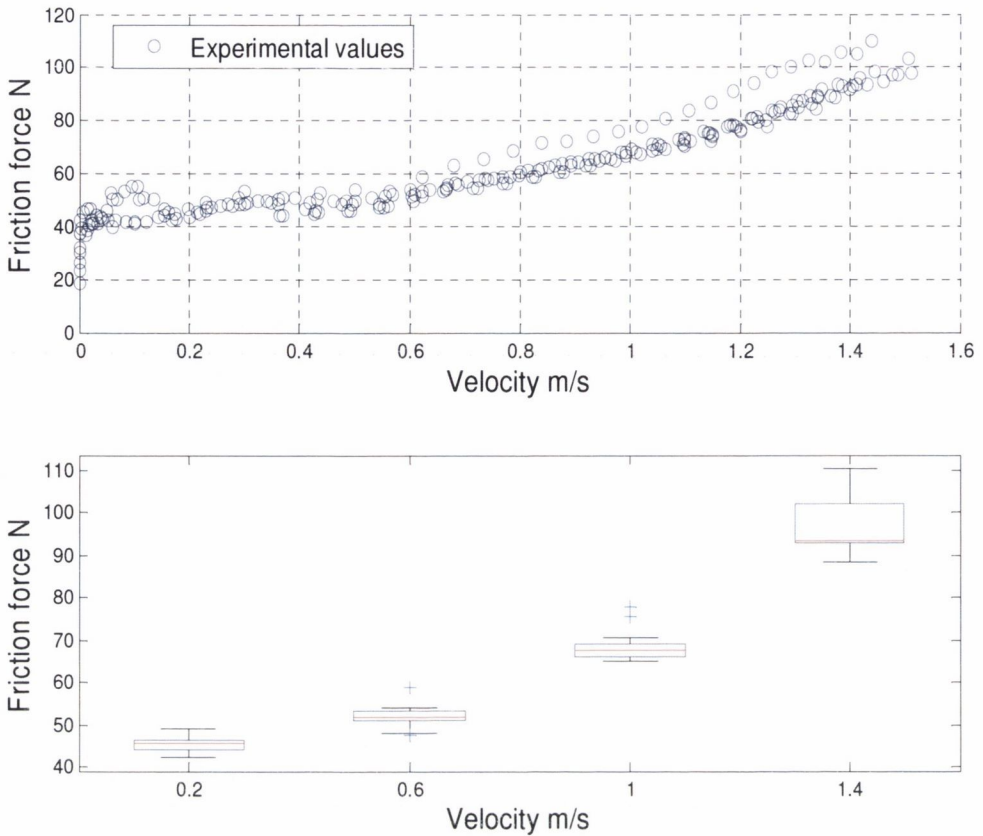


Figure 4.13: Overall results of friction with velocity for extend stroke and selected bar plots

In figure 4.14 the Stribeck effect, of negative viscous friction, is very much evident for the extend stroke. Similar to work of Hildebrandt et al [49], the dry friction is high in comparison to full theoretical force produced by the drive of 295N. Of note is the fact that friction force is not symmetric for extend and retract strokes. Belforte et al [76] have attributed this behaviour to two causes; 1/ Directionality of the seals. The piston and rod seals act differently according to the direction of motion. 2/ Tribological factors. The tolerance between cylinder barrel and seals, roughness of the cylinder barrel and amount of lubricant are different along the cylinder. However, in the study by Belforte the difference in friction forces for the extend and retract stroke is relatively small. In comparison, the difference in static friction for both strokes is approximately 47%. The average friction parameter results for the second payload, based on 5 test runs, are shown in table 4.5.

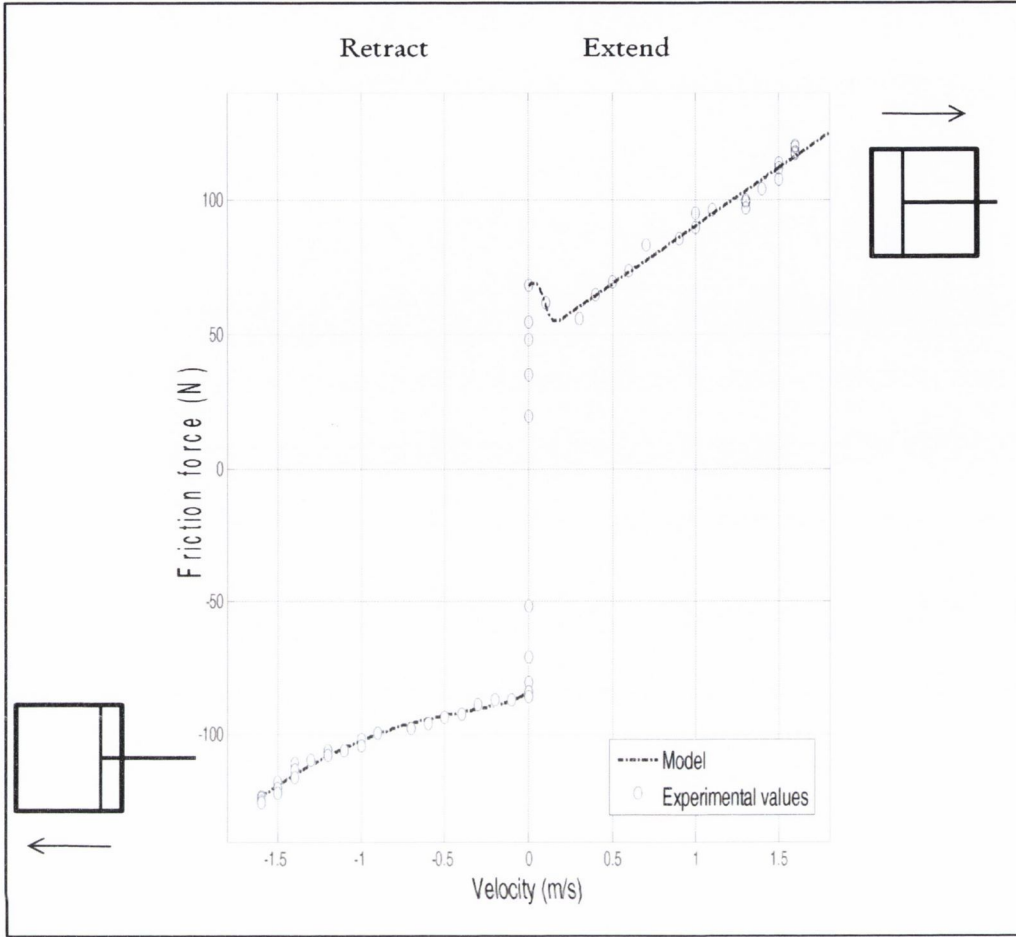


Figure 4.14: Measured friction force with velocity and fitted model (extend and retract)

M2	Extend	Retract
Mean F_s	43.029	81.871
Std dev	1.184	0.657
Mean F_c	7.137	69.217
Std dev.	3.609	3.113
Mean B	62.135	13.774
Std dev.	6.512	1.836
Mean vs	0.458	0.375
Std dev.	0.029	0.023
Mean d	1.756	2.815
Std dev.	0.184	0.545

Table 4.5: Selected friction parameter results for payload M2

Friction model development

Based on the results in the parameter identification section, the friction model was further developed, using an additional if-case loop, to account for asymmetric frictional effects during extend and retract (eq 4.15).

$$F_f = \begin{cases} F_{df1} + (F_{sf1} - F_{df1})e^{\left(\frac{-|\dot{y}|}{sv1}\right)^{\delta1}} + \beta_1\dot{y} \dots \text{if } \dot{y} > 0 \\ F_{df2} + (F_{sf2} - F_{df2})e^{\left(\frac{-|\dot{y}|}{sv2}\right)^{\delta2}} + \beta_2\dot{y} \dots \text{if } \dot{y} < 0 \end{cases} \quad (4.15)$$

4.3 Model validation

A double acting asymmetric cylinder was used to validate the modelling approach. Bang Bang control was implemented through a PLC (OMRON CQM), solenoid activated 5/2 directional control valve and magnetic reed limit switches. A one way flow control (meter out type) was used for the extend stroke and both exhaust paths terminated with a silencer. The pneumatic cylinder's properties are described in figure 4.15. The total weight of the cylinder was 0.293kg. The pneumatic circuit diagram for the experimental setup is illustrated in figure 4.16 and represents a typical industrial type pneumatic drive system. In order to validate the modelling approach, three experiments were conducted with different payloads (figure 4.4) but constant supply pressure of approximately 5 bar absolute.

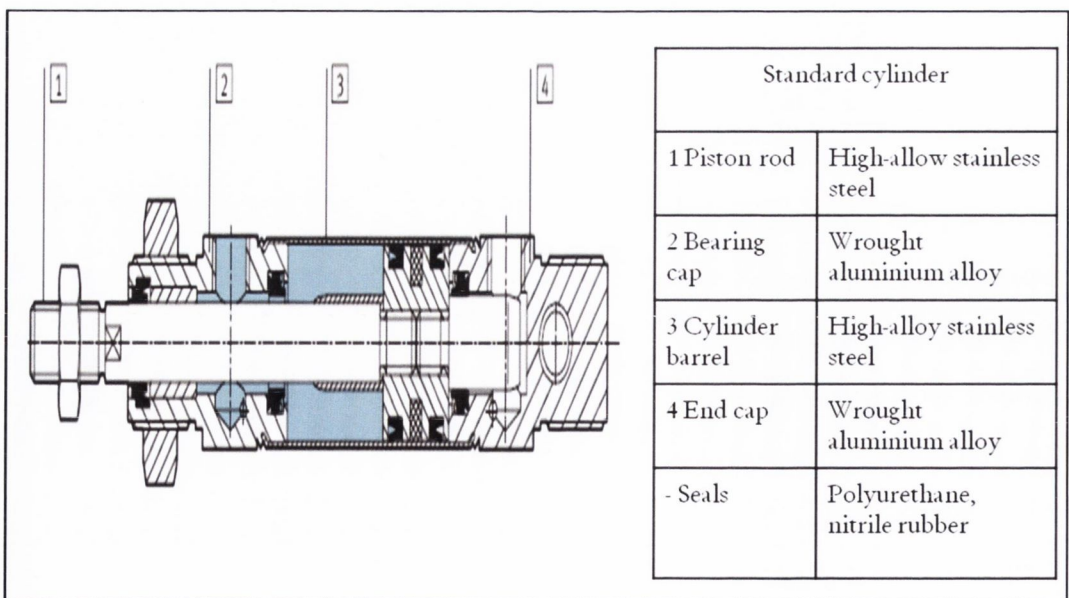


Figure 4.15: Actuator properties [166]

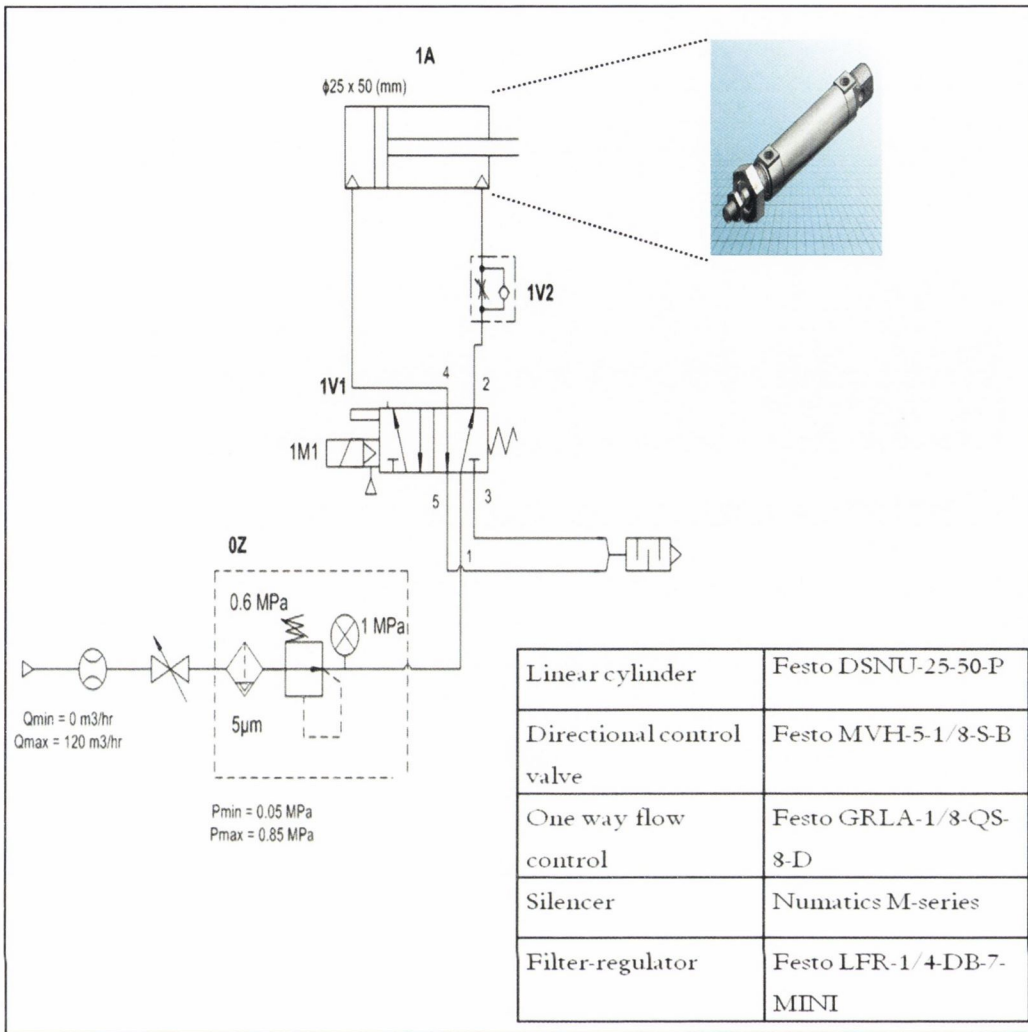


Figure 4.16: Pneumatic circuit diagram for drive system and equipment details

Figures 4.17a and 4.17b illustrate the measured and predicted position trajectory of the first payload for extend and retract strokes. Figure 4.18 shows the position and velocity trajectories for the second payload during extend stroke. The displacement measurements are subject to an error of 0.03% using the MTS sensor. All figures show excellent agreement between modelled and experimental curves in terms of both time alignment and steady state accuracy. Summary results from the residual analysis of measured versus simulated position are shown in table 4.6. The analysis is based on the difference between experimental and modelled trajectories during the transient state. Steady state error is not appropriate in this case since the position is saturated at both ends. The root mean square error was between 0.57mm to 1.7mm for both payloads. The mean error shows that the model generally under-estimates the extend stroke and over-estimates

the retract stroke. However, the mean absolute error is less than 1mm in both cases, indicating a good level of prediction accuracy. The results compare favourably to previous published work in the literature. Richer et Hurmuzlu state an average error of 2mm and max error of 3.42mm [15]. Najafi et al report a positioning error of less than 1.8mm [89]. Both used actuators of similar size.

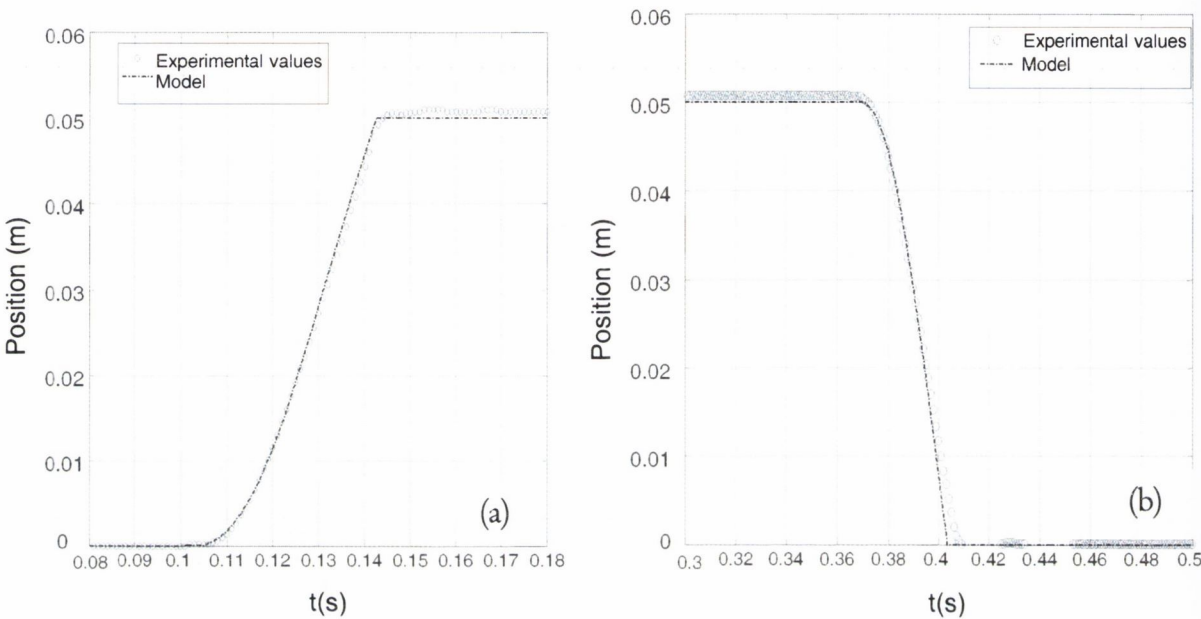


Figure 4.17: Model v measured position with payload1, (a) extend, (b) retract

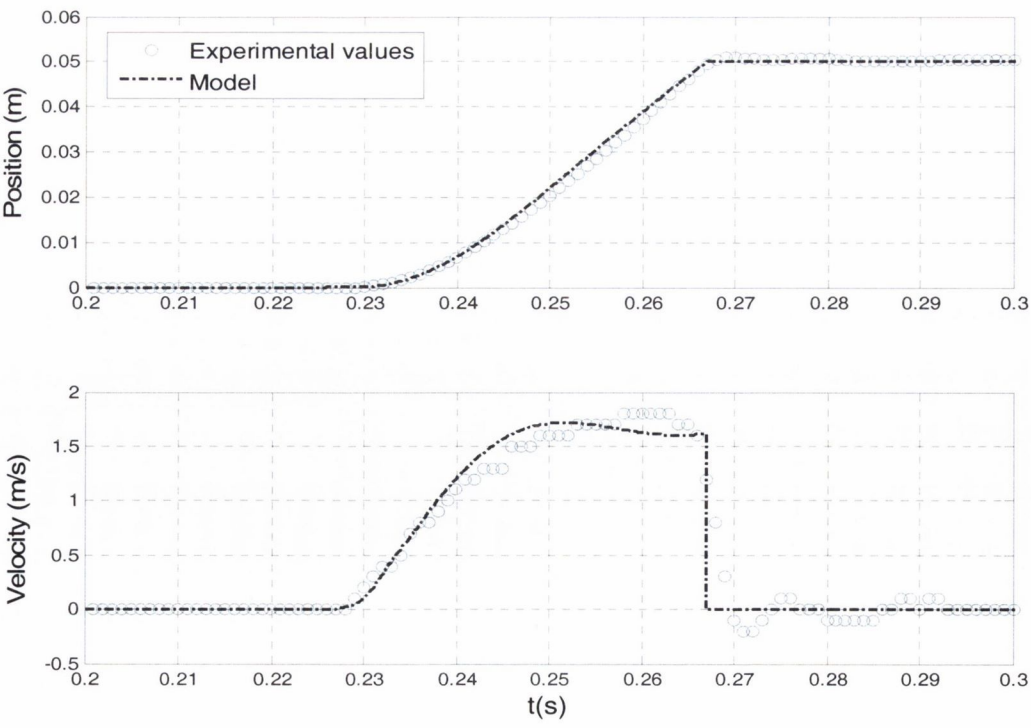


Figure 4.18: Model v measured position and velocity with payload2 (extend)

The model was checked with Model advisor tool in Simulink to check for inefficient system simulation or code generation and to assess its compliance with IEC61508 (ISO26262) and DO-178B standards on software for safety critical applications. An issue raised by the advisor tool was that in order to generate code for real-time embedded applications, using real time workshop for example, a fixed step solver is necessary. To test the model in cycle, the simulation was run with a fixed step solver and automatic step size. Figure 4.19 demonstrates that the dynamic behaviour of the system in cycle is sufficiently approximated.

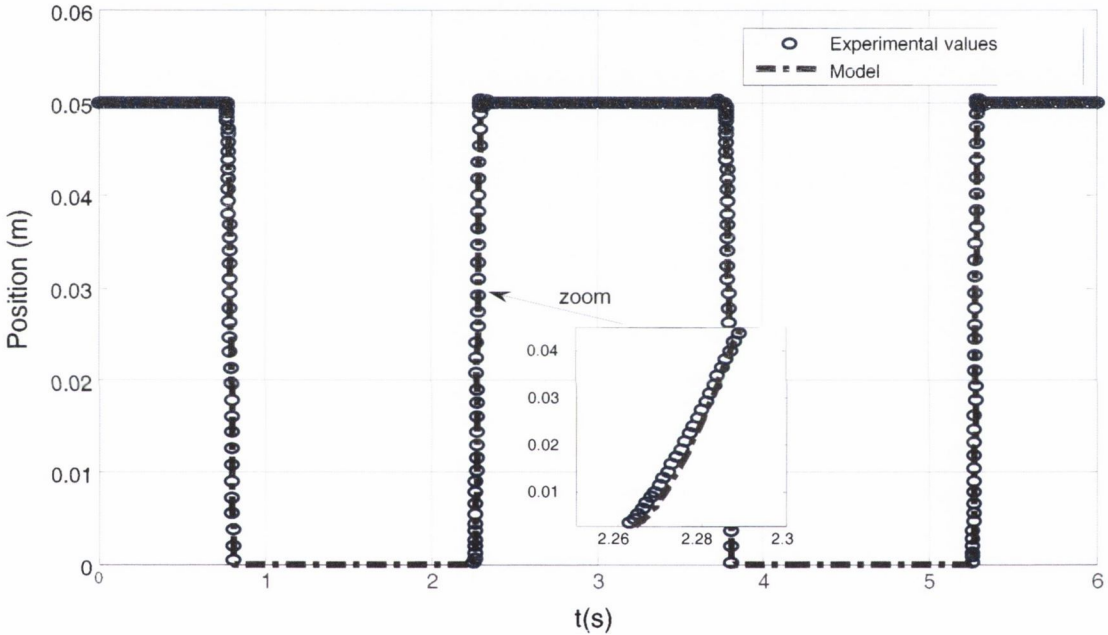


Figure 4.19: In cycle modelled and measured position with payload2

Position	ME (mm)	MAE (mm)	RMSE (mm)	MXR (mm)
Extend M1	+0.28	0.54	0.57	1.1
Retract M1	-0.02	0.79	0.91	1.64
Extend M2	+0.92	0.93	1.7	5.24
Retract M2	-0.79	0.83	0.92	1.6

Table 4.6: Residual analysis for measured and simulated position (In cycle)

Figure 4.20 and figure 4.21 illustrate the pressure prediction accuracy of the model for the extend stroke with third payload. Figure 4.23 and figure 4.24 show the measured and modelled pressure for the retract stroke in both chambers. It can be seen from table 4.7 that the pressure is well approximated by the model with a root mean square error of 0.14 to 0.34 bar. The pressure during discharge (chamber 2) is more difficult to predict with an increased mean absolute error of approximately 21.5kPa in comparison to 0.58 kPa MAE for the pressure prediction in chamber 1. Hildebrandt et al have also noted model errors in pressure prediction [49]. This is likely due to the flow parameters identified for the exhaust circuit line. The flow characteristics of the cylinder exhaust circuits are difficult to identify since they do not have access to an unlimited energy supply. In order to allow for the steady state based flow method of identification the pneumatic circuit must be modified and this implies that circuit used for identification is not identical to its final configuration. This highlights an important limitation of the current identification by steady flow method, in particular for industrial environments, where there may be limited flexibility to re-arrange components. Nonetheless the modelled resultant pneumatic force, for both extend and retract, (figures 4.22 and 4.25) provide a good match with experimental results. The root mean square error was 16.3N for the extend stroke. The average difference of 8.3N indicates that the model generally under predicts experimental values, due in this case to an over-estimation of exhaust pressure.

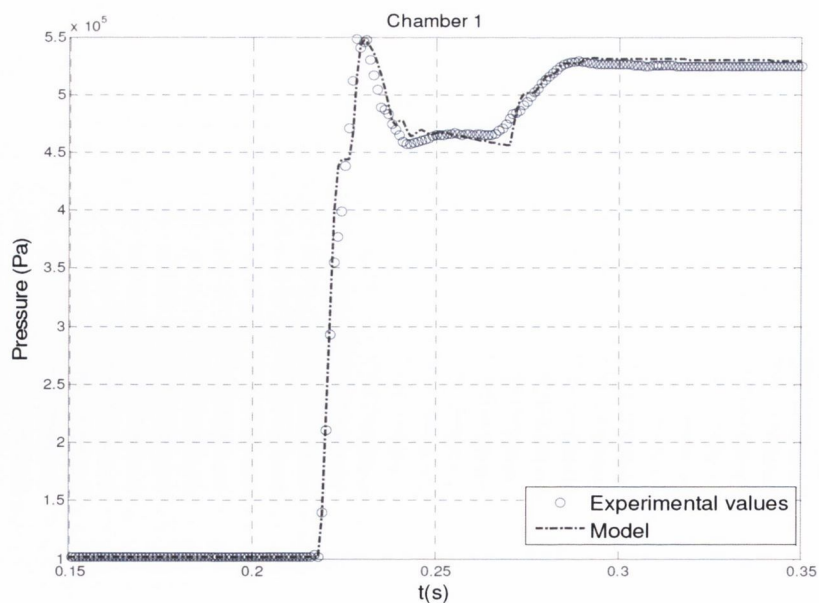


Figure 4.20: Measured and simulated pressure during extend stroke with M3 payload

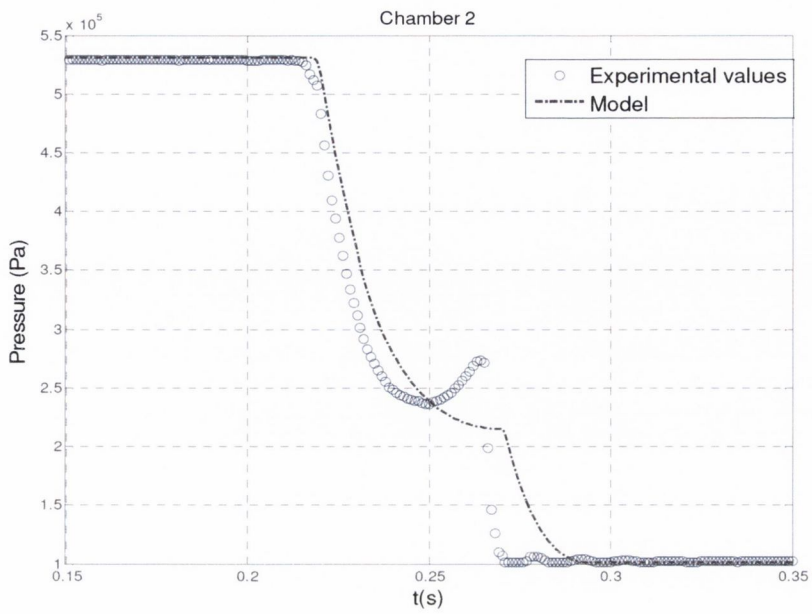


Figure 4.21: Measured and simulated pressure during extend stroke with M3 payload

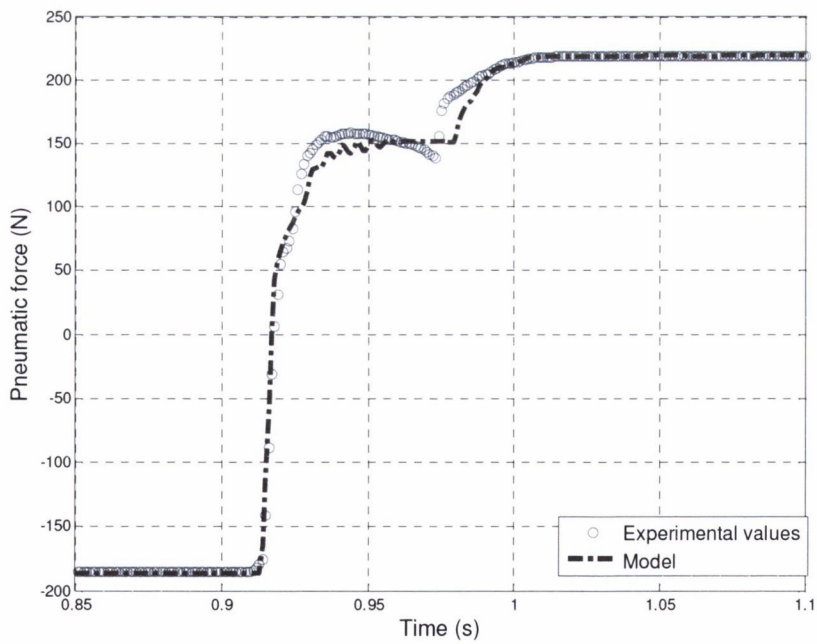


Figure 4.22: Measured and simulated pneumatic force during extend stroke with M3 payload

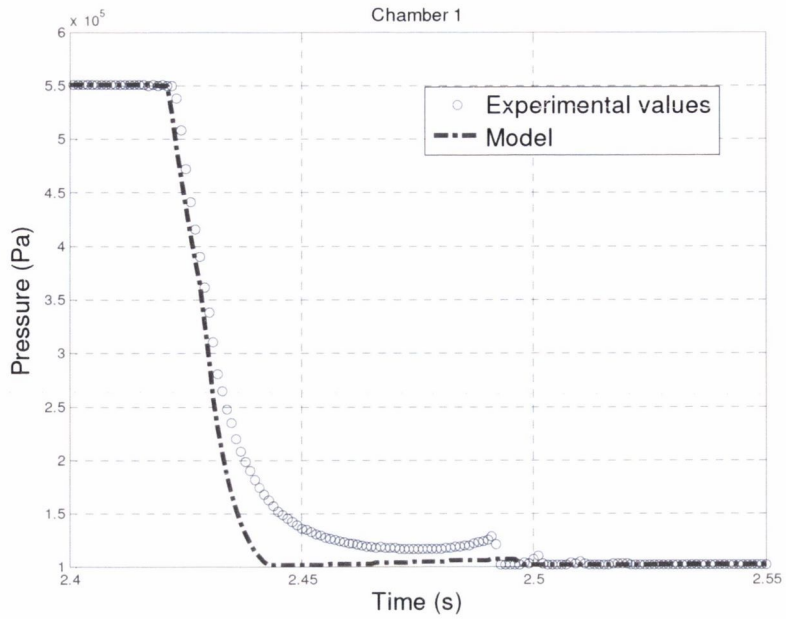


Figure 4.23: Measured and simulated pressure during retract stroke with M3 payload

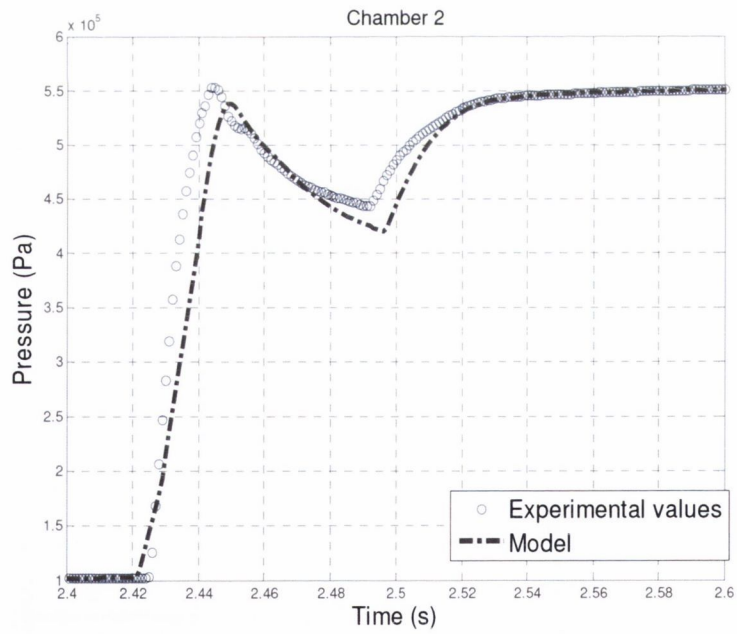


Figure 4.24: Measured and simulated pressure during retract stroke with M3 payload

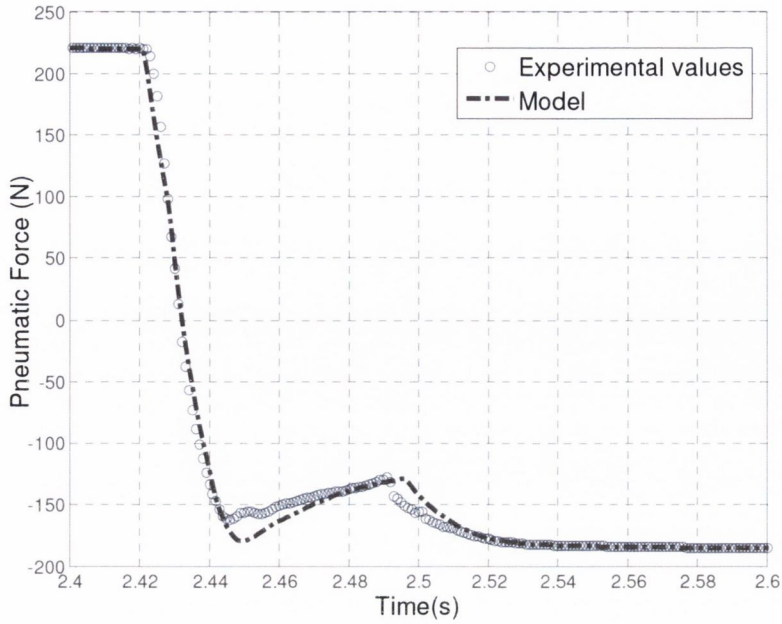


Figure 4.25: Measured and simulated pneumatic force during retract stroke with M3 payload

	ME	MAE	RMSE
Pressure (Ch1)	-0.8 kPa	0.58 kPa	14.3 kPa
Pressure (Ch2)	-19 kPa	21.5 kPa	33.9 kPa
Pneumatic force	+8.3 N	9.6 N	16.3 N

Table 4.7: Residual analysis for measured and simulated pressure and pneumatic force (Extend)

4.4 Summary

- The contribution of this work has been to fully model the dynamics of an open loop controlled pneumatic drive system, common in industry.
- An extended flow function, proposed by Kagawa [103], has been used to accurately describe the non-linear flow behaviour of a typical pneumatic drive circuit, and both charge and exhaust flow paths have been carefully identified. Based on the latest research, heat transfer was explicitly included in the cylinder's thermodynamic model and the friction model chosen based on experimental data with parameters identified at specific operating conditions.
- The improved ISO identification method, proposed by Kuroshita [98] for component characterisation, has been successfully applied to the identification of extended pneumatic circuits and as such is deemed suitable for industrial circuits.
- The model provided good results in terms of tracking position and pneumatic force trajectories and as such should be useful for future simulation, design and analysis of industrial type pneumatic actuator systems. The mean absolute error, in position prediction was less than 1mm, in pressure prediction was less than 22 kPa, and for pneumatic force was estimated to be 9.6N. The position error in terms of the stroke length of the cylinder is 2%. The pneumatic force error in terms of the maximum theoretical force produced at a pressure of 5 bar is 3.9%.
- This chapter has provided the theoretical foundation for understanding the consumption of compressed air by pneumatic drives. However, in order to practically model industrial type production systems (i.e. to scale), some simplifications and the consideration of other air consumer types is necessary.

5. Predictive Consumption Models for Electro-Pneumatic Production Systems

5.1 Model development

With a view to improving the overall energy efficiency of pneumatic systems, it is proposed here that the air consumption of production systems should be coupled with machine state and activity. The approach taken is based on the fact that theoretically (e.g. excluding leakage) the air consumption function transitions from one value to another at moments when individual loads are activated and deactivated [31]. The challenge is thus to efficiently model the systems response to changing activation profiles. In an industrial system, this profile is determined by a programmable controller and initiated by a products/work piece presence. Using this approach, the consumption characteristics can be related to physical phenomenon, and the required production of air can potentially be predicted.

The model development consists of the development of the mathematical models of individual consumers within an electro-pneumatic system, the overall system itself, and model implementation in Matlab-Simulink. The main issues motivating the model development are:

- Scalability: To accurately model the consumption of large machine's consisting of multiple pneumatic devices
- Identification: To reduce the time and air consumed by current parameter identification techniques
- Interoperability: To allow for integration into current production environments
- Dynamic: To allow for changing production conditions
- Universal: To account for all types of consumers, active and passive, within a typical factory environment

The proposed model architecture is shown in figure 5.1. Any pneumatic production machine consists of multiple types of actuators and blow device, controlled by a PLC via electro-pneumatic valves. The approach taken is to use simplified linear consumption

models, developed in Matlab-Simulink, and an OPC server to interface the simulation model and the PLC. A benefit of using OPC is that it is an open protocol and widely used in industry.

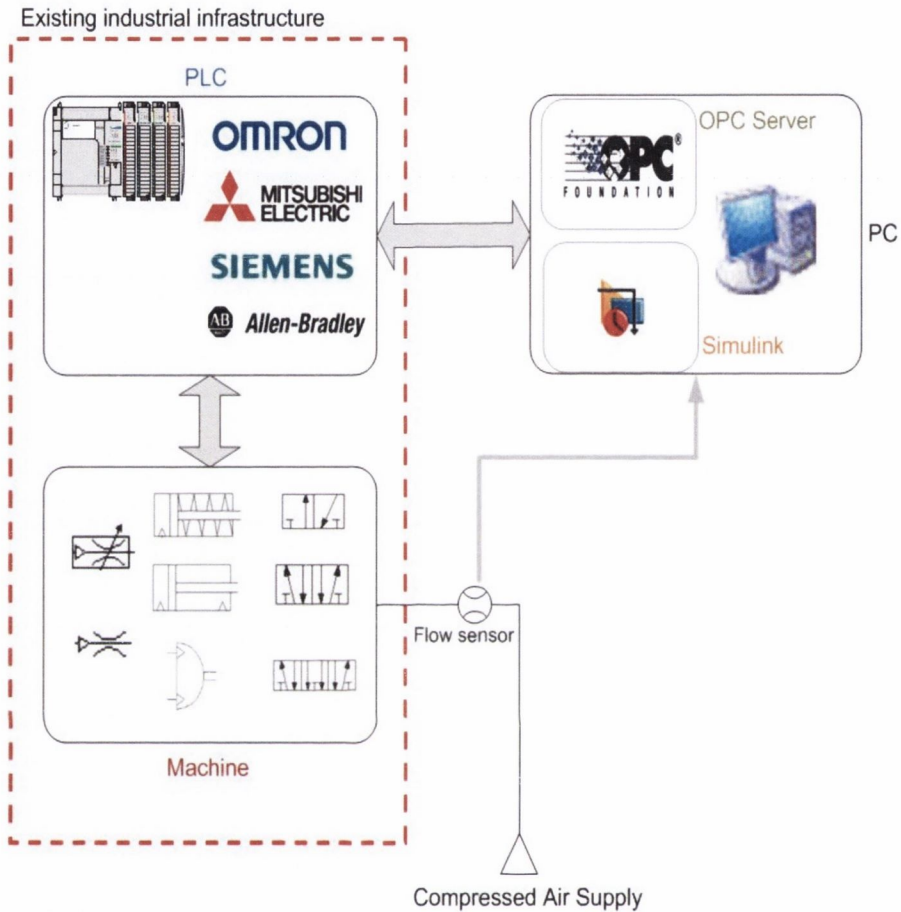


Figure 5.1: Modelling approach

5.1.1 Consumption dynamics of production systems

Typical air consumers in a pneumatic production system consist of cylinders, motors, tools, open blow/blasts. Consumption may be constant during certain time period, it may change periodically, stepwise, linearly or randomly depending on the characteristics of the consumer [119]. Previous research by Parkinnen [31] considered the consumption function as stochastic, in that consumers in pneumatic network are activated temporally at random instants of time. The objective of compressor control has thus been to respond to time dependant consumption. However, if the addition of random demand loads on the system are neglected (e.g. air gun use by operator), then the consumption

function can be viewed as quasi-deterministic due to the fact that component activation is dependent on the controlling program in the PLC. An event based model is therefore a suitable simulation paradigm.

The most commonly utilised active consumer in an industrial system is the linear cylinder. Pressurised air is consumed in extending and retracting the cylinder. The consumption of a stroke is estimated using a simplified equation (eq 5.1), derived from the Boyles law assuming a closed system with constant temperature. The consumption equation consists of two parts: the active volume of the drive and dead volume in tubing between the directional control valve and actuator. This equation can be used for all types of linear drives, single or doubling acting, single rod, double rod or rodless, and cylinder based semi-rotary actuators. For rodless cylinders equation 5.1a can be used for extend and retract strokes. Equation 5.1b is suitable for both strokes on double rod cylinders. For single rod cylinders the difference in active volume on the retract stroke due to piston rod is also accounted for by using equation 5.1b. Single acting cylinders consume air on the extend stroke only.

$$m = \left\{ s \cdot \frac{\pi \cdot D^2}{4} + l \cdot \frac{\pi d^2}{4} \right\} \left[\frac{P_1}{P_2} \right] \cdot \rho \quad (5.1a)$$

$$m = \left(s \cdot \left[\frac{\pi D^2}{4} - \frac{\pi d^2}{4} \right] + l \cdot \frac{\pi d^2}{4} \right) \left[\frac{P_1}{P_2} \right] \cdot \rho \quad (5.1b)$$

Beater reports that maximum consumption can always be found for meter out drive circuits, the minimum for meter in [13]. Cai et Kagawa have investigated the exergy distribution in actuation of cylinder [167]. Hildebrandt et al have shown that the air consumption index depends on the piston area in a monotonically non-decreasing way [49]. This is interesting since it implies that minimisation of acquisition cost also minimises air consumption [49].

Passive consumers, such as air knives, nozzles and open blow devices are modelled with the Sanville/ISO6358 flow model (eq 5.2), assuming a stable pressure supply and sonic conditions e.g. $\varphi_i = 1$. This simplifies the model to a linear equation without discontinuities e.g. no switching required. Since most passive consumers operate at 2 to 4 bar (absolute) pressure range and the theoretical critical pressure ratio is 0.52, the choked

flow assumption is reasonable. Additionally, in an advanced manufacturing facility, most consumers, active and passive, are regulated and have an adequately sized supply line to maintain pressure. The assumption of a pressure stable supply is therefore also reasonable.

The sonic conductance is empirical which implies that some system identification is still required. Alternatively if empirical measurements for C are not available or feasible, the orifice flow equation (5.3) can be used, again assuming sonic conditions. The discharge coefficient C_d is then selected based on nozzle geometry.

$$\dot{m}_i = \rho_o \cdot C_i \cdot P_u \cdot \sqrt{\frac{T_o}{T_u}} \quad (5.2)$$

$$\dot{m}_c = \frac{C_d \cdot A \cdot P_u}{\sqrt{T_u}} \left\{ \frac{\gamma}{R} \left(\frac{2}{\gamma+1} \right)^{\frac{\gamma+1}{\gamma-1}} \right\}^{0.5} \quad (5.3)$$

In industrial practise it is common to refer to volumetric flow or consumption [94]. Thus the mass flow equations are converted using equation 5.4 with the density of air defined under standard DIN1343 reference conditions. In addition to the bore sizes, stroke lengths, tubing volume and sonic conductance parameters of a given electro-pneumatic system, if the compression ratios and upstream pressures are considered constants, the system's air consumption is then a function of the activation of individual components.

The time interval under consideration is divided into N subintervals. The number of consumers attached to the network is n and the activations of loads at subintervals can be described by the activation matrix \underline{A} [31]. Each row then represents the activation of an individual actuator at subintervals. The subscripts i and j refers to individual consumers and subintervals respectively. For a system of multiple components, matrix multiplication can be used to solve the total consumption for sub-periods. Applying the superposition theorem means that the overall compressed air usage of the system is the sum of the individual component usage (eq. 5.5). Execution of the matrix multiplication leads to equation 5.6. Passive consumers, once activated, consume air on a continuous basis and the consumption over the interval is defined by equation 5.7. Note the term consumption throughout this paper refers to the total amount of air consumed in cycle or operation (e.g. integration of air flow rate). As pointed out by Xiaocong et al [151] it is common

practise to treat consumption, and the required flow rate of a pneumatic drive in cycle, as equivalent terms.

$$q_v = \frac{\dot{m}}{\rho_0} \quad (5.4)$$

$$q_v = A^T q_v = \begin{bmatrix} a_{11} & a_{12} & \dots & a_{1N} \\ a_{21} & \dots & \dots & \dots \\ \dots & \dots & \dots & \dots \\ a_{n1} & \dots & \dots & a_{nN} \end{bmatrix}^T \begin{bmatrix} q_{v1} \\ q_{v2} \\ \dots \\ q_{vN} \end{bmatrix} \quad (5.5)$$

Where $a_{ij} = \begin{cases} 1 & \text{if device } i \text{ activated during time interval } j \\ 0 & \text{otherwise} \end{cases}$

$$q_v = [\sum_{i=1}^n a_{i1} q_i \quad \sum_{i=1}^n a_{i2} q_i \quad \dots \dots \dots \sum_{i=1}^n a_{iN} q_i]^T \quad (5.6)$$

$$q_{\text{passive}} = \int q_v dt \quad (5.7)$$

Parkkinen (R) used equations 5.5/5.6 to model the instantaneous flow of all types of consumers for a defined loading situation [31]. Hyvarinen used a similar analytical based approach but focused on developing a simulator tool to optimise the sizing of pneumatic networks [119,120]. Later work by Parkkinen (J) used the modelling approaches of Parkkinen (R) and Hyvarinen to develop a CA efficiency index in order to reduce energy consumption in compressed air systems [118]. The focus of this work is the development of a dynamic consumption model to account for changing production conditions.

However, while the above approach can be used for estimating total passive usage, active consumers such as cylinders do not consume air on a continuous basis but when they are switched. Parkkinen estimated the average flow of active consumers by including, the number of cycles per time unit a cylinder executes, in equation 5.1. However, this may not be practical since the actuation frequency, f , of the drive may not be known and may change with production conditions. Additionally in order to interface with the PLC, the inputs to the model must be of an equivalent form to the binary PLC outputs. For example the approach here considers ‘ $a=1$ ’ to mean the cylinder is extended (e.g. DCV ‘on’) whereas Parkkinen used ‘ $a=1$ ’ to mean an actuator was in cycle for subinterval. In order to allow for such active consumers a transition matrix \underline{Z} , shown in equation 5.8, was defined. An individual transition represents if an active consumer changes state and is based on the activation matrix. An activation is clarified as the state of the controlling valve i.e. on (1) or off (0). If the future control states (PLC outputs) are known, the air

consumption can be predicted over a finite horizon. Alternatively the subinterval consumption of pneumatic system, q_{sub} , is calculated using equation 5.9 and is useful for modelling the dynamic consumption. The subinterval depends on the simulation time step. The same equation (5.9) can be used for passive consumers by replacing the transition index with an activation index. The total active consumption over full test interval, q_{total} , is calculating using the cumulative sum of the inputs over the test time period. The total system consumption, q_{sys} , is a function of both active and passive consumption (eq. 5.10).

$$q_{active} = \begin{bmatrix} z_{11} & z_{12} & \dots & z_{1N} \\ z_{21} & \dots & \dots & \dots \\ \dots & \dots & \dots & \dots \\ z_{n1} & \dots & \dots & z_{nN} \end{bmatrix}^T \begin{bmatrix} q_1 \\ q_2 \\ \dots \\ q_n \end{bmatrix} \quad (5.8)$$

$$\text{Where } z_{ij} = \begin{cases} 1 & \text{if } |a_{ij} - a_{i(j-1)}| = 1 \\ 0 & \text{otherwise} \end{cases}$$

$$q_{sub} = \sum_{i=1}^n z_{ij} q_i \quad (5.9)$$

$$q_{sys} = q_{active} + q_{passive} \quad (5.10)$$

5.1.2 Software implementation

Matlab Simulink and the Open Process Control (OPC) toolbox add-on were used for building the model. The top level Simulink diagram for a pneumatic system consisting of two double acting linear drives and one air knife is illustrated in figure 5.2. The inputs to the model are the current values of the output bit addresses on the PLC. The PLC therefore drives the model and forms the dynamic aspect to the simulation. The model employs a fixed step solver to solve the simulation. The actuator subsystems were masked to allow for easy changes to parameters and to highlight the model function with an ISO standard symbol i.e. consumption of double/single acting cylinder or blower. The model was also assessed with Simulink model advisor. The top level subsystem depth is 4. For large systems, the individual device models can be grouped by machine sub-assembly or module, as shown in appendix B, to simplify the top level diagram, but still allow for complete visibility of energy use to device or machine subsystem level.

Additionally, two other input configurations were developed for offline testing and validation purposes (appendix B). The first allowed previously recorded control signals to

be used as inputs to the model. The second used a signal builder block in Simulink to enable an investigation of predicted consumption with user defined activation profile.

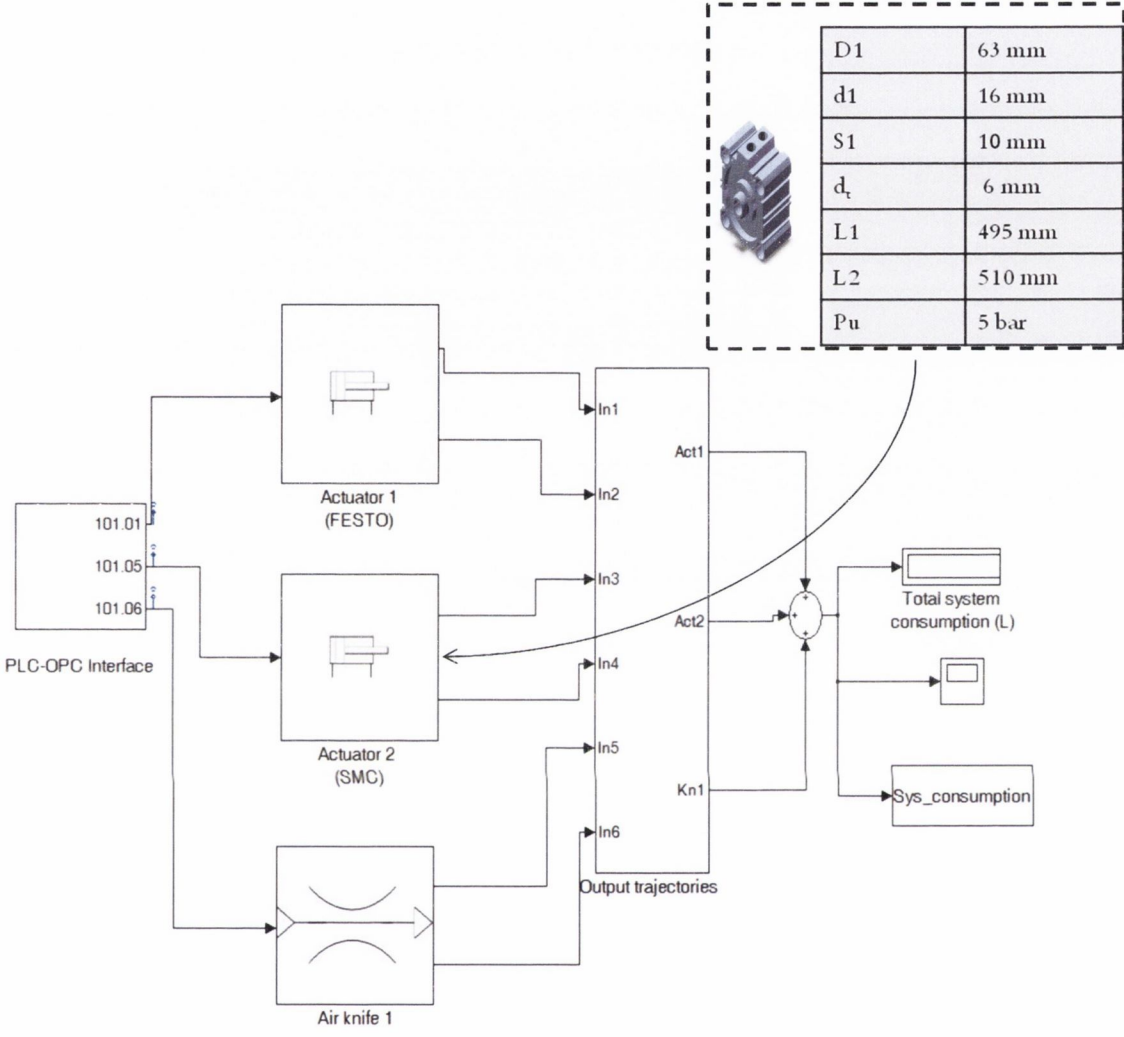


Figure 5.2: Top level diagram in Simulink and required model parameters for actuators

Subsystems

The interface subsystem configures and reads data items from the OPC server. A MATRIKON OPC server was utilised to interface the PLC with model. OPC architecture involves using a server to read data from a device such as a PLC and provide this data to a client, in this case the Simulink model. The benefit of using OPC is that it eliminates the need for custom coding between the model and vendor specific communication protocols. Additionally the model can interface with any OPC server, to Data Access specification 2.05, ensuring modularity. The frequency at which the model

samples OPC data items, and the OPC server samples the PLC bit addresses, can be based on cycle times of the system under study. In this case a 20-30 Hz sampling rate was deemed sufficient.

To ensure scalability, the actuator models are piece part such that they can be added or removed depending on the pneumatic system configuration. The actuator subsystems (figure 2.2) consists of the relevant consumption equations described by equations 5.1 to 5.3 and edge evaluation. Active and passive consumers require different edge evaluation strategies due to the fact that active components consume air during transition periods (e.g. 0-1, 1-0), whilst passive type's consume air for the duration of a positive bit input signal. The consumption of active consumers can be viewed as a pulsed response to a step input, while passive consumers exhibit a step response to the input. Additional differences arise between actuators. Single acting cylinders consume air on extend stroke only and thus require a rising edge detection capability. Double acting cylinders require both rising and falling edges to be detected. The initial activation states are all set to zero.

The output trajectories subsystem consists of display scopes for instantaneous and cumulative air consumption of individual actuators. The simulation results are also written to a workspace for further analysis and visualisation. The model flow for a single pneumatic drive example is shown in figure 5.3. Pseudo real-time simulation refers to the model execution time matching the system clock as closely as possible by slowing down the simulation appropriately. The client manager configures and associates the OPC client with the Simulink model. Pseudo real-time latency refers to the time spent (in seconds) waiting for the system clock during each step. If model runs slower than real-time, pseudo real-time latency violation occurs e.g. the simulation step takes longer to compute than the time between steps. A negative value implies the simulation runs slower than real-time, while positive number means that the model is running faster than the system clock. If latency oscillates around zero, violations can be ignored. Violations can be minimised through; 1/ Asynchronous read operations 2/ Slower OPC read rates 3/ Simulink accelerator 4/ Closing all scopes 5/ Increasing model sample times [168].

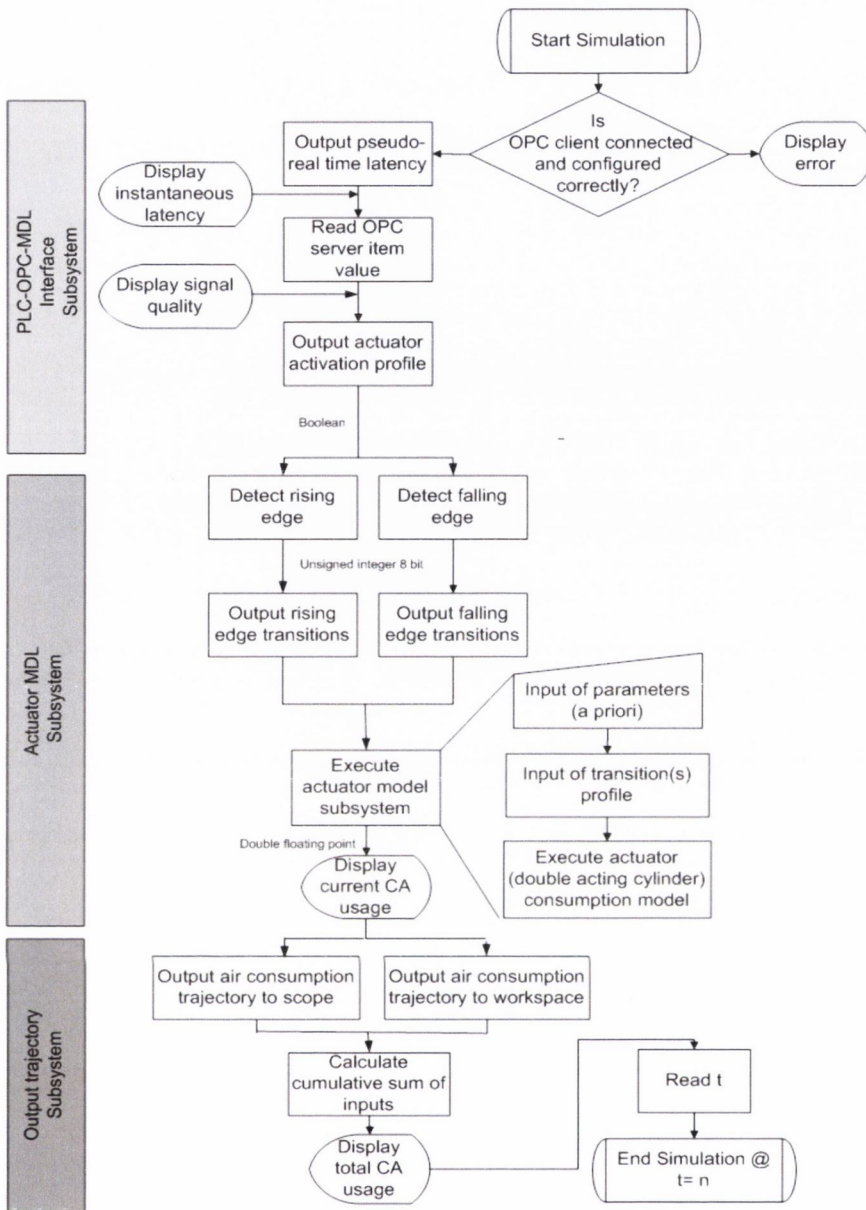


Figure 5.3: Model flowchart for single pneumatic drive

5.2 Experimental setup

In order to validate the proposed modelling approach, a prototype automation system was developed. Figure 5.4 shows the schematic illustration of the experimental setup that consists of the electro-pneumatic system to be modelled and the DAQ system. The system was designed to replicate assembly type module typical in industry. The power, signal and control elements of the system are shown in table 5.1. The upstream air supply was typically regulated to 5 bar and the air filtered to a quality of 5 micron. A

variety of speed control methods were implemented. On the first drive meter out control was employed for the extend stroke, for the second drive no flow controls were used, and for the third drive meter out was used for both extend and retract strokes. Magnetic-reed limit switches were attached to the cylinder ends and used for proximity sensing. One PC was used for programming the PLC and hosting the OPC server, the other for DAQ purposes. The electrical circuit diagram for the rig and PLC details can be found in appendix C.

The pneumatic circuit diagram for the fluid power part of the system is shown in figure 5.5. The consumption of three types of drives was investigated; standard; compact type with large bore and short stroke; and standard bore with longer stroke. The air knives were similar to those used for cleaning and drying purposes in the industrial case study. All the directional control valves were the same type: Festo tiger 5/2 solenoid actuated, with spring return and manual over-ride.

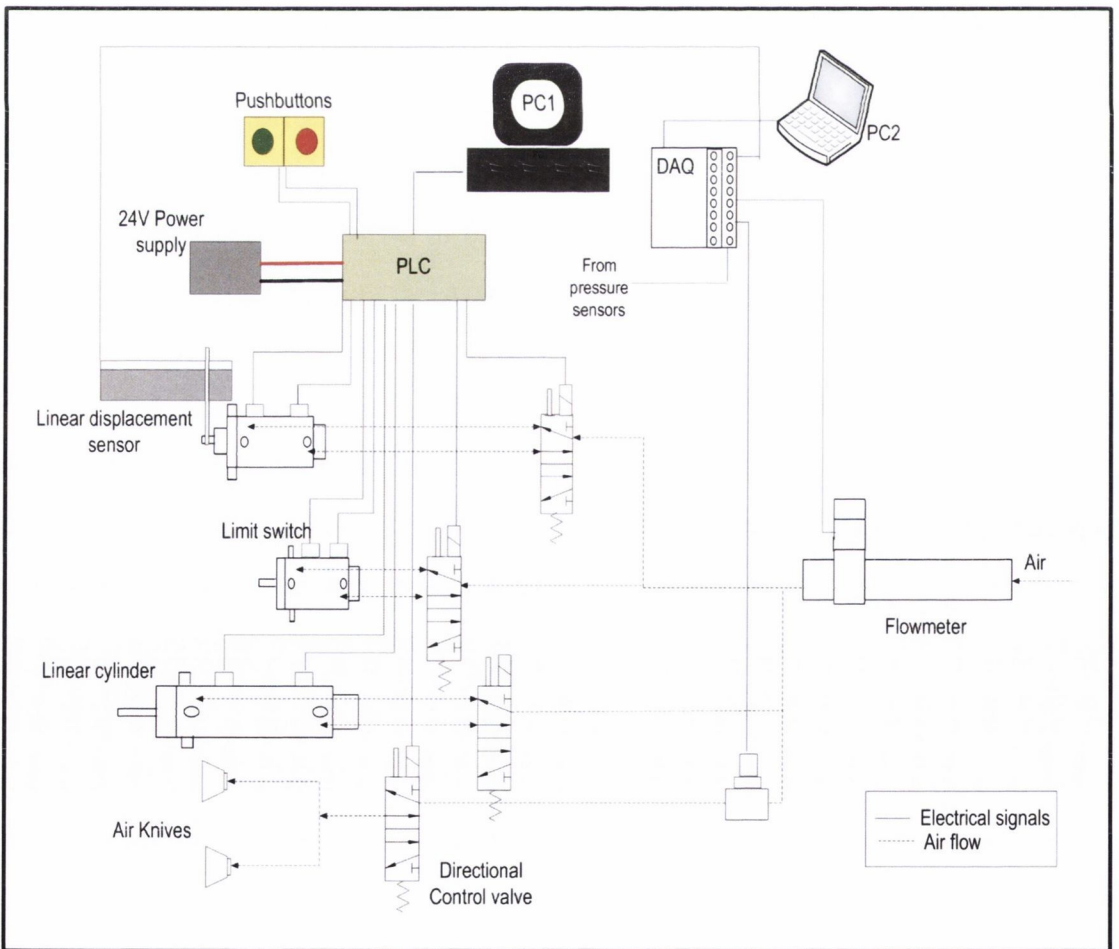


Figure 5.4: Schematic illustration of prototype automation system

Component	QTY	OEM	Model	Details
Linear Cylinder	1	FESTO	DSNU-25-50	Double acting, standard
Linear Cylinder	1	SMC	NCDQ2-B63-10D	Double acting, compact
Linear Cylinder	1	FESTO	DSNU-16-125	Double acting
Directional Control Valve	4	FESTO	MVH-5-1/8-S-B	5/2 solenoid actuated
Air Knife	1	Exair	2" Super air nozzle	16 orifices
Air Knife	1	Delevan	AJ150	16 orifices
PLC	1	OMRON	CQM1-CPU21	Max I/O points: 128

Table 5.1: Rig equipment details

A range of flow sensors, for ultra low to industrial scale flow rates, were employed as part of the measurement system. The flow sensors were used for parameter identification and passive consumption measurement. Pressure sensors were used, in conjunction with a model, to estimate the consumption of the drive units. Additionally a magneto-restrictive type linear displacement sensor was utilised for measuring position of one of the drives. The position of the flow and pressure sensors is illustrated in figure 5.5 and details for the sensors can be found in table 5.2. The circuits refer to the tubing, fittings and valves supplying the individual drives and are labelled correspondingly i.e. Cr1 is the circuit supplying 1A1.

The DAQ system was the same as that described in Chapter 4 and allowed for simultaneous sampling with high bandwidth. Signal express software from National Instruments was used to record the data. A sampling rate of 1000Hz was used for sensor data acquisition in all the experiments with the exception of switching time measurement, which required a higher sample frequency.

5.2.1 Consumption measurement

It is not possible to measure the flow and consumption of fast acting cylinders due to the slow response time of commercially available sensors. The fastest sensor response available was 15ms, for the Festo SFAB sensor. However the upper range limit of 50 L/min was not sufficient to capture the instantaneous flow rates to any of the drives. The larger Testo flow meter had a response time of approximately 500ms, which was greater than the cycle time of the cylinders under study. Since, it has been shown in Chapter 4 that it is possible to model the dynamics of a pneumatic drive with reasonable accuracy the approach taken was to use a comprehensive non-linear model as a datum model for comparison with the simplified consumption equations.

The mass flow can be modelled using a thermodynamic approach, equation 5.11, considering the cylinder chamber as an open and reversible thermodynamic system and assuming no leakage across the chambers. It can be seen from equation 5.11 that the mass flow is affected by three main processes; pressure change, volumetric work and heat transfer. However, even assuming negligible heat exchange influence on mass flow, the thermodynamic based modelling approach still requires measurement of downstream pressure for both chambers, the position of piston, model or measurement of the temperature and numerical differentiation (and consequently noise filtering) of experimental measurements for rate of volume and pressure change. The temperature is generally modelled as a polytropic process with implies identification of the tuneable index n is also necessary. In equation 5.9, the first and second terms account for the effect of piston motion and pressure differential respectively on air consumption.

$$\dot{m}_i = \frac{P \frac{dV}{dt} + V \frac{dP}{dt} + \frac{\gamma - 1}{\gamma} \frac{dQ}{dt}}{RT} \quad (5.11)$$

Miyajima et al [121] developed a linearised consumption model, suitable for servo-pneumatic actuator system, based on the consumption required to expand volume and that required to accelerate the piston. However this approach still requires the measurement of piston velocity and jerk.

Alternatively a fluid dynamics approach can be taken where the flow through a pneumatic resistance is considered. Using the Kagawa equation (5.12), the flow can be modelled with just the use of upstream and downstream pressure sensors. The switching

time of the valve must also be considered, since it can be significant for binary mode control valves. The control signal from PLC must also be measured but this does not require a sensor. The drawback of this approach is that the flow parameters must be identified for each circuit. Nevertheless, this approach is deemed most suitable for analysing multiple circuits since it reduces the amount of sensors required and associated costs.

$$\dot{m}_i = \rho_o \cdot C_i \cdot P_u \cdot \sqrt{\frac{T_o}{T_u}} \cdot \varphi_i(\text{Pr}, b, a, \text{ms}) \quad (5.12)$$

$$\text{Where } \varphi_i = \begin{cases} \left[1 - \left(\frac{\text{Pr} - b_i}{a_i - b_i} \right)^2 \right]^{\text{ms}} & \dots \text{ if } \text{Pr} > b \\ 1 & \dots \text{ if } \text{Pr} \leq b \end{cases}$$

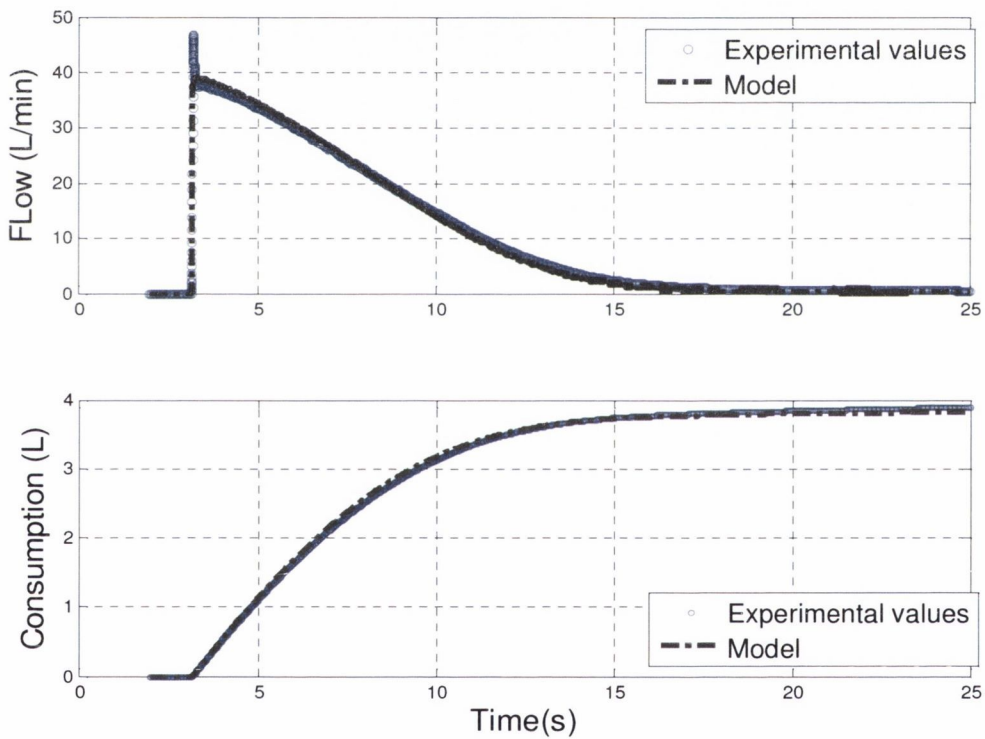
$$\dot{m}_i = \begin{cases} C_i \cdot P_u \cdot \sqrt{\frac{T_o}{T_i}} \cdot \varphi_i \cdot \rho_o \dots \text{ if } \tilde{u} \geq u_{\text{th}} \\ 0 \dots \text{ if } \tilde{u} < u_{\text{th}} \end{cases} \quad (5.13)$$

5.2.2 Flow model validation

In order to validate the non-linear flow/consumption model (eq 5.13) a special experiment was designed. In order to make effective use of SFAB flow sensor, a charge circuit was throttled by using the smallest tubing available, 2mm internal diameter of long enough length, and a one way flow control. The inclusion of the additional resistance of the flow sensor inline decreased the overall conductance of the circuit further. Using this circuit allowed maximum flow rate to be restricted to below 50 L/min at a pressure of 1.5 bar. Then by charging a fixed volume tank of sufficient capacity, 2.5L, with the lower flow rate allowed for a response time of the order of approximately 20 seconds. The combined low conductance circuit and large capacity receiver allowed the dynamic flow response to be captured by the sensor.

The flow parameters of the pneumatic circuit were identified by the improved ISO method discussed in Chapter 4 and had a similar (flow function curve) form to earlier circuits. Since the directional control valve was operated with a pilot supply pressure lower than recommended (i.e. less than 2 bar for Festo Tiger DCV's), the switching time for the valve was also re-identified and was approximately twice the time of that for normal operation. The measured and simulated flow, and consumption, for the fixed volume charging process are shown in figure 5.6. The residuals analysis included in the

figure indicate a mean error, and absolute mean error, of 0.17 L/min and 0.537 L/min respectively. Considering the average flow rate over the charging process was approximately 10.8 L/min, this represents a good level of prediction. The largest residuals, between measured and simulated flow, occur at the start of the charging process and can be attributed to the fact that the valve switching is modelled as a simple step change. This aspect of the model could be improved by considering the linear model [89]; $C = (C_{max} \cdot t) / t_{rise/fall}$ for opening and closing of the valve. Nevertheless the root mean square error of 0.8 L/min demonstrates a good overall level of accuracy, even with outliers due to the step switching model.



	ME	MAE	RMSE
Flow, L/min	0.175	0.537	0.804

Figure 5.6: Measured and simulated, flow and consumption during charging of fixed volume tank and residual analysis

The overall consumption of compressed air for the tank charging process is shown in table 5.3. It can be seen from the table that the difference between the measured consumption and consumption calculated from the non-linear flow model is 0.0064L. This

is equivalent to a 0.16% error relative to measured consumption, indicating an excellent overall approximation. It is interesting to note that the simplified consumption equation over-predicts the consumption of air in the pressurisation process by 2.4L. This is a significant difference, equivalent to a 60% error, considering the total measured consumption of 3.9L.

	Consumption (L)
Measured	3.891
Kagawa flow model	3.827
Difference, flow model - measured	-0.0064
Simplified consumption model	6.25
Difference, consumption model - measured	2.359

Table 5.3: Total consumption of fixed volume charging process

The extended ISO6358 model is therefore used as the datum model for testing the linear cylinders. The reference model was developed in Simulink, and has four inputs: the DCV control signal from PLC, upstream pressure and chamber pressures. It can be seen from table 5.4, that the estimated overall accuracy of the datum model is approximately 7% based on the accuracy of the pressure sensors and identified flow parameters. The flow rate of passive consumers (air knives and leakage) can be measured directly using the flow sensors, which means the error in predicting consumption is slightly improved (table 5.4). The volumetric consumption, in both cases, is the integral of the modelled or measured flow to the device over specified period (5.14). For drives, the integral only considers positive flow rates i.e. influx air to both chambers.

$$q = \int_{t_{start}}^{t_{stop}} q_v(> 0) dt \tag{5.14}$$

Parameter of measurement system	Sensor/system accuracy
Pressure, % (x2)	±2.83
Conductance, %	±6.32
Consumption (drive),%	±6.92
Consumption (nozzle), %	±6

Table 5.4: Accuracy of sensors and measurement system for consumption measurements

5.3 Parameter identification

The improved steady flow test method described in Chapter 4 was used to identify the flow characteristics of the pneumatic circuits. Ambient conditions were also the same as given in Chapter 4. Two flow sensors were employed to compensate for limited range of the flow meters, in order to identify the characteristics of lower conductance circuits. Due to the use of two sensors the estimated error in measuring flow is increased to 6.7%. A modified characteristic identification algorithm was developed in Matlab to allow for integration of both sensors. The sampling time was increased to 5 kHz for measuring the switching time.

5.3.1 Circuit identification

The mean circuit characteristics for the four circuits of the pneumatic system are shown in table 5.5 and are based on 5 test runs. Only the input flow paths are necessary for consumption identification and all results are independent of leakage effects i.e. circuits isolated for identification. The cracking pressure was unity for all circuits. The pneumatic circuit for drive 2A1 was similar to circuit 1 in terms of flow capability, and due to a symmetric setup had very similar characteristics for both charge flow paths. The flow characteristics of third drive circuit are of note for the low conductance and high subsonic index values. This can be attributed to long small diameter tubing and flow controls in the circuit. The fourth circuit consisted of the two air knives with a common supply, and was identified without leakage by isolating the pilot supply to DCV4. As shown in figure 5.9, since the conductances of the two air knives are additive, the circuit was identified and modelled as one unit. The subsonic index of 0.55 indicates the flow function corresponds closely to the Sanville ellipse model. It is interesting to note the reduced critical pressure ratio of 0.22 for the air knives, caused by multiple restrictions in the circuit. The standard deviations indicate a reasonable level of precision similar to that of other published work by Kuroshita [98]. It is important to note that when an exhaust circuit is throttled with meter out flow control, the conductance of the influx flow is also affected considerably.

Charge paths only	Cr1		Cr2		Cr3		Cr4
	Fp1	Fp2	Fp1	Fp2	Fp1	Fp2	Fp
C, Mean Std. Dev.	1.79E-08	8.69E-09	1.73E-08	1.73E-08	3.57E-09	3.43E-09	6.56E-09
	2.76E-10	1.64E-10	1.65E-10	3.54E-10	5.18E-11	1.36E-11	7.81E-11
b, Mean Std. Dev.	0.23	0.29	0.24	0.25	0.19	0.19	0.22
	0.035	0.02	0.014	0.026	0.028	0.019	0.039
m, Mean Std. Dev.	0.5	0.52	0.56	0.58	0.59	0.62	0.55
	0.042	0.056	0.046	0.038	0.017	0.023	0.023

Table 5.5: Circuit characteristics for input flow circuits

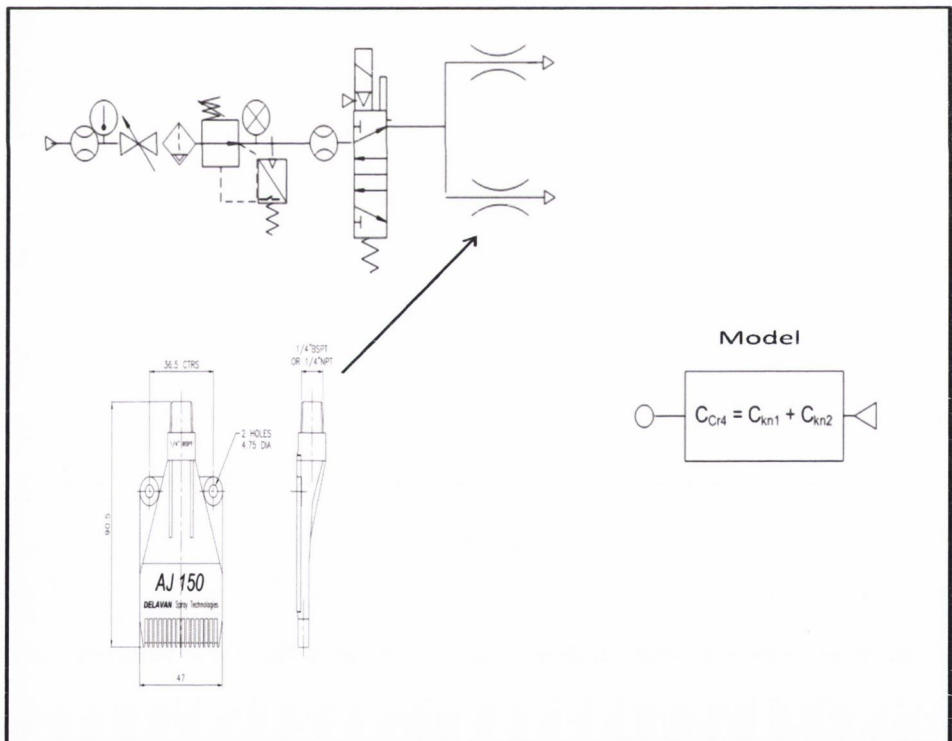


Figure 5.9: Cr4 identification circuit, air knife dimensions and simplified block model

5.3.2 Leakage characteristics

A leak was present in pilot supply to DCV4 (4V1 in figure 5.5) on the pneumatic circuit. The leak was due to an elastomeric seal between pilot supply and solenoid (see figure 5.8) becoming loose. Since drive 3A1 shared a common supply with circuit 4, it was also affected by leakage. Leakage can be viewed as an additional load in parallel. The total conductance of the overall circuit (figure 5.7) is increased but not the mass flow through the drive circuit.

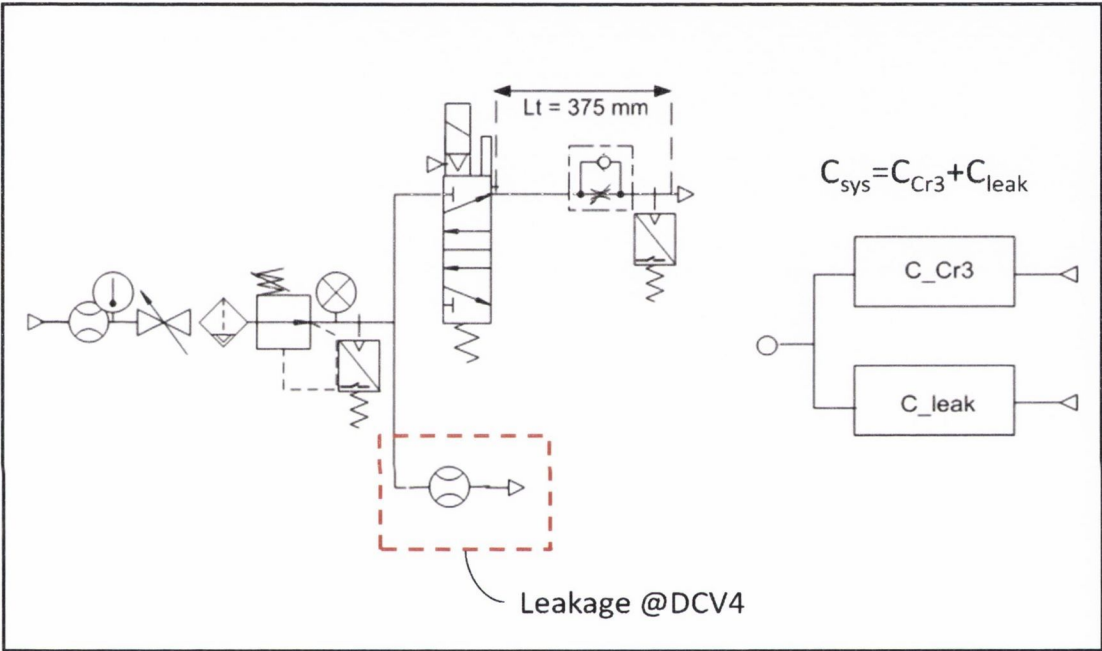


Figure 5.7: Pneumatic circuit for identification of Circuit 3 and conceptual model of leakage load in parallel

There are two options for flow identification of a drive with leakage. The first approach is to isolate the leak, so that the drive circuit can be identified without leakage and then the leak characteristics identified separately. This approach follows the logic of the model development whereby leakage is modelled as a standalone passive consumer if required. Modelling leakage may be useful in the case of low friction type directional control valves with lapped spools. From a simulation development perspective, leakage is as modelled a standalone consumer since it can occur upstream of valve-actuator subsystems and is therefore independent of control actions in many cases. Additionally if the leak is located upstream of the filter regulator it may be at a higher network pressure.

However since in an industrial environment it may not be possible to reconfigure circuits easily, a second identification approach would be to identify the combined system flow characteristics, then identify the leakage characteristics separately and finally solve for the drive circuit flow using equation 5.15.

$$\dot{m}_{in} = C_{sys}\rho_o P_u \varphi(Pr, b, m, a) - C_L \rho_o P_u \varphi(Pr, b, m, a) \quad (5.15)$$

The first approach was taken here. To test for leakage the working ports of DCV4 were blocked and pressure increased successively as in the improved ISO identification method. An example of the leakage flow function is shown in figure 5.8 with summary flow characteristics. The results are based on 5 test runs. The cracking pressure, a , was unity for all tests. It can be seen from the figure that the subsonic index is high which means the extended Kagawa equation is necessary for accurate characterisation. According to the identification results in figure 5.8, the critical pressure ratio is 0.12. However, from the figure it is clear that the critical pressure ratio may not have been reached. Since the computed critical pressure ratio is close to the minimum pressure ratio actually achieved during the identification process, the ISO6358 standard, stipulates re-testing with lower downstream or higher upstream pressure in order to ensure choked flow has been achieved. However, from practical point of view attaining such a low pressure ratio is very difficult. In any case, the typical operating pressure of industrial drives is less than 8 bar, so the model is sufficiently defined over its normal operating conditions i.e. the pressure ratio will never likely be less than 0.12. Nevertheless, the low pressure ratio is important to note as it means the assumption of sonic flow for leakage does not hold in all cases.

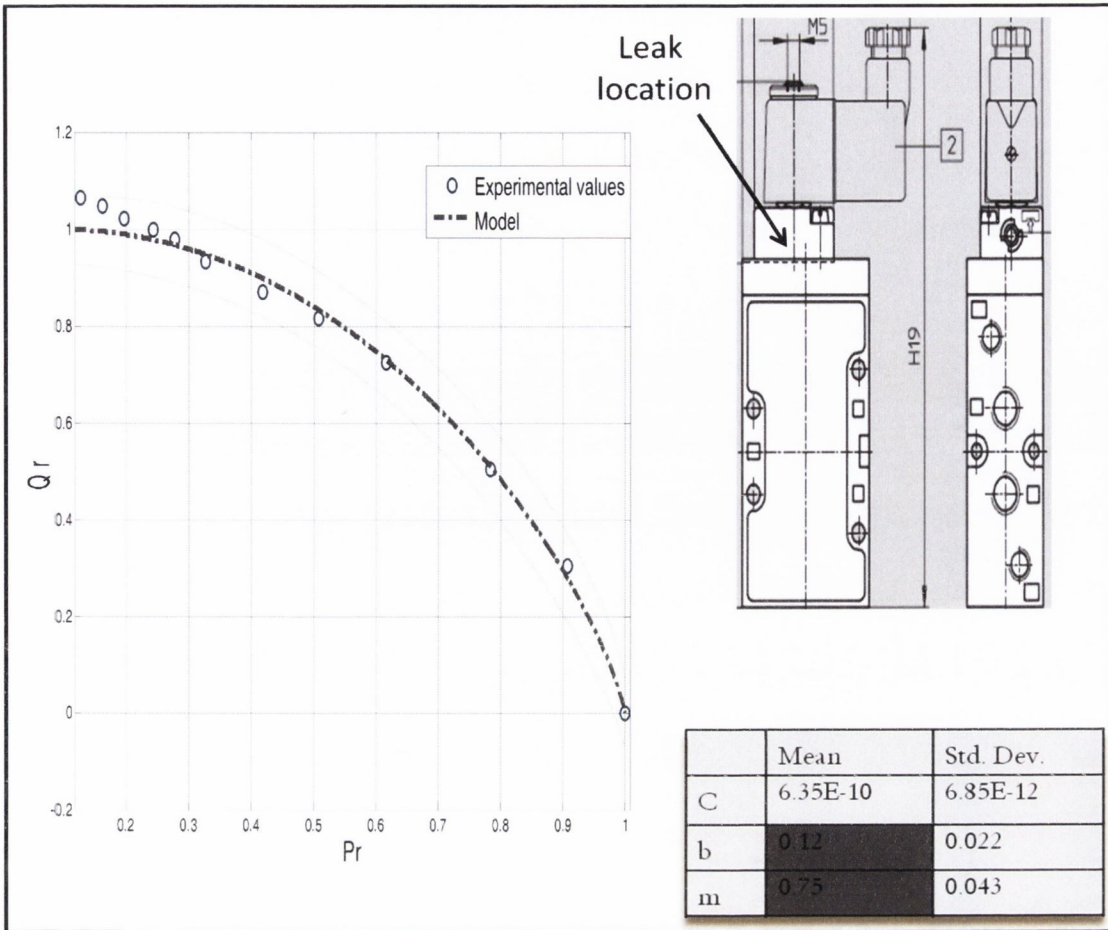


Figure 5.8: Leakage location, flow function and summary flow characteristic results

5.3.3 Consumption model estimation

The benefit of using simplified consumption equations, in addition to reducing model complexity, is to reduce the amount of parameter identification required. The main parameters required for estimating the consumption of a pneumatic drive are shown in figure 5.2 and include the bore diameter and stroke of the cylinder, inner diameter of connecting tubing and length. The bore diameter, rod diameter and stroke are available from the component data sheets or international standards ISO6432 [70] and ISO15552 [169]. The tubing lengths can be measured. For passive consumers, the conductance is the only required parameter and is identified experimentally (table 5.5), or taken from component data sheets. If experimental identification is not possible, it is important to consider the aggregate conductance of the circuit. This can be done using the Eckersten equations [117] and a tubing attenuation factor [15] if necessary. The upstream temperature is taken as constant at 298K.

At a regulated supply pressure of 5 bar, the estimated consumption for the three drives, with supply tubing, under study, for extend and retract strokes, is shown in table 5.6. It was observed that the actual measured upstream pressure would vary about the regulated set point with approximately 5% difference. Using the modelled consumption values, the consumption can be predicted over an interval based on a user defined activation profile, as shown in figure 5.10.

	Extend (L)	Retract (L)	Cycle (L)
Drive 1A1	0.176	0.185	0.361
Drive 2A1	0.226	0.218	0.444
Drive 3A1	0.128	0.114	0.242

Table 5.6: Consumption model results for three drives

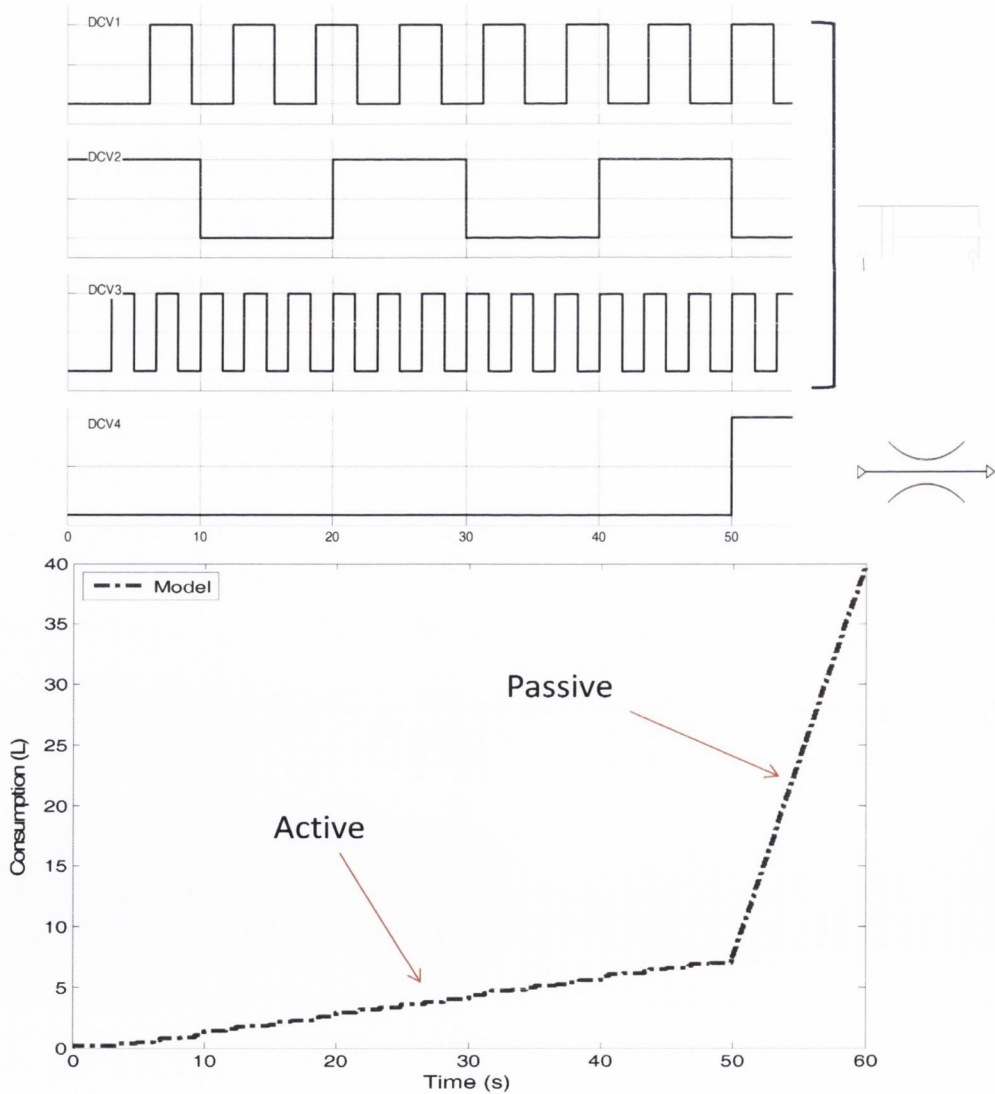


Figure 5.10: Predicted consumption for user defined activation profile

5. 4 Results and model validation

To validate the accuracy of the simplified consumption models, the simulated and experimental results were compared at an individual device and system level. For the individual drives, the simplified consumption equation results were compared with the consumption of the fully developed flow model. Passive consumption was measured directly with flow sensors. An example of the non-linear flow/consumption model's input and output variables is shown in figure 5.11. The control signal voltage was reduced from 0-24VDC to 0-7VDC with a voltage divider. The required compressor capacity and running cost calculation is based on average flow rate over specified time period. This is calculated by taking the product of consumption per cycle and actuation frequency as shown in equation 5.14. An allowance/safety factor is usually included to account for leakage losses in the air system, consumption by drain and pilot valves and temperature drops. However, it is important to note that pneumatic circuit must be sized to allow for the maximum instantaneous flow rate. In the case of figure 5.11 the cylinder consumes approximately 0.22L of air in 0.13s. This is equivalent to an average flow rate per stroke of 101.5 L/min, while maximum consumption is over 200L/min. If multiple actuators are on the same supply line, the circuit must be sized to allow for simultaneous actuation of all drives. It has also been documented in the OEM literature [170,171] that at high cycle rates, the pressurised chambers of cylinders are not fully exhausted, which means the air consumption can be significantly less than that estimated in equation 5.14.

$$q_v(av) = \left[\left(S \cdot \frac{\pi D_1^2}{4} + L_1 \cdot \frac{\pi d_t^2}{4} \right) + \left(S \cdot \left(\frac{\pi D_1^2}{4} - \frac{\pi D_2^2}{4} \right) + L_2 \cdot \frac{\pi d_t^2}{4} \right) \right] \left\{ \frac{P_u}{P_d} \right\} \cdot f \quad (5.14)$$

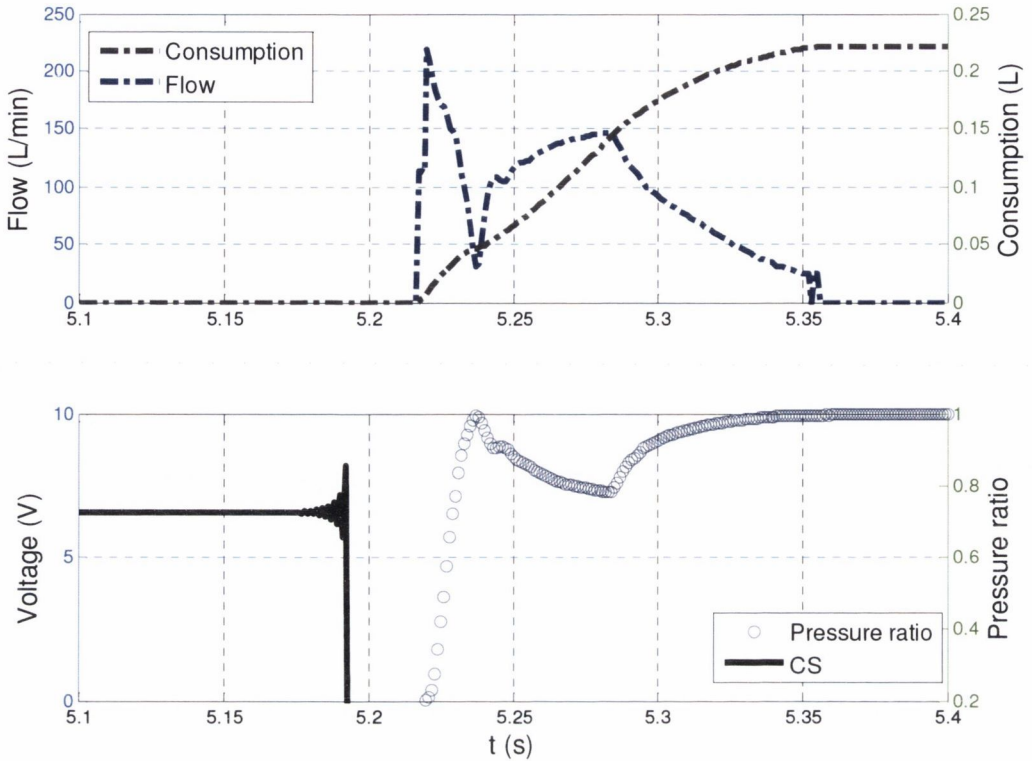


Figure 5.11: Simulated flow with measured pressure and control signal during extension of linear drive

5.4.1 Active consumers

The modelled and measured cumulative consumption of drive 3A1 over a number of cycles is shown in figure 5.12. The consumption function increases monotonically with time. The accuracy of the simulated results was quantified by comparing the simplified consumption model results with that of the non-linear flow model, figure 5.13.

The average difference is calculated by subtracting the simulated results from the average consumption, based on five tests, determined from the flow model. A positive result therefore indicates an over prediction, while a negative indicates an under prediction. A cycle consists of an extend and retract stroke. It can be seen from figure 5.13 that the consumption of drives 2A1 and 3A1 is well approximated with an average difference under 0.02L in both cases. This is equivalent to under a 10% error considering the total air consumed by both drives. However, the consumption model consistently over predicts the consumption of drive 1A1 under all load conditions. The average difference of

0.06L per cycle is significant considering the total consumption of drive 1A1 is only 0.29L. This results in a 20% prediction error approximately per cycle. This confirms the OEM’s observation that the theoretical models over predict air consumption. It can also be seen from figure 5.13 that the payloads appear to have little influence on air consumption of drive 1A1. A paired t-test was performed to determine if the payload had a statistical significant effect on air consumption. The air consumption for single cycle of drive 3A1 with no load (M0) and a 2.37 kg payload (M3) were assessed (table 5.7). Since the T statistic is less than critical value and the p value is greater than the selected alpha level of 0.05, the null hypothesis is accepted, that the tested loads had no affect on air consumption. However, it is important to note that the maximum load investigated was approximately 30% of the cylinder’s capacity.

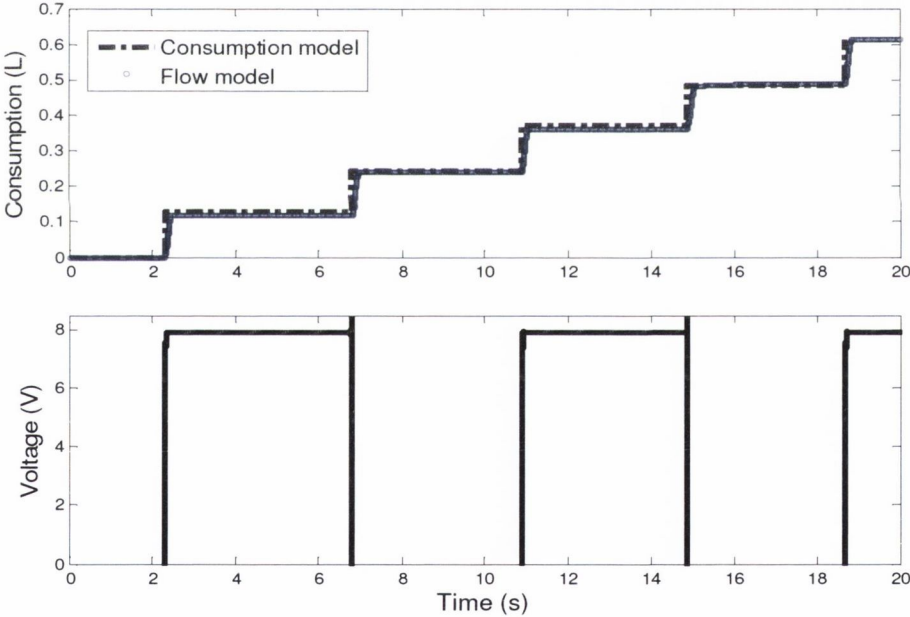


Figure 5.12: Cumulative consumption of drive 3A1 in cycle

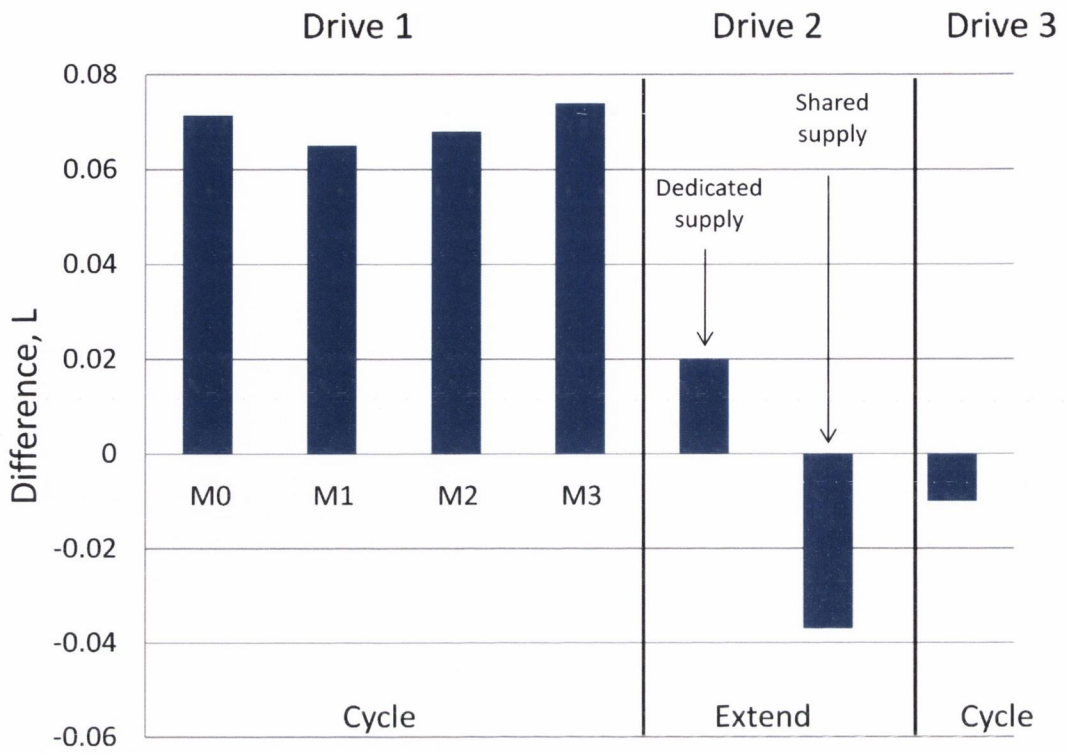


Figure 5.13: Difference between simplified consumption estimate and flow model for linear drives

	M0	M3
Mean (consumption/cycle), L	0.28928	0.28682
Variance	4.3107E-05	0.000030777
Observations	5	5
Hypothesized Mean Difference	0	
df	8	
t Stat	0.639948329	
P(T ≤ t) one-tail	0.27004827	
t Critical one-tail	1.859548033	
P(T ≤ t) two-tail	0.54009654	
t Critical two-tail	2.306004133	

Table 5.7: Paired t-test results to determine payload effect on air consumption

To calculate the consumption of multiple drives in parallel, the flow model was further developed to account for both drives. It can be seen from figure 5.13 that the consumption of air by drive 2A1 appears to change with a different supply line configuration. A typical industrial circuit setup allows for multiple drives with a shared pressure source/regulator. With such a configuration, the difference between linear consumption equation and non-linear is $0.035L$, an approximately 15% under-prediction. A paired t-test was conducted to determine the significance of circuit layout on air consumption. The results of the test show that the t statistic is greater than the critical value, and the probability is less than the selected alpha level of 0.05. The null hypothesis of no statistically significant difference is rejected. Therefore, the alternative hypothesis is accepted, the consumption of the drive is increased with shared supply. This is likely due to the extra volume to be pressurised in the circuit. Figure 5.14 expands the Pneumatic Wheatstone Bridge model for two cylinders with a common supply and demonstrates the pressure response in the circuit during charging of a single drive. When the control valve of actuator 2A1 is turned on, air flows from the supply to chamber 1 of the second drive. The rapid drop in supply pressure causes compressed air to flow from chamber 2 of the first drive, which is in a holding position, to the supply junction for both drives. The sum of the flows at the junction is equal to zero. This allows for quick recovery of the supply pressure and thus faster pressurisation of second cylinder's charging end. However, an additional volume of air is consumed in then pressurising the additional fixed volume in the first drive. This process is shown schematically in figure 5.14. The same phenomenon occurs during staggered sequential actuation of cylinders with common supply. Note if check valves are used in the circuit, the flow behaviour will be the same as a single drive circuit.

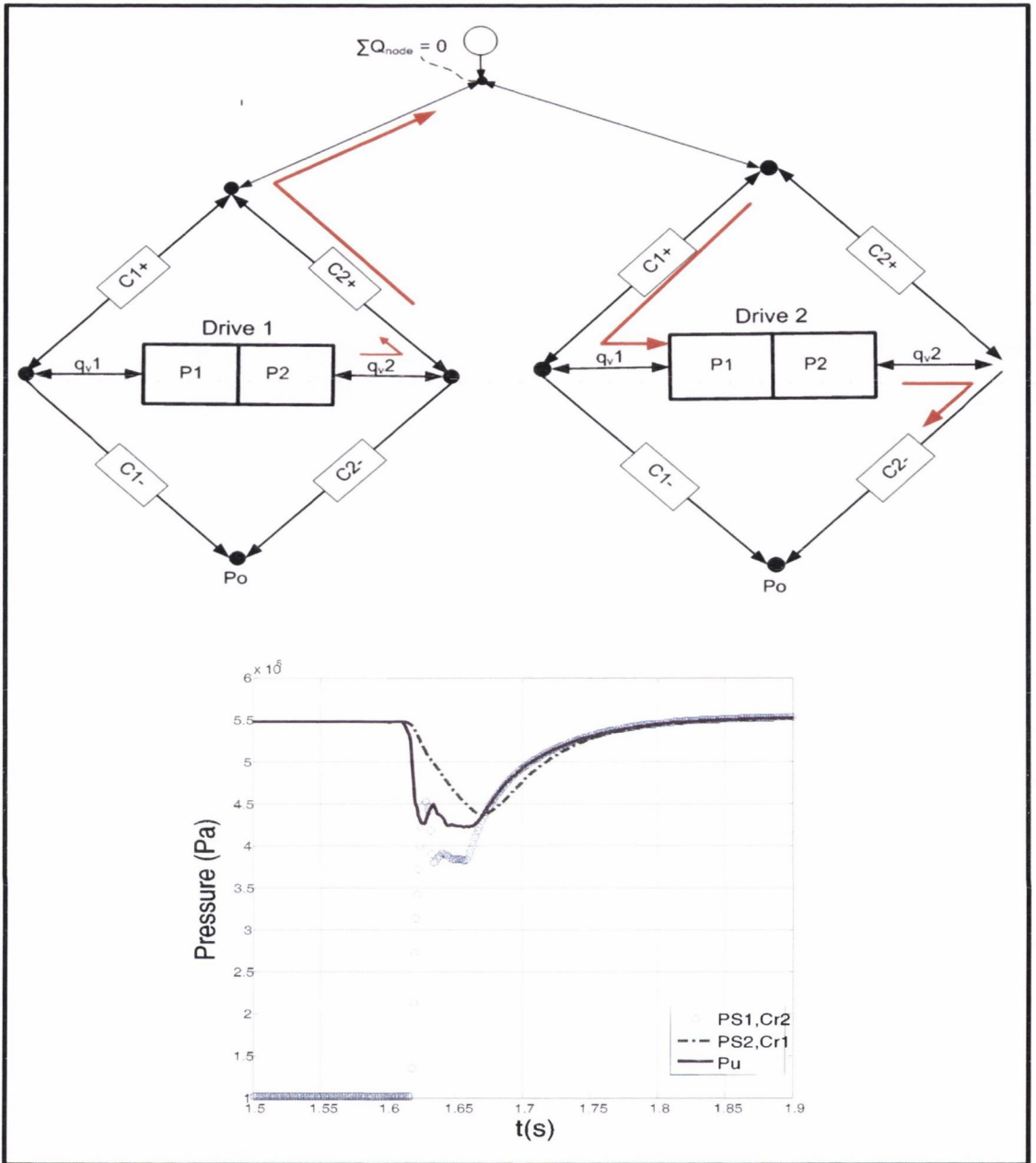


Figure 5.14: Modified Pneumatic Wheatstone Bridge for network model and pressure response in multiple drive circuit

5.4.2 Passive consumers

The measured and modelled flow rate of the two air knives in circuit 4 is shown on the left in figure 5.15. The measured and modelled flow values, for leakage at the pilot supply of DCV4, are shown on the right of figure 5.15. The residuals in both cases are highest in the subsonic regions as would be expected since the linear model assumes sonic conditions. The difference between the simulated flow and measured values as a percentage

of measured flow for combined passive consumption is shown in table 5.8, for a range of selected pressures. It is clear from both figure 5.15 and table 5.8 that the linear flow model is capable of approximating the combined passive consumption with an accuracy of around 5% for pressures above 3.5 bar. The linear model is therefore suitable for blow devices operating at suitably higher pressures.

However, for passive systems operating at pressure below 3 bar it may be necessary to use the full non-linear Sanville/ISO6356 flow model, since the error is increased to greater than 15% for pressures below 2.5 bar. For the individual passive consumers, while the absolute deviations for pressures above 2 bar are not considerably different to that in the sonic region, see residuals in figure 5.15, the relative percentage error is increased due to the lower overall flow rates. In particular for individual leaks, the high subsonic index may lead to large deviations between the linear flow model and measured values for pressure below 4 bar. Therefore, if the leakage load is significant with respect to overall passive consumption, and cannot be reduced or eliminated, the full Kagawa equation is necessary. The decision on flow model for passive consumers should therefore be made depending on plant conditions.

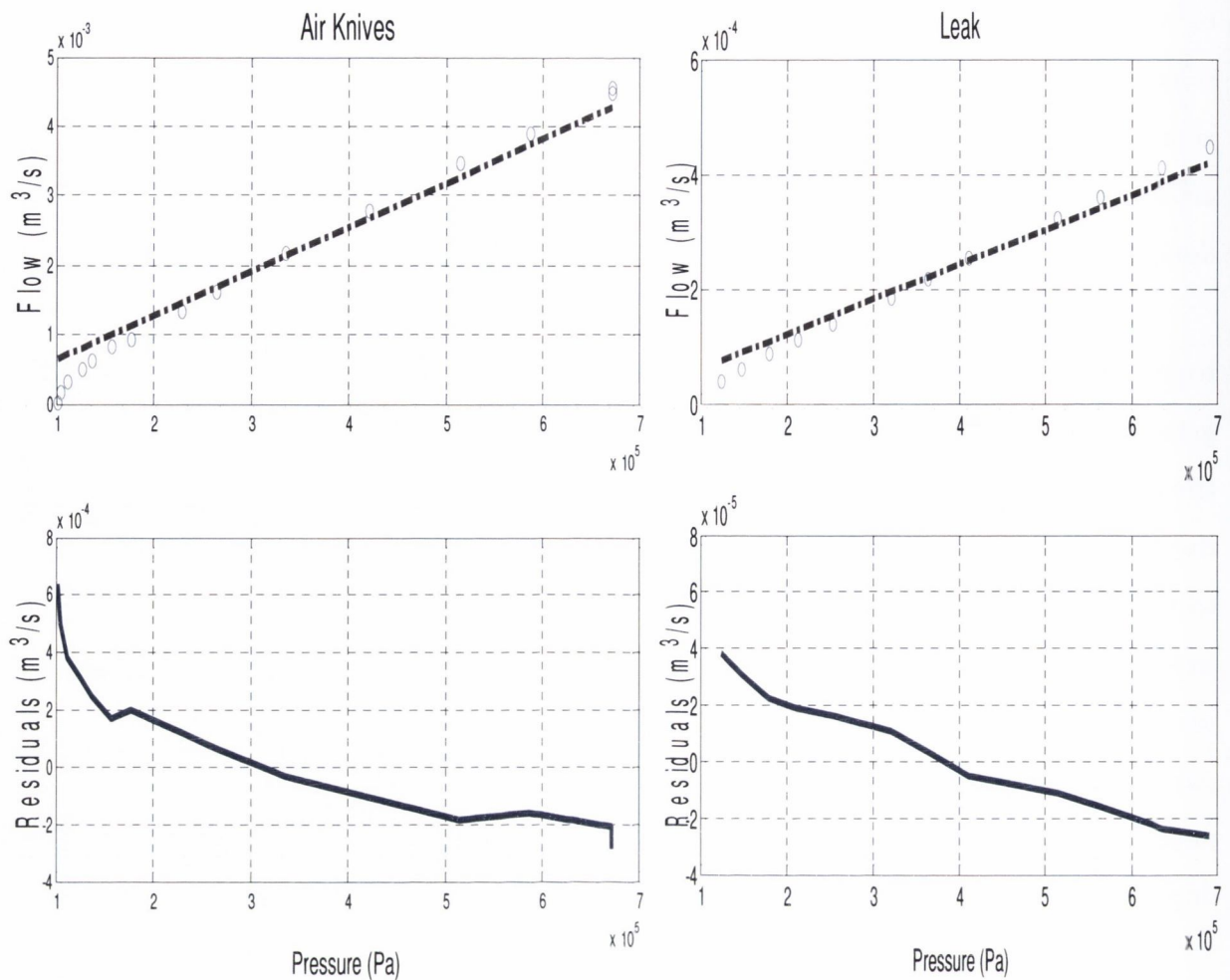


Figure 5.15: Measured flow values and linear flow model over pressure range

	2.5 bar	3.5 bar	5 bar
Model, L/min	104	145	207
Measured, L/min	91	138	198
Difference, L/min	13	7	9
Difference, %	14.3	5	4.5

Table 5.8: Total consumption rate of passive consumers at selected pressures

5.4.3 Full system

A sequential program was developed to study the air consumption of the full prototype system. The operation of the system is a replica of many industrial applications whereby a work piece or product is clamped in place, a machine tool or punch is brought

into contact with the work piece for a set period of time, after which the tool is removed and the work piece cleaned and ejected. In terms of the sequence of events, cylinder 1A1 extends, followed by cylinder 2A1 shortly after, followed by an extension and retraction of cylinder 3A1 and activation of air knives by DCV4. The entire operation occurs in approximately 20 seconds. The function chart for the operation can be found in appendix C. The measured and modelled cumulative consumption over the test period is shown in figure 5.16. The measured flow for the same test is shown in figure 5.17. The continuous increase in measured consumption at the start of the operation is due entirely to leakage. The large final difference in air consumption of approximately 4.6L, a -25.9% discrepancy, between the theoretical model and measured results is due to leakage in the system.

If the system contains a known leakage due to the use of a particular device it may be considered part of the consumption load and modelled accordingly. In this case, leakage at the valve is independent of the control state and therefore represents a constant load on the system. The consumption model including leakage is also shown in figure 5.16, and the difference between modelled and measured consumption is reduced to 1.54L, a +8.6% increase in comparison to total measured consumption. It can be seen from the figure that air knife consumption is over predicted due to the use of the linear (sonic) flow model.

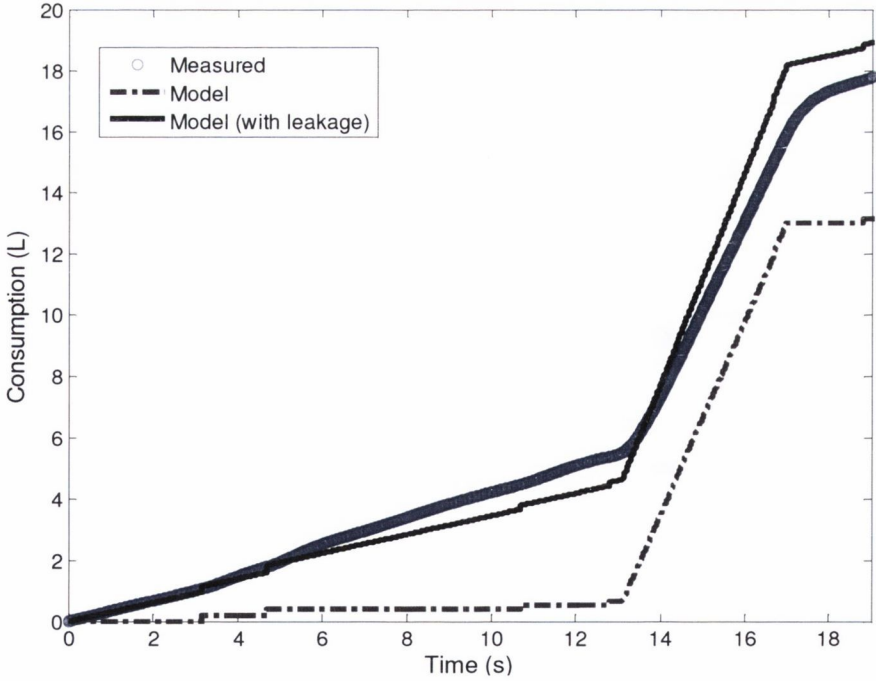


Figure 5.16: Cumulative consumption over sequence

The limitations of the flow sensor in measuring all aspects of consumption can be seen clearly in figure 5.17. The instantaneous flow rate requirements of the, fast acting, pneumatic drives are not captured accurately due to the response time of the flow sensor. The sensor can therefore be characterised as a type of low pass filter whereby the consumption of high frequency actuators is rejected. This limitation may be particularly relevant when measuring the consumption of machines with active air consumer dominated loads. It is interesting to note in the case of sequence 1 with a constant passive load, figure 5.16, that the sensor appears to overestimate the consumption during the first part of the cycle (up to 13s), since at 4 bar(g) the leakage flow rate is well approximated.

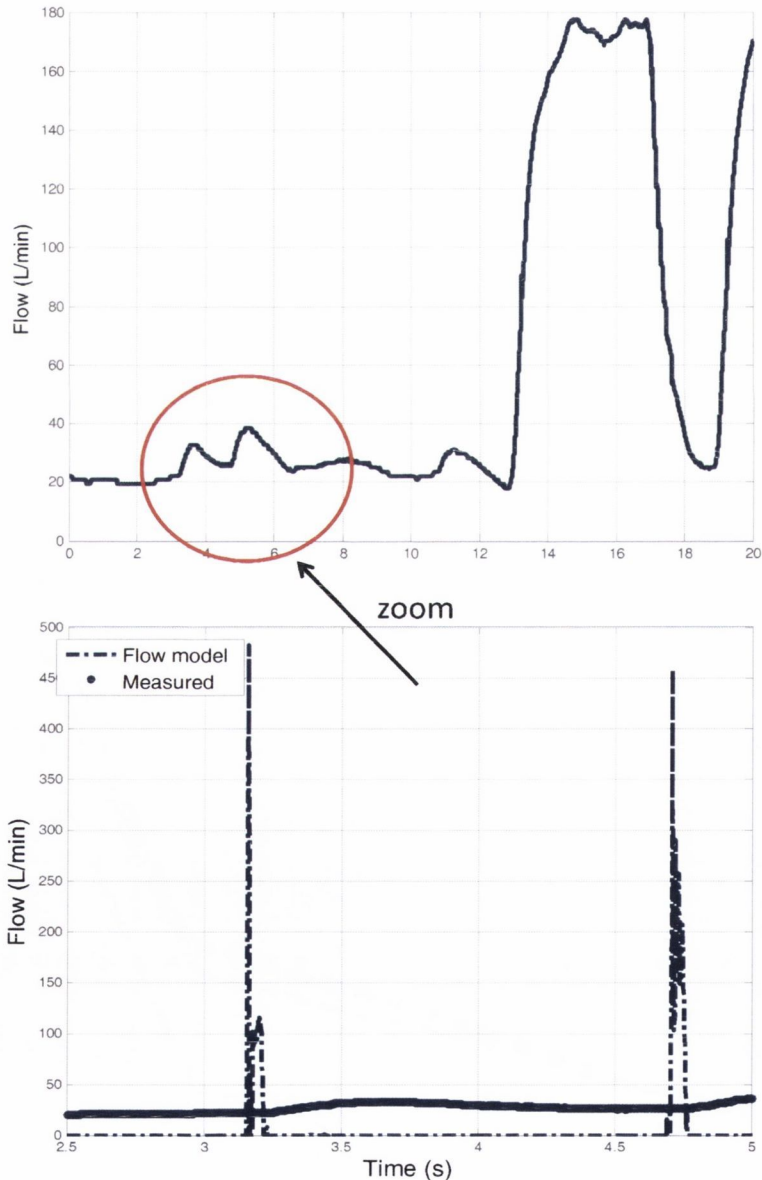


Figure 5.17: Measured flow over sequence 2

To assess the accuracy of the consumption model for the operation without leakage, the consumption model was compared with the non-linear flow model. Summary results for the total consumption by both models are shown in table 5.9. The total consumption over the test period was predicted with a difference of 0.84L. This is equivalent to an error of 6.8% in comparison to total consumption. However it must be pointed out that since the consumption function is dominated by the passive consumers in this case study, the accuracy of the result is mainly due to the accuracy of air knife consumption model. Therefore a second operation based sequence scenario with more balanced active-passive load was developed. In a one minute operation, drive 1A1 cycles 30 times, drive 2A1 extends once and drive 3A1 cycles at an actuation frequency of 50 cycles per minute. The air knives are active for a short 10s burst and operate at a lower pressure of 2 bar(g). This operation can also be considered a reasonable replica of industrial process conditions. The difference in modelled consumption of 4.76L equates to a 12.8% prediction error, an increase on the previous operation. Nevertheless, the overall accuracy of the proposed model in tracking the air consumption of the prototype pneumatic production system is encouraging. Note in table 5.9, the time intervals are of different magnitude for both operations.

	Seq 1 (20s)	Seq 2 (60s)
Modelled consumption, L	13.13	41.98
Modelled (non-linear) consumption, L	12.29	37.22
Difference, L	0.84 (6.8%)	4.76 (12.8%)

Table 5.9: Summary results of predicted and measured consumption for two application examples

5.5 Summary

- A novel PLC driven consumption model of a pneumatic system has been presented in this work. The proposed systems type approach allows for the air consumption model to be scaled for use in production processes by minimising identification and modelling effort. The use of an OPC server allows for integration with most industrial control systems. All types of linear cylinders, semi-rotary actuators, air blow devices and leakage can be accounted for in the model.
- At a component level, results indicate that the consumption of a single drives can be modelled with reasonable accuracy using the simplified model approach. The average error in consumption for three drives was estimated was 13%. Common supply for multiple drives are factors not accounted for in simplified modelling approach. Passive consumers are well approximated at higher pressures. However, for lower pressure it is recommended to use the full Sanville/ISO6358 model.
- The accuracy of the developed system model in predicting the consumption of the prototype system under two sequential operations ranged from approximately 7% to 13%. The work has therefore demonstrated the PLC driven model will work in practise with sufficient level of accuracy for engineering applications.
- The model can be used to breakdown pneumatic energy drivers to any level. In its present form the model has potential application in leakage detection, in conjunction with a flow sensor, and local level metric deployment and cost allocation. The model also allows very easy changes to parameters and could be useful as a means of quantifying design/maintenance consumption savings arising from; changed pressure levels for individual device or system; replacement of open pipe with nozzle; the addition of control valve to blower circuits.
- The limitations of flow sensors in tracking consumption have been highlighted and it is suggested there use is based on the consumption characteristics of the machine under study.

6. Conclusions and Recommendations for Future work

6.1 Conclusions

The energy efficiency of pneumatic systems is an area of significant importance within manufacturing industry. Practically every production facility has a compressed air infrastructure and energy costs related to compressed air can be considerable. Accurate models are essential in optimising the energy efficiency of pneumatic systems through model based design and control techniques. This study therefore aims to explore the dynamics, and in particular consumption characteristics, of pneumatic production processes with a focus on the development of scientific process models for industrial electro-pneumatic systems.

An industrial case study was undertaken to examine compressed air consumption and efficiency in automated production. The module investigated was a quality testing unit that formed part of a larger automated assembly line. Air usage under a variety of production rates and machine conditions was recorded and analysed. This allowed a breakdown of consumption and characterisation of losses. Additionally the relationship between production output and air consumption was studied using regression analysis.

A theoretical model was developed to predict the dynamics of an individual pneumatic drive system. The process model was developed mathematically from first principles. The simulation results were compared with the experimental results under different loading conditions using flow, pressure, position and acceleration sensors. A scalable air consumption model for pneumatic systems was developed, using simplified linear equations, and interfaced with a programmable logic controller. The simulation and experimental results were compared for a number of different cylinders, air knives, pneumatic circuit configurations and loading conditions. The overall simulated and experimental consumption for a prototype automation system was also examined. All models were developed in Matlab-Simulink.

6.1.1 Industrial investigations

The efficiency of compressed air consumption on an automated production module was investigated in the industrial case study. The analysis focused on two aspects in particular: An assessment of air usage and losses, and the development of a statistical model to predict machine air consumption.

Based on the investigations of two assembly stations, average losses were estimated to account for 34% of total machine air consumption. Leakage accounted for 21% of the losses and the remaining 13% was attributed to lack of control of passive consumers. It is noted that a significant amount of such energy losses can be addressed with current technology, little investment and better maintenance. The losses estimate does not include further energy savings possible using more advanced methods in design. It was observed that a system model would be useful in order to understand the dynamics of machine consumption, quantifying and classifying air usage, clarifying losses and highlighting savings due to improvements in design or control.

With regard to the statistical model development, it has been found that linear regression, a widely employed industry tool, is of limited use in predicting machine air consumption with confidence. This is due to the dependence of air consumption on multiple predictor variables. Additionally the variability of leakage flowrate during machine shutdown mode has been highlighted. This has been attributed to a number of factors including: functional degradation of the pneumatic component (seals etc) over time, type of maintenance strategy employed (i.e. breakdown, time or condition based) and network pressure fluctuations.

6.1.2 Pneumatic drive dynamics model

A dynamics model of an open loop controlled pneumatic drive system, common in industry, was developed, identified and validated. The mathematical model took into consideration non-linear flow through extended pneumatic circuit, direction dependant friction, dead volume in cylinder chambers, fittings and tubing, leakage between actuator chambers, time delays due to valve switching and long lengths of tubing, and polytropic

temperature model with optimisation of index. Finally based on the latest research the heat transfer was explicitly included in the cylinder's thermodynamic model.

In terms of identification, the improved ISO method, proposed by Kuroshita [98] for component characterisation, has been successfully applied to the identification of extended pneumatic circuits and as such is deemed suitable for industrial circuits. It has been highlighted that application of the model to open loop controlled systems requires that the flow parameters of charge and exhaust lines in the drive circuit be identified. Additionally it has been observed that the friction parameters should be estimated for extend and retract strokes, and parameters identified at specific operating conditions.

The model provided good results in terms of tracking position and pneumatic force trajectories and should therefore be useful in the simulation, design and analysis of industrial type pneumatic actuator systems. The mean absolute error, in position prediction was less than 1 mm, and for pneumatic force was estimated to be 9.6N. These results are good considering the maximum stroke length and theoretical force of the cylinder (at 5 bar) are 50mm and 245N respectively. The results also compare favourably to the published data with mean errors in position of 1.7mm reported in the literature most recently [89].

6.1.3 Pneumatic system consumption model

A dynamic consumption model for pneumatic production system was developed, identified and validated. The model was developed with a view to implementation in an industrial environment. The mathematical models account for most types of active and all passive consumers. A transition matrix was defined to allow easy interface with a logic controller. An OPC server was used to interface the model with a PLC. The consumption can also be predicted using a user defined activation profile.

The limitations of flow sensors in measuring drive consumption, due primarily to slow a response time and range limited range ability, were highlighted. It is suggested there use, at present, is based on the consumption characteristics of the machine under study. However, it is likely that the development of flow sensor technology will lead to sufficient performance, in terms of response time and range, to allow accurate characterisation of

pneumatic systems in the future. In order to validate the consumption of a drive, the Kagawa flow model was used in conjunction with pressure sensors. A special experiment was designed to validate this approach using a low conductance circuit and larger capacity tank. It has been shown that the extended flow function can accurately describe the non-linear flow behaviour of a typical pneumatic drive circuit. The mean absolute error during charging of a fixed volume tank was 0.537 L/min. This is a good result considering the average flow over the process was 10.8 L/min, equivalent to 5% error with respect to the average flow-rate.

At a component level, results indicate that the consumption of a single drive can be modelled with mixed accuracy using the developed Simulink model. Two linear cylinders were modelled with less than 10% error. However the difference in consumption between modelled and measured for a third cylinder was 20%. It has been pointed out that a common supply for multiple drives is a factor not accounted for in the simplified modelling approach. Passive consumers have been shown to be well approximated at higher pressures, with an accuracy of 5% with supply pressure greater than 3.5 bar. However, for lower pressure it is recommended to use the full Sanville/ISO6358 model, since the accuracy decreases to less than 15%. At a system level, it has been observed that the discrepancy between simulated and measured consumption of an individual drive is less of an issue, in particular if air requirements are dominated by passive consumers. The accuracy of the model in predicting the consumption of a prototype automated production type machine under two sequential operations ranged from approximately 7% to 13%.

The work has demonstrated the PLC driven model will work in practice with sufficient level of accuracy for engineering applications. The model can be used to breakdown pneumatic energy drivers to any level. In its present form the model has potential application in leakage detection, in conjunction with a flow sensor, and local level metric deployment and cost allocation. The model allows for very easy changes to parameters and could be useful as a means of quantifying return on investment due to design or maintenance improvements. For example the resulting savings in compressed air arising from reduced pressure levels for individual device or system, replacement of an open pipe with a nozzle, or the addition of control valve to a blower circuit can be calculated.

6.1.4 Concluding remarks

Reliable models are core component of simulation, estimation and control applications and thus essential to the development of technical intelligence and energy efficiency in pneumatic systems. System models are also useful in validating air loss estimates and developing accurate quality metrics, such as consumption efficiency.

It has been observed that a significant portion of the compressed air requirements, for an industrial production module, is driven by non-functional usage. The industrial case study has demonstrated non-functional usage can account for over a third of total consumption. A priority for industrial users should be reducing such air losses. Improved control of passive consumers, air knives and blowers, resulted in an approximately 8% reduction in air consumption. According to best practise, the percentage of compressed air lost to leakage should be less than 10% in a well maintained system [125]. Based on the above figures, it is recommended that the target for total non-functional usage should be a maximum of 15% of total usage. It is noted that inefficiencies in energy usage due to poor pneumatic design (e.g. over sizing or over pressurisation) and exergy type losses due to pressure drop, friction and backpressure are difficult to quantify using only a flow sensor.

The work has contributed to the development of a comprehensive system model and identification method for industrial type pneumatic drive systems. While previous research has developed various aspects of the flow model [103,19,75], thermodynamic model [89,80,15] and friction model [83,76], this work brings together all elements and applies to the development of an open loop pneumatic drive model. The accuracy of the model and identification method was experimentally validated. Since the results compare favourably to the literature, the model can be considered state of art. The model could be useful for simulation based design of pneumatic drive systems, though it requires reconfiguration to allow for typical design objectives i.e. move payload a certain distance with a pre-defined cycle time. The modelling approach is also useful in the model development stage of controller synthesis for servo-pneumatic drives [49]. In context of a control law, non-linear models have in the past been considered computationally expensive and complex [73]. This is the reason most control orientated research has neglected some dynamics, to utilise

reduced order models. However with development of micro-processors and data acquisition equipment, processing speed is now less of an issue [73]. Finally, in terms of application, the model could be used for condition monitoring since such models are now being used, in combination with flow sensors, for fault diagnostics in pneumatic systems [74].

A novel PLC driven consumption model of a pneumatic system has been presented in this work. The proposed systems type approach allows for the air consumption model to be scaled for use in production processes by minimising identification and modelling effort. The use of an OPC server allows for integration with most industrial control systems. All types of cylinders, semi-rotary actuator types and blowers can be accounted for in the model. Consumption due to leakage can also be included if the pneumatic system under study contains valves with static consumption. The results of the model validation on a prototype automation system indicate that the approach can be used with sufficient accuracy for engineering applications. It is observed that the model can be used in static form for many purposes discussed: cost allocation, energy breakdown and to calculate the return on investment due to design changes. Nonetheless, the focus for this work is the development of an online flow and consumption modelling tool for dynamic production environments. This may eventually allow for the model-based optimisation of control variables. Ultimately such a model could form the basis for a predictive compressor control strategy.

6.2 Recommendations for Future work

Two main areas of work have been identified: in the development of the models, both individual and system, and identification methods. It is envisaged that the development of the models and identification methods are key to any future energy saving applications.

6.2.1 Drive model and identification method development

The identification of circuit flow characteristics is an essential aspect of both models implementation. The rationale for further development of the current identification method is three fold. Firstly, the steady flow method is time consuming and heavy on air consumption, so reducing both forms of consumption would be beneficial for efficiency. Secondly it is difficult to identify the characteristics of exhaust circuits since they are not directly connected to an air source/pressure regulator. In order to identify the circuits, reconfiguration is necessary which may lead to a loss of accuracy in identification results and may not be feasible in an industrial environment. Finally there is a time dependent aspect to flow parameters in the industrial context, due to constantly changing production conditions. For example the throttling or tuning of circuits by technicians will alter the flow characteristics. It would be useful to account for such realistic conditions. These reasons are mainly relevant to modelling the full dynamics of individual pneumatic drives. However, since passive consumers in the system consumption model also require identification, these issues are also of relevance albeit to a lesser extent.

There are two elements of the identification method that could be investigated with a view to improvement:

1. Inverse or thermal based methods for the characterisation of components have been proposed by De Giorgi et al [110,85] . It would be useful to examine and develop further such approaches in particular for industrial circuits. For example the actuators could be used in their extended positions as constant volume sources. The actuator could be charged to a sufficiently high pressure, then the air discharged through the circuit to atmosphere. Based on the pressure response in the cylinder, and the inverse thermodynamic model, the flow characteristics of the circuit could be determined. The temperature response can be calculated by the stop method proposed by Kawashima [106]. Particular focus should be on the applicability of such methods to high conductance circuits with small volume actuators, where short pressure response times may be an issue due to the limited response time of pilot assisted valves.

2. An online identification tool would be useful to account for the sensitivity of flow parameters to throttling by technicians or wear (e.g. pinched tube). The use of recursive estimation algorithms could be investigated. A black box approach was taken by

Saleem et al [172] who employed an ARMA model for online system identification using a Mixed Reality Environment.

Also of interest from an identification perspective, is the estimation of the subsonic index, m , for components in series. Such calculations are possible for the critical pressure ratio, b , and Sonic Conductance, C , using Eckersten's equations [117]. Additionally the experimental rig requires shock absorber for parameter identification during movement of heavy payloads (> 4 kg).

A potential interesting development of the dynamics model could be to interface the model with the PLC using the same OPC architecture proposed for the system consumption model. If the simulation model is simplified by assuming constant upstream pressure, then the only required input variable to the model is the PLC-to-valve control signal. This would simplify the setup of dynamics model further, since analog control signal would no longer required.

6.2.2 Consumption model development

Further model development and validation work is required to ensure the system consumption model accounts for all pneumatic components on a production machine. Specifically in terms of consumers, models of air motors and servo-drive consumption could be developed and validated. An isothermal tank could be used as an alternative method for measuring the consumption of pneumatic drives. An edge detection configuration for bi-stable directional control valves should also be developed. Current edge detection is configured for spring return valves only, so there is a need to account for pneumatic return types. It would be useful to create a block library of consumption equations for all pneumatic consumers in the Simulink browser. The air consumption of drain and pilot assisted valves should also be investigated.

While it is envisaged that a predictive flow model will form the basis for compressor control strategy, there remain a number of model related issues to be addressed:

1. Average flow requirements.

At present only the consumption per stroke of actuators is considered. The average flow required depends on the stroke time of the actuator, and is important from a capacity

planning point of view and thus a fundamental development issue. While the instantaneous flow required is much higher than the average rate, the receiver acts as a buffer between the supply and end use systems. One potential solution is to calculate the average stroke time of the actuator based on the time between limit switch input signals to the PLC. This would make effective use of the OPC interface infrastructure. Alternatively the activation frequency of the actuator's controlling valve could be calculated based on the previous PLC (to DCV) output signals. Typically an allowance/safety factor is also incorporated into capacity planning calculations. It would be interesting to examine the use of a dynamic allowance factor based on estimated system leakage using the proposed model in conjunction with a flow sensor.

2. Predictive and CA system model development

The predictive element of the model could also be further developed. Since most pneumatic systems are controlled in a sequential or logical manner, it may be possible to forecast the PLC states, and thus consumption, based on the PLC program. It would be interesting to examine the use of ladder logic in Simulink (stateflow) for this purpose. The current modelling approach does not consider the addition of random loads to the system, for example, through the use of air guns by operators or leakage. The use of an artificial neural network may aid in predicting short term demand fluctuations.

Since in many cases, consumers such as air guns and leaks are unregulated (i.e. pressure unstable), the network pressure is then also an important consideration. Development of a full system model may be useful to allow for complete understanding of compressed air system dynamics and interaction between supply and demand. In particular losses due to pressure and temperature drops, leakage, and time delays in the network need to be accounted for. Additionally in its present form, the consumption model allows for design changes to be assessed only. Exergy based analysis, proposed by Cai et Kagawa [127,173,167,126], allows for the work-producing potential of compressed air to be assessed and could be incorporated into future work.

3. Model development for real-time system use

For real time applications or hardware in the loop testing, C code generation will be necessary. C code is necessary to run both models on any microprocessor or real time

operating system. Then performance in real time can be assessed and improved for example by loop reduction. This can be done for example in Matlab real time workshop/Simulink coder which generates and executes C or C++ code from Simulink diagrams. Prior to any C code generation, the models require development to ensure conformance with the relevant model based design standards i.e. IEC61508 and DO178.

Finally, a vision for future energy efficient pneumatic systems may be characterised by continuous condition monitoring for cost allocation and leak detection, control for automated pressurisation based on load, and recycling of exhaust air for passive consumers. This could potentially be combined with the localised generation of pressurised air to allow a tighter coupling of compressor output with machine demand using predictive flow models and operational energy minimisation strategies.

References

1. Jovane F, Yoshikawa H, Alting L, Boër CR, Westkamper E, Williams D, Tseng M, Seliger G, Paci AM (2008) The incoming global technological and industrial revolution towards competitive sustainable manufacturing. *CIRP Annals - Manufacturing Technology* 57 (2):641-659
2. Seliger G (2007) *Sustainability in Manufacturing: Recovery of Resources in Product and Material Cycles* Springer, Berlin
3. Gutowski T, Murphy C, Allen D, Bauer D, Bras B, Piwonka T, Sheng P, Sutherland J, Thurston D, Wolff E (2001) *WTEC Panel Report on Environmentally Benign Manufacturing* International Technology Research Institute
4. Gutowski T, Murphy C, Allen D, Bauer D, Bras B, Piwonka T, Sheng P, Sutherland J, Thurston D, Wolff E (2005) Environmentally benign manufacturing: Observations from Japan, Europe and the United States. *Journal of Cleaner Production* 13 (1):1-17
5. Van Brussel H Foreword. In: *Second International Workshop on Intelligent Manufacturing Systems* Leuven, Belgium, September 1999.
6. Tanaka K (2008) Assessment of energy efficiency performance measures in industry and their application for policy. *Energy Policy* 36 (8):2887-2902
7. *Annual Competitiveness Report 2008: Volume 1 Benchmarking Ireland's Performance (2008)*. Forfas, Department of Enterprise, Trade and Employment, Dublin, Ireland
8. *Delivering a sustainable energy future for Ireland: Irish Government White Paper (2007)*. Dublin, Ireland
9. Erkman S (1997) Industrial ecology: An historical view. *Journal of Cleaner Production* 5 (1-2):1-10
10. Yoshikawa H Sustainable Manufacturing. In: *41st CIRP Conference on Manufacturing Systems*, Tokyo, Japan, May 27 2008.
11. Pearce M (2005) Is there an alternative to fluid power? *Computing & Control Engineering Journal* 16 (2):8-11
12. Sands S (1999) *Pneumatics: A Practical Engineer's Handbook*. Kamtech Publishing Ltd., Surrey, Uk
13. Beater P (2007) *Pneumatic Drives: System Design, Modelling and Control*. Springer Berlin
14. Moore P, Jun Sheng P Pneumatic servo actuator technology. In: *IEE Colloquium on Actuator Technology: Current Practice and New Developments*, 1996. pp 3/1-3/6

15. Richer E, Hurmuzlu Y (2000) A High Performance Pneumatic Force Actuator System: Part 1 - Nonlinear Mathematical Model. *ASME Journal of Dynamic Systems, Measurement and Control* 122 (3):416-525
16. Kazerooni H (2005) Design and analysis of pneumatic force generators for mobile robotic systems. *Mechatronics, IEEE/ASME Transactions on* 10 (4):411-418
17. Granosik G, Borenstein J (2005) Pneumatic actuators for serpentine robot. Paper presented at the 8th International Conference on Walking and Climbing Robots London, UK, 12-15 Sept.
18. Hesse S (2001) 99 Examples of Pneumatic Applications. *Blue Digest on Automation*. Festo AG, Esslingen, Germany
19. Thomas MB, Gary PM (2009) Considerations on a Mass-Based System Representation of a Pneumatic Cylinder. *Journal of Fluids Engineering* 131 (4):041101
20. Winter CA, Bredau J From component supplier to solution provider In: 7th International Fluid Power Conference, Aachen 2010. pp 203-220
21. Van Ormer H Will an air receiver cut energy consumption? *Hydraulics & Pneumatics* v. 54 no. 8 (August 2001) p. 41-2.
22. Yuan CY, Zhang T, Rangarajan A, Dornfeld D, Ziemba B, Whitbeck R (2006) A decision-based analysis of compressed air usage patterns in automotive manufacturing. *Journal of Manufacturing Systems* 25 (4):293-300
23. Lovrec D, Tic V Reduction in air consumption when air-blowing using an energy saving nozzle. In: 7th International Fluid Power Conference, Aachen, 2010. pp 303-316
24. *Compressed Air: Introducing energy saving opportunities for business* (2007). Carbon Trust London, UK
25. Eret P, Harris C, De Lasa T, Meskell C, O'Donnell GE Industrial Compressed Air Usage - Two Case Studies. In: 7th International Fluid Power Conference, Aachen, Germany, 22-24 March 2010. pp 355-366
26. Radgen P, Blaustein E (2001) *Compressed Air Systems in the European Union: Energy, Emissions, Savings Potential and Policy Actions*. Fraunhofer ISI, Stuttgart
27. Risi JD (1995) Energy savings with compressed air. *Energy Engineering* 92 (6):49-58
28. Kaya D, Phelan P, Chau D, Sarac HI (2002) Energy conservation in compressed-air systems. *International Journal of Energy Research* 26 (9):837-849
29. Saidur R, Rahim NA, Hasanuzzaman M (2010) A review on compressed-air energy use and energy savings. *Renewable and Sustainable Energy Reviews* 14 (4):1135-1153
30. Andersen BW (1967) *The Analysis and Design of Pneumatic Systems* John Wiley & Sons, New York, NY

31. Parkkinen R, Lappalainen P A consumption model of pneumatic systems. In: Conference Record of the IEEE Industry Applications Society Annual Meeting, 1991. pp 1673-1677
32. Fleischer H (1995) Manual of Pneumatic Systems Optimisation. McGraw-Hill, New York, NY
33. Doll M, Sawodny O Energy Optimal Open Loop Control of Standard Pneumatic Cylinders. In: 7th International Fluid Power Conference, Aachen, 2010. pp 259-270
34. Jovane F, Koren Y, Boër CR (2003) Present and Future of Flexible Automation: Towards New Paradigms. CIRP Annals - Manufacturing Technology 52 (2):543-560
35. Alting DL, Jørgensen DJ (1993) The Life Cycle Concept as a Basis for Sustainable Industrial Production. CIRP Annals - Manufacturing Technology 42 (1):163-167
36. Gungor A, Gupta SM (1999) Issues in environmentally conscious manufacturing and product recovery: a survey. Computers & Industrial Engineering 36 (4):811-853
37. Tridech S, Cheng K (2008) Low Carbon Manufacturing: Characterization, Theoretical Models and Implementation. Paper presented at the The 6th International Conference on Manufacturing Research (ICMR08), Brunel University, U.K., 9-11th September 2008
38. Jeswiet J, Kara S (2008) Carbon emissions and CES(TM) in manufacturing. CIRP Annals - Manufacturing Technology 57 (1):17-20
39. Westkamper E Technical Intelligence for Manufacturing. In: Second International Workshop on Intelligent Manufacturing Systems, Leuven, Belgium, 2000. pp k3-k14
40. Jovane F, Westkamper E, Williams D (2009) The Manufuture Road: Towards Competitive and High-adding-value Manufacturing. Illustrated edn. Springer, Berlin, Germany
41. Tangen S (2005) Demystifying productivity and performance. International Journal of Productivity and Performance Management 54 (1):34-46
42. Groover MP (2007) Automation, production systems, and computer-integrated manufacturing. 3rd, Illustrated edn. Prentice Hall, Upper Saddle River, NJ
43. Koren Y, Heisel U, Jovane F, Moriwaki T, Pritschow G, Ulsoy G, Van Brussel H (1999) Reconfigurable Manufacturing Systems. CIRP Annals - Manufacturing Technology 48 (2):527-540
44. O'Donnell GE (2007) Sensor Technology for Process Monitoring in Flexible Machining Systems. AMS Research Centre, University College Dublin Ireland
45. Rembold U, Nnaji BO, Storr A (1993) Computer Integrated Manufacturing and Engineering. Addison-Wesley Publishing Company, Boston, MA

46. Carpanzano E, Jovane F (2007) Advanced Automation Solutions for Future Adaptive Factories. *CIRP Annals - Manufacturing Technology* 56 (1):435-438
47. Harding EC Energy Saving Potential by Optimising the Process of Air Generation and Consumption. In: 4th European Conference on Electrical and Instrumentation Applications in the Petroleum & Chemical Industry 2007. pp 1-7
48. Lotter B (1997) *Manufacturing Assembly Handbook*. Blue Digest on Automation. Festo AG, Esslingen, Germany
49. Hildebrandt A, Neumann R, Sawodny O (2010) Optimal System Design of SISO-Servopneumatic Positioning Drives. *IEEE Transactions on Control Systems Technology* 18 (1):35-44
50. Zanki A (2006) *Milestones in Automation: From the Transistor to the Digital Factory*. Publicis Corporate Publishing Erlangen, Germany
51. Vijayaraghavan A, Sobel W, Fox A, Dornfeld DA, Warndorf P Improving Machine Tool Interoperability using Standardised Interface Protocols: MTConnect. In: International Symposium on Flexible Automation Atlanta, GA, June 23-26 2008.
52. Anonymous (1998) OPC overview.
53. Gutowski T, Dahmus J, Thiriez A (2006) Electrical energy requirements for manufacturing processes. Paper presented at the 13th CIRP International Conference on Life Cycle Engineering Leuven, May 31st - June 2nd
54. Kordonowy DN (2001) *A Power Assessment of Machining Tools*. B.S., Massachusetts Institute of Technology, Cambridge, MA
55. Dahmus J, Gutowski T An Environmental Analysis of Machining In: ASME International Mechanical Engineering Congress and RD&D Expo, Anaheim, CA, 2004.
56. McCloy D, Martin HR (1980) *Control of Fluid Power: Analysis and Design*. 2nd edn. John Wiley & Sons, New York
57. Elliott BS (2006) *Compressed Air Operations Manual* McGraw-Hill, New York, USA
58. Shearer JL (1956) Study of Pneumatic Processes in the Continuous Control of Motion with Compressed Air, Parts 1 and 2. *Transactions of the ASME* 78:233-249
59. Fleming JS, Tang Y, Cook G (1998) The Twin Helical Screw Compressor Part 1: Development, Applications and Competitive Position. *Proceedings of the Institution of Mechanical Engineers -- Part C -- Journal of Mechanical Engineering Science* 212 (5):355-367
60. Foszcz J, L. (2002) Controls increase compressor efficiency. *Plant Engineering* 56 (5):34
61. Lutfy E (2002) Innovative compressed air solutions. *Plant Engineering* 56 (3):57

62. Wagner H (2002) Compressed air quality. *Plant Engineering* v. 56 no. 10 p. 81, 83, 85.
63. Hand R, White M (2007) Keep your compressed air high and dry. *Hydraulics & Pneumatics* v. 60 no. 2 (February 2007) p. 40, 42.
64. Overby K (2002) Keeping dried compressed air dry. *Plant Engineering* v. 56 no. 9 p. 42-4.
65. Bernhardt E (2005) Keep Compressed Air from Going Down the Drain. *Hydraulics & Pneumatics* v. 58 no. 9 p. 42-3.
66. Rattenbury JM (2001) How to optimize an instrument air system. *Plant Engineering* v. 55 no. 2 p. 88-92.
67. Hand R (2004) Double play. *Hydraulics & Pneumatics* v. 57 no. 11 p. 36, 38-40.
68. Hitchcox AL (2006) Clean air at the right pressure. *Hydraulics & Pneumatics* 59 (11):36-40
69. Barber A (1997) *Pneumatic Handbook*. 8th edn. Elsevier Advanced Technology, Oxford, UK
70. Anonymous (1985) BS ISO 6432 Pneumatic fluid power - Single rod cylinders - Bores from 8 to 25mm. International Organisation for Standardisation,
71. SMC Basic Pneumatics: A manual for fluid power components and practical applications. Indianapolis, IN
72. Carneiro JF, De Almeida FG (2007) Heat transfer evaluation of industrial pneumatic cylinders. *Proceedings of the Institution of Mechanical Engineers Part I: Journal of Systems and Control Engineering* 221 (1):119-128
73. Richer E, Hurmuzlu Y (2000) A High Performance Pneumatic Force Actuator System: Part 2 - Nonlinear Control Design *ASME Journal of Dynamic Systems, Measurement and Control* 122 (3):426-434
74. Gonzalez RG Fault diagnosis of a pneumatic subsystem. In: 7th International Fluid Power Conference, Aachen, 2010. pp 537-548
75. Nouri BMY, Al-Bender F, Swevers J, Vanherck P, Van Brussel H Modelling a pneumatic servo positioning system with friction. In: *Proceedings of the American Control Conference* 2000. pp 1067-1071
76. Belforte G, Mattiazzo G, Mauro S, Tokashiki LR (2003) Measurement of friction force in pneumatic cylinders. *Tribotest* 10 (1):33-48
77. Sorli M, Gastaldi L, Codina E, de las Heras S (1999) Dynamic analysis of pneumatic actuators. *Simulation Practice and Theory* 7 (5-6):589-602

78. Andrighetto PL, Valdiero AC, Carlotto L Study of the friction behavior in industrial pneumatic actuators. In: ABCM symposium in Mechatronics, Rio de Janeiro, Brazil, 2006. ABCM, pp 369-376
79. Ning S, Bone GM Development of a nonlinear dynamic model for a servo pneumatic positioning system. In: IEEE International Conference on Mechatronics and Automation, 2005. pp 43-48
80. Carneiro JF, de Almeida FG (2006) Reduced-order thermodynamic models for servo-pneumatic actuator chambers. Proceedings of the Institution of Mechanical Engineers, Part I: Journal of Systems and Control Engineering 220 (4):301-314
81. Kagawa T, Tokashiki LR, Fujita T (2002) Influence of Air Temperature Change on Equilibrium Velocity of Pneumatic Cylinders. Journal of Dynamic Systems, Measurement, and Control 124 (2):336-341
82. Mullins E (2003) Statistics for the quality control chemistry laboratory. The Royal Society of Chemistry Cambridge, UK
83. Nouri BMY (2004) Friction identification in mechatronic systems. ISA Transactions 43 (2):205-216
84. Swevers J, Al-Bender F, Ganseman CG, Projogo T (2000) An integrated friction model structure with improved presliding behavior for accurate friction compensation. IEEE Transactions on Automatic Control 45 (4):675-686
85. De Giorgi R, Kobbi N, Sesmat S, Bideaux E Thermal model of a tank for simulation and mass flow rate characterization purposes. In: 7th JFPS International Symposium on Fluid Power, Toyama, September 15-18 2008.
86. Schumacher M, Corves B, Husing M, Barej M, Hemmerich D Simulation of pneumatic actuators at the application example of windscreen wiper systems. In: 7th International Fluid Power Conference, Aachen, 2010. pp 287-300
87. Al-Ibrahim AM, Otis DR Transient air temperature and pressure measurements during the charging and discharging processes of an actuating pneumatic cylinder. In: 45th National Conference on Fluid Power, Chicago, 1992. pp 233-239
88. De las Heras S Gas compression process inside oleopneumatic suspensions. In: International Fluid Power Exposition and Technical Conference, 1996. National Fluid Power Association, pp 11-18
89. Najafi F, Fathi M, Saadat M (2009) Dynamic modelling of servo pneumatic actuators with cushioning. The International Journal of Advanced Manufacturing Technology 42 (7):757-765
90. Anonymous (2001) BS ISO 10099 Pneumatic fluid power - Cylinders - Final examination and acceptance criteria. International Organisation for Standardisation, Geneva

91. Zhang H, Oneyama N, Kagawa T, Kuroshita K Standard proposal on flow-rate characteristics of pneumatic components. In: 50th National Conference on Fluid Power, 2005.
92. Sanville FE (1971) New method of specifying the flow capacity of pneumatic fluid power valves *Hydraulic Pneumatic Power* 17 (195):120-126
93. Purdue DR, Wood D, Townsley MJ (1969) DESIGN OF PNEUMATIC CIRCUITS. *Fluid Power International* 34 (401):27-31, 36
94. Sanville FE (1972) Some Simplified Flow Calculations for Pneumatic Circuits *Hydraulic Pneumatic Power* 18 (214):452-457
95. Shannak BA (2002) Experimental investigation of critical pressure ratio in orifices. *Experiments in Fluids* 33 (4):508-511
96. Anonymous (1990) ISO6358 Method for Determination of flow-rate characteristics of pneumatic fluid power components International Organisation for Standardisation, Geneva
97. Anonymous (2008) BS ISO5598: Fluid power systems and components - Vocabulary. International Organisation for Standardisation, Geneva
98. Kuroshita K, Oneyama N Improvements of test method of flow-rate characteristics of pneumatic components. In: SICE Annual Conference, 4-6 Aug. 2004. pp 147-152
99. Hubert D, Sesmat S, De Giorgi R, Gautier D, Bideaux E Analysis of flow behaviour and characteristics of pneumatic components. In: 7th JFPS International Symposium on Fluid Power, Toyama, Japan, 2008. pp 719-724
100. Sesmat S, Hubert D, Gautier D, Bideaux E Pneumatic component characterization: Use of measured stagnation pressures. In: 7th International Fluid Power Conference, Aachen, 2010. pp 223-234
101. White FM (2003) *Fluid Mechanics*. 5th edn. McGraw-Hill, New York, NY
102. Jungong M, Juan C, Ke Z, Mitsuru S Flow-rate characteristics parameters of pneumatic component. In: IEEE International Conference on Automation and Logistics (ICAL) 1-3 Sept. 2008. pp 2946-2949
103. Kagawa T, Cai M, Kawashima K, Wang T, Nagaki T, Hasegawa T, Oneyama N Extended representation of flow-rate characteristics for pneumatic components and its measurement using isothermal discharge method. In: Bath Workshop on Power Transmission and Motion Control (PTMC), University of Bath, UK, 2004. Professional Engineering Publishing pp 271-282
104. Jungong M, Baolin W, Juan C, Zhiyong T, Oneyama N Error comparison between ISO/WD6358-2 and ISO6358:1989. In: 7th International Symposium on Instrumentation and Control Technology, 2008.

105. Kuroshita K, Sekiguchi Y, Oshiki K, Oneyama N Development of new test method for flow-rate characteristics of pneumatic components. In: Burrows CR, Edge KA, Johnston DN (eds) Bath Workshop on Power Transmission and Motion Control (PTMC), University of Bath, UK, 2004. Professional Engineering Publishing, pp 243-256
106. Kawashima K, Kagawa T, Fujita T (2000) Instantaneous Flow Rate Measurement of Ideal Gases. *Journal of Dynamic Systems, Measurement, and Control* 122 (1):174-178
107. Kawashima K, Fujita T, Kagawa T (2001) Flow rate measurement of compressible fluid using pressure change in the chamber. *Transactions of the Society of Instrument and Control Engineers* 1 (1)
108. Kawashima K, Ishii Y, Funaki T, Kagawa T (2004) Determination of Flow Rate Characteristics of Pneumatic Solenoid Valves Using an Isothermal Chamber. *Journal of Fluids Engineering* 126 (2):273-279
109. Ji-Seong J, Sang-Won J, Bo-Sik K Study on the Measurement Method of Leakage Flow-rate for Pneumatic Driving Apparatus. In: SICE-ICASE, International Joint Conference, 18-21 Oct. 2006. pp 4116-4120
110. De Giorgi R, Sesmat S, Bideaux E Using inverse models for determining orifices mass flow rate characteristics In: 6th JFPS International Symposium on Fluid Power, Tsukuba 2005.
111. Yang L-h, Liu C-l (2006) Measuring flow rate characteristics of a discharge valve based on a discharge thermodynamic model. *Measurement Science and Technology* 17 (12):3272
112. Qian Y, Xiang MG (2008) Identification of the flow-rate characteristics of a pneumatic valve by the instantaneous polytropic exponent. *Measurement Science and Technology* 19:1-5
113. Lin-Chen YY, Wang J, Wu QH (2003) A software tool development for pneumatic actuator system simulation and design. *Computers in Industry* 51 (1):73-88
114. Wang J, Pu J, Moore P (1999) A practical control strategy for servo-pneumatic actuator systems. *Control Engineering Practice* 7 (12):1483-1488
115. Tressler JM, Clement T, Kazerooni H, Lim A Dynamic behavior of pneumatic systems for lower extremity extenders. In: IEEE International Conference on Robotics and Automation 2002. pp 3248-3253
116. Bobrow J, McDonell B (1998) Modelling, Identification and Control of a Pneumatically Actuated, Force Controllable Robot. *IEEE Transactions on Robotics and Automation* 14 (5):732-742
117. Eckersten J Simplified flow calculations for pneumatic components. In: Atlas Copco Compendium, Stockholm, Sweden, 1975. Atlas Copco, pp 183-192

118. Parkkinen J, Zenger K (2008) A New Efficiency Index for Analysing and Minimising Energy Consumption in Pneumatic Systems. *International Journal of Fluid Power* 9 (1):45-52
119. Hyvarinen K, Lappalainen P A lumped circuit parameter model of pneumatic networks. In: *International IEEE/IAS Conference on Industrial Automation and Control: Emerging Technologies*, 22-27 May 1995. pp 735-742
120. Hyvarinen K, Lappalainen P A novel simulator of pneumatic networks. In: *Proceedings of the IEEE International Conference on Industrial Technology*, 2-6 Dec 1996. pp 343-347
121. Miyajima T, Kawashima K, Fujita T, Sakaki K, Kagawa T (2005) Air Consumption of Pneumatic Servo Table System. In: *Systems Modeling and Simulation: Theory and Applications*. pp 324-333
122. Yang A, Pu J, Wong CB, Moore P (2009) By-pass valve control to improve energy efficiency of pneumatic drive system. *Control Engineering Practice* 17 (6):623-628
123. Zhang Y, Cai M, Kong D Overall Energy Efficiency of Lubricant-Injected Rotary Screw Compressors and Aftercoolers. In: *Asia-Pacific Power and Energy Engineering Conference 2009*. pp 1-5
124. Talbott EM (1986) *Compressed Air Systems - A Guidebook on Energy and Cost savings*. The Fairmont Press, Atlanta, GA
125. *Improving Compressed Air System Performance: A Sourcebook for Industry* (1998). Compressed Air Challenge, Office of Energy Efficiency and Renewable Energy, U.S.
126. Cai M, Kawashima K, Kagawa T (2006) Power Assessment of Flowing Compressed Air. *Journal of Fluids Engineering* 128 (March)
127. Cai M, Kagawa T, Kawashima K Energy conversion mechanics and power evaluation of compressible fluid in pneumatic actuator systems. In: *37th Intersociety Energy Conversion Engineering Conference (IECEC)*, 2002. pp 438-443
128. Zhang Y, Cai M, Kagawa T Study of cost and energy consumption for pneumatic actuator and electric actuator In: *7th International Fluid Power Conference*, Aachen, 2010. pp 195-210
129. Herrmann C, Kara S, Thiede S (2011) Dynamic life cycle costing based on lifetime prediction. *International Journal of Sustainable Engineering* 4 (3):224-235. doi:10.1080/19397038.2010.549245
130. Gauchel W (2006) Energy-saving pneumatic systems. *O + P Olhydraulik und Pneumatik* 50 (1)
131. Fleischer H (1999) Stop oversizing pneumatic components. *Machine Design* 71 (11):101

132. Heilala J, Helin K, Montonen J (2006) Total cost of ownership analysis for modular final assembly systems. *International Journal of Production Research* 44 (18):3967 - 3988
133. Heilala J, Montonen J, Helin K, Salonen T, Väätäinen O, Pham DT, Eldukhri EE, Soroka AJ (2006) Life Cycle and Unit Cost Analysis for Modular Re-Configurable Flexible Light Assembly Systems. In: *Intelligent Production Machines and Systems*. Elsevier Science, Oxford, pp 395-400
134. Cai M, Kagawa T Simulation for Energy Savings in Pneumatic Systems. In: *Systems Modelling and Simulation: Theory and Applications*, 2007. Springer,
135. Senoo M, Zhang H, Oneyama N (2005) Research and development on energy saving in pneumatic system. Paper presented at the 50th National Conference on Fluid Power
136. Shi Y, Cai M-l Study on efficiency and flow characteristics of two kinds of pneumatic booster valves. In: *International Conference on Computer, Mechatronics, Control and Electronic Engineering (CMCE)*, 24-26 Aug. 2010. pp 45-50
137. Otis DR, Al-Shaalan T, Weiss E Reducing compressed air consumption by utilising expansion energy during the actuation of a pneumatic cylinder. In: *45th National Conference on Fluid Power*, 1992.
138. Li TC, Wu HW, Kuo MJ (2006) A study of gas economizing pneumatic cylinder. *Journal of Physics: Conference series* 48:1227-1232
139. Mutoh H, Kawakami Y, Hriata Y, Kawai S An approach to energy conservation in pneumatic systems with meter out circuit In: *7th JFPS International Symposium on Fluid Power*, TOYAMA, September 15-18 2008.
140. Sweeney R (2002) Cutting the cost of compressed air systems. *Machine Design* 74 (21):76
141. Cai M, Xu W (2010) Self-sustained oscillation pulsed air blowing system for energy saving. *Chinese Journal of Mechanical Engineering* 23
142. Kambli S (2008) Monitoring pneumatics makes all the difference. *Machine Design* 80 (16):89
143. Coll S (2005) Pulling money OUT OF THIN AIR. *Machine Design* 77 (4):148
144. Fryer CW (2006) Improving pneumatics bottom line. *Machine Design* 78 (3):80
145. Christian B (2007) SELF-MONITORING pneumatic systems. *Machine Design* 79 (8):70
146. Xiangrong S, Michael G (2007) Energy Saving in Pneumatic Servo Control Utilizing Interchamber Cross-Flow. *Journal of Dynamic Systems, Measurement, and Control* 129 (3):303-310

147. Al-Dakkan KA, Barth EJ, Goldfarb M A Multi-objective sliding mode approach for the energy saving control of pneumatic servo systems. In: ASME International Mechanical Engineering Congress & Exposition, Washington, D.C., November 15-21 2003.
148. Granosik G, Borenstein J Minimizing air consumption of pneumatic actuators in mobile robots. In: Proceedings of the IEEE International Conference on Robotics and Automation (ICRA), 2004. pp 3634-3639
149. Al-Dakkan KA, Barth EJ, Goldfarb M (2006) Dynamic constraint-based energy-saving control of pneumatic servo systems. *Journal of Dynamic Systems, Measurement, and Control* 128:655-662
150. Al-Dakkan KA, Goldfarb M, Barth EJ Energy saving control for pneumatic servo systems. In: Proceedings of the IEEE/ASME International Conference on Advanced Intelligent Mechatronics (AIM) 2003. pp 284-289
151. Xiaocong Z, Jian C, Guoliang T, Bin Y Energy-saving method of pneumatic position control system based on separate control of motion trajectory and pressure trajectory. In: 7th International Fluid Power Conference, Aachen, 2010. pp 329-342
152. Ke J, Wang J, Jia N, Yang L, Wu QH Energy efficiency analysis and optimal control of servo pneumatic cylinders. In: Proceedings of IEEE Conference on Control Applications, 2005. pp 541-546
153. The Carbon Zero compressor recovers 100% of the input energy (2009). Atlas Copco, Stockholm, Sweden
154. Anonymous Energy efficient compressed air systems. Carbon Trust,
155. Koski MA (2002) Compressed air energy audit--"the real story". *Energy Engineering* 99 (3):59-70
156. Plackett-Smith M (1998) Optimizing energy efficiency in compressed air filtration. *Filtration & Separation* 35 (3):251-253
157. Sanville FE Two-level compressed air systems for energy saving. In: 7th International Fluid Power Symposium, Bath, England, 1986. pp 375-383
158. The Lean and Energy Toolkit (2008). U.S. Environmental Protection Agency, Washington, D.C.
159. Kissock K, Seryak J Lean Energy Analysis: Identifying, Discovering and tracking energy savings potential. In: Proceedings of Society of Manufacturing Engineers: Advanced Energy and Fuel Cell Technologies Conference, Livonia, MI, 2004.
160. Järvensivu M, Saari K, Jämsä-Jounela SL (2001) Intelligent control system of an industrial lime kiln process. *Control Engineering Practice* 9 (6):589-606

161. Mouzon G, Yildirim MB, Twomey J (2007) Operational methods for minimization of energy consumption of manufacturing equipment. *International Journal of Production Research* 45 (18):4247 - 4271
162. Compressed Air Counter testo 6440: Saving costs with consumption measurement (2006). Testo,
163. PicoScope 2000 Series PC Oscilloscopes: User guide (2005). Pico Technology,
164. Dwyer T (2004) Making pneumatics an energy miser. *Machine Design* 76 (4):110
165. Anonymous (2005) The Truth About Compressed Air! *Machine Design* 77 (13):19
166. Standard cylinders DSNU data sheet. Festo, Esslingen, Germany
167. Cai M, Kagawa T Energy consumption assessment of pneumatic actuating systems including compressor. In: *International Conference on Compressors and their systems*, City University, London, UK, 2001. IMechE Conference Transactions. Professional Engineering Publishing, pp 381-390
168. Simulink Dynamic System Simulation for Matlab (2000). Version 4 edn. The MathWorks Natick, MA
169. Anonymous (2004) BS ISO15552 Pneumatic fluid power - Cylinders with detachable mountings - Bores from 32mm to 320mm. International Organisation for Standardisation, Geneva
170. Cylinder air consumption (2010). 1.6 edn. Festo AG, Esslingen, Germany
171. Energy Saving Program (2010). 3.5 edn. SMC Corporation, Tokyo, Japan
172. Saleem A, Abdrabbo S, Tutunji T (2009) On-line identification and control of pneumatic servo drives via a mixed-reality environment. *The International Journal of Advanced Manufacturing Technology* 40:518-530
173. Cai M, Kagawa T Design and application of air power meter in compressed air systems. In: *Proceedings of EcoDesign the Second International Symposium on Environmentally Conscious Design and Inverse Manufacturing* 2001. pp 208-212

Appendix A OPC data exchange protocol

OLE (object linking and embedding) for process control is a series of industry specifications, defined by the OPC foundation, for allowing communication between numerous data sources, including devices, controllers, databases and other applications, and is based on Microsoft's OLE/COM technology (OPC overview, 1998). OPC can be represented conceptually as an abstraction layer that allows a data sink and data source to exchange data without knowing specific communication protocols and internal data organisation structures. This device abstraction layer is realised by using two components, an OPC server and OPC client (figure A.1)

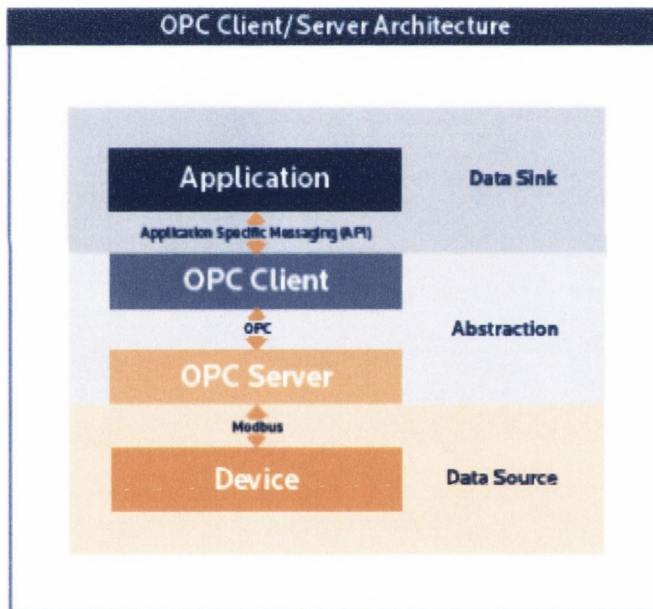


Figure A.1: OPC client server architecture (OPC overview, 1998)

An OPC server is a software application, written to comply with one or more OPC specifications, that acts as a translator between OPC and original device communication protocols. The server can read and write to the data source, but only if the OPC client commands it to. OPC clients are software modules that control communication with compliant OPC connectors (servers), based on embedded application requests (figure A.2). Typically OPC clients are embedded in applications such as Human Machine Interfaces (HMI's) and other data trending packages. The client configures the

rate at which the OPC server provides data to the client. The main OPC specifications include OPC Data Access, OPC Alarm and Events and OPC Historical Data Access.

The OPC data access server is comprised of several objects: the server, the group and the item. The server maintains information about itself and hosts the groups. The groups represent containers for one or more server items and provide a way for clients to organise data. Within the groups are items which represent connections to data sources within the server (OPC overview, 2008).

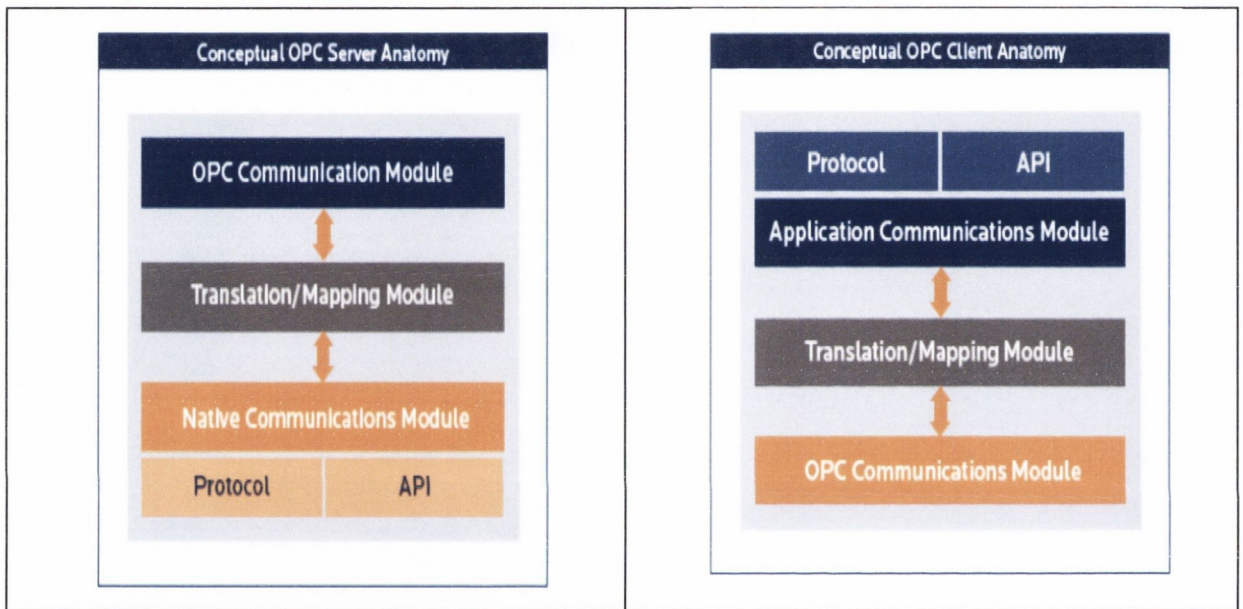


Figure A.2: Conceptual OPC server and client anatomy

Appendix B Matlab and Simulink programs

B1 Pneumatic drive Simulink models

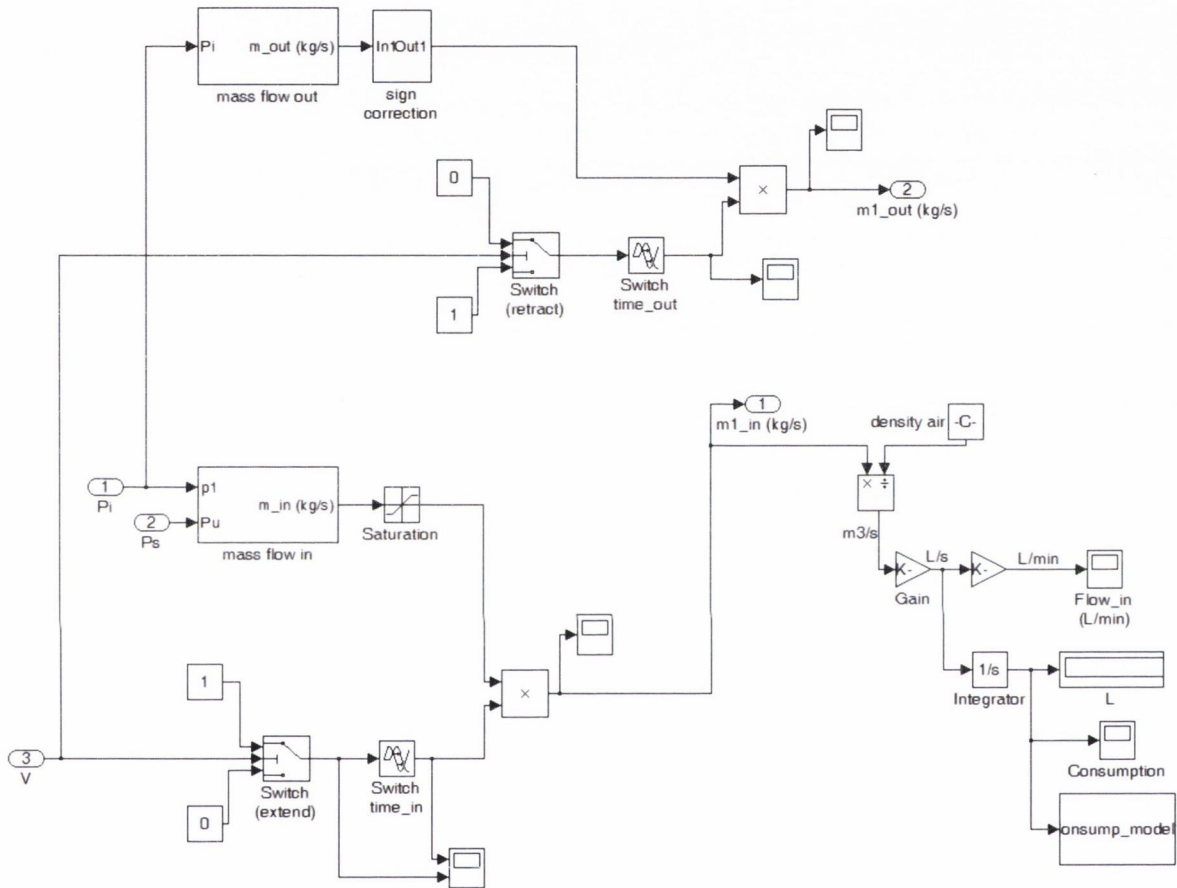


Figure B1: Level 3 flow model (Chamber 1 example)

B2 Identification scripts

```
%% ***** Circuit characteristics identification***** %%
%%%%%%%%%%%%%%%%%%%%%%%%%%%%%%%%%%%%%%%%%%%%%%%%%%%%%%%%%%%%%%%%%%%%%%%%
%Improved ISO method 2

disp(textdata)

v1 = data(:,1);
v2 = data(:,2);

dv1 = decimate(v1,4) %reduce data by factor of n, employs
filter also
dv2 = decimate(v2,4);

sdv1 = round2((smooth(dv1, 300)),0.01); %use large span
to account for increased noise due to reduced damping on FS
sdv2 = round2(smooth(dv2),0.01); %unweighted 5pt
moving average with rounding to 2 decimal places

clear('v1','var', 'v2', 'var');

%% All flow rates to DIN standard reference conditions

%Testo sensor
q_te = (((sdv1-1.57)/0.1067)*1000/60)*0.9479; % L/min
q_te(q_te < 0) = 0; % setting negative values
to zero
Q = (q_te/1000/60); % m3/s

%Festo SFAB sensor
s = whos('data');
if s.size(2) == 3 %if third (sensor) data column exists....
    v3 = data(:,3);
    dv3 = decimate(v3,4);
end

clear('s','v3');

ans = exist('dv3');
if ans == 1
    q_fe = dv3./0.2; % L/min
    Q_fe = (q_fe./1000)./60;
end

clear('ans','dv3');

%% Pressure unit: bar(g)
Pu = ((10-((5-sdv2)/0.3992))); % bar(g)
```

```

Pu (Pu<0) = 0;
Pu = Pu + 1.01325;           % bar(a)
P = (Pu*100000);           %Pa

%*****%

t = 0:0.001:(length(Pu)*0.001);           %1000 Hz sampling
t(:,length(Pu))=[];
t = t(:);

clear('dv1','var','dv2','var','sdv1','sdv2');

Pr = 101325./P;

To = 273;   % Air temperature at DIN reference conditions (K)
Tu = 298;   %Upstream (measured) temperature of air (K)

%% plots

r = detrend(Q); %to allow for easier computation of local
maxima

%peakdet function: http://billauer.co.il/peakdet.html
[maxtab, mintab] = peakdet(r, 0.0001, t);           %1st argument
is vector to examine, 2nd is peak threshold (to avoid many
local maxima),
%3rd argument is vectors x-axis

%Note must use local minima if decreasing regulated pressure
during test
figure(1);
plot(t,r);
xlabel('time (s)');
ylabel('Residuals');
hold on
scatter(maxtab(:,1), maxtab(:,2), 'r*');

ti = maxtab(:,1);           %must use time as pressure values non-
distinct

% if decreasing pressure during test....

%figure(1);
%plot(t,r);
%xlabel('time (s)');
%ylabel('Residuals');
%hold on
%scatter(mintab(:,1), mintab(:,2), 'r*');
%ti = mintab(:,1);

```



```

%lookup table
Pi = interp1(t, P, ti);
Qi = interp1(t, Q, ti);
Qi = Qi*(sqrt(Tu/To)); %Flow corrected to ref. temperature

% Conductance (m3/s.Pa) to DIN reference conditions
Ci = Qi./Pi;
C = max(Qi)/max(Pi);

er = 6; %combination of sensor inaccuracy
n = 1:length(Ci);
test = ((C - Ci(n))/C)*100; %difference from original mean

C = [];
%if difference within error of sensors recalculate mean as
average of values within error range
for n = 1:length(Ci)
    if test(n) < er
        C = [C, Ci(n)];
    end
end

C = mean(C)
Pri = 101325./Pi;

clear('test','n','er');

figure(2);
x(1) = subplot(2,1,1);
plot(Pi,Qi,'o','MarkerSize',8)
xlabel('Upstream pressure (Pa)');
ylabel('Flow (m3/s)');
hold on
x = [0, max(Pi)];
y = [0, max(Qi)];
plot(x,y,'--g','Linewidth',3);
grid on
x(2) = subplot(2,1,2);
scatter(Pri, Ci);
xlabel('Pressure ratio');
ylabel('Conductance');
grid on

Qimax = C*Pi*(sqrt(To/Tu)); %temperature correction
Qri = Qi./Qimax;

%Extended ISO representation (b,m)
figure(3);
[cf_,gof] = ISOe_curve_fit(Pri, Qri)

%ISO6358 fit (b)

```

```

%[cf_, gof] = ISO1_curve_fit(Pri,Qri)

%Full Kagawa model (b,m,a)
%showfit ISOee      %Ezyfit toolbox

%% Determine number of points in subsonic region

ans = find(Pri > 0.5);
disp('Approximate number of data points in subsonic region')
Data_points = length(ans)      % number of data points in
subsonic region

```

B3 Pneumatic system Simulink models

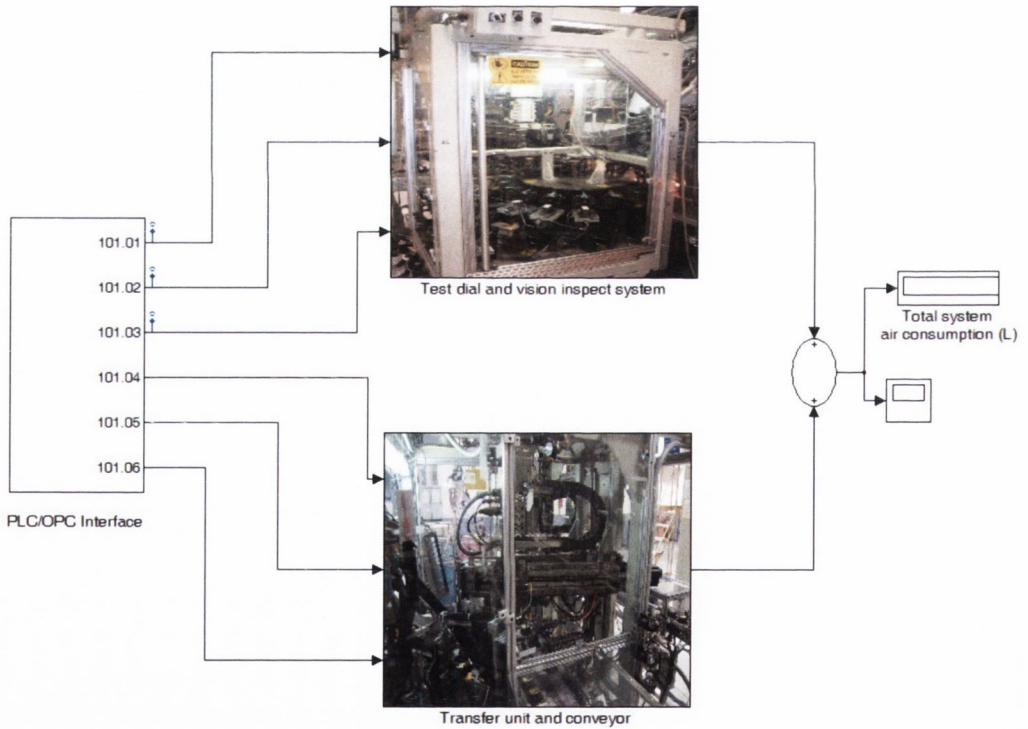


Figure B4: Top level diagram AQT unit

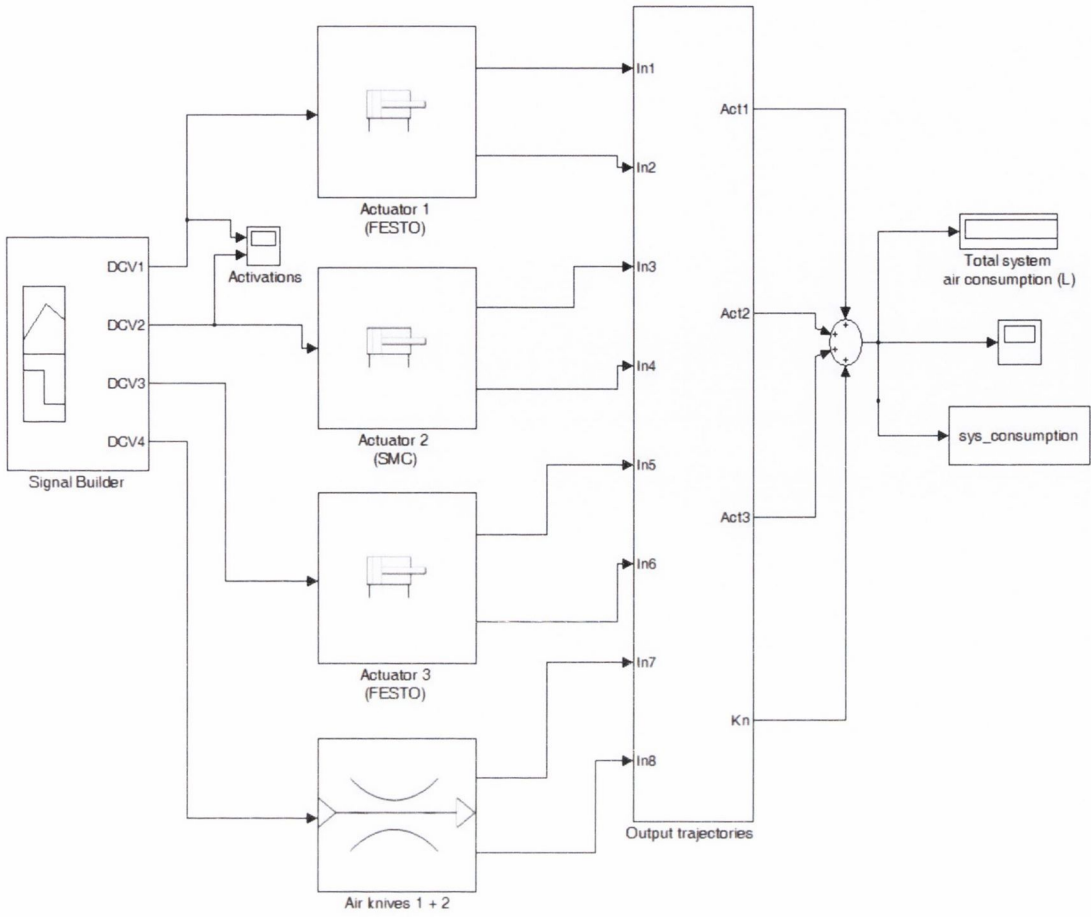
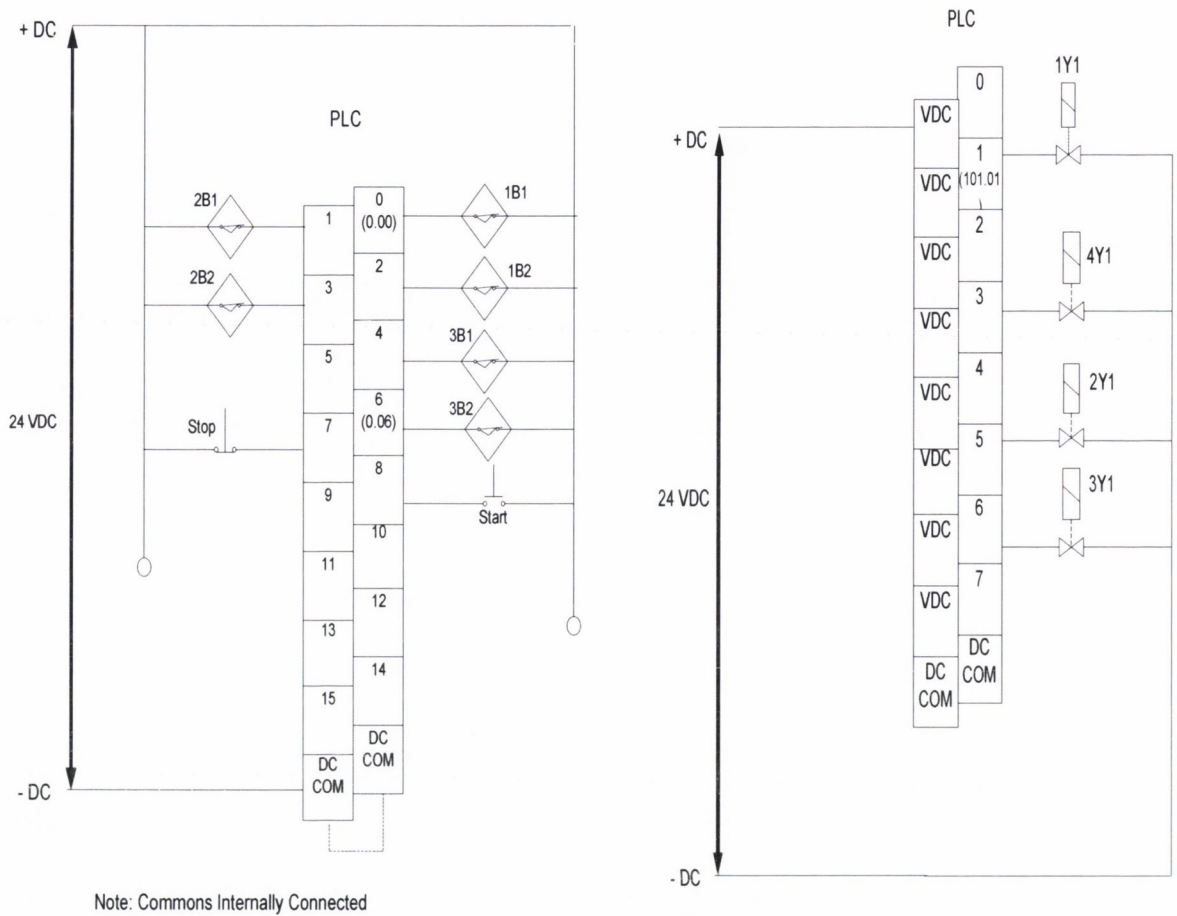


Figure B5: Top level diagram of prototype pneumatic system with user defined loading profile

Appendix C Prototype system details



ASSIGNMENT SHEET			
INPUTS			
SYMBOL	DATA	ADDRESS	COMMENT
PB1	BOOL	0.08	N/O Start button
PB2	BOOL	0.07	N/C Stop button
1B1	BOOL	0.00	Cylinder 1
1B2	BOOL	0.02	Cylinder 1
2B1	BOOL	0.01	Cylinder 2
2B2	BOOL	0.03	Cylinder 2
3B1	BOOL	0.04	Cylinder 3
3B2	BOOL	0.06	Cylinder 3
OUTPUTS			
SYMBOL	DATA	ADDRESS	COMMENT
1Y1	BOOL	101.01	Solenoid 1
2Y1	BOOL	101.05	Solenoid 2
3Y1	BOOL	101.06	Solenoid 3
4Y1	BOOL	101.03	Solenoid 4

Figure C1: Electrical circuit diagram for prototype system; inputs and outputs, and PLC assignment sheet

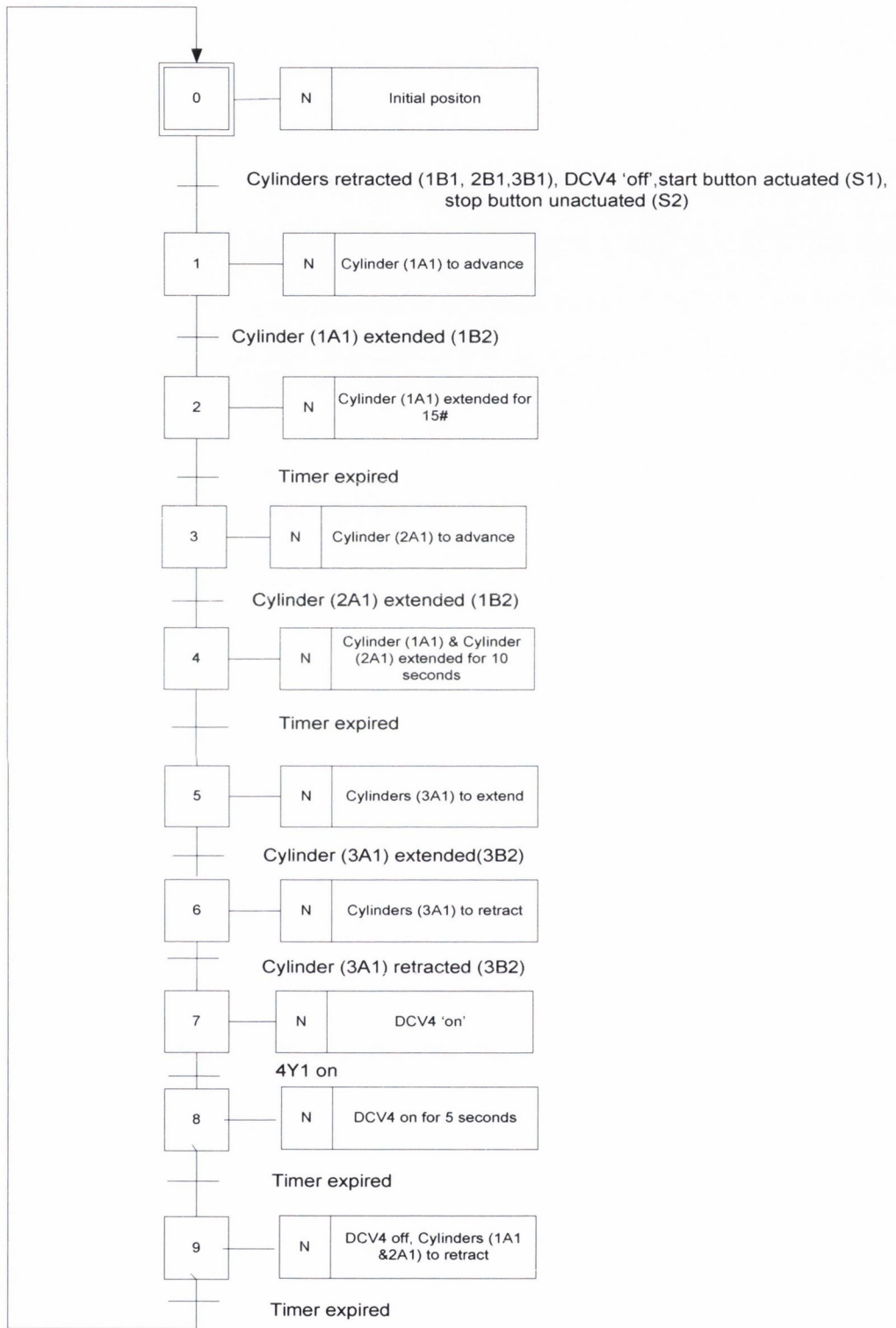


Figure C2: Function chart for sequence 1 (prototype system)